Structures of some Silyl- and Germyl- Transition Metal Carbonyl Complexes.

by

Alastair Robertson

A thesis presented for the degree of Doctor of Philosophy.

University of Edinburgh. September 1976.

ACKNOWLEDGEMENT

Special thanks are due to Professor E.A.V. Ebsworth, my supervisor, whose enthusiastic help and advice made this thesis possible. Many thanks are also due to Dr. D.W.H. Rankin and Dr. S. Cradock for their immeasurable assistance in the electron diffraction and photoelectron studies.

I am also very grateful to many people in the chemistry department, especially those in inorganic research, for their help, co-operation and comradeship throughout this study.

Further thanks are due to the Dewar Foundation for financial support and the University of Edinburgh for the provision of laboratory facilities.

I would also like to thank Professor D.W.J. Cruikshank, Dr. F. Beagley and Mrs. V. Ulbrecht of the University of Manchester Institute of Science and Technology for the provision of electron diffraction facilities.

SUMMARY

The He(I) photoelectron spectra of $HMn(CO)_5$, $SiH_3Mn(CO)_5$, $SiCl_3Mn(CO)_5$, $SiF_3Mn(CO)_5$, $GeH_3Mn(CO)_5$, $GeMe_3Mn(CO)_5$, $HRe(CO)_5$, $CH_3Re(CO)_5$, $SiH_3Re(CO)_5$, $SiF_3Re(CO)_5$, $GeH_3Re(CO)_5$, $Re_2(CO)_{10}$, $HCo(CO)_4$, $SiH_3Co(CO)_4$, $SiMe_3Co(CO)_4$ and $GeH_3Co(CO)_4$ were recorded. These spectra and published photo-electron spectra of $CH_3Mn(CO)_5$, $CF_3Mn(CO)_5$ and $SiMe_3Mn(CO)_5$ are discussed in terms of $(d \rightarrow d)\ \pi$ bonding in the silicon-transition metal and germanium-transition metal bonds. Due to the overlapping of peaks in the above mentioned spectra the assignment of all but a few electronic energy levels to peaks in the photo-electron spectra was impossible. However these spectra did indicate that, in at least the manganesepentacarbonyl derivatives, $(d \rightarrow d)\ \pi$ bonding was unimportant in the metal-metal bonds. The main change in substituting a silyl- or germyl- group for a methyl- group on manganesepentacarbonyl appeared to be an increase in σ acceptor power of the ligand. Rheniumpentacarbonyl and cobalttetracarbonyl derivatives gave photo-electron spectra which are consistent with this observation.

The gas phase molecular structures of $SiH_3Mn(CO)_5$, $SiF_3Mn(CO)_5$, $GeH_3Mn(CO)_5$, $GeH_3Co(CO)_4$, $CH_3Re(CO)_5$, $SiH_3Re(CO)_5$ and $GeH_3Re(CO)_5$ were determined by electron diffraction. Difficulties were encountered in the structure determinations of the rhenium derivatives owing to an oscillation in the published scattering factor for rhenium. This oscillation had to be removed to enable these structure determinations to be carried out. The discussion of the above structures and those available for $CH_3Mn(CO)_5$, $CF_3Mn(CO)_5$, $SiMe_3Mn(CO)_5$, $SiH_3Co(CO)_4$, $SiCl_3Co(CO)_4$, $SiF_3Co(CO)_4$ and $GeCl_3Co(CO)_4$ was also largely in terms of $(d \rightarrow d)\ \pi$ bonding in the bonds between silicon or germanium and transition metals. These

metal-metal bonds were always found to be shorter than would be predicted from the covalent radii of the atoms involved and this could be taken as an indication of (d⟶d) π bonding. However, these relatively short silicon- and germanium- transition metal bond lengths are also consistent with σ acceptor power increasing as silyl- and germyl- groups are substituted for methyl- groups. Halogenation of a silyl- or germyl- group bound to a transition metal atom shortens the metal-metal bond. This again could be due to an increase in (d⟶d) π bonding. The very large reduction in the methyl carbon-manganese bond length on fluorination of $CH_3Mn(CO)_5$ and the fact that the silicon-manganese bond length in $SiF_3Mn(CO)_5$ is only slightly shorter than would be predicted from the methyl carbon-manganese bond length in $CF_3Mn(CO)_5$ indicate that halogenation of silyl- and germyl- groups in transition metal carbonyl complexes does not cause an increase in (d⟶d) π bonding in the metal-metal bonds. It also seems likely that the methyl carbon-manganese bond in $CH_3Mn(CO)_5$ is anomalously weak and long rather than the manganese-silicon and manganese-germanium bonds in $SiH_3Mn(CO)_5$ and $GeH_3Mn(CO)_5$ being anomalously short and strong.

At the start of this work it was hoped that the molecular structures would also enable more information to be obtained from the photoelectron spectra. However, the photoelectron spectra and molecular structures of Si_2H_6, Si_2F_6, $SiH_3Mn(CO)_5$ and $SiF_3Mn(CO)_5$ demonstrated the difficulties involved in trying to correlate bond lengths with binding energies of the σ bonding level. Fluorination of Si_2H_6 results in an increase in binding energy of the electrons in the Si-Si σ bond but no significant decrease in bond length whereas fluorination of $SiH_3Mn(CO)_5$ resulted both in an increase in binding energy of the electrons in the Si-Mn σ bond and a decrease in Si-Mn bond length.

Appendix one describes an attempt to determine the gas phase molecular structure of trifluoromethylisocyanate by electron diffraction. This failed since all the bond lengths are too close together, as are the two-bonded distances.

Appendix two describes the gas phase molecular structure of hydridotetrakis (trifluorophosphine) rhodium (I) determined by electron diffraction. This structure indicates that, with trifluorophosphine ligands, (d$\rightarrow$d) π bonding is important in rhodium-phosphorus bonds.

CONTENTS

INTRODUCTION

In 1941 Hein et al. established the possibility of bonding between Group IVB elements and transition metal atoms with the preparation of some tin-cobalt derivatives[1]. Later in the same decade some trialkyllead derivatives of tetracarbonyliron were prepared by the same group of workers[2] but it was not until 1956 that the first simple silyl transition metal carbonyl complex, dicarbonyl (η^5-2,4-cyclopentadien-1-yl) (trimethylsilyl) iron, was prepared[3]. Many other silyl and germyl transition metal carbonyl complexes have since been synthesised, especially after 1965 when Chalk and Harrod published the preparations of a series of substituted silyl-cobalttetracarbonyl complexes[4] and Aylett and Campbell published the preparation of tetracarbonylsilylcobalt(I)[5]. These two papers described methods of preparation which are now frequently used for silyl and germyl derivatives of transition metal carbonyl complexes:

$$xM1R_3H + M2_x(CO)_y \rightarrow xM1R_3M2(CO)_{y/x} + x/2H_2$$

as in reference 4,

and

$$xM1H_3X + M2(CO)^{x-}_y \rightarrow (M1H_3)_x M2(CO)_y + xX^-$$

as in reference 5,

where M1 = Si, Ge; R = alkyl, alkoxy, aryl, halogen; M2 = transition metal, normally Group VIa, VIIa or VIII

All the silyl and germyl transition metal carbonyl complexes studied in this work were prepared using one or other of the above two methods.

In these compounds there exists the possibility of multiple bonding between the silicon or germanium atom and the transition metal atom involving, in addition to the metal-metal σ bond, π interaction between the unfilled d-orbitals of silicon or germanium and the filled d-orbitals of the transition metal. This will result in a bond which

will hereafter be referred to as a $(d\rightarrow d)\pi$ bond. This type of bonding is similar to $(d\rightarrow p)\pi$ and $(d\rightarrow d)\pi$ bonding which are generally accepted as being important in the metal-carbon and metal-phosphorus bonds in transition metal carbonyl and phosphine complexes respectively. Similar $(p\rightarrow d)\pi$ bonding has also been postulated in the bonds between silicon and main group elements with lone pairs, for example, in the silicon-chlorine bond in SiH_3Cl[6] and the silicon-oxygen bonds in $(SiH_3)_2O$[7].
Much work has been carried out, using several techniques, to assess the importance of $(d\rightarrow d)\pi$ bonding in silicon-transition metal and germanium-transition metal bonds and there follows a brief literature survey of the evidence obtained.

Some chemical properties of methyl-, silyl- and germyl-transition metal carbonyl complexes.

Several silyl- and germyl- transition metal carbonyl complexes have been found to be thermally more stable than the analogous alkyl compounds. For example, tetracarbonylsilylcobalt(I)[5] and tetracarbonylgermylcobalt(I)[8] have both been found to be fairly stable in vacuo at room temperature but tetracarbonylmethylcobalt(I)[9] decomposes in vacuo at temperatures below $0^{\circ}C$.
The silicon-transition metal and germanium-transition metal bonds in silyl- and germyl- transition metal carbonyl complexes are also less susceptible to chemical attack than the alkyl carbon-transition metal bonds in analogous alkyl derivatives. Carbon monoxide readily inserts into the C_{met}-Mn bond of pentacarbonylmethylmanganese(I)[10] but no such insertion occurs into the metal-metal bond of either pentacarbonylgermylmanganese(I)[11] or pentacarbonylsilylmanganese(I)[12].
Silyl- and methyl- derivatives of manganesepentacarbonyl

also behave differently towards hydrogenchloride

$$CH_3\,Mn(CO)_5 + HCl \rightarrow HMn(CO)_5 + CH_3Cl$$ [13]

but

$$SiH_3Mn(CO)_5 + xHCl \rightarrow SiH_{3-x}Cl_xMn(CO)_5 + xH_2$$ [12]

The differences in the above two reactions are probably accounted for by differences in the reaction mechanisms. It appears that the former reaction involves electrophilic substitution on the manganese atom whereas the latter reaction involves nucleophilic substitution on the silicon atom. These two reaction mechanisms could arise through nucleophilic substitutions being easier at silicon than at a methyl carbon atom or if the Mn-Si bond were stronger than the Mn-C bond or by a combination of both effects.

If thermodynamic factors dominate, the above chemical evidence indicates that silicon-transition metal bonds and germanium-transition metal bonds in silyl- and germyl-transition metal carbonyls are stronger than alkyl carbon-transition metal bonds in the analogous alkyl complexes. Such observations have been rationalised in terms of bonding in the metal-metal bonds of silyl- and germyl-transition metal complexes[4].

Vibrational Spectra of silyl- and germyl- transition metal carbonyl complexes.

Much of the earlier work in this field was on force constant calculations on carbonyl stretching frequencies. Such calculations on substituted silyl- and germyl- cobalttetracarbonyl complexes, [14, 15] published in 1967, led to the conclusion that (d→d) π bonding was important in the metal-metal bonds in these compounds. Force constant calculations published a year later, also on substituted silyl- and germyl- cobalttetracarbonyl derivatives[16] gave rise to different conclusions, the results of the calculations being interpreted in terms of a ligand field effect.

Similar calculations on substituted silyl- and germyl-manganesepentacarbonyl derivatives were published by the same group[17] and these results could also be rationalised in terms of ligand field effects. However, also in 1968 in a review of Group IVB transition metal complexes[18] it was noted that the difference between force constants for axial and equatorial A_1 carbonyl stretching vibrations was always greater for alkyl- cobalt and alkyl- manganese carbonyl derivatives than in analogous silyl-, germyl- and stannyl- complexes. The author explained this fact in terms of the presence of (d→d)π bonding in the latter group of compounds. Several other force constant calculations on Group IVB transition metal carbonyl complexes have been interpreted as showing that (d→d)π bonding is important in the metal-metal bond (including references 19, 20, 21, 22). Around the same time as the above work was published it was noted, in a paper on the molecular structure of $SiH_3CO(CO)_4$ that little credence could be given to estimations of (d→d)π bonding in silyl- and germyl- transition metal carbonyl complexes from calculations based on carbonyl stretching frequencies due to the succession of approximations inherent in the method [23].

In a paper published in 1971[24] on force field calculations on germyl- and stannyl- cobalttetracarbonyl complexes, (d→d)π bonding was declared important. This paper also upheld the view that force constant calculations on carbonyl stretching frequencies of Group IVB transition metal carbonyl complexes could not be used to estimate accurately the importance of (d→d)π bonding in the metal-metal bonds of these complexes.

More recently, force field calculations on some substituted germyl- cobalttetracarbonyl complexes indicated (d→d)π bonding was significant in the Ge-Co bond[25]. Most of the above mentioned force constant and force field calculations have been interpreted in terms of (d→d)π bonding in the metal-metal bonds. However, the validity of conclusions

from the earlier force constant calculations has been questioned [23, 24]. One limitation on the validity of the conclusions based on these calculations is the difficulty in evaluating the mixing of vibrations within the molecule. Also, since there is no rigorous relationship between force constants and bond energies, not to mention between force constants and the nature of bonding, there must be some doubt over the validity of all conclusions as to the presence, or otherwise, of $(d \rightarrow d)\pi$ bonding in these compounds that are based on force field and force constant calculations.

Bond energies of metal-metal bonds in Group $\overline{IVB}$ transition metal carbonyl complexes derived from their mass spectra.

Metal-metal bond energies in several Group $\overline{IV}$B transition metal carbonyl complexes have been determined using mass spectrometry. The bond energies of Si-Co bonds in $F_3Si\ Co(CO)_4$, $F_2(CH_3)Si\ Co(CO)_4$ and $Cl_3Si\ Co(CO)_4$ have been determined and rationalised in terms of variations in $(d \rightarrow d)\pi$ bonding in the Si-Co bonds[26]. The Si-Mn bond energies in the series $Me_3SiMn(PF_3)_x(CO)_{5-x}$ (where $x = 0$ to 5) have been determined[27] and these are said to indicate that $(d \rightarrow d)\pi$ bonding is important in the Si-Mn bonds. Other bond energies for silicon- and germanium-transition metal bonds have been determined this way[28, 29] but no attempt was made by the authors to correlate these results with the presence or absence of $(d \rightarrow d)\pi$ bonding. A very strong Sn-Re bond in $Me_3SnRe(CO)_5$ has been found but $(d \rightarrow d)\pi$ bonding need not be invoked to explain this[29]. Bond dissociation energies of these metal-metal bonds do not, in themselves, give a complete insight into the nature of these bonds as they only give the strength of a bond. There is also the problem that it may be the bond energy of the positive ion rather than that of the neutral molecule which is being measured.

Molecular structures of Group IVB transition metal carbonyl complexes

The metal-metal bond lengths and other structural parameters of these compounds may be expected to give some insight into the nature of the metal-metal bond. The molecular structures of several Group IVB transition metal carbonyl complexes have been determined and the metal-metal bond lengths found are given in Table 1.
In the series, $H_3SiCo(CO)_4$, $F_3SiCo(CO)_4$ and $Cl_3SiCo(CO)_4$ the Si-Co bond length is seen to decrease with increasing electronegativity of the substituent on silicon. This has been rationalised in terms of increasing $(d\rightarrow d)\pi$ bonding with increasing electronegativity of the substituent on the silicon atom[41]. However, there is a similar difference between the C_{met}-Mn bond lengths in $H_3CMn(CO)_5$[30] and $F_3CMn(CO)_5$[31], where there is no possibility of $(d\rightarrow d)\pi$ bonding. This must cast doubt on whether it is increasing $(d\rightarrow d)\pi$ bonding that is causing the shortening of the Si-Co bond in the silyl- derivatives of cobalttetracarbonyl. The Mn-Ge bond in $Br_3GeMn(CO)_5$[33] is very much shorter than that in $Ph_3GeMn(CO)_5$[34] but both these Mn-Ge bond lengths and the Mn-Si bond length in $Me_3SiMn(CO)_5$[32] are shorter than would be expected from calculations from covalent radii (using the molecular structures of C_2H_6[43], SiH_3CH_3[44], GeH_3CH_3[45] and $CH_3Mn(CO)_5$[30] to obtain covalent radii for C, Si, Ge and Mn). The same Sn-Mn bond length is found for both $Me_3SnMn(CO)_5$[35] and $Ph_3Sn(CO)_5$[36] and this is considerably less than the sum of Sn and Mn covalent radii. A similar pattern for Sn-Fe bond lengths is seen in $Br_3SnFe(CO)_2(C_5H_5)$, $Cl_3SnFe(CO)_2(C_5H_5)$[38] and $Ph_3SnFe(CO)_2(C_5H_5)$[39] the Fe-Sn bond lengths in the trichlorostannyl- and tribromostannyl- derivatives are significantly shorter than that in the triphenylstannyl derivative. It was suggested that this shortening of the

TABLE 1 Metal-Metal bond lengths in some Group IVB transition metal carbonyl complexes.

Compound	R(M1-M2) (pm)	Method of determination	Reference
$H_3CMn(CO)_5$	218.5(11)	e.d	30
$F_3CMn(CO)_5$	205.6 (4)	e.d	31
$Me_3SiMn(CO)_5$	249.7(5)	X-ray	32
$Br_3GeMn(CO)_5$	244	X-ray	33
$Ph_3GeMn(CO)_5$	254(2) 253(2)	X-ray	34
$Me_3SnMn(CO)_5$	267.4(2)	X-ray	35
$Ph_3SnMn(CO)_5$	267.4(4)	X-ray	36
$(Cl_3Si)_2FeH(CO)(C_5H_5)$	225.2(3)	X-ray	37
$Cl_3SnFe(CO)_2(C_5H_5)$	246.6(2)	X-ray	38
$Br_3SnFe(CO)_2(C_5H_5)$	246.5(3)	X-ray	38
$Ph_3SnFe(CO)_2(C_5H_5)$	253.7(3)	X-ray	38
$H_3SiCo(CO)_4$	238.1(7)	e.d	23
$Cl_3SiCo(CO)_4$	225.4(3)	X-ray	39
$F_3Si\ Co(CO)_4$	222.6(5)	X-ray	40
$GeCl_3Co(CO)_4$	231.0(7)	X-ray	41
$Cl_3SiRhHClP(C_6H_5)_3)_2$	220.3(4)	X-ray	42

Fe-Sn bond was indicative of the Sn-Fe bonds being purely σ[38]. The Fe-Si bond length in $(C_5H_5)Fe(SiCl_3)_2(CO)$ has been interpreted in terms of $(d \rightarrow d)\pi$ bonding in that bond[37]. The Rh-Si bond in $RhHCl(SiCl_3)(P(C_6H_5)_3)_2$ was the shortest transition metal-silicon bond then determined[42]. The author's explanation for this was that $(d \rightarrow d)\pi$ bonding was most important in silicon-transition metal bonds when there was no competing bonding ligand trans to the silyl-group.
The molecular structures so far determined of Group IVB transition metal carbonyl complexes are consistent with $(d \rightarrow d)\pi$ bonding being important in the metal-metal bonds. However, since the metal-metal bond length decreases as the electronegativity of the substituent on the Group IVB atom increases these shortenings are also consistent with a ligand field effect being the predominant cause of any such change in metal-metal bond length. A wider range of known metal-metal bond lengths may help clarify this bonding problem and this was the stimulus for the structure determinations in this thesis.

U.V. Photoelectron spectra of, ultra violet spectra of and molecular orbital calculations on Group IVB transition metal carbonyl complexes and metal compounds.

Prior to the start of this work in 1971, ultraviolet photoelectron spectroscopy had seldom been applied to transition metal carbonyl complexes. The only work published was by Green et al. on a series of manganese-pentacarbonyl derivatives[46], $RMn(CO)_5$ (where R = H, Cl, Br, I, CH_3, CF_3, CH_3CO, CF_3CO, $Mn(CO)_5$). These spectra were interpreted as indicating large energy splittings, up to 1.6ev, between the Mn 3d e and Mn 3d b_2 formally non-bonding energy levels. The Mn 3d e energy level is the electronic energy level on manganese most likely

to participate in (d→d)π bonding in Si-Mn and Ge-Mn bonds. The above assignments indicated that (d→d)π bonding, were it to occur in silyl- and germyl- transition metal carbonyl complexes, would be readily detectable using photoelectron spectroscopy. This work was therefore the stimulus for the photoelectron work in this thesis. Recently many of the assignments made by Green et al have been challenged and new assignments made for both the halogen [47, 48, 49] and methyl- and trifluoromethyl-[50, 51, 52] manganesepentacarbonyl derivatives on the basis of ab initio molecular orbital calculations and correlations with the photoelectron spectra of series of related compounds. The consensus opinion of these papers is that Green et al over estimated the binding energy of the electrons in the Mn-X a_1 bonding level by several electron volts and the Mn-X a_1 bonding level lies close in energy to the Mn 3d b_2 and Mn 3d e, formally non-bonding, energy levels. As a result, in these PE spectra, peaks arising from the excitation of electrons out of the Mn 3d e and b_2 and Mn-X a_1 energy levels overlap. This causes difficulties in the exact assignments of these peaks and there is little agreement on that subject. No ab initio molecular orbital calculations have been published for any silyl or germyl transition metal carbonyl complexes. Extended Hückel theory calculations on $F_3SiCO(CO)_4$ and $Cl_3SiCo(CO)_4$ [53] indicated that there is a significant (d→d)π character in the Si-Co bonds in both complexes, but to a greater extent in $F_3SiCo(CO)_4$. This was in agreement with predictions made from Si-Co bond lengths [40, 41] but mass spectra indicated that the Si-Co bond is stronger in $Cl_3SiCo(CO)_4$ [26]. A review paper recently published [54] on the UV spectra of some methyl, silyl, germyl and halogen derivatives of pentacarbonylmanganese concluded, on the basis of these

spectra, related published photoelectron spectra and ab initio calculations, that (d→d)π bonding is important in the silyl- and germyl- complexes.

Studies on Group IVB transition metal carbonyl complexes using nuclear resonance techniques.

Some ^{59}Co nuclear quadrupole resonance frequencies have been determined for Group IVB cobalttetracarbonyl complexes. A paper on ^{59}Co n.q.r. spectra over a wide range of Group IVB cobalttetracarbonyl complexes gave no evidence for (d→d)π bonding in any silyl- derivatives of cobalttetracarbonyl, found the $SiCl_3$ group a good σ donor and gave some evidence for (d→d) π bonding in Sn-Co and Ge-Co bonds in stannyl- and germyl- cobalttetracarbonyl derivatives[55]. The authors did not quantify the importance of (d→d)π bonding in these compounds. A later paper[56] gave ^{59}Co n.q.r. frequencies for the series $X_3SnCo(CO)_4$ (X=Cl,Br,I) and these were rationalised in terms of (d→d)π bonding in the Sn-Co bonds.

Molecular orbital calculations have indicated that ^{55}Mn n.m.r. chemical shifts are largely dependent on the σ polarity of the Mn-Sn bond in tin(IV) derivatives of manganesepentacarbonyl and it has been suggested that the amount of π bonding in those bonds is reflected in the line width of the resonance[57]. The ^{55}Mn chemical shift has also been seen to vary linearly with the ^{119}Sn Mössbauer isomer shift[57], and ^{55}Mn and ^{1}H n.m.r. chemical shifts. ^{119}Sn Mössbauer studies have also indicated that $Mn(CO)_5$ is a better σ-donor than Me, Ph or halogen and there is a σ transfer Mn to Sn onsubstitutionof alkyls or aryls by halogens on the tin atom[57]. A more recent study of ^{55}Mn chemical shifts over a wide range of Group IVB manganesepenta-

carbonyl derivatives[58] found, in accordance with the molecular orbital calculations mentioned above, that the ^{55}Mn chemical shift was probably dependent on the Mn-Mlσbond. However the ^{55}Mn resonance line width was found to be dependent on the square of the ^{55}Mn chemical shift and therefore these results, which do not preclude (d→d)πbonding, must cast doubt about the accuracy of the molecular orbital calculations mentioned earlier.

The ^{119}Sn Mössbauer effect has been observed for many tin(IV) transition metal carbonyl complexes where there is a tin transition metal bond (including references 59, 60, 61, 62, 63). The general conclusion from this effect is that (d→d)π bonding is not important in tin-transition metal bonds. Results obtained from the ^{119}Sn Mössbauer effect in some tin-manganese and tin-iron carbonyl complexes indicated that the main effect in changing the substituent at tin was to change the tin-transition metal bonds. A 1973 review[57] of the subject explained the ^{119}Sn Mössbauer spectra of tin(IV) transition metal carbonyl complexes in terms of changes in the tin-transition metal bond. However, since these ^{119}Sn Mössbauer spectra may be unaffected by (d→d)π bonding, owing to the insensitivity of this effect to the occupancy of Sn 5d orbitals, these spectra do not preclude the presence of (d→d)π bonding in the metal-metal bonds.

In the preceding survey there is no direct evidence for (d→d)π bonding in metal-metal bonds of silyl-, germyl- and stannyl- transition metal carbonyl

complexes. Much of the evidence cited is consistent with $(d \rightarrow d)\pi$ bonding being important in these bonds and there is no evidence which proves conclusively that $(d \rightarrow d)\pi$ bonding does not occur. However, many of the results mentioned can be satisfactorily explained by differences in the electronegativities of the ligands without invoking $(d \rightarrow d)\pi$ bonding. This together with the ^{119}Sn Mössbauer spectra of stannyl transition metal carbonyl complexes, which indicate important changes in the metal-metal bond as the substituent on tin is changed, make it seem doubtful that $(d \rightarrow d)\pi$ bonding is important in Group IVB element-transition metal bonds.

The following study of the PE spectra and molecular structures of some silyl- and germyl- transition metal carbonyl complexes was undertaken with the aim of obtaining some more concrete evidence on the presence, or otherwise, of $(d \rightarrow d)\pi$ bonding in silicon- and germanium- transition metal bonds. It was also hoped that some useful correlations between molecular structures and PE spectra could be demonstrated and that this would enable extra information to be obtained from the PE spectra.

CHAPTER ONE

The Photo-electron Spectra of some silyl- and germyl- transition metal carbonyl Complexes

CHAPTER 1

1.1 INTRODUCTION

The He(I) photoelectron spectra of the following compounds were recorded: $LMn(CO)_5$ (where L = SiH_3, $SiCl_3$, SiF_3, GeH_3 $GeMe_3$), $LRe(CO)_5$ (where L = H, CH_3, SiH_3, SiF_3, GeH_3, $Re(CO)_5$), $LCo(CO)_4$ (where L = H, SiH_3, $SiMe_3$, GeH_3). Photoelectron spectra of $HMn(CO)_5$, $CH_3Mn(CO)_5$, $CF_3Mn(CO)_5$[46] and $SiMe_3Mn(CO)_5$[64] had previously been recorded and are used in this work for comparison.

Photoelectron spectroscopy is a relatively recent method of determining ionisation potentials of molecules. Ultraviolet photoelectron spectroscopy was developed by Dr. D. W. Turner whose first results were published in 1962[65]. Since then an extensive literature including books [66, 67] and reviews[68, 69, 70] has been built up on the subject especially since 1969 when Perkin-Elmer Ltd. introduced a commercial photoelectron spectrometer.

The basic process involved is photoionisation; the interaction of a photon and a molecule results in the ejection of an electron. The energy of the photon determines the level from which the electron is ejected. High energy photons (X-ray) can be used resulting in the ejection of core electrons (e.g. 1s) and valence electrons. This is known as electron spectroscopy for chemical analysis, E.S.C.A.. The technique used in this work is ultraviolet photoelectron spectroscopy (U.V.P.E. or simply P.E.) where low energy photons (He(I) U.V.) are used. The electrons ejected are from valence energy levels.

In the interaction

$$M + h\nu \rightarrow M^+ + e^-$$

the relation

$$E = h\nu - I \qquad (A)$$

holds where E is the kinetic energy of the electron, $h\nu$ the energy of the incident photon and I the ionisation potential of that electron. From equation (A) it is seen that measurement of the kinetic energy of the ejected electron makes possible the determination of the ionisation potential of the electron which has been removed.

Koopmans' theorem states that there is no electronic rearrangement before complete ionisation.[71] Assumption of this theorem enables the ionisation potentials to be equated with the molecular energy levels. Therefore, by measurement of the energies of the ejected electrons, a molecular energy level diagram may be drawn up. Molecular orbital calculations have cast doubts on the precise validity of Koopmans' theorem but it is possible that the invalidity lies within the calculations rather than in the assumption of Koopmans' theorem which, in the absence of proof of its invalidity, appears to be at least the best basis for assigning peaks in U.V. photoelectron spectra.

The Franck-Condon principle states that electronic transitions are fast when compared with vibrational and rotational transitions. The ionisation process can therefore occur from the molecular ground state to variously defined excited states of the ion. Relation (A) would therefore be better written

$$E = h\nu - I - \Delta E_{vib} - \Delta E_{rot}$$

where ΔE_{vib} and ΔE_{rot} represent changes in rotational and vibrational energies on ionisation. Photoionisation especially from bonding energy levels, can lead either to a progression of peaks due to various changes in vibrational quanta on excitation or simply to a broad peak if the vibration involves dissociation. For this reason broad peaks are often assigned to bonding levels rather than non-bonding levels.

Arising from the Franck-Condon principle there are two ways of defining ionisation potential. The adiabatic ionisation potential is the difference in energy between the vibrational ground states in the potential energy curves of the excited and ground state species whereas the vertical ionisation potential is the most probable transition from the ground state to an ionic state which may be vibrationally excited.

There are serious limitations to this technique when it is applied to complex molecules. With large molecules there are many electronic energy levels and consequently much overlap of peaks can occur in their PE spectra. This occurs in all the PE spectra observed in this work. In every spectrum given here there is a region between about 13 and 17 ev which is unassignable and the region between 8 and 11ev is always complicated by overlapping peaks. The PE spectra of the series $LRe(CO)_5$, are further complicated by observation of spin-orbit coupling.

Due to the complexity of these PE spectra it was assumed that peak intensity gave some indication of orbital degeneracy. In doing this it was noted that peak intensity is also dependent on the photoionisation cross-section so any assignments based on peak intensity can only be tentative. (The photo-electron spectrum of $NMe_3Cr(CO)_5$ demonstrates the limitations assigning peaks from their relative intensities:[72] the peak assigned to the Cr-N a_1 bonding level is of the same intensity as the peak assigned to both the Cr 3d e and b_2 levels). The assignment of the peaks in the following photo-electron spectra have been made by considering the spectra of series of compounds rather than by taking each spectrum individually. It is also stressed that definitive assignments cannot be made for most peaks and the assignments made are no more than consistent with the spectra observed.

1.2 Results

The spectra obtained are illustrated in figures 1.1 to 1.13 and the vertical ionisation potentials are collected in tables 1.1 to 1.5. In all spectra between 13 and 17 ev there is a set of overlapping bands, described by an onset-to-tail range. The onset is always sharp but the tail is less well defined. Table 1.6 gives some data from free transition metal atoms for comparison. Attempts were made to obtain P.E. spectra of $SiF_3Co(CO)_4$ and $GeF_3Co(CO)_4$ but both these compounds decomposed before reaching the ionisation chamber.

1.3 Assignments

To analyse the spectra an approximate scheme must be drawn up to describe the molecular orbitals of the molecules being studied.

Molecules of the form $X_3M1M2(CO)_5$ are treated as belonging to the point group C_4v, the three-fold symmetry of the $M1X_3$ group being over-ridden by the four-fold symmetry of the $M2(CO)_5$ group. The occupied orbitals can be divided into five groups (four if X = H): those associated with the CO groups and M2-C bonds, those associated with the M1-X bonds (a_1 and e), the M1-M2 σ bond (a_1), the formally non-bonding M2 d-orbitals (e and b_2) and, unless X = H, those of the X lone pairs (2e, a_1 and a_2).

Molecules of the type $X_3M1Co(CO)_4$ are assumed to have C_3v symmetry and the orbitals can be classed in terms similar to the above, the most important difference being that the formally non-bonding Co 3d levels now comprise two doubly degenerate sets.

The spectra could be complicated by Jahn-Teller distortions which could lead to a broadening or doubling of the Mn 3d e and Co 3d e energy levels.

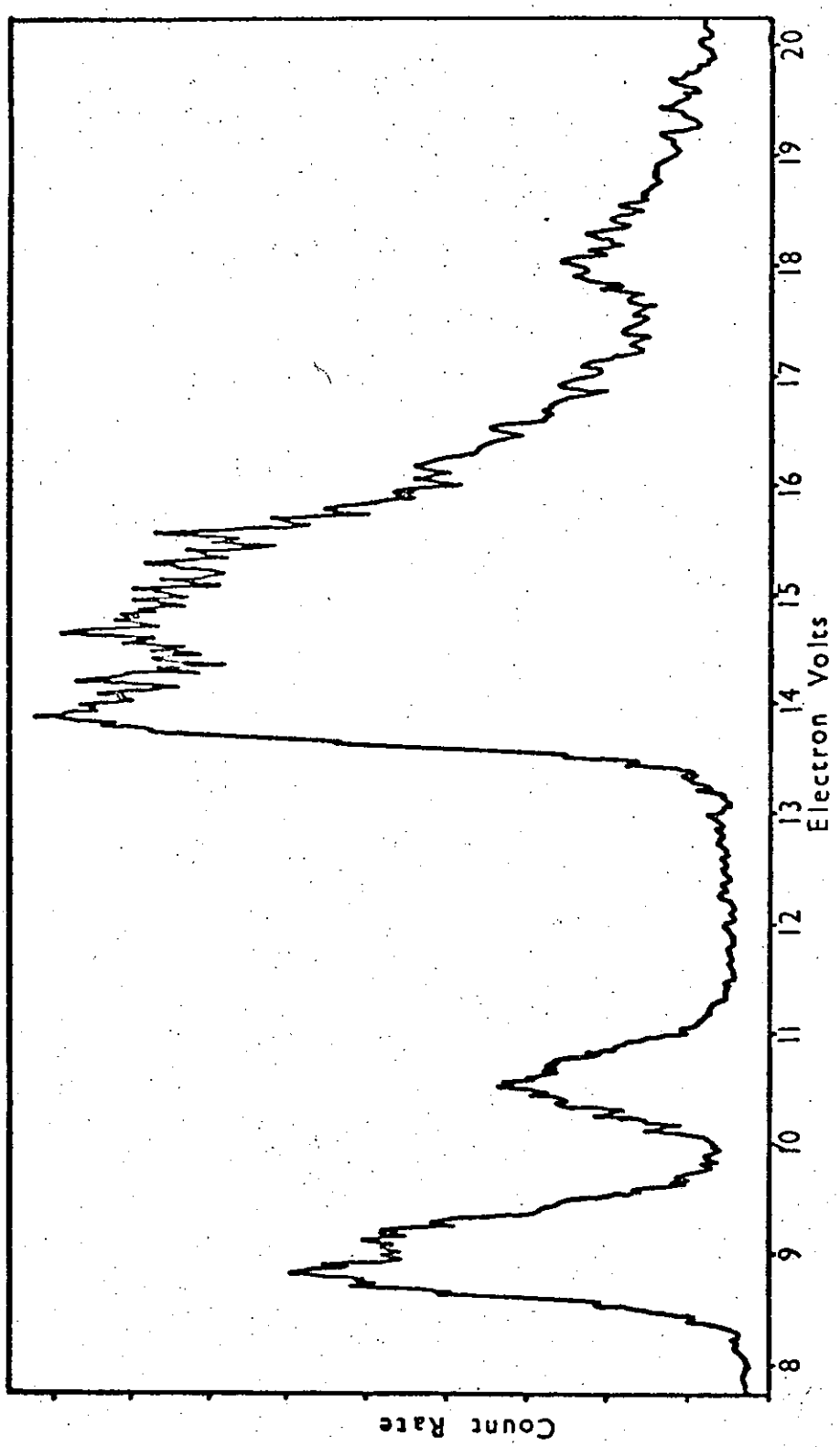

Figure 1.1 - Photoelectron spectrum of $HMn(CO)_5$.

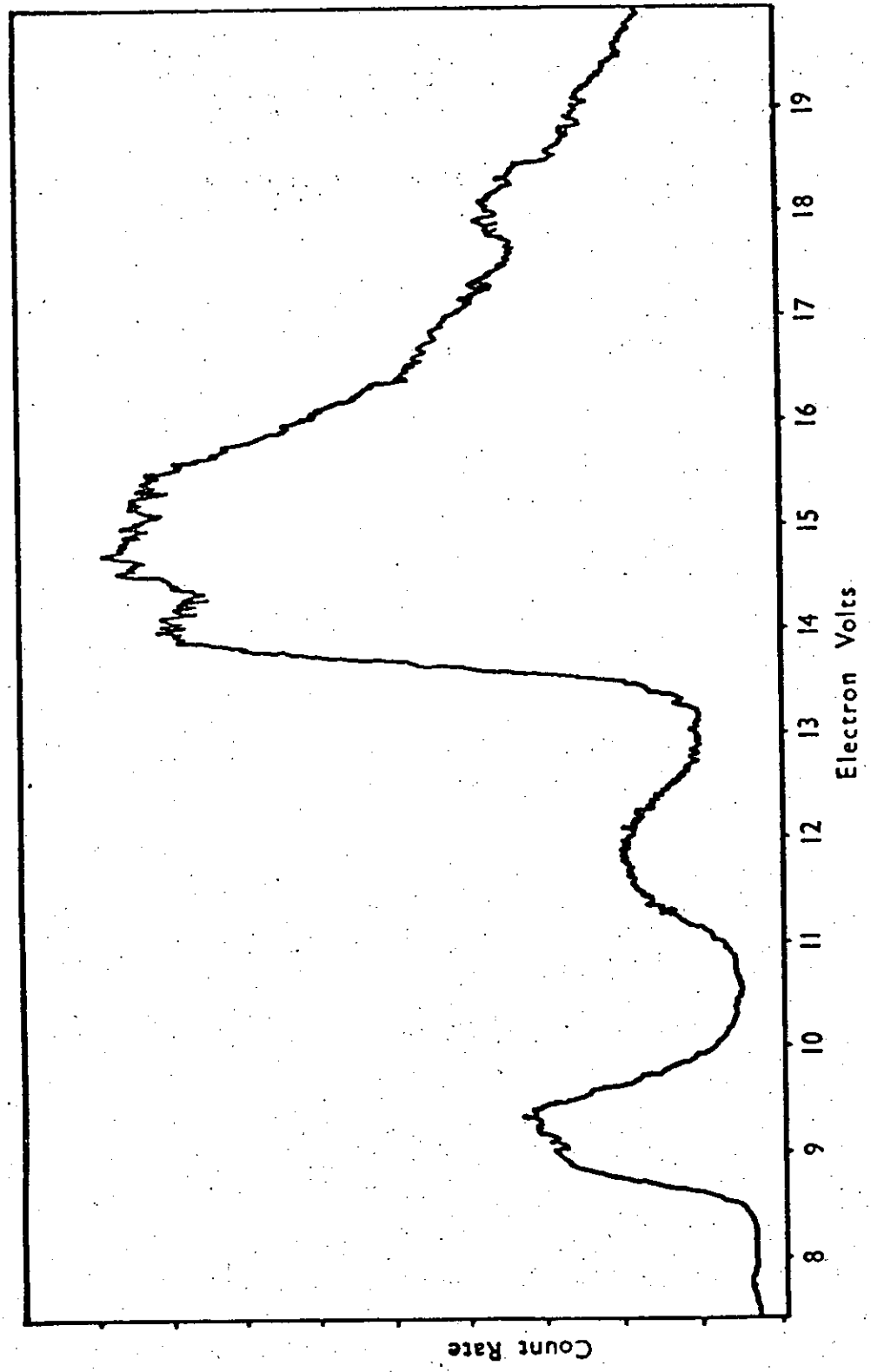

Figure 1.2 Photoelectron spectrum of $SiH_3Mn(CO)_5$

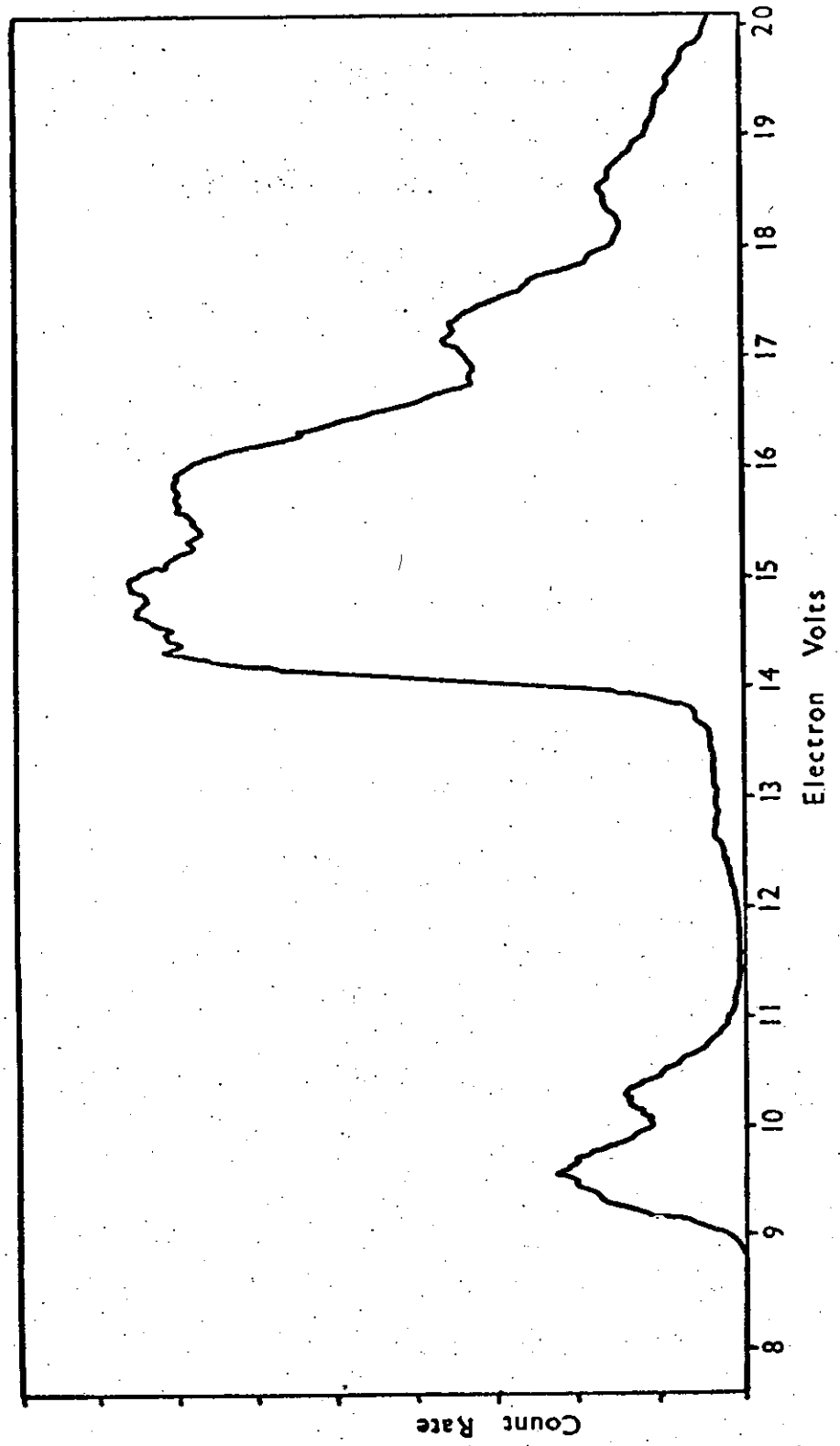

Figure 1.3 Photoelectron spectrum of $SiF_3Mn(CO)_5$

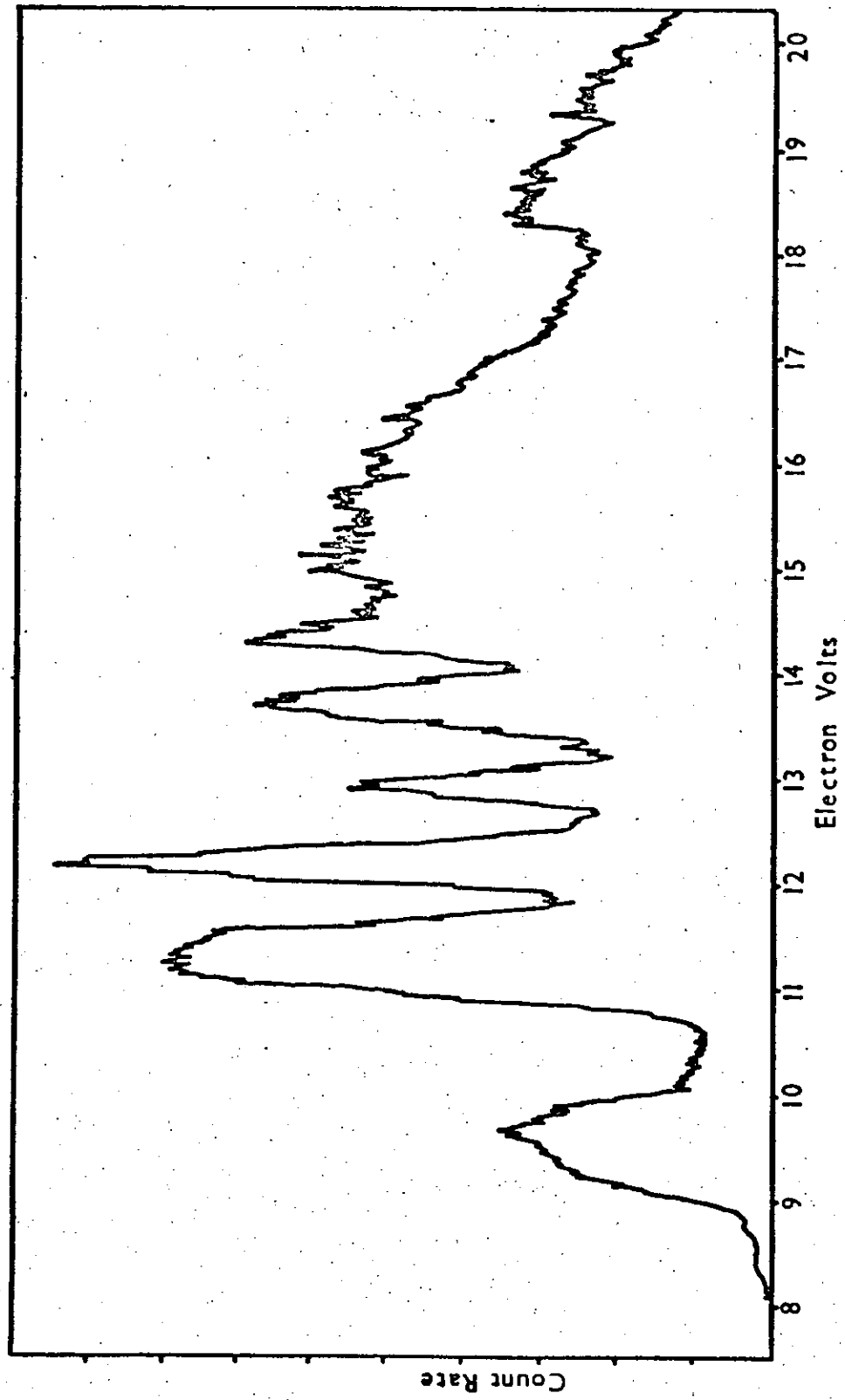

Figure 1.4 Photoelectron spectrum of $SiCl_3Mn(CO)_5$

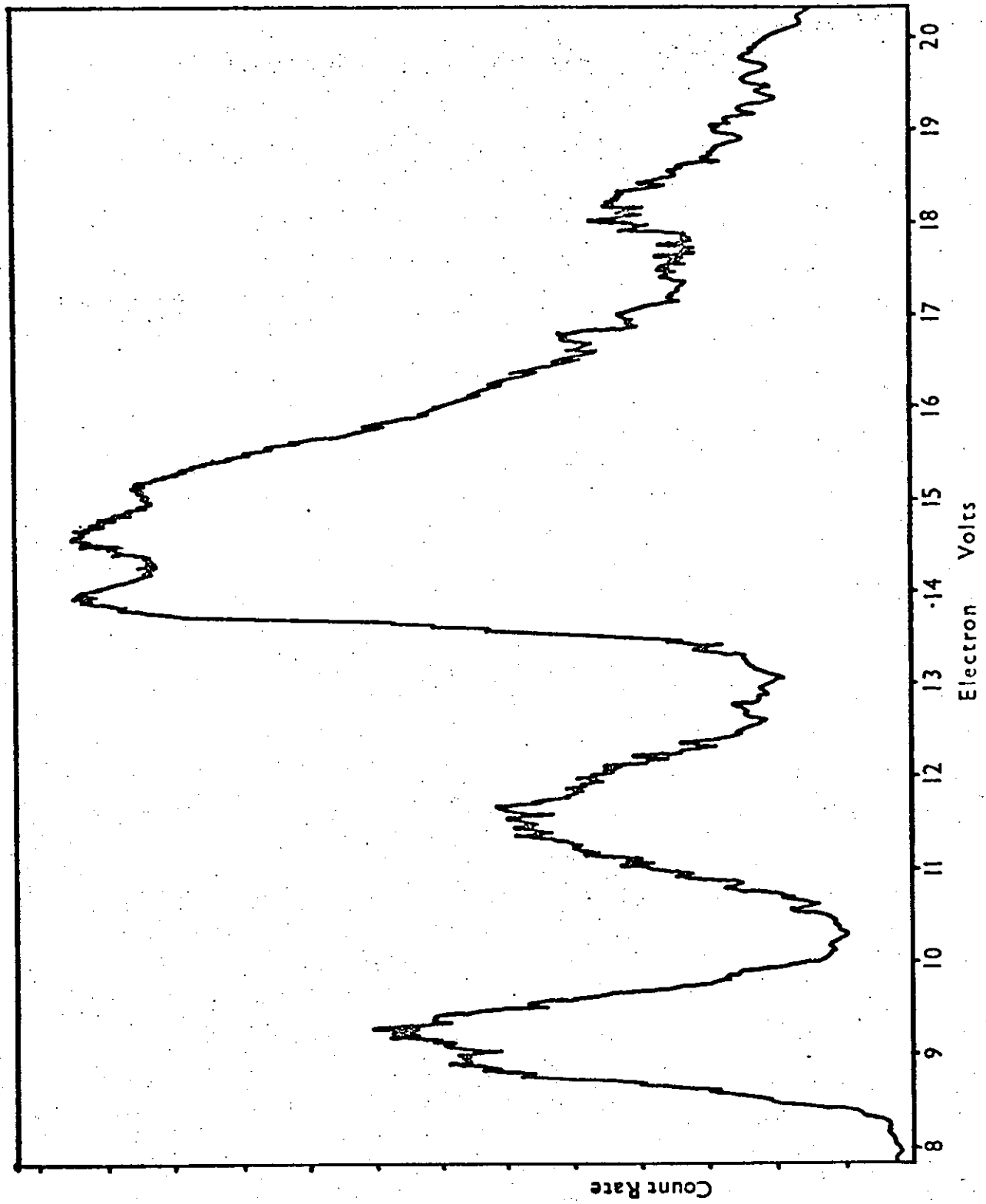

Figure 1.5 Photoelectron spectrum of $GeH_3Mn(CO)_5$

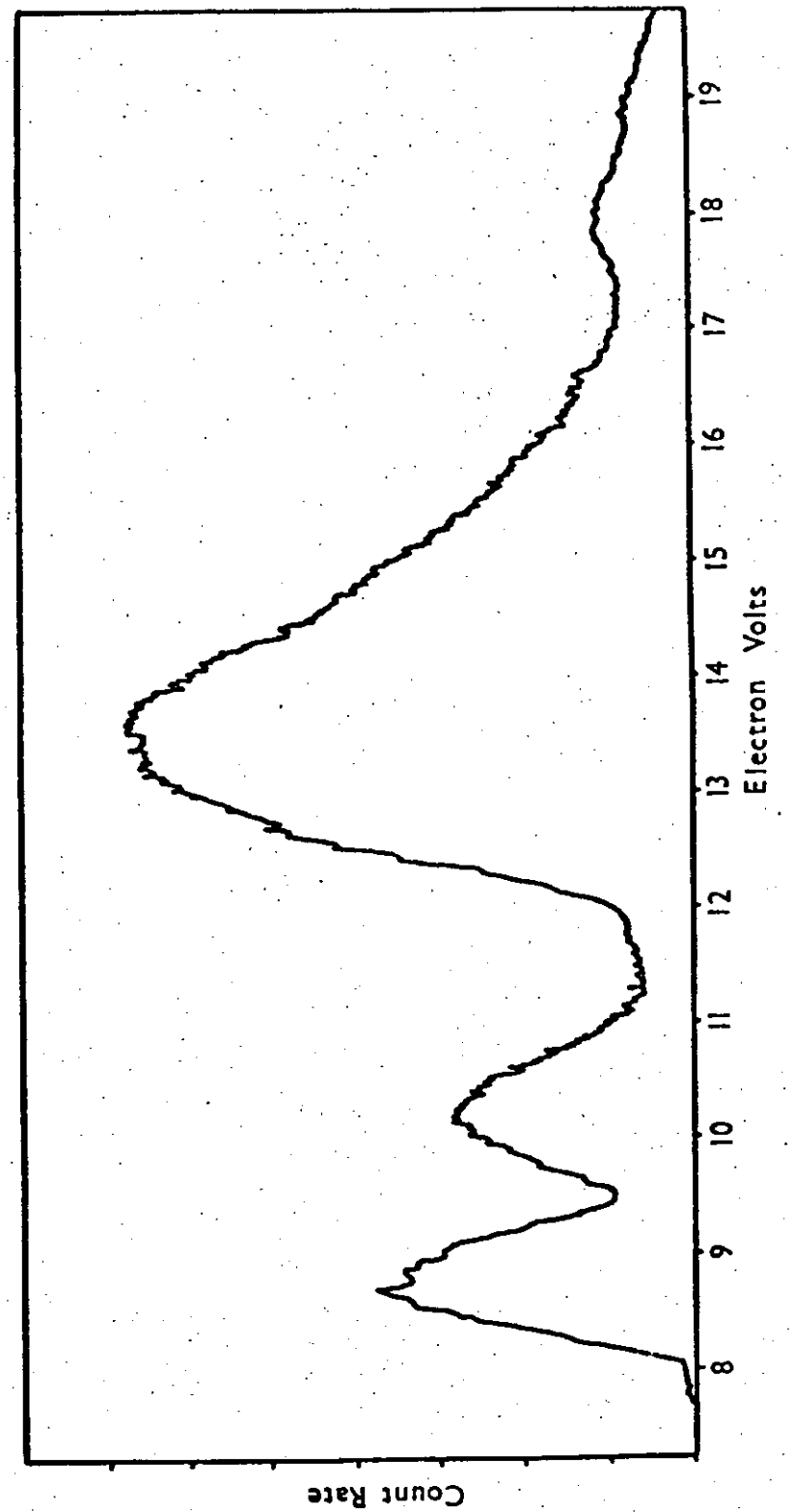

Figure 1.6 Photoelectron spectrum of $GeMe_3Mn(CO)_5$

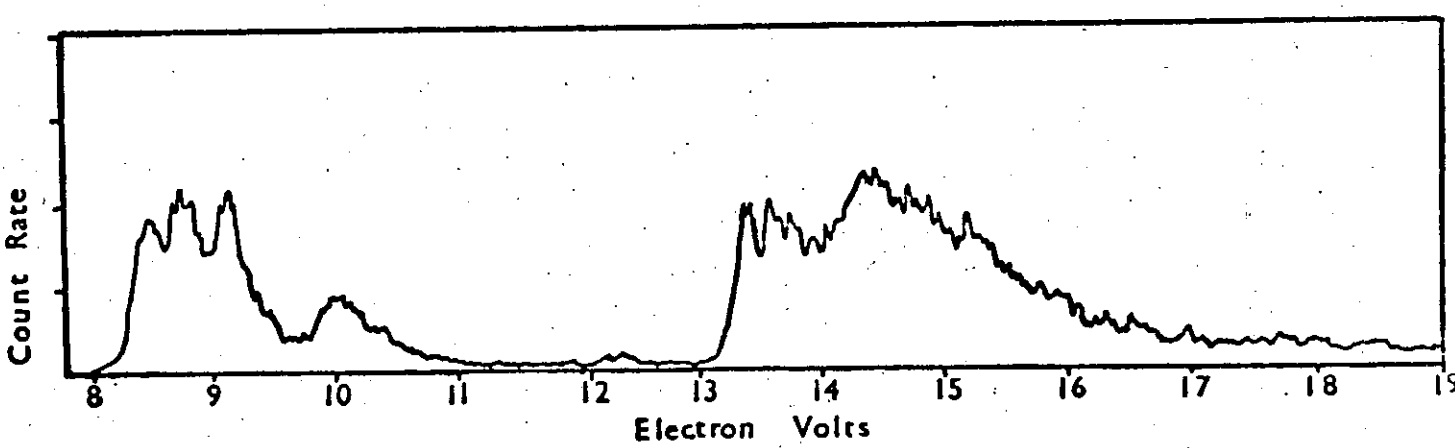

Figure 1.7 Photoelectron spectrum of $HRe(CO)_5$

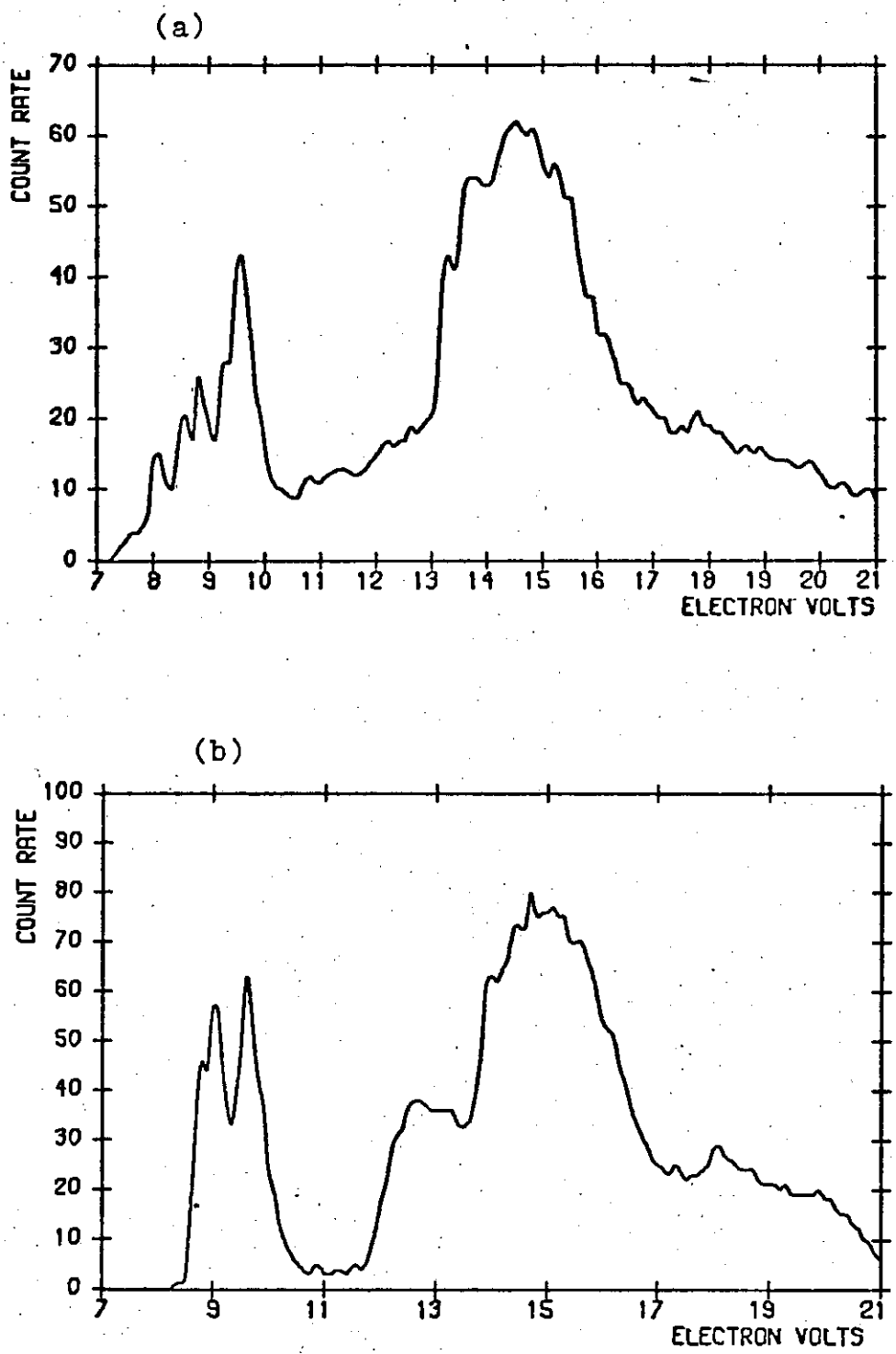

Figure 1.8 Photoelectron spectra of (a) $Re_2(CO)_{10}$ (b) $CH_3Re(CO)_5$

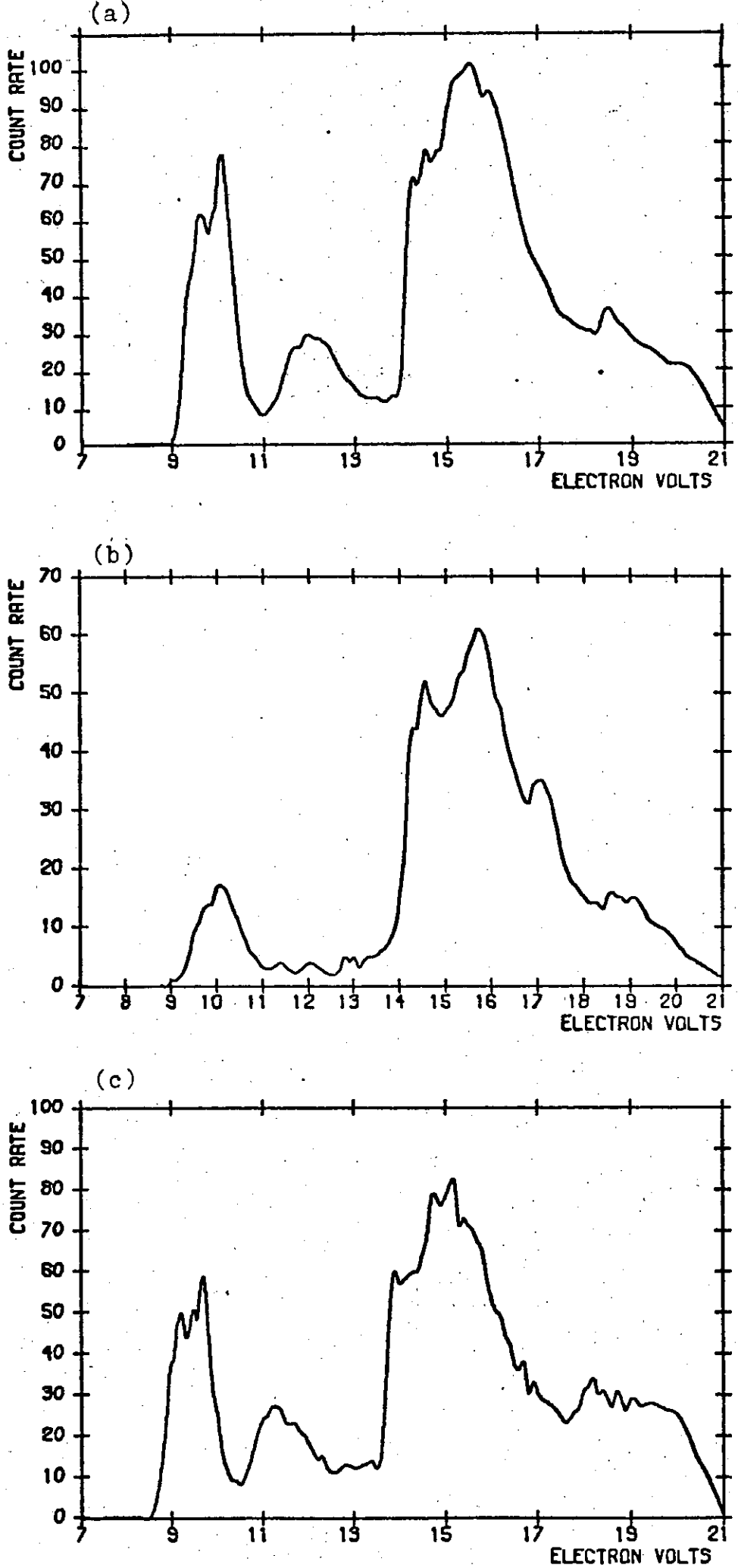

Figure 1.9 Photoelectron spectra of (a) $SiH_3Re(CO)_5$, (b) $SiF_3Re(CO)_5$ and (c) $GeH_3Re(CO)_5$

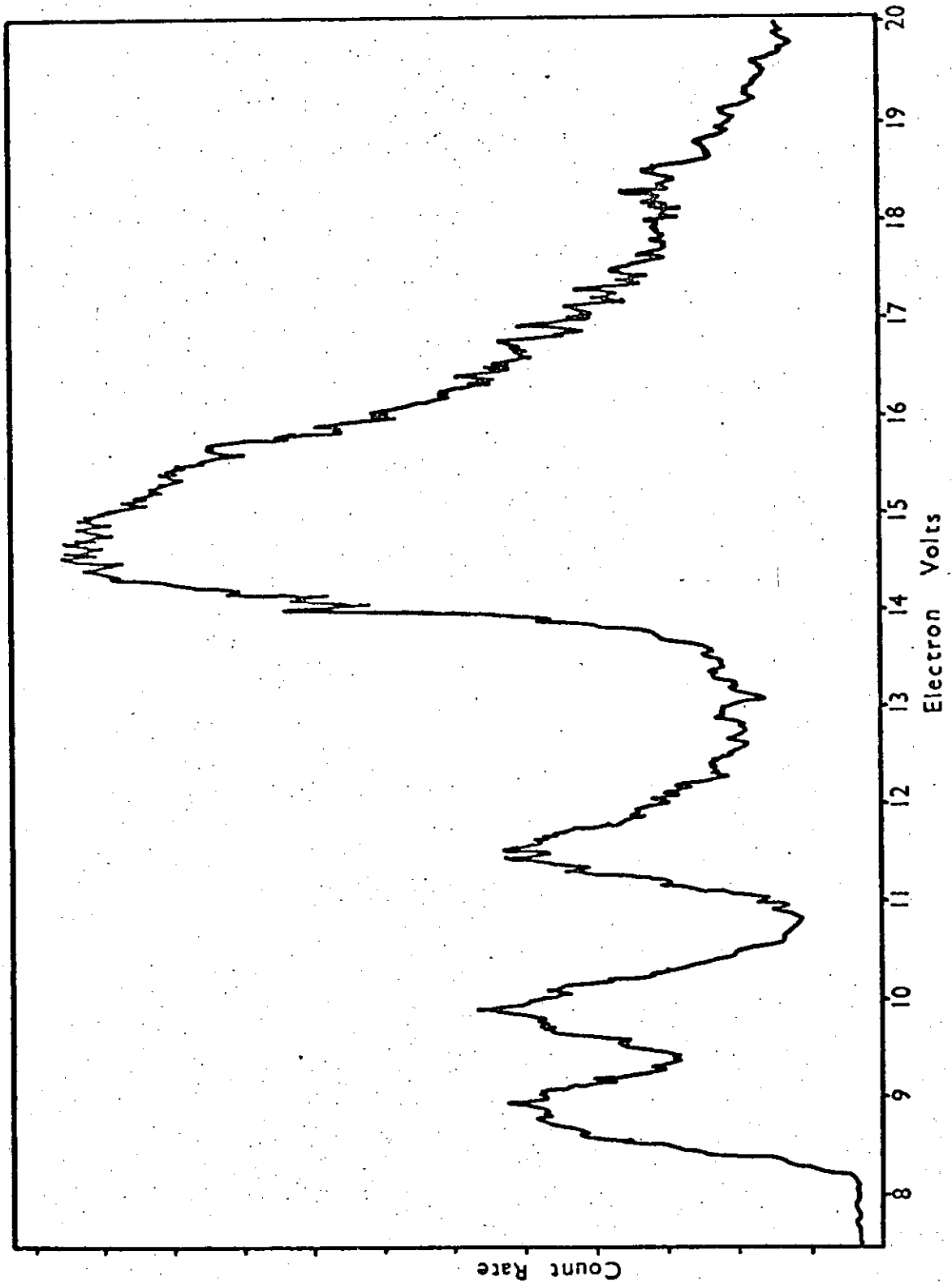

Figure 1.10 Photoelectron spectrum of $HCo(CO)_4$

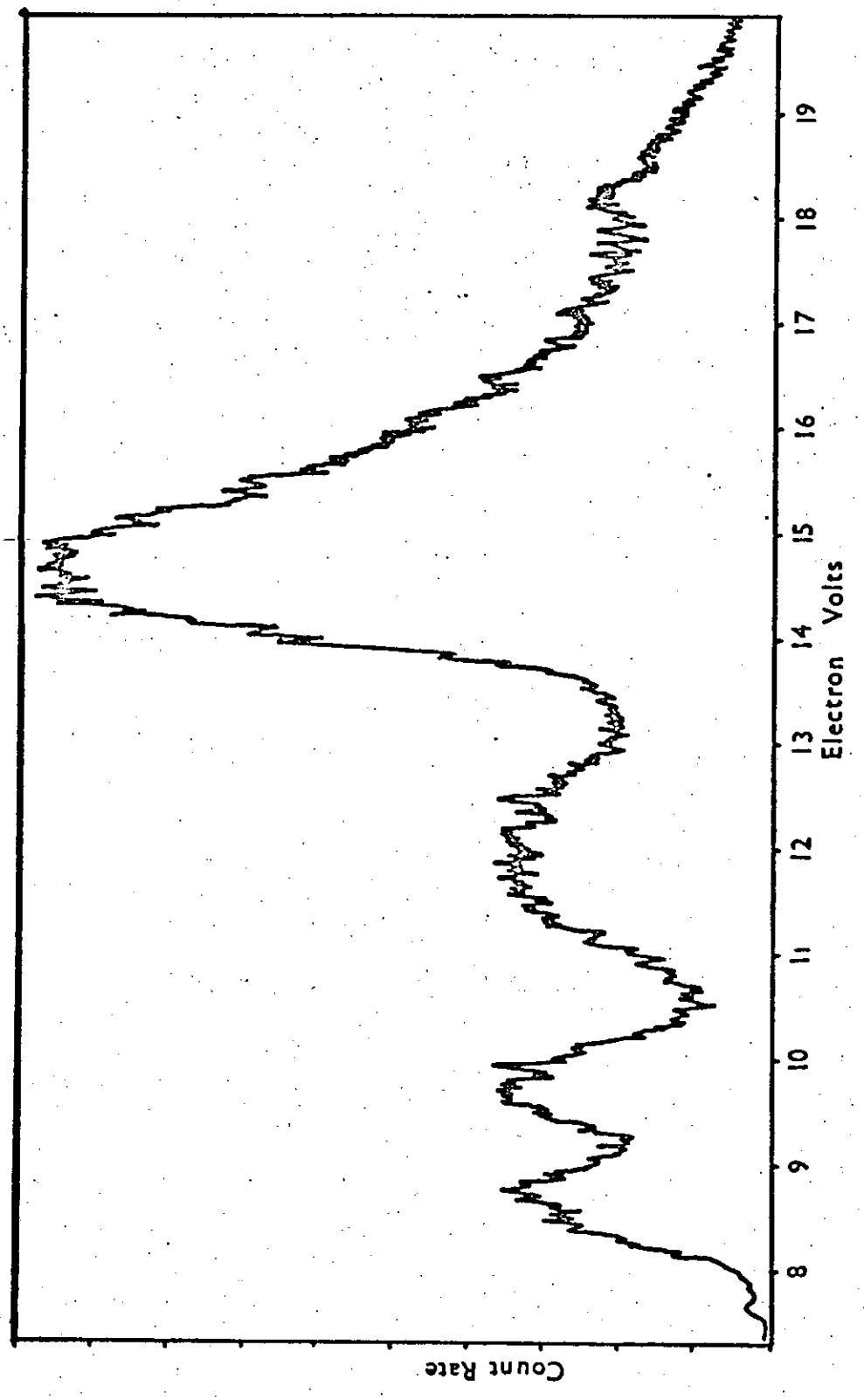

Figure 1.11 Photoelectron spectrum of $SiH_3Co(CO)_4$

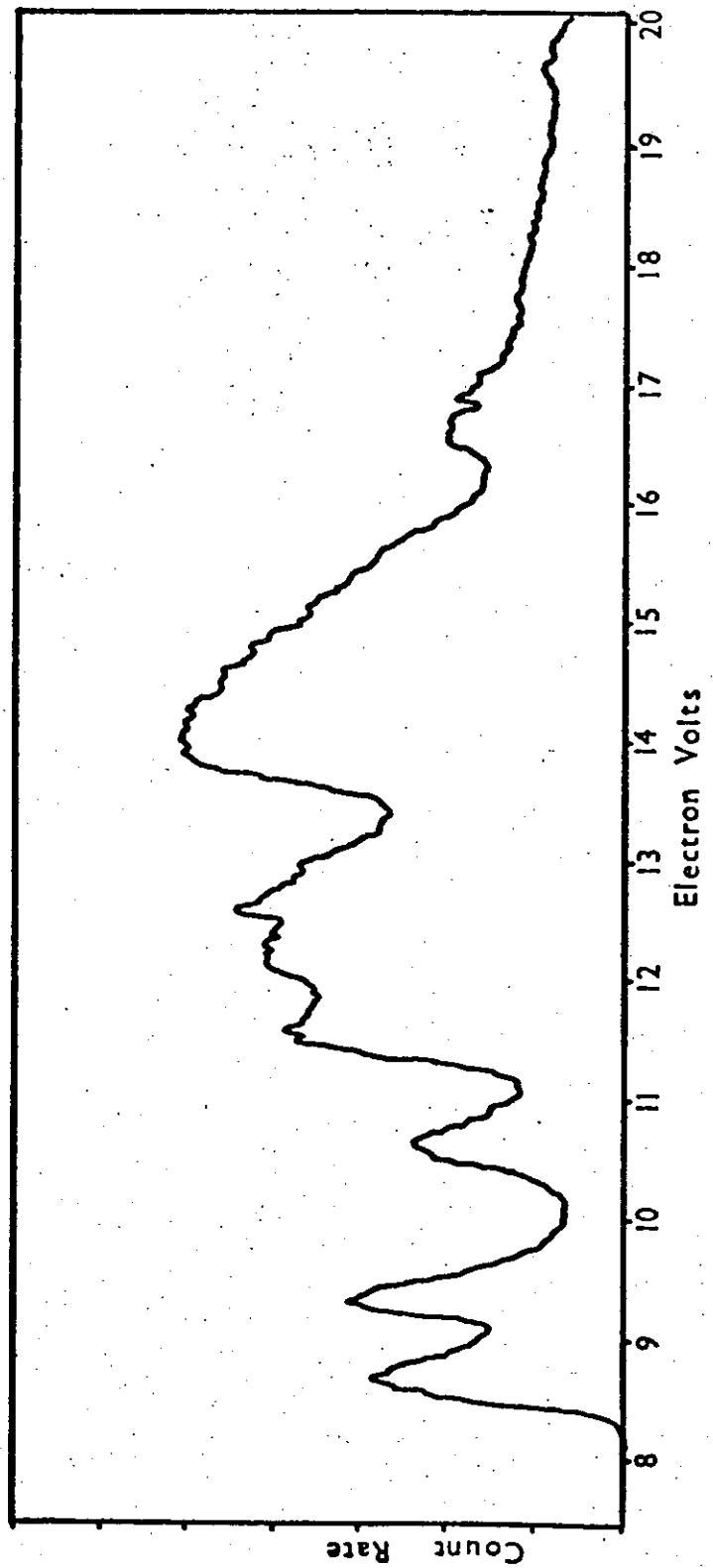

Figure 1.12 Photoelectron spectrum of $SiMe_3Co(CO)_4$

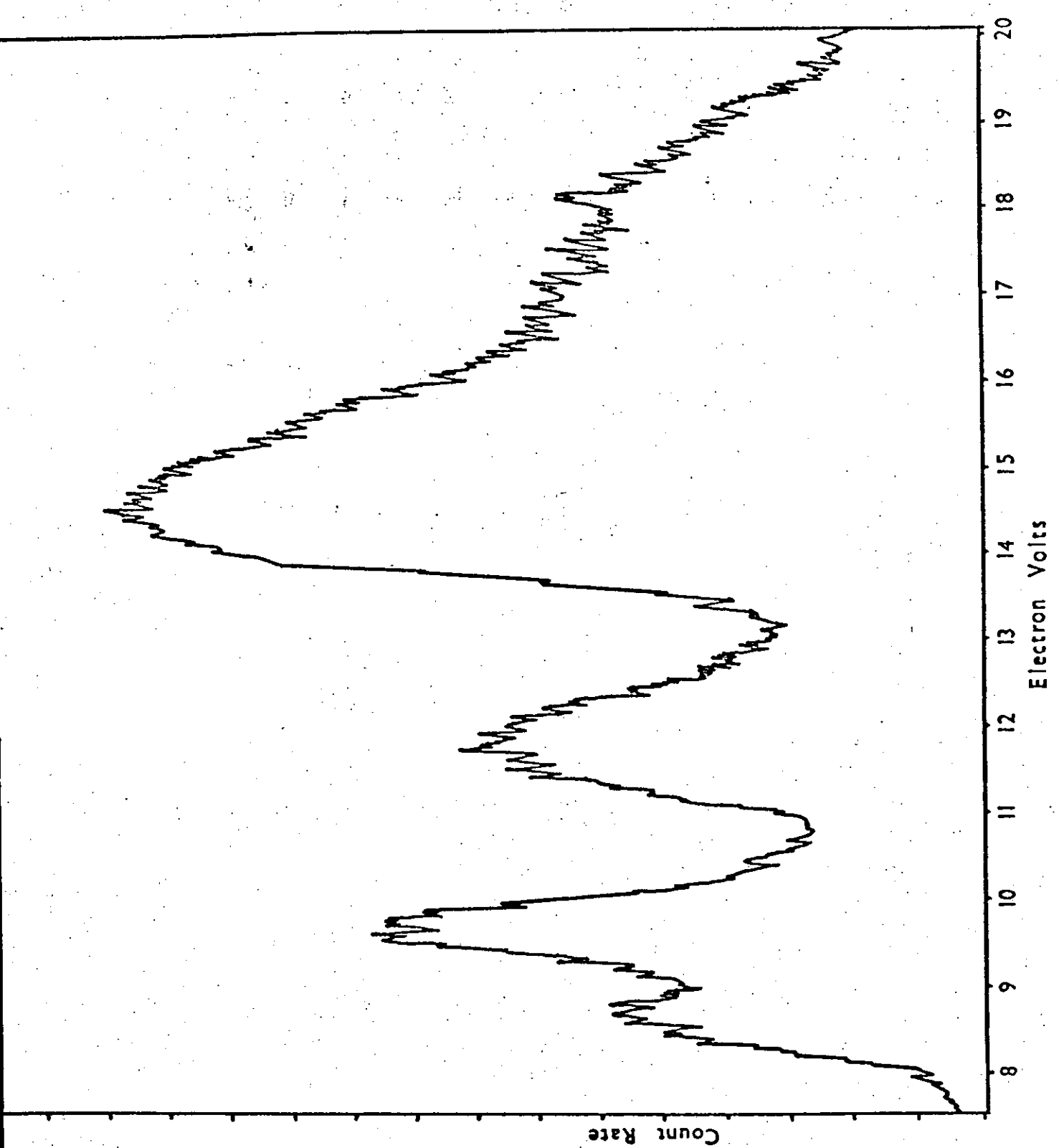

Figure 1.13 Photoelectron spectrum of $GeH_3Co(CO)_4$

Table 1.1 Vertical ionisation potentials and assignments for $LMn(CO)_5$

	IP (e.v.)	assignments
$HMn(CO)_5$		
A	8.85	Mn 3d e
	9.14	Mn 3d b_2
	10.5	Mn-H a_1
B	13.4	Mn-C σ on set
	17	C-O π tail
C	18.0	C-O σ
$CH_3Mn(CO)_5$		
A	8.46, 9.10	Mn 3d e, Mn 3d b_2 and Mn-C a_1
	12.6	C-H
B	13.5	Mn-C σ on set
	17	C-O π tail
C	18.0	C-O σ
$CF_3Mn(CO)_5$		
A	9.20	Mn 3d e, Mn 3d b_2
	10.30	Mn - C a_1
B	13.5	Mn-C σ on set
	17.6	C-O π tail
C	18.5	C-O σ

Table 1.2 Vertical ionisation potentials and assignments for $LMn(CO)_5$

		I.P. (e.v.)	assignment
$SiH_3Mn(CO)_5$	A	8.99, 9.38	Mn 3d e, Mn 3d b_2 and Mn-Si a_1
		11.9	Si-H e
	B	13.7	Mn-C σ on set
		17	C-O π tail
	C	18.0	C-O σ
$SiF_3Mn(CO)_5$	A	9.80	Mn 3d e, Mn 3d b_2
		10.40	Mn-Si a_1
	B	13.9	Mn-C σ on set
		17.6	C-O π tail
	C	18.4	C-O σ
$SiCl_3Mn(CO)_5$	A	9.30, 9.65	Mn 3d e, Mn 3d b_2 and Mn-Si a_1
		11.3, 12.2, 12.9 and 13.7	Si-Cl e and Cl lone pairs

Table 1.2 cont.

B	14.0	Mn-C σ on set
	17	C-O π tail
C	18.3	C-O σ

$SiMe_3Mn(CO)_5$

A	9.0, 9.3	Mn 3d e, Mn 3d b_2 and Mn-Si a_1
	10.8	Si-C e
	13.2	C-H σ
B	13.5	Mn-C σ on set
	17	C-O π tail
C	18.1	C-O σ

Table 1.3 Vertical ionisation potentials and assighments for $LMn(CO)_5$

		I.P (e.v.)	assignment
$GeH_3Mn(CO)_5$			
	A	8.90, 9.26	Mn 3d e, Mn 3d b_2 and Mn-Ge a_1
		11.5	Ge-H e
	B	13.4	Mn-C σ on set
		17	C-O π tail
	C	18.0	C-O σ
$GeMe_3Mn(CO)_5$			
	A	8.7, 9.1	Mn 3d e, Mn 3d b_2 and Mn-Ge a_1
		10.2	Ge-C e
	B	13.6	Mn-C σ on set
		17	C-O π tail
	C	18	C-O σ

Table 1.4 Vertical ionisation potentials[a] and assignments for $LRe(CO)_5$

	$HRe(CO)_5$	assignment	$CH_3Re(CO)_5$	$SiH_3Re(CO)_5$	$SiF_3Re(CO)_5$	$GeH_3Re(CO)_5$	$Re_2(CO)_{10}$	assignment
A	8.86	Re 5d e	8.80	9.1		9.0	8.05	
	9.15		9.03	9.30	9.7	9.18	8.55	Re 5d e, Re 5d b_2
	9.53	Re 5d b_2	9.60	9.57	10.05	9.48	8.86	Re-Ml a_1
	10.5	Re-H a_1		9.75		9.68	9.27, 9.60, 9.92.	
			12.7	11.7	-	11.3	-	Ml-X e
B	13.5		13.7	13.7	14.0	13.6	13.1	Re-Cσ on set
	17		17	17		17.5	17	C-Oπ tail
C			18.0	18.1	19 tail	18.1	17.8	C-Oσ

a, vertical ionisation potentials are given in electron volts

Table 1.5 Vertical ionisation potentials[a] and assignments for $LCo(CO)_4$

	$HCo(CO)_4$	$SiH_3Co(CO)_4$	$SiMe_3Co(CO)_4$	$GeH_3Co(CO)_4$	assignment
A	8.90	8.85	8.7	8.80	Co 3d e,
	9.90	9.90	9.3	9.80	Co 3d e, Co-Ml a_1
	-	11.9	10.6	11.9	Ml-X e
	11.5	-	-	-	Co-H a_1
	-	-	11.3 - 13.3	-	C-H
B	13.8	13.8	13.5	13.5	Co-C σ on set
	17	17	17	17	C-O π tail
C	18.2	18.2	-	18.1	C-O σ

a, vertical ionisation potentials are given in electron volts.

Following Green et al.[46] the spectra are divided into three regions (A from 8 to 13ev, B from 13-17ev and C from 17 to 19ev) for the purposes of assignment and discussion.

The PE spectra of the hydrides give some help in the assignments of peaks in the other PE spectra. The peaks between 8 and 10ev can be assigned to the formally non-bonding, metal d-orbitals and the weaker peak at around 11 ev in each case to the M2-Hσ bonding level. Green et al.[46] only resolved one maximum in the large peak at about 9ev in the PE spectrum of $HMn(CO)_5$ and assigned this peak to the Mn 3d e energy level and the peak at 10.6ev to the Mn 3d b_2 energy level with the Mn-H a_1 bonding level being thought to come in region B of the PE spectrum. However the PE spectra of $HMn(CO)_5$, $HRe(CO)_5$ and $HCo(CO)_4$ run for this thesis all showed more than one maximum at around 9ev and a smaller peak at around 11ev. It therefore seems more reasonable to assign the peak at around 11ev to the Mn-H bonding level and the peaks at around 9ev to the metal d-orbital energy levels. The PE spectra of the $M1H_3$ derivatives are superficially similar so, by analogy, the peaks at around 9ev must be due, at least in part to the metal d-orbitals. Also with $M1H_3$ derivatives there are two energy levels arising from the M1-H σ bonds. By comparison with other $M1H_3$ derivatives the energy level of symmetry species a_1 would be expected to come in region C or even higher I.P. in the PE spectra whereas those of symmetry species e would be expected at much lower ionisation potential. In methyl halides the C-H e levels come at about 15ev and in silyl and germyl halides the corresponding levels come at about 13ev. Furthermore as the electronegativity of the group bound to M1 decreases so does the ionisation potential of the M1-H e bonding level The assignment of the broad peak at about 12ev in all the PE spectra of the $M1H_3$ derivatives described here to the

M1-H e bonding level is consistent with the above observations. Further comparison of $M1H_3$ derivatives and hydrides indicates that the binding energy of the M2-H a_1 bonding level will be about 2ev greater than the corresponding M1-M2 a_1 bonding level. This means that, in most cases, the M1-M2 bonding level will lie amongst the formally non-bonding metal d levels. Molecular orbital calculations and PE spectra of both $CH_3Mn(CO)_5$ and $CF_3Mn(CO)_5$ indicate that, in both cases electrons in the Mn-C σ bonding energy level and those in the Mn 3d e and b_2 energy levels have similar binding energies.[50,51,52] The same has been said about electrons in the Mn-X σ bond (X = halogen) and the Mn 3d e and b_2 levels in the series $XMn(CO)_5$.[47, 48, 49.]

With SiF_3 derivatives the Si-F a_1 and e bonding levels and the levels due to the fluorine lone pairs lie in region B or at higher ionisation potential and hence cannot easily be distinguished in these PE spectra. However in the PE spectrum of $Cl_3SiMn(CO)_5$ peaks at 11.3, 12.2, 12.9 and 13.7 ev can be assigned to the Si-Cl e bonding level and the chlorine lone pair levels; the Si-Cl a_1 bonding level probably lies in region B and cannot be seen.

In the PE spectrum of $Me_3GeMn(CO)_5$ there is a peak at 10.2 ev which can reasonably be assigned to the Ge-C e bonding level. Here the Ge-C a_1 bonding level will lie in region B or at higher ionisation potential. The peak at 10.6 ev in the PE spectrum of $Me_3Si(CO)_4$ is assigned to the Si-C e bonding level. The series of peaks between 11.4 and 13.6 ev in that spectrum appears to be due to C-H bonding levels.

If region A of the PE spectra of the series $M1H_3Mn(CO)_5$ is now considered (M1=C, Si, Ge) it can be seen that in each spectrum there are two peaks in this region, the peak at higher ionisation potential always being more intense than that at lower ionisation potential. From the general assignments made earlier it would appear that there are

three energy levels (Mn 3d e , Mn 3d b_2 and Mn-Ml a_1) to assign to these two peaks. Peak intensities indicate that in each case the peak at higher ionisation potential is due, at least in part, to the Mn 3d e level but it is impossible to assign specifically either the Mn 3d b_2 or Mn-Ml a_1 energy levels as there is insufficient evidence for such an assignment.

Peaks in the PE spectrum of $CH_3Mn(CO)_5$ at 8.46 ev and 9.10 ev have been assigned by Greenet al.[46] to the Mn 3d e and b_2 levels respectively. However, with evidence from the PE spectra of $HMn(CO)_5$, $SiH_3Mn(CO)_5$ and $GeH_3Mn(CO)_5$ that the Mn-C a_1 bonding level also lies in this region, these assignments seem unjustifiable. In the P.E. spectra of $SiCl_3Mn(CO)_5$, $SiMe_3Mn(CO)_5$ and $GeMe_3Mn(CO)_5$ there is only a single broad peak at about 9ev and it would appear that all three energy levels (Mn 3d e and b_2 levels and the Mn-Ml a_1 bonding level) lie under this peak.
In the P.E. spectrum of $SiF_3Mn(CO)_5$ there are two peaks in this region: a large broad peak at 9.80 ev and a smaller peak at 10.40 ev. Substitutionof fluorines for hydrogens in SiH_3Cl shifts the Si-Cl a_1 bonding level from 13.4 ev in SiH_3Cl to 15.33 ev in SiF_3Cl. In organic molecules with planar skeletons a perfluoro effect is observed; substitution of fluorine for hydrogen has a much larger stabilising effect on the σ molecular orbitals than the π molecular orbitals.[73] The assignment of the peak at 9.80 to the Mn 3d e and b_2 energy levels and the peak at 10.40 ev to the Mn-Si a_1 bonding level in the PE spectrum of $SiF_3Mn(CO)_5$ is consistent with both the above observations. The PE spectrum of $CF_3Mn(CO)_5$ is similar to that of $SiF_3Mn(CO)_5$ and the differences between the PE spectra of $CH_3Mn(CO)_5$ and $CF_3Mn(CO)_5$ are similar to the differences between the PE spectra of $SiH_3Mn(CO)_5$ and $SiF_3Mn(CO)_5$. It therefore seems reasonable to assign the peaks in region A of the PE spectra of $CF_3Mn(CO)_5$

in a similar manner to those in $SiF_3Mn(CO)_5$, the peak at 9.20 ev is due to the Mn 3d e and b_2 levels and the peak at 10.30 ev to the Mn - C a_1 bonding level. This is contrary to both previous published assignments for the PE spectrum of $CF_3Mn(CO)_5$; Green et al.[46] assigned the peak at 9.20 ev to the Mn 3d e energy level and the peak at 10.30 ev to the Mn 3d b_2 energy level while, more recently, the peak at 9.20 ev was assigned to the Mn 3d e and the Mn - C a_1 energy levels and the peak at 10.30 ev to the Mn 3d b_2 energy level. The assignment of the large peak at 9.20 ev to the Mn 3d e and b_2 energy levels and the peak at 10.30 ev to the Mn - C a_1 bonding level does seem more reasonable as fluorination of the methyl group bound to a manganesepentacarbonyl group would be expected to affect the energy of the Mn - C a_1 more than the Mn 3d b_2 level, especially if the "perfluoro effect" holds.

The photoelectron spectra of pentacarbonylrhenium derivatives are similar to those of the pentacarbonyl-manganese derivatives but are affected by spin-orbit coupling. The spin-orbit coupling parameter, ξ_{5d}, for Re is about 0.3 ev whereas ξ_{3d} for Mn is of the order of 0.03 ev. This explains the appearance of four peaks in region A of the PE spectrum of $HRe(CO)_5$ while in this region of the PE spectrum of $HMn(CO)_5$ there are only three peaks; the fourth peak in the former case is probably caused by spin-orbit coupling in the ^2E state of $HRe(CO)_5^+$. The first ionisation potential of atomic rhenium is 0.44 ev higher than that of atomic manganese. This indicates that the peak at 9.53 ev in the PE spectrum of $HRe(CO)_5$ is due to the Re 5d b_2 energy level and the peak at 9.14 ev in the PE spectrum of $HMn(CO)_5$ is due to the Mn 3d b_2 energy level. In region A of the PE spectrum of $HRe(CO)_5$ this leaves a doublet and 8.86 and 9.15 ev to be assigned and, in the same region of the PE spectrum of $HMn(CO)_5$, a single peak at

8.85 ev remains to be assigned. The doublet in the PE spectrum of $HRe(CO)_5$ can be reasonably assigned to the Re 5d e energy level, split by spin-orbit coupling and the single peak in the PE spectrum of $HMn(CO)_5$ can then be assigned to the Mn 3d e energy level.

The photelectron spectra of $CH_3Re(CO)_5$, $SiH_3Re(CO)_5$, $SiF_3Re(CO)_5$ and $GeH_3Re(CO)_5$ are less clearly defined in region A than is the PE spectrum of $HRe(CO)_5$ since the Re - Ml a_1 bonding level lies in this region. In the MlH_3 derivatives spectra three maxima can be distinguished in region A and, where Ml = Ge, an extra shoulder can be distinguished at low ionisation potential. In the PE spectrum of $SiF_3Re(CO)_5$ a broad hump is observed in the region between 9 and 11 ev. The maximum is at about 10.0 ev but there is little structure to this peak. Little justification could be given for any particular assignments made for these peaks. Doublets, of separation just under 0.3 ev could be due to ionisation from the Re 5d e level but, other than this, little else can be logically assigned with no help being derived from peak intensities as all energy levels in this region are non-degenerate as a result of spin-orbit coupling. The photoelectron spectrum of $Re_2(CO)_{10}$ was also run, largely as a check on the purity of the sample of SiF_3-$Re(CO)_5$. Predictably this spectrum was very complex with six maxima being observed in region A. It is possible to account for 6 bands in this region but no assignments can be made. If a $Re(CO)_5$ group is considered separately it can be seen that the formally non-bonding Re 5d levels will be split into two energy levels of symmetry species e and b_2; the e level will be further split by spin-orbit coupling giving three energy levels. If the two $Re(CO)_5$ groups are considered together this number of energy levels will be doubled and, as the Re - Re a_1 bonding level will also lie in this region, there

are a total of 7 energy levels to assign to the six peaks observed.

The PE spectrum of $HCo(CO)_4$, in region A, shows peaks at 8.90, 9.90 and 11.5 ev. The first two peaks are assigned to the two Co 3d e levels and the last the Co-H a_1 bonding level.

The patterns of peaks observed in the PE spectra of $SiH_3Co(CO)_4$ and $GeH_3Co(CO)_4$ are similar to that observed in $HCo(CO)_4$ though for the germyl compound the peak at lowest binding energy is of lower intensity than that adjacent to it. These peaks, as in the hydrides, are probably due to the Co 3d e energy levels but here they probably conceal the Co-Ml a_1 bonding level. In the PE spectra of both the silyl- and germyl- compounds the Ml-H e bonding level can be assigned to a broad peak just below 12 ev. The PE spectrum of $Me_3SiCo(CO)_4$ is slightly different from that of $SiH_3Co(CO)_4$. The two peaks at lowest ionisation potential are only 0.65 ev apart, compared with 1.0 ev in the PE spectrum of $SiH_3Co(CO)_4$, there is a peak at 10.6 ev and a series of peaks from 11.4 ev to 13.0 ev is also present. The two peaks at low binding energy are again assigned to the Co 3d e energy levels with the Co - Si a_1 bonding level being concealed, the peak at 10.6 ev is assigned to the Si - C e bonding level and the peaks from 11.4 ev to 13.0 ev are assigned to some of the C - H bonding levels. (It is possible that the maximum at 11.4 ev is due to a trace of $HCo(CO)_4$ impurity). It is seen that the Si - C e bonding level is very much closer in energy to the Co 3d e levels in $Me_3SiCo(CO)_4$ than the Si-H e bonding level in $H_3SiCo(CO)_4$ is to the Co 3d e levels and therefore interaction between the Si-C e bonding level and the Co 3d e levels in $SiH_3Co(CO)_4$ is likely. Such interaction would explain the small difference in energy between the two Co 3d e energy levels.

In none of the above PE spectra could any reasonable attempt be made to assign peaks in regions B and C due to the complexity of these regions of the spectra and the large number of energy levels in the molecules.

1.4 Discussion.

Recent work on the PE spectra of and molecular orbital calculations for pentacarbonylmanganese halides[47, 48, 49] and methyl- and trifluormethyl-pentacarbonyl- manganese [50, 51, 52] has led to criticisms of the assighments of the PE spectra of the above compounds made by Green et al[46]. In each case the main criticism is the assignment of the Mn-X (X = Cl,Br,I,C) a_1 bonding level to region B of the PE spectrum. These recent papers stated that the peak in the PE spectrum due to excitation of electrons from the Mn-X a_1 bonding level lay in region A of the PE spectrum, generally close to the Mn 3d energy levels. The PE spectra obtained for this thesis are consistent with these recent criticisms in that the M1 - M2 a_1 bonding level (M1 = H, C, Si, Ge; M2 = Mn, Co, Re) is always assigned to region A of the PE spectrum.

Since any difference in energy between either Mn 3d e and Mn 3d b_2 energy levels or Re 5d e and Re 5d b_2 cannot be determined from the photoelectron spectra of the series $LMn(CO)_5$ (L = CH_3, CF_3, SiH_3, $SiCl_3$, SiF_3, $SiMe_3$, GeH_3, $GeMe_3$) and $LRe(CO)_5$ (L = CH_3, SiH_3, SiF_3, GeH_3) these spectra do not shed much light as to the importance, or otherwise, of $(d\rightarrow d)\pi$ bonding in the metal-metal bonds of the silyl and germyl derivatives.

However the differences which arise in the PE spectra of methyl-, silyl- and germyl- transition metal carbonyls can be explained without invoking $(d\rightarrow d)\pi$ interactions between the transition metal and silicon or germanium atoms. If the PE spectra of the series, $CH_3Mn(CO)_5$,

$GeH_3Mn(CO)_5$ and $SiH_3Mn(CO)_5$ are considered it is seen that the group of peaks in region A of the spectra, assigned to the Mn 3d e and b_2 levels and the Mn-Ml a_1 bonding level, moves to higher binding energy as one moves along the series $CH_3 \ll GeH_3 < SiH_3$. This indicates that the positive charge on manganese is increasing in that order. A possible explanation is that the σ acceptor properties of the substituents increase in the order $CH_3 \ll GeH_3 < SiH_3$. This is different from the generally accepted order of $SiH_3 \approx GeH_3 < CH_3$. Such shifts in π orbitals on atoms adjacent to silicon or germanium have previously been attributed to interactions with the empty d energy levels on the silicon or germanium atoms but the shift of the Mn 3d b_2 energy level to lower energy on substitution of methyl- by germyl- or silyl- on the $Mn(CO)_5$ group appears to preclude this type of π interaction as a major factor in these metal-metal bonds. Also, the Mn-Si bonding level is apparently shifted much more in energy than the Mn 3d e and b_2 levels on fluorination of the silyl- group of silylmanganesepentacarbonyl and this indicates that $(d \rightarrow d)\pi$ interaction is unimportant in the Mn-Si bond: what determines the ionisation potential of the metal-metal σ bonding level and the Mn 3d levels in these compounds is the σ acceptor power of the substituents. The PE spectra of the series $X_3SiMn(CO)_5$ (X = H,Me,Cl,F) are also consistent with the hypothesis that it is the σ acceptor power of the substituent which determines the position of the peaks in region A of their PE spectra. An order of σ acceptor power of these groups from these PE spectra is $SiMe_3 \approx SiH_3 < SiCl_3 < SiF_3$ and this is similar to the expected order from electronegativities. The PE spectra of the Group IVB derivatives of tetracarbonylcobalt and pentacarbonylrhenium studied are consistent with the above hypothesis. Another indication of the relative unimportance of $(d \rightarrow d)\pi$ bonding in these com-

pounds is the general similarity of the PE spectra of methyl- and germyl- or silyl- transition metal carbonyl complexes.

It is emphasised that the above is just a hypothesis and definitely not a proof of the absence of (d⟶d)π bonding in these compounds. The general shift upwards in energy of the Mn-C_{met} a_1 bonding level and Mn 3d e and b_2 energy levels in $CH_3Mn(CO)_5$ relative to the corresponding levels in $SiH_3Mn(CO)_5$ could be due to the $(CH_3Mn(CO)_5)^+$ ion being more stable than the $(SiH_3Mn(CO)_5)^+$ ion, possibly because the shorter Mn-C_{met} bond leads to an increase in electron densityround the manganese atom. Other explanations of trends in the afore-mentioned spectra may, of course, be hidden by the breakdown of Koopmans' Theorem.

The photoelectron spectra described in this chapter also indicate that, at present, PE spectroscopy is not a particularly helpful tool for determining the relative positions of electronic energy levels in molecules as complex as those studied here.

CHAPTER TWO

Electron Diffraction Determination of the Molecular Structures of silyl-, trifluorosilyl- and germyl- manganesepentacarbonyl and germylcobalttetracarbonyl in the gas Phase

CHAPTER 2

2.1 Introduction

Gas phase electron diffraction data were taken for silylmanganesepentacarbonyl, germylmanganesepentacarbonyl and germylcobalttetracarbonyl on a Balzer's KD.G2 gas diffraction apparatus at the University of Manchester Institute of Science and Technology.[74] Data were taken for trifluorosilylmanganesepentacarbonyl on a Balzer's KD.G2 Eldigraph at Oslo[76, 77]. These samples were prepared as described in chapter 6. Details of the nozzle to plate distances, sample temperatures and nozzle temperatures are given in table 2.1.

Data analyses for silyl- and germyl- manganesepentacarbonyl and germylcobalttetracarbonyl were carried out as described in chapter 6. For trifluorosilylmanganesepentacarbonyl data were reduced to uphill curves on a CDC3300 computer using established programs[78]. Subsequent data analysis was carried out as described in chapter 6.

Shrinkage corrections applied to the manganesepentacarbonyl derivatives were those applied to pentacarbonyl-(trifluorophospine)molybdenum[79] as these were believed to be a reasonable approximation. Shrinkage corrections applied to germylcobalttetracarbonyl were adapted from those calculated for ironpentacarbonyl[80]. The complex scattering factors of Cox and Bonham[81] were used.

2.2 Molecular Structure of Silylmanganesepentacarbonyl

The weighting points (used to set up the off diagonal weight matrix), correlation parameters and scale factors are shown in table 2.2.

Table 2.1 Nozzle heights, sample and nozzle temperatures.

compound	nozzle height (mm)	sample temperature(K)	nozzle temperature(K)
$SiH_3Mn(CO)_5$	250	323	333
	500		
	1000		
$GeH_3Mn(CO)_5$	250	328	333
	500		
	1000		
$SiF_3Mn(CO)_5$	190	338	348
	580	334	343
$GeH_3Co(CO)_4$	250	313	328
	500		
	1000		

The molecular model used for the purposes of the least squares refinements assumed: 1) the manganesepentacarbonyl group had local $C_{4}v$ symmetry, 2) the silyl group had local $C_{3}v$ symmetry, 3) all carbon-oxygen and carbon-manganese distances were equal, and 4) free rotation about the manganese-silicon bond since there is a twelve-fold barrier to rotation about this bond. These assumptions allowed the molecule to be described using the four bonded distances and the following angles: $H\text{-}\hat{Si}\text{-}H$, $C_{eq}\text{-}\hat{Mn}\text{-}C_{ax}$ and $Mn\text{-}\hat{C}_{eq}\text{-}O_{eq}$.

The assumption that the manganese-carbon distances are all equal might have proved unjustified but it is unlikely that the difference is greater than 4pm (as in methylmanganesepentacarbonyl) and it may be nearer 2pm (as in manganesepentacarbonylhydride). Such small differences within a molecule are difficult to determine using electron diffraction. There is no evidence for any asymmetry in the Mn-C peak in the radial distribution curve nor are the Mn-C or Mn...O amplitudes of vibration significantly greater than values found in other manganesepentacarbonyl derivatives.

In the least squares refinements the Si-Mn, Mn-C and C-O bonded distances and their amplitudes of vibration all refined satisfactorily as did the $Mn\text{-}C_{eq}\text{-}O_{eq}$ and $C_{ax}\text{-}Mn\text{-}C_{eq}$ angles. The overlapping of large numbers of peaks in the radial distribution curve (figure 2.1) necessitated the refinement of groups of amplitudes of vibration as single parameters (see table 2.3). Most groups other than those involving hydrogen atoms refined satisfactorily; the amplitudes of vibration of $Si...C_{ax}$ and $Si...O_{ax}$ non-bonded distances being the only exceptions. These amplitudes, along with all parameters involving hydrogen, were set at reasonable values.

The final R- factor (R_G) was 0.16. The molecular para-

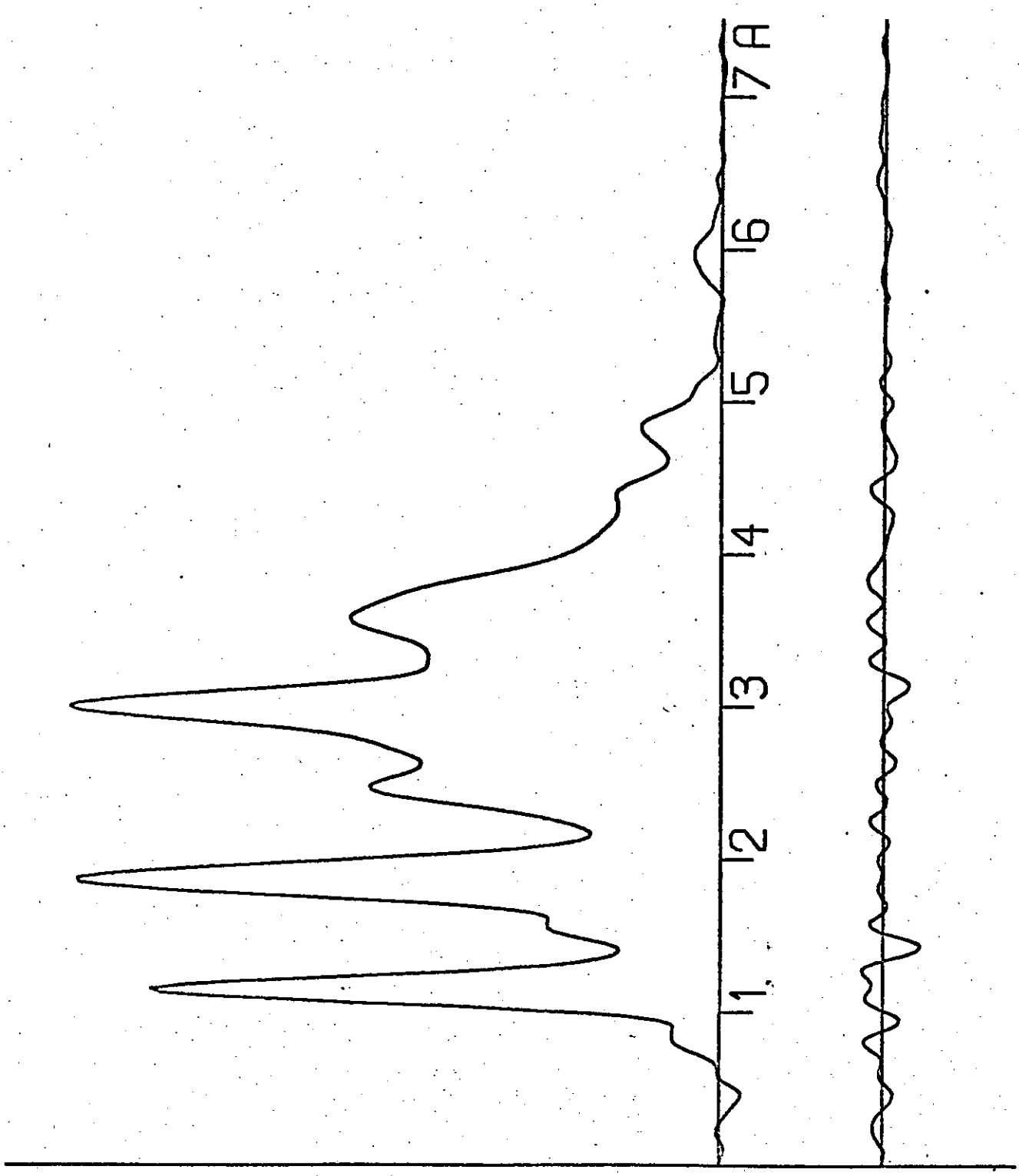

Figure 2.1 Radial distribution curve, P(r)/r, and final deviations between experimental and theoretical curves for $SiH_3Mn(CO)_5$. Before Fourier inversion the data were multiplied by s. $\exp((-0.000025s^2)/(z_{Mn}-f_{Mn})(z_O-f_O))$

Table 2.2 Weighting points for Silylmanganesepentacarbonyl

Nozzle Height (mm)	$dels_1$ (nm^{-1})	s_{min}	s_1	s_2	s_{max}	$P/_h$	Scale Factors
250	4	68	108	250	280	0.4448	1.056 ± 0.038
500	2	36	60	135	155	0.4763	1.168 ± 0.029
1000	1	10	17.5	62.5	70	0.4920	0.900 ± 0.047

Table 2.3 Molecular Parameters for $SiH_3Mn(CO)_5$

	Distance	Amplitude	Shrinkage Correction
a Independent distances			
r_1 (C-O)	113.2 (0.3)	4.2 (0.8)	
r_2 (Mn-C)	184.7 (0.2)	7.5 (0.6)	
r_3 (Mn-Si)	240.7 (0.5)	7.4 (0.9)	
r_4 (Si-H)	149.0 (fixed)	8.45 (fixed)	
b Dependent distances			
d_5 ($Mn...O_{ax}$)	297.4 (1.0)	8.2 (0.6)	0.59
d_6 ($Mn...O_{eq}$)	297.4 (1.0)		0.59
d_7 ($C_{eq}...O_{eq}$)	474.2 (1.7)	11.5 (1.4)	2.27
d_8 ($O_{eq}...O_{eq}$)	590.6 (2.0)		3.42
d_9 ($C_{eq}...C_{eq}$)	367.0 (1.1)		1.33
d_{10} ($C_{eq}...C_{eq}$)	271.2 (0.6)	10.7 (1.4)	0.25
d_{11} ($C_{eq}...C_{ax}$)	260.1 (0.7)		0.25
d_{12} ($O_{eq}...O_{eq}$)	436.0 (0.7)	28.7 (3.6)	1.40
d_{13} ($O_{eq}...O_{ax}$)	418.6 (1.4)		1.40
d_{14} ($C_{eq}...O_{eq}$)	362.0 (0.7)		0.82
d_{15} ($C_{ax}...O_{eq}$)	362.0 (0.7)	18.4 (0.9)	0.82
d_{16} ($C_{eq}...O_{ax}$)	348.8 (1.0)		0.82

Table 2.3 cont.

d_{17} ($Si...C_{ax}$)	424.0 (1.1)	19.4	1.43
d_{18} ($Si...O_{ax}$)	536.3 (1.5)	21.7	2.38
d_{19} ($Si...C_{eq}$)	291.3 (1.4)	25.0 (fixed)	0.28
d_{20} ($Si...O_{eq}$)	367.0 (1.8)	36.0	0.90
d_{21} (H...Mn)	322.9 (0.9)	12.0 (fixed)	0.59
d_{22} ($H...C_{ax}$)	494.3 (1.1)	15.0 (fixed)	2.27
d_{23} ($H...O_{ax}$)	602.6 (1.8)	18.0 (fixed)	3.42
d_{24} (H...H)	242.4 (0.2)	10.0 (fixed)	0.07
($H...C_{eq}$)	Between 242.4 and 423.4		
($H...O_{eq}$)	Between 313.7 and 508.5		

c Independent angles

$\angle 1$ (H-Si-H)	110° (fixed)
$\angle 2$ (C_{ax}-Mn-C_{eq})	94.5° (2°)
$\angle 3$ (Mn-C_{eq}-O_{eq})	180° (fixed)

Table 2.4

Least squares correlation matrix multiplied by 1000 for $SiH_3Mn(CO)_5$

R1	R2	R3	<2	U1	U2	U3	U5	U7	U10	U12	U14	U17	K1	K2	K3
1000	-23	-114	-635	11	70	6	71	19	60	77	108	30	27	142	84
	1000	-15	-481	9	33	-11	38	2	19	20	-79	52	46	-7	-30
		1000	47	-33	-94	195	53	-57	272	23	-18	1	-49	-97	-40
			1000	-78	-141	16	-87	-6	50	-150	-268	-19	-145	-169	-30
				1000	459	109	374	124	-69	16	188	1	586	438	52
					1000	39	467	152	-113	17	230	0	682	589	104
						1000	228	39	542	28	1	0	195	123	-52
							1000	146	258	19	59	7	602	502	104
								1000	-23	472	3	-422	188	199	86
									1000	22	-170	11	-106	-116	-16
										1000	167	-756	33	12	-25
											1000	-137	292	260	-56
												1000	14	-27	-74
													1000	572	72
														1000	52
															1000

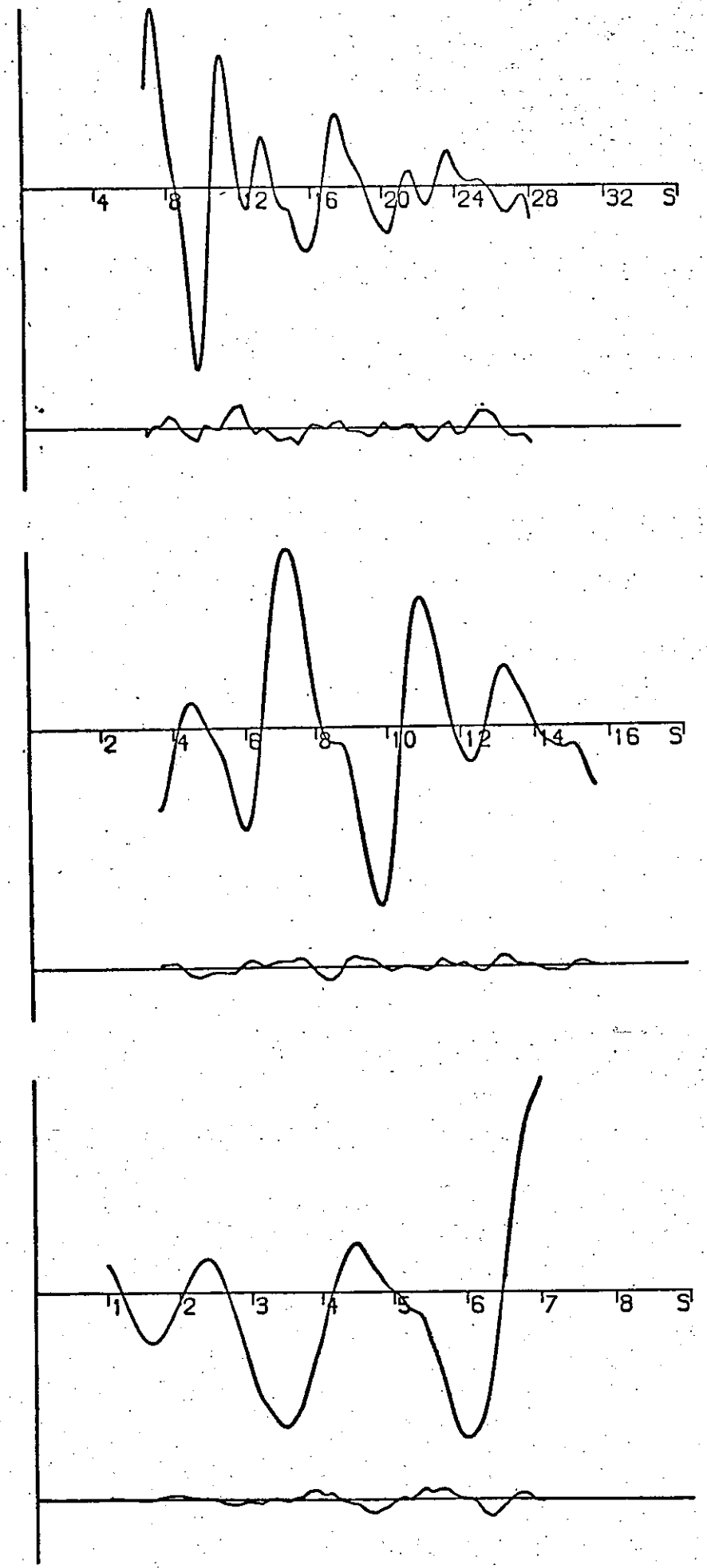

Figure 2.2 Observed and final weighted difference molecular intensities for $SiH_3Mn(CO)_5$ for data sets obtained with nozzle to plate distances of 250, 500 and 1000mm.

meters are shown in table 2.3 and the final least squares correlation matrix in table 2.4. The observed and final weighted difference molecular intensity curves are shown in figure 2.2.

2.3 Molecular Structure of Germylmanganese-pentacarbonyl

Weighting points (used to set up the off diagonal weight matrix), correlation parameters and scale factors are shown in table 2.5.

The molecular model used was the same as that used for silylmanganesepentacarbonyl. Here also the assumption that all manganese-carbon distances were equal may have proved unjustified. However, any difference would be of the same order of magnitude as that in silylmanganese-pentacarbonyl and there is neither evidence of any asymmetry in the Mn-C peak in the radial distribution curve (figure 2.3.) nor of the amplitudes of vibration of the Mn-C or Mn...O distances being significantly greater than values in other manganesepentacarbonyl derivatives.

Refinements were similar to those in silylmanganese-pentacarbonyl. The Mn-Ge, Mn-C and C-O bonded distances and their amplitudes of vibration all refined satisfactorily along with the $Mn-C_{eq}-O_{eq}$ and $C_{eq}-Mn-C_{ax}$ angles. Here also there is overlapping of peaks in the radial distribution curve (figure 2.3) so groups of vibrational amplitudes were constrained to refine as single parameters (see table 2.6). Amplitudes of vibration involving right-angled C...C, C...O and O...O distances did not refine nor did any parameters involving hydrogen atoms. All non-refining parameters were set at typical values.

The final R-factor(R_G) was 0.13. Table 2.6 shows molecular parameters for germylmanganesepentacarbonyl and the final least squares correlation matrix is shown

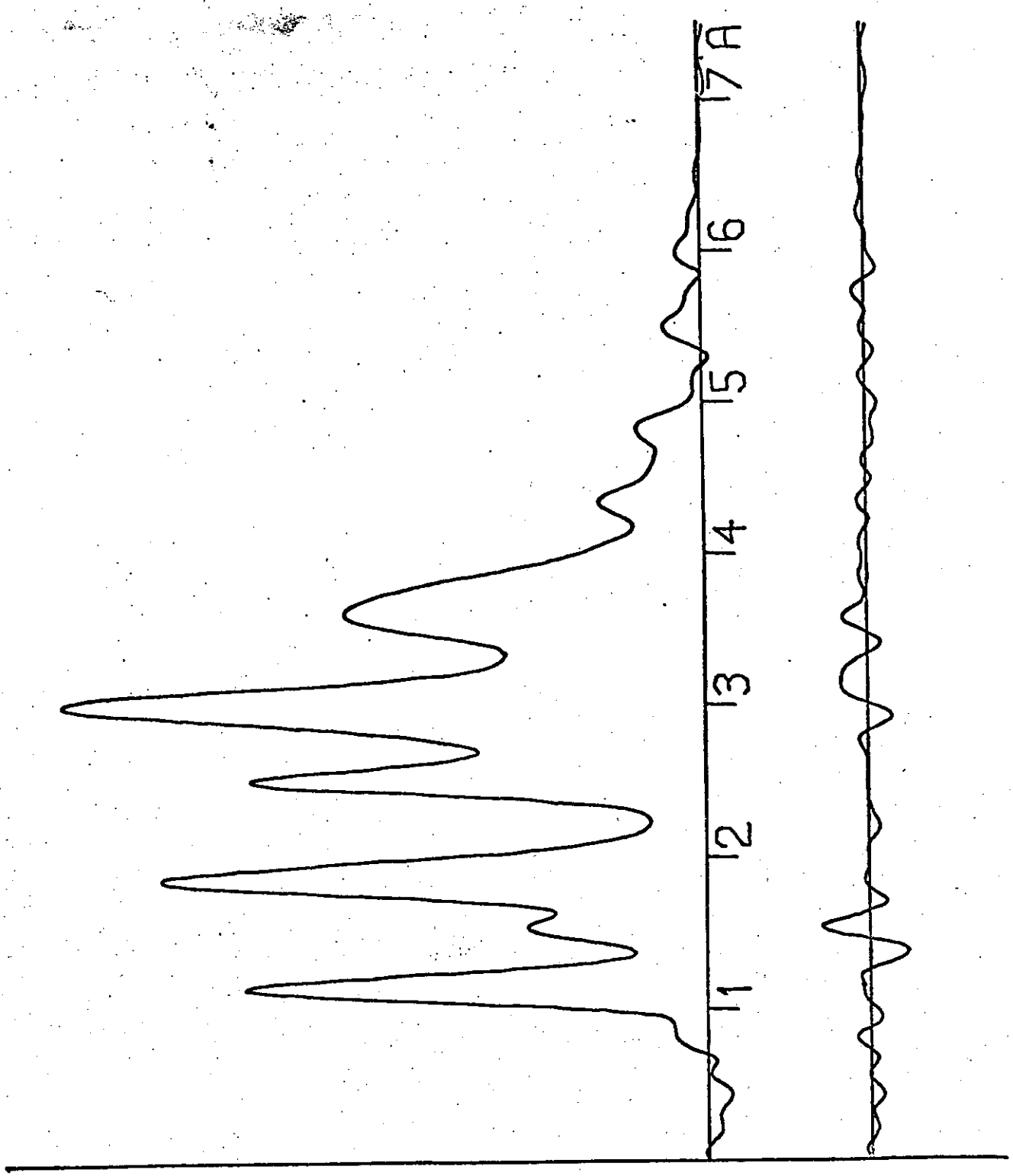

Figure 2.3 Radial distribution curve, P(r)/r, and final differences between experimental and calculated curves for $GeH_3Mn(CO)_5$. Before Fourier inversion the data were multiplied by s.exp $((0.000025s^2)/(z_{Mn}-f_{Mn})(z_O-f_O))$

Table 2.5 Weighting points etc. for Germylmanganesepentacarbonyl

Nozzle Height (mm)	dels^{-1} (nm^{-1})	s_{min}	s_1	s_2	s_{max}	P/h	Scale Factors
250	4	68	108	248	288	0.4207	1.067 ± 0.033
500	2	28	53	130	150	0.2475	0.907 ± 0.020
1000	1	12	20	65	73	0.4587	0.851 ± 0.039

Table 2.6 Molecular Parameters for $GeH_3Mn(CO)_5$ (pm)

	Distance		Amplitude		Shrinkage Correction.
a Independent distances					
r_1 (C-O)	113.9	(0.2)	4.3	(0.8)	
r_2 (Mn-C)	184.9	(0.2)	6.8	(0.6)	
r_3 (Mn-Ge)	248.7	(0.2)	5.7	(0.6)	
r_4 (Ge-H)	153.5	(fixed)	12.0	(fixed)	
b Dependent distances					
d_5 (Mn...O_{ax})	298.2	(1.0)	6.8	(0.6)	0.59
d_6 (Mn...O_{eq})	298.2	(1.0)			0.59
d_7 (C_{eq}...O_{eq})	478.2	(1.5)			2.27
d_8 (O_{eq}...O_{eq})	590.0	(2.0)	8.5	(1.3)	3.42
d_9 (C_{eq}...C_{eq})	365.9	(1.1)			1.33
d_{10} (C_{eq}...C_{eq})	276.3	(0.6)	15.9	(fixed)	0.25
d_{11} (C_{eq}...C_{ax})	259.4	(0.7)			0.25
d_{12} (O_{eq}...O_{eq})	445.5	(1.4)	27.7	(fixed)	1.40
d_{13} (O_{eq}...O_{ax})	418.1	(1.4)			1.40
d_{14} (C_{eq}...O_{eq})	368.8	(0.7)			0.82
d_{15} (C_{ax}...O_{eq})	368.8	(0.7)	19.3	(fixed)	0.82
d_{16} (C_{eq}...O_{ax})	348.8	(1.0)			0.82

Table 2.6 cont.

d_{17} (Ge...C_{ax})	432.2 (1.0)	7.1 (1.5)	0.43
d_{18} (Ge...O_{ax})	545.1 (1.4)	7.9	2.38
d_{19} (Ge...C_{eq})	291.9 (0.8)	15.5 (1.0)	0.28
d_{20} (Ge...O_{eq})	364.5 (1.4)	19.4	0.90
d_{21} (H...Mn)	333.3 (1.0)	12.0 (fixed)	0.59
d_{22} (H...C_{ax})	504.8 (1.3)	15.0 (fixed)	2.27
d_{23} (H...O_{ax})	613.6 (1.7)	18.0 (fixed)	3.42
d_{24} (H...H)	249.7 (0.7)	10.0 (fixed)	0.07

($H...C_{eq}$) between 249.7 and 427.7

($H...O_{eq}$) between 309.7 and 510.5

c Independent angles

$\angle 1$ H-Ge-H	110° (fixed)
$\angle 2$ C_{ax}-Mn-C_{eq}	97° (2°)
$\angle 3$ Mn-C_{eq}-O_{eq}	180° (fixed)

Table 2.7 Least squares correlation matrix multiplied by 1000 for $GeH_3Mn(CO)_5$

R1	R2	R3	<2	U1	U2	U3	U5	U7	U17	U19	K1	K2	K3
1000	51	25	-606	8	85	54	42	83	16	-95	18	101	96
	1000	-59	-615	38	112	134	107	48	59	50	113	122	85
		1000	-120	-65	-181	- 28	-36	-44	-29	-224	-92	-146	-178
			1000	-83	-177	-156	-46	-89	-30	-132	-150	-225	-140
				1000	445	335	259	117	100	318	530	511	157
					1000	410	338	151	124	384	624	656	247
						1000	176	118	104	344	579	496	135
							1000	161	113	-131	480	369	86
								1000	-65	-3	199	172	92
									1000	49	180	136	5
										1000	438	542	293
											1000	636	227
												1000	258
													1000

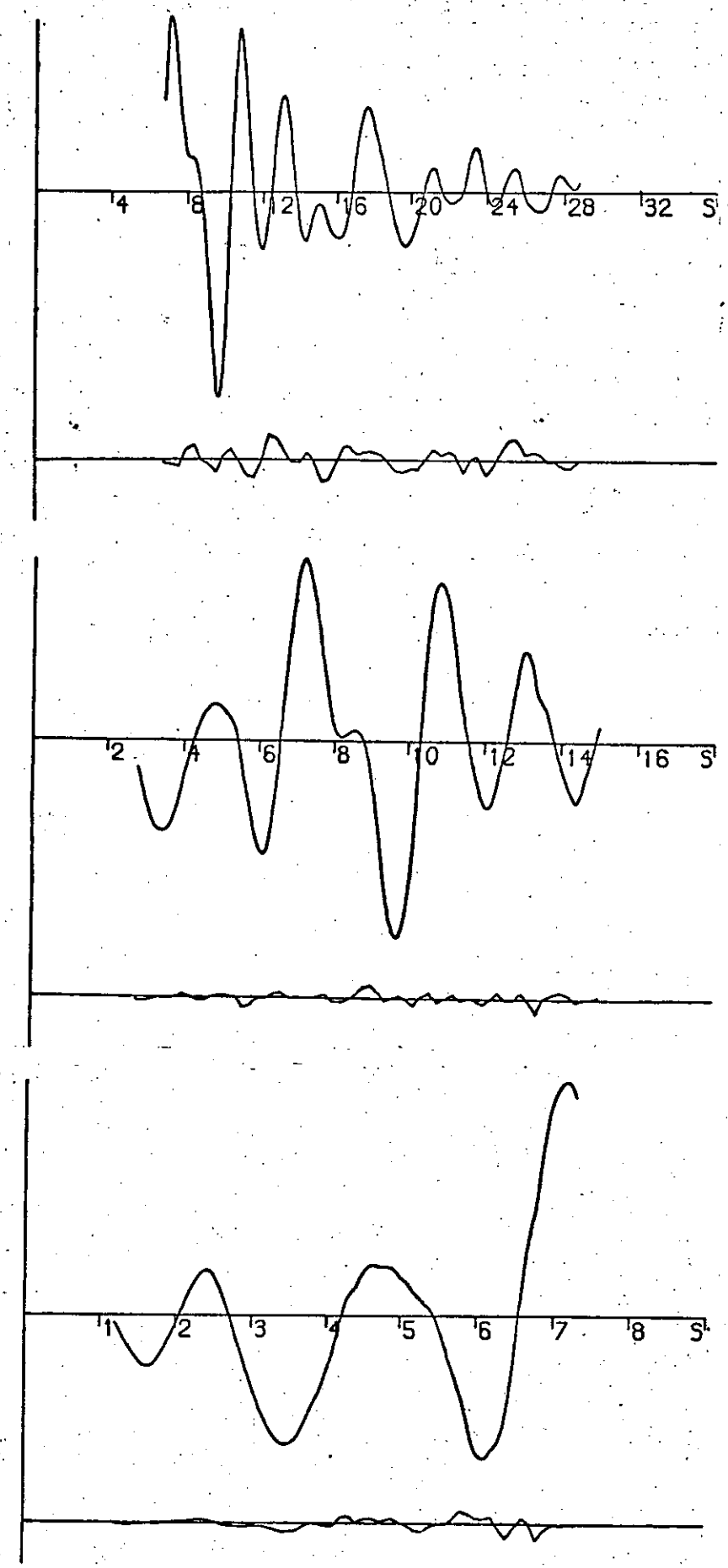

Figure 2.4 Observed and final weighted difference molecular intensities for $GeH_3Mn(CO)_5$ for data sets taken with nozzle-to-plate distances of 250, 500 and 1000mm.

in table 2.7. The observed and weighted final difference molecular scattering curves are given in figure 2.4.

2.4 Molecular Structure of Trifluorosilylmanganesepentacarbonyl

Table 2.8 shows weighting points (used to set up the off diagonal weight matrix), correlation parameters and scale factors.

The molecular model used for the purposes of least squares refinements was similar to that used for silylmanganesepentacarbonyl but, since the data appeared to be of higher quality, allowance was made for differences between the axial and equatorial carbon-manganesebond lengths. This meant the molecule could be described using the silicon-fluorine, carbon-oxygen and manganese-silicon bond lengths, the average manganese-carbon bond length, the difference between axial and equatorial carbon-manganese bond lengths and the following angles: F-Si-Mn, C_{eq}-Mn-C_{ax} and Mn-C_{eq}-O_{eq}.

All bonded distances and their amplitudes of vibration, save that of carbon-oxygen, refined satisfactorily as did the C_{eq}-Mn-C_{ax} and F-Si-Mn angles. Here also the overlap of large numbers of peaks in the radial distribution curve (figure 2.5) necessitated the refinement of certain groups of amplitudes as single parameters (table 2.9). All groups bar the following refined satisfactorily, right-angled C...C, right-angled O...O, F...C_{ax} and F...O_{ax}. These vibrational amplitudes along with those of F...F and C-O were set at typical values. The difference between axial and equatorial carbon-manganese bond lengths and the Mn-C_{eq}-O_{eq} angle were both set by doing series of refinements with different fixed values of those parameters and comparing the R-

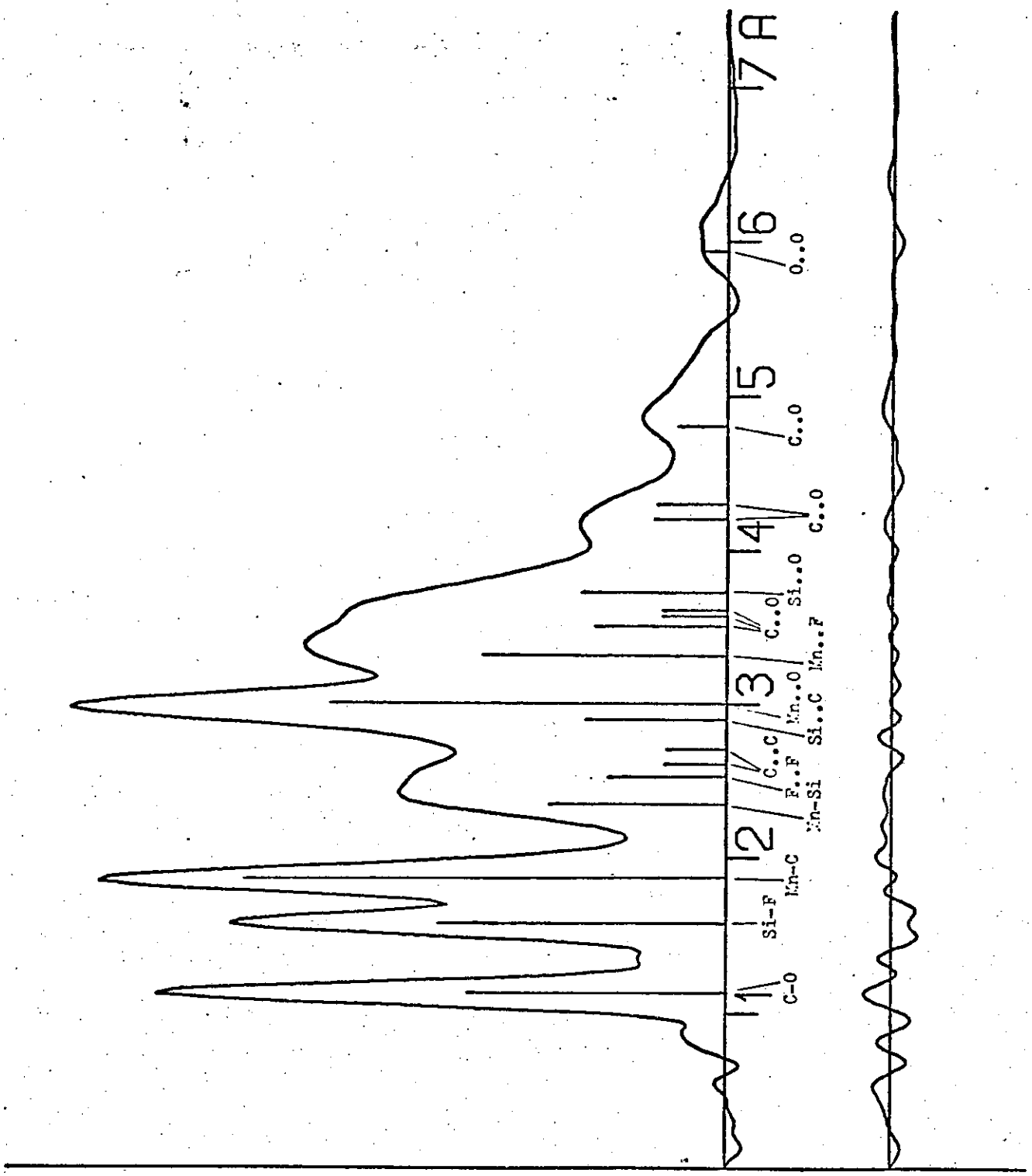

Figure 2.5 Radial distribution curve, P(r)/r, for $SiF_3Mn(CC)_5$ showing principal interatomic distances. Before Fourier inversion the data were multiplied by $s.\exp(-0.000015s^2/(z_{Mn}-f_{Mn})(z_0-f_0))$

Table 2.8 Weighting Factors etc. for Trifluorosilylmanganesepentacarbonyl

Nozzle Height (mm)	dels (nm^{-1})	s_{min}	s_1	s_2	s_{max}	$P/_h$	Scale Factors
190	4	48	76	300	340	0.4549	0.979 ± 0.021
580	2	24	36	120	130	0.4902	0.836 ± 0.021

Table 2.9 Molecular parameters for $SiF_3Mn(CO)_5$ [a]

a Independent distances and amplitudes [b]

r_1	(C-O)	113.0 (3)	3.5 (fixed)
r_2	$(Mn-C)_{av}$	185.8 (6)	5.4 (5)
r_3	(Mn-Si)	235.8 (7)	7.6 (7)
r_4	(Si-F)	158.1 (4)	4.7 (5)

b Dependent distances, amplitudes and shrinkage corrections applied [c]

d_5	$(Mn-C_{eq})$	185.4 (8)	5.4 (5)
d_6	$(Mn-C_{ax})$	187.4 (8)	5.4
d_7	$(Mn\ldots O_{eq})$	297.8 (13)	6.8 (5)
d_8	$(Mn\ldots O_{ax})$	299.8 (13)	
d_9	$(C_{eq}\ldots C_{eq})$	369.0 (20)	11.4 (14)
d_{10}	$(C_{eq}\ldots O_{eq})$	481.00 (24)	
d_{11}	$(O_{eq}\ldots O_{eq})$	592.8 (28)	
d_{12}	$(C_{eq}\ldots C_{eq})$	270.2 (12)	14.6 (fixed)
d_{13}	$(C_{eq}\ldots C_{ax})$	261.6 (15)	
d_{14}	$(O_{eq}\ldots O_{eq})$	430.1 (16)	25.0 (fixed)
d_{15}	$(O_{eq}\ldots O_{ax})$	420.1 (19)	

0.00	
0.00	
0.59	
0.59	
1.33	
2.27	
3.42	
0.25	
0.25	
1.40	
1.40	

Table 2.9 cont.

d_{16} ($C_{eq}...O_{eq}$)	360.0(15)]		0.82
d_{17} ($C_{ax}...O_{eq}$)	357.6 (13)]	15.9 (fixed)	0.82
d_{18} ($C_{eq}...O_{ax}$)	350.1 (18)]		0.82
d_{19} (Si...C_{ax})	421.8 (15)]	[11.9 (28)	1.43
d_{20} (Si...O_{ax})	533.8 (20)]	[13.2	2.38
d_{21} (Si...C_{eq})	292.2 (16)]	[15.3 (14)	0.28
d_{22} (Si...O_{eq})	372.1 (20)]	[18.5	0.90
d_{23} (Mn...F)	329.8 (8)	10.5 (7)	0.59
d_{24} (F...C_{ax})	503.0 (14)	16.7 (fixed)	2.27
d_{25} (F...O_{ax})	610.9 (18)	16.7 (fixed)	3.42
d_{26} (F...F)	252.9 (12)	9.9 (fixed)	0.07
(F...C_{eq}) between 292 and 435			
(F...O_{eq}) between 326 and 523			

c Angles

∠1 (F-Si-F)	112.5 (4)	
∠2 (C_{ax}-Mn-C_{eq})	92.9 (4)	
∠3 (Mn-C_{eq}-O_{eq})	178.3 (fixed)	

a All distances and amplitude are given in pm; angles in degrees.

b Independent distances are r_a.

c Shrinkage applied were the same as those used for $SiH_3Mn(CO)_5$.

Table 2.10 Least squares correlation matrix multiplied by 100 for $SiF_3Mn(CO)_5$

r1	r2	r3	r4	<1	2	u3	u4	u5	u7	u9	u16	u19	u21	u23	k1	k2
100	16	12	13	-25	-17	9	-4	4	6	12	-32	0	-24	-25	3	-8
	100	24	44	-43	-57	6	3	-11	2	5	-40	1	- 9	-11	-8	-8
		100	1	-62	28	-10	-11	-5	-10	1	2	-11	12	7	-22	-13
			100	-5	-38	-10	-2	-18	-1	-11	2	3	-16	4	-15	-16
				100	-39	19	5	0	29	-30	37	13	-39	4	8	13
					100	-30	-4	8	-30	19	2	-13	48	-2	2	1
						100	9	7	19	-3	5	6	-20	1	20	12
							100	11	15	2	-1	5	3	- 3	34	7
								100	21	8	3	6	11	-1	53	25
									100	-3	11	8	-42	1	41	18
										100	-17	-32	5	-9	11	6
											100	-8	-1	58	3	6
												100	1	-2	12	5
													100	33	12	8
														100	-4	-7
															100	26
																100

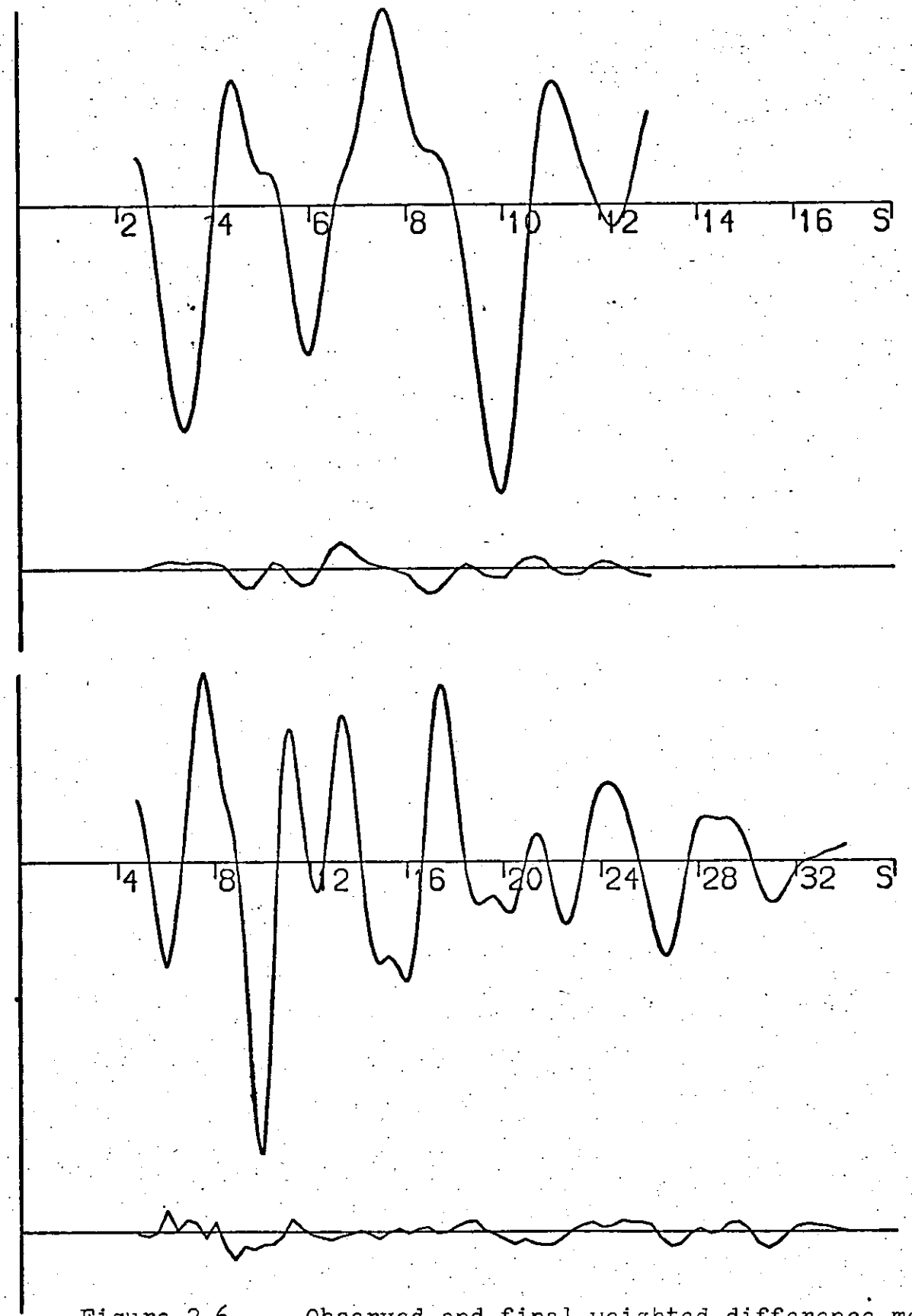

Figure 2.6 Observed and final weighted difference molecular scattering intensities for $SiF_3Mn(CO)_5$ for data sets obtained with nozzle-to-plate distances of 190mm and 580mm

factors for these refinements. These would not refine normally owing to high correlation with other parameters.

The final R-factor was 0.129. Table 2.10 shows the least squares correlation matrix and figure 2.6 shows the observed and final weighted difference molecular scattering curves.

2.5 Molecular Structure of Germylcobalttetracarbonyl.

In table 2.11 the weighting points (used to set up the off diagonal weight matrix), correlation parameters and scale factors are given.

For the least squares refinements the molecular model assumed the molecule had C_3 symmetry and all carbon-oxygen bond lengths were equal. The molecule could then be described using the Ge-H, C-O and Ge-Co bond lengths, the average cobalt-carbon bond length, the difference between axial and equatorial carbon-cobalt bond lengths and the following angles: C_{eq}-Co-C_{ax}, Co-C_{eq}-O_{eq}, Co-Ge-H and a twist angle describing the configuration of the germyl group with respect to the cobalttetracarbonyl group (at zero degrees the configuration was eclipsed).

The Ge-Co and C-O bond lengths and their amplitudes of vibration, the average cobalt-carbon bond length, the difference between axial and equatorial cobalt-carbon bond lengths and the C_{eq}-Co-Ge and Co-C_{eq}-O_{eq} angles all refined satisfactorily. Again, due to the overlap of several peaks in the radial distribution curve certain groups of amplitudes were refined as single parameters. All groups, other than those involving hydrogen atoms refined satisfactorily. The twist angle was determined by carrying out a series of refinements with various twist angles and comparing the R-factors. All other

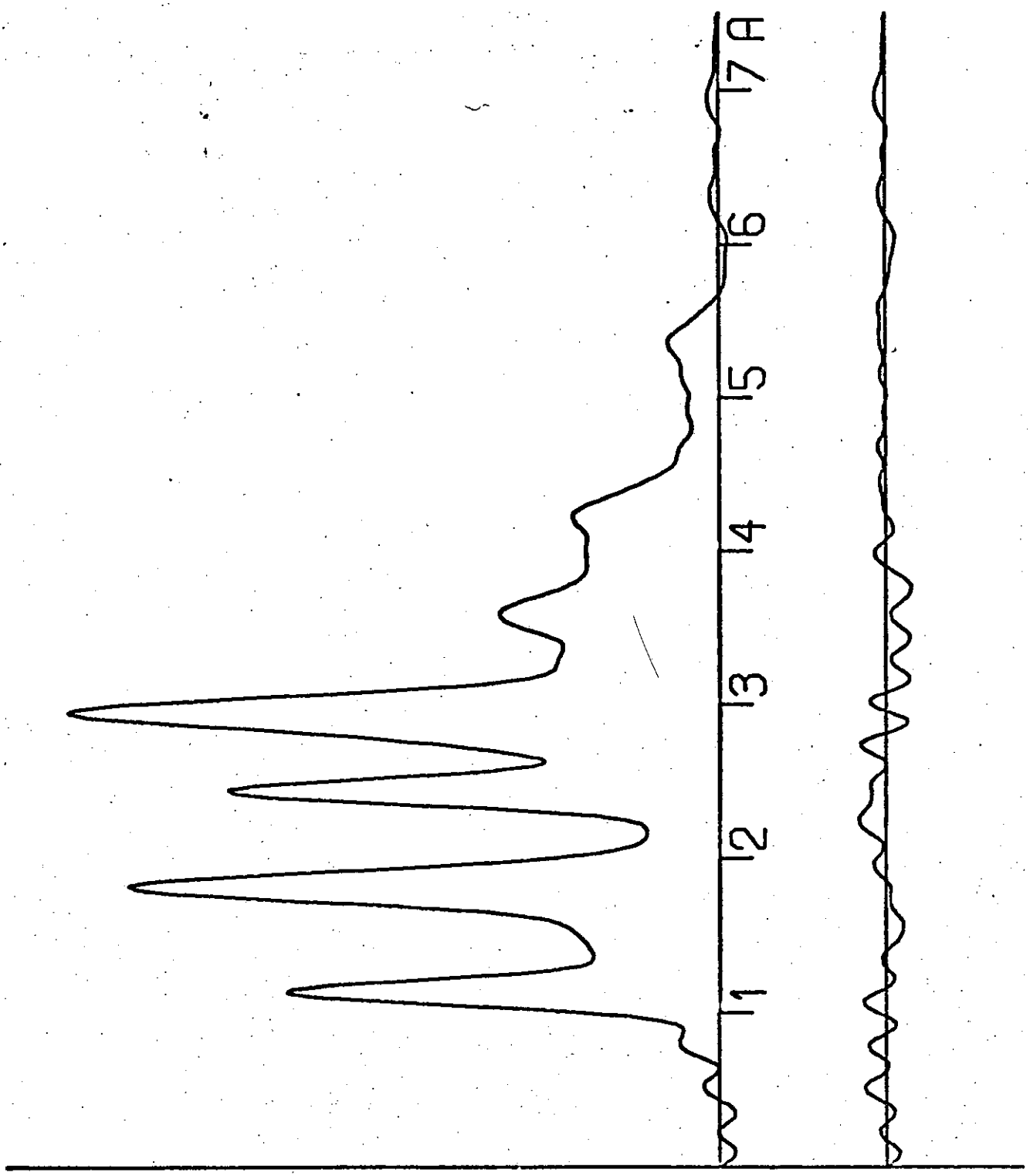

Figure 2.7 Radial distribution curve, P(r)/r, and final deviations between experimental and theoretical curves for $GeH_3Co(CO)_4$. Before Fourier inversion the data were multiplied by $s.\exp((0.000025s^2)/(z_{Co}-f_{Co})(z_O-f_O))$

Table 2.11 Weighting Points etc. for Germylcobalttetracarbonyl

Nozzle Height (mm)	dels (nm^{-1})	s_{min}	s_1	s_2	s_{max}	$P/_h$	Scale Factor
250	4	76	105	260	300	0.4201	1.069 ± 0.032
500	2	28	40	120	140	0.4795	1.020 ± 0.026
1000	1	10	17	64	72	0.4994	1.033 ± 0.052

Table 2.12 Molecular parameters of $GeH_3Co(CO)_4$

a Independent distances and amplitudes (pm)

r_1	(Co-C) (mean)	180.0 (6)	
δ	(Co-C) (eq-ax)	-1.0 (16)	
r_2	(C-O)	112.8 (4)	5.2 (7)
r_3	(Co-Ge)	241.6 (4)	6.9 (5)
r_4	(Ge-H)	152.5 (fixed)	10.0 (fixed)

b Dependent distances and amplitudes

d_5	($Co-C_{eq}$)	179.8 (8)	6.1 (6)
d_6	($Co-C_{ax}$)	180.8 (15)	6.1 (tied to u 5)
d_7	($Co\ldots O_{eq}$)	291.7 (13)	6.8 (5)
d_8	($Co\ldots O_{ax}$)	292.8 (18)	6.8 (tied to u 7)
d_9	($C_{eq}\ldots C_{eq}$)	308.7 (14)	13.0 (18)
d_{10}	($C_{eq}\ldots O_{eq}$)	408.6 (18)	15.7 (tied to u 9)
d_{11}	($O_{eq}\ldots O_{eq}$)	500.2 (25)	18.6 (tied to u 9)
d_{12}	($C_{ax}\ldots C_{eq}$)	268.3 (18)	14.5 (fixed)
d_{13}	($C_{ax}\ldots O_{eq}$)	361.3 (24)	17.5 (fixed)
d_{14}	($C_{eq}\ldots O_{ax}$)	360.0 (23)	17.5 (fixed)
d_{15}	($O_{ax}\ldots O_{eq}$)	437.4 (30)	21.0 (fixed)
d_{16}	($Ge\ldots C_{ax}$)	420.3 (19)	10.0 (16)

Table 2.12 cont.

d_{17} (Ge...O_{ax})	532.1 (23)	11.0 (tied to u 16)
d_{18} (Ge...C_{eq})	284.2 (6)	16.5 (14)
d_{19} (Ge...O_{eq})	355.0 (8)	19.9 (tied to u 18)
d_{20} (Co...H)	325.1 (12)	15.0 (fixed)
d_{21} (H...C_{eq})	274.8 (8)	15.0 (fixed)
d_{22} (H...C_{eq})	379.1 (9)	15.0 (fixed)
d_{23} (H...C_{eq})	395.1 (11)	15.0 (fixed)
d_{24} (H...O_{eq})	295.0 (8)	15.0 (fixed)
d_{25} (H...O_{eq})	445.5 (13)	15.0 (fixed)
d_{26} (H...O_{eq})	472.7 (14)	15.0 (fixed)
d_{27} (H...C_{ax})	491.7 (22)	20.0 (fixed)
d_{28} (H...O_{ax})	599.6 (29)	20.0 (fixed)
d_{29} (H...H)	248.9 (fixed)	11.0 (fixed)

c Angles

$\angle$ 1 (Co-Ge-H)	109.1 (fixed)
$\angle$ 2 (C_{eq}-Co-Ge)	83.8 (3)
$\angle$ 3 (twist)	10.0 (see text)
$\angle$ 4 (Co-C_{eq}-O_{eq})	178.3 (fixed)

Note: Distances (r_a) are given in pm, and angles in degrees. The angle Co-C-O, fixed in the final refinement, had been included in earlier refinements, in which the quoted value was obtained.

Table 2.13 Least squares correlation matrix multiplied by 100 for $GeH_3Co(CO)_4$

r1	δ	r2	r3	<2	u3	u4	u5	u7	u9	u16	u18	k1	k2	k3	
100	-4	36	-4	-86	3	11	8	-5	-15	-3	10	17	15	-1	r1
	100	4	11	-2	4	7	17	24	54	32	-5	6	15	19	δ
		100	-4	-67	0	1	7	-4	-1	-3	-5	4	3	-1	r2
			100	-2	0	8	-3	7	-4	3	-17	4	-2	-9	r3
				100	-6	-12	-15	5	12	4	-19	-30	-19	1	<2
					100	30	28	25	10	8	19	-44	30	6	u3
						100	40	30	14	13	25	65	44	5	u4
							100	37	22	16	28	62	52	15	u5
								100	29	21	-9	54	42	16	u7
									100	16	15	18	27	26	u9
										100	-14	39	41	11	u16
											100	17	16	10	u18
												100	57	12	k1
													100	14	k2
														100	k3

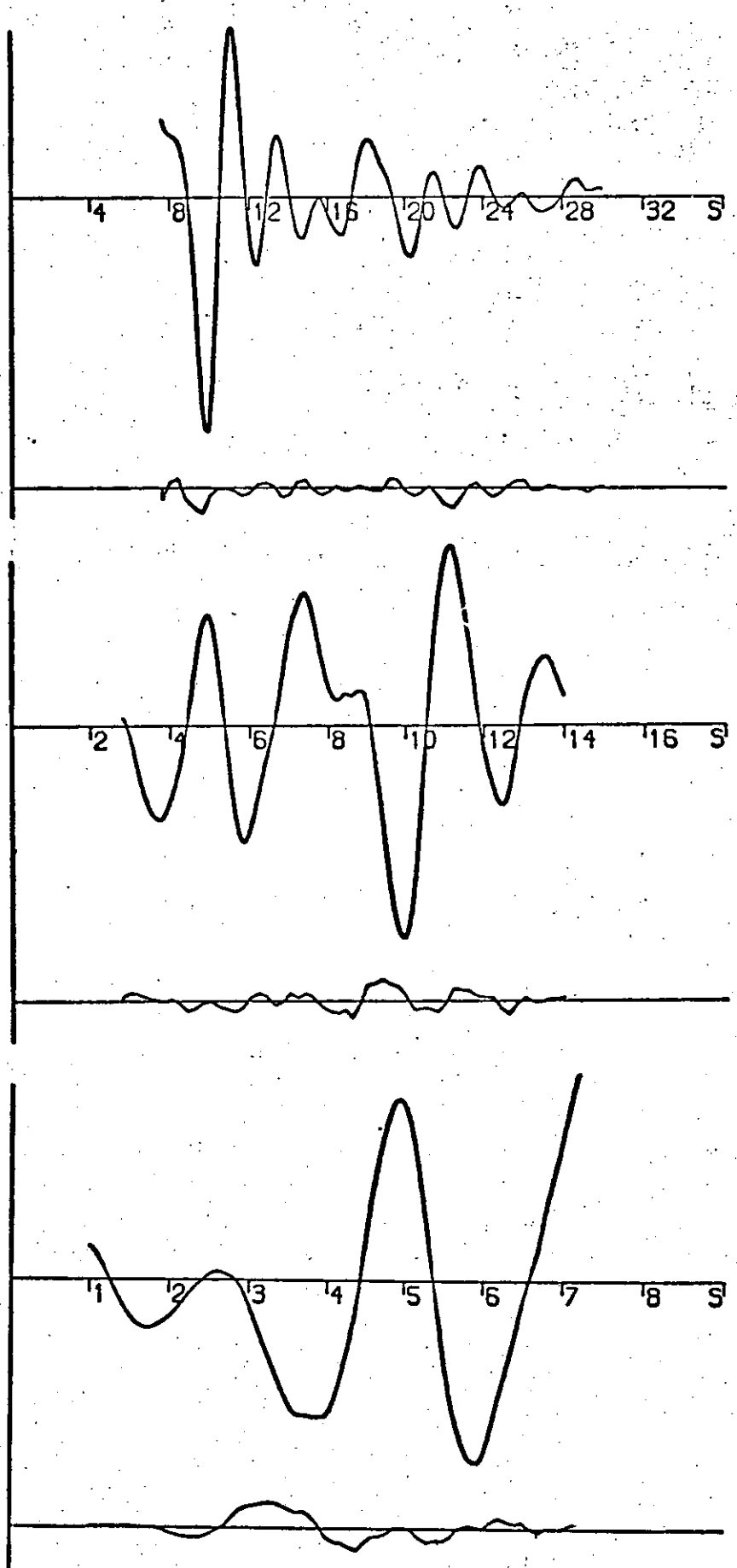

Figure 2.8 Observed and final weighted difference molecular scattering intensities for $GeH_3Co(CO)_4$ for data sets obtained with nozzle-to-plate distances of 250, 500 and 1000 mm.

parameters involving hydrogen were set at fixed values. The final R-factor(R_G) was 0.14.

Table 2.12 shows molecular parameters and table 2.13 the final least squares correlation matrix. Final weighted difference and observed molecular scattering intensity curves are shown in figure 2.8.

2.6 Discussion

If it is assumed that the Mn-C_{met} bond in methylmanganesepentacarbonyl is a pure σ bond the covalent radius of manganese in manganesepentacarbonyl derivatives can be deduced to be 141.8pm from r(Mn-C_{met}) in $CH_3Mn(CO)_5$ [30] and r(C-C) in C_2H_6 [43]. (This value is in broad agreement with other values published for this parameter [82, 83] but there is a wide spread of published values). Consequently, using covalent radii of silicon and germanium predicted from the molecular structures of C_2H_6 [43], SiH_3CH_3 [44] and GeH_3CH_3 [45], Mn-Si and Mn-Ge single covalent bond lengths can be calculated for $SiH_3Mn(CO)_5$ and $GeH_3Mn(CO)_5$. The actual values for r(Si-Mn) and r(Ge-Mn) in $SiH_3Mn(CO)_5$ and $GeH_3Mn(CO)_5$ are much smaller than those calculated in the above manner (see table 2.14). A possible explanation for these discrepancies would be the presence of (d $\rightarrow$ d) π bonding in the Si-Mn and Ge-Mn bonds. However PE spectra of these, and other manganesepentacarbonyl derivatives indicate that such π bonding is unimportant and that the main effect of substituting silyl- or germyl- for methyl- on manganesepentacarbonyl is to increase the σ-acceptor power of the ligand (chapter 1). This effect would also result in r(Si-Mn) and r(Ge-Mn) in $SiH_3Mn(CO)_5$ and $GeH_3Mn(CO)_5$ being shorter than predicted from r(C_{met}-Mn) in $CH_3Mn(CO)_5$.

There is a shortening of 5pm in r(Si-Mn) on fluorination

Table 2.14 Some Mn - Group IVB element bond lengths

Compound	observed r(Mn-M')	Predicted r(Mn-M')a	Method	Reference
$CH_3Mn(CO)_5$	218.5 (11)		e.d.	30
$SiH_3Mn(CO)_5$	240.7 (5)	251.9	e.d.	this work
$GeH_3Mn(CO)_5$	248.7 (2)	259.6	e.d.	this work
$CF_3Mn(CO)_5$	205.6 (4)	218.5	e.d.	31
$SiF_3Mn(CO)_5$	236.0 (7)	251.9	e.d.	this work
$GeBr_3Mn(CO)_5$	244	259.6	X-ray	33
$SiMe_3Mn(CO)_5$	249.7 (5)	251.9	X-ray	32

a Predicted r(Mn-M') calculated using covalent radii for Mn, C, Si and Ge described in the text.

of $SiH_3Mn(CO)_5$ to $SiF_3Mn(CO)_5$. This is very much a typical value for a reduction in r(Si-X) on fluorination of SiH_3X. However fluorination of $CH_3Mn(CO)_5$ to $CF_3Mn(CO)_5$ results in a reduction of $r(Mn-C_{met})$ by 13pm[31]. In fact, r(Mn-Si) in $SiF_3Mn(CO)_5$ is only slightly shorter than would be predicted from $r(Mn-C_{met})$ in $CF_3Mn(CO)_5$. These observations and the low bond dissociation energy of the $Mn-C_{met}$ bond indicate that $r(Mn-C_{met})$ in $CH_3Mn(CO)_5$ is longer than might be expected rather than r(Si-Mn) and r(Ge-Mn) in $SiH_3Mn(CO)_5$ and $GeH_3Mn(CO)_5$ being shorter than expected. This could arise because both the methyl and the manganese-pentacarbonyl- groups are strong σ donors so the bond between these groups is likely to be long and weak. Other possible reasons could involve steric or antibonding interactions between the methyl and manganesepenta-carbonyl groups.

If it is the $Mn-C_{met}$ bond in $CH_3Mn(CO)_5$ which is long and weak it is unnecessary to invoke $(d \rightarrow d)\pi$ bonding in the Si-Mn bond of $SiH_3Mn(CO)_5$. The reduction in r(Mn-Si) on fluorination of $SiH_3Mn(CO)_5$ also seems best explained in terms of an increase in σ acceptor power of the SiF_3 group relative to the SiH_3 group. Also, the fact that r(Mn-Si) in $SiF_3Mn(CO)_5$ is only slightly shorter than would be predicted from $r(Mn-C_{met})$ in $CF_3Mn(CO)_5$ can be taken as an indication that $(d \rightarrow d)$ π bonding is unimportant in the Si-Mn bond of $SiF_3Mn(CO)_5$.

Neither the Si-F bond length nor the F-Si-F angle in $SiF_3Mn(CO)_5$ indicate any interaction between F-Si bonding or anti-bonding levels or fluorine lone pairs and the $Mn(CO)_5$ group.

Other molecular parameters of any of these manganese-pentacarbonyl derivatives give little information on the nature of metal-metal bonding in these compounds.

For example there is no simple relationship between the C_{eq}-Mn-C_{ax} angle and the differences between observed and predicted metal-metal bond length. This is most probably due to the large number of factors which affect that angle though it could be because the angle is difficult to determine accurately by electron diffraction owing to its high correlation with other parameters.

A cobalt covalent radius of 133pm has been suggested for cobalttetracarbonyl derivatives on the basis of the Co-Co bond length in $Co_2(CO)_6(PBu^t_3)_2$[84]. By analogy with the Mn-Mn bond length in $Mn_2(CO)_8(PEt_3)_2$[85] this value for the covalent radius of cobalt may be too large. Little therefore can be deduced from the fact that both r(Co-Si) and r(Co-Ge) in $SiH_3Co(CO)_4$[23] and $GeH_3Co(CO)_4$ are shorter than predicted from this value of the cobalt covalent radius and the covalent radii of silicon and germanium determined as described earlier. A more useful comparison would be with the Co-C_{met} bond length in $CH_3Co(CO)_4$, but this has not yet been determined.

Some Co-Si and Co-Ge bond lengths in some silyl- and germyl- derivatives of cobalttetracarbonyl are listed in table 2.15. From this table it can be seen that r(Co-Si) in $SiH_3Co(CO)_4$ has been found only 3pm shorter than r(Co-Ge) in $GeH_3Co(CO)_4$. Also, chlorination of $SiH_3Co(CO)_4$ results in a 13pm reduction in r(Si-Co)[40] whereas r(Ge-Co) in $GeH_3Co(CO)_4$ is only reduced by 10pm on chlorination[41]. These surprising figures seem best explained by assuming the published molecular structure of $SiH_3Co(CO)_4$ to be inaccurate; it is likely that r(Si-Co) is between 2 and 5pm shorter than stated. Such an assumption is not unreasonable. The molecular structure of $SiH_3Co(CO)_4$ was determined by electron diffraction but only one nozzle-to-plate distance was used and the final R-factor was high(0.28).

Table 2.15 Some Co- Group IVB element bond lengths

Compound	r(Co-M')	method	reference
$SiH_3Co(CO)_4$	238.1 (7)	e.d.	23
$SiCl_3Co(CO)_4$	225.4 (3)	X-ray	39
$SiF_3Co(CO)_4$	222.6 (5)	X-ray	40
$GeH_3Co(CO)_4$	241.6(4)	e.d.	this work
$GeCl_3Co(CO)_4$	231.0 (7)	X-ray	41

Nevertheless it is still apparent that halogenation of $SiH_3Co(CO)_4$ and $GeH_3Co(CO)_4$ has a greater effect on r(Si-Co) and r(Ge-Co) than halogenation of $SiH_3Mn(CO)_5$ and $GeH_3Mn(CO)_5$ has on r(Si-Mn) and r(Ge-Mn). This could be attributed to (d→d) π bonding being important in the halogenated silyl- and germyl- cobalttetracarbonyl derivatives but it may be significant that fluorination of $CH_3Mn(CO)_5$ results in a reduction in $r(C_{met}-Mn)$ similar to the reduction in r(Si-Co) on fluorination of $SiH_3Co(CO)_4$[23, 40] and no (d→d) π bonding can be reasonably expected to occur in $CF_3Mn(CO)_5$. These observations in methyl- and trifluoromethyl- manganesepentacarbonyl obviously do not rule out the possibility of (d→d) π bonding in silyl- and germyl- cobalttetracarbonyl but it is difficult to argue in favour of (d→d)π bonding being important in silyl- and germyl-cobalttetracarbonyl complexes when on the basis of the same type of evidence it seems unimportant in silyl- and germyl-manganesepentacarbonyl complexes. On the other hand, as ^{119}Sn Mössbauer studies of Sn(IV) derivatives of $Co(CO)_4$ and $Mn(CO)_5$ have indicated that $Mn(CO)_5$ is a stronger σ donor than $Co(CO)_4$, it would seem reasonable that Si-Co and Ge-Co bond lengths would be less affected by changes in acceptor power of the silyl- and germyl- groups than Si-Mn and Ge-Mn bond lengths of analogous manganesepentacarbonyl complexes.

Determination of the molecular structures of $CH_3Co(CO)_4$ and $CF_3Co(CO)_4$, in particular the difference between the Co-C_{met} bond lengths of these two compounds, may help to clarify this situation.

CHAPTER THREE

Electron Diffraction Determination of the molecular Structures of methyl-, silyl- and germyl- rheniumpentacarbonyl in the gas Phase

CHAPTER 3

3.1 Introduction

Samples of methylrheniumpentacarbonyl, silylrheniumpentacarbonyl and germylrheniumpentacarbonyl were prepared (chapter 6) and their gas phase molecular structures were determined by electron diffraction using data obtained on the Balzer's KD.G2 gas diffraction apparatus at Manchester[74]. The nozzle to plate distances used (table 3.1) gave data over a range of scattering variable, s, of about 10 to 280nm^{-1}. Data analyses were carried out as described in chapter 6. Table 3.2 shows weighting points (used to set up the off-diagonal weight matrix), correlation parameters and scale factors.

The complex scattering factors of Schäfer, Yates and Bonham[86] were initially used but superimposed on the molecular scattering curves of each of these rhenium derivatives was a large oscillation of frequency 80nm^{-1}. An oscillation of similar frequency was also observed on the scattering factor of rhenium (figure 3.1) and removal of this oscillation from the scattering factor resulted in the removal of the oscillation from the molecular scattering curves. Similar oscillations in the rhenium scattering factor were also encountered and removed during the structure determinations of ReF_6 and ReF_7[87, 88].

The molecular model used in the structure determinations of $SiH_3Mn(CO)_5$ and $GeH_3Mn(CO)_5$ (Chapter 2) was used in all the structure determinations described in this chapter. No attempt was made to differentiate between the $Re-C_{ax}$ and $Re-C_{eq}$ bond lengths. Any difference would probably be no greater than 4 pm, the value found in $CH_3Mn(CO)_5$[30], and differences of this magnitude are difficult to determine accurately using electron diffraction techniques, especially using data of the

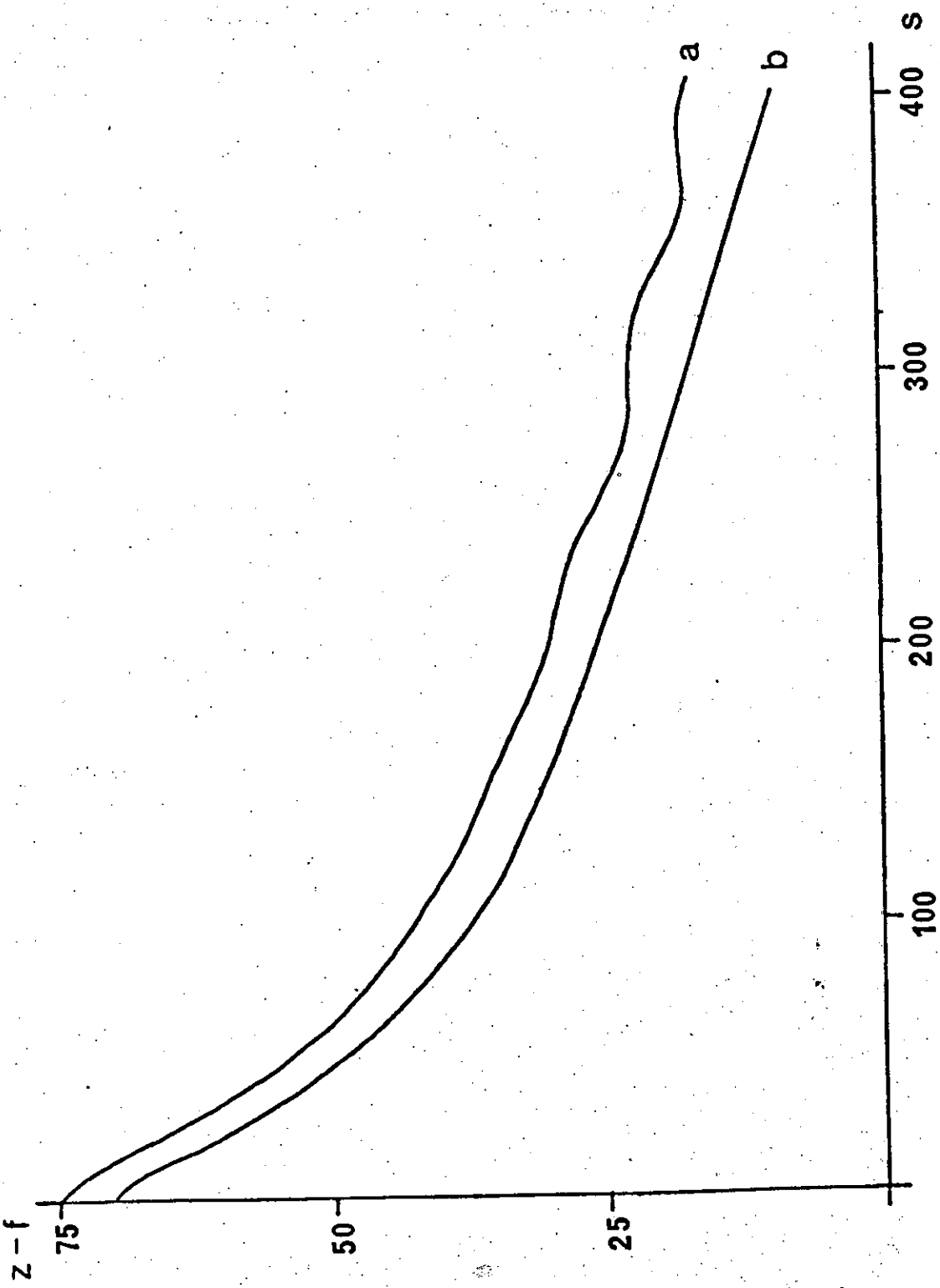

Figure 3.1 Scattering factor, z-f, for rhenium, a, derived from data by Schäfer et al. and, b, modified and used for this work. The second curve is displaced 5 units downwards for clarity.

Table 3.1 Nozzle heights, nozzle and sample temperatures.

Compound	Nozzle Height (mm)	Sample Temperature (K)	Nozzle Temperature (K)
$CH_3Re(CO)_5$	1000 500 250	333	340
$SiH_3Re(CO)_5$	1000 500 250	333	340
$GeH_3Re(CO)_5$	1000 500 250	333	340

quality obtained here. This assumption appears justified as there is no asymmetry of the Re-C peak in the radial distribution curves nor are any of the Re-C amplitudes of vibration abnormally high.

3.2 Refinements and Results

a. Methylrheniumpentacarbonyl.

The $Re-C_{met}$, $Re-C_{carbonyl}$ and C-O bond lengths and their amplitudes of vibration all refined satisfactorily as did the $C_{ax}-Re-C_{eq}$ angle. Just as in the structure determinations of the manganese and cobalt carbonyl complexes, described in chapter 2, there is much overlapping of peaks in the radial distribution curve (figure 3.2). This necessitated the refinement of groups of amplitudes of vibration as single parameters (table 3.3). All groups, other than those involving hydrogen atoms and the group consisting of linear C...C, C...O and O...O amplitudes of vibration, refined satisfactorily. All non-refining parameters were set at reasonable values.

The final molecular parameters are shown in table 3.3. The final R-factor was 0.121. It is noticeable that with all these rheniumpentacarbonyl derivatives the individual R-factor for the data from the plate exposed at 250mm. from the nozzle is very high. This could be partly due to incorrect calculation of the phase shifts and insufficient smoothing in the scattering factor for rhenium. Here the R-factor is particularly high at 0.38; the probable cause is that there is very little molecular scattering intensity at s values greater than $100nm^{-1}$ and therefore it is the sum of intensities which is particularly low rather than the sum of the differences being unusually high.

The least squares correlation matrix is given in table 3.4 and the observed and final weighted difference molecular scattering curves are given in figure 3.3.

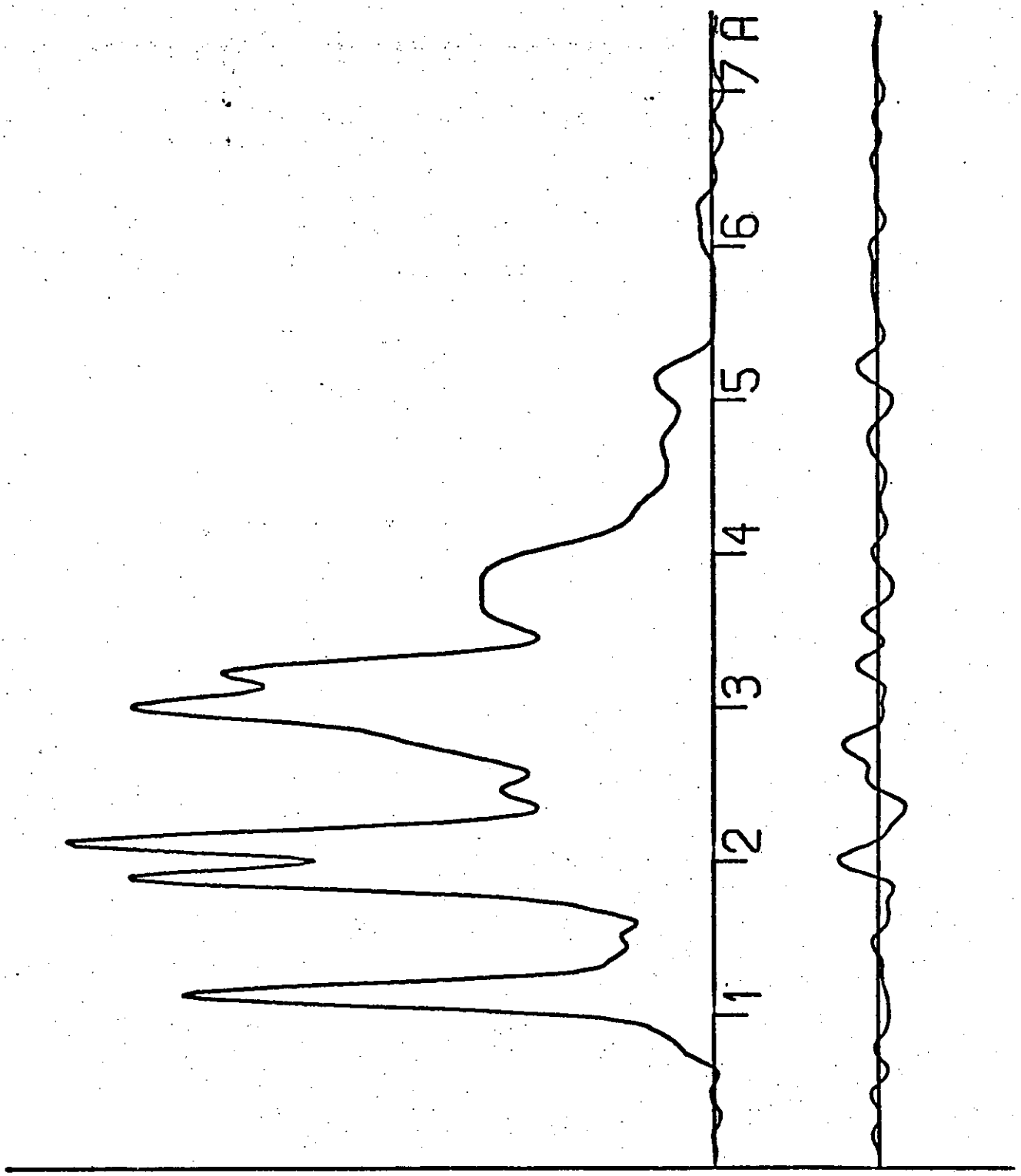

Figure 3.2 Radial distribution curve, P(r)/r, and difference curve for $CH_3Re(CO)_5$. Before Fourier inversion the data were multiplied by $s.\exp((-0.00001\ s^2)/(z_{Re}-f_{Re})(z_O-f_O))$

Table 3.2 Weighting functions, correlation parameters and scale factors

Compound	camera height mm	del s nm^{-1}	s_{min} nm^{-1}	s_1 nm^{-1}	s_2 nm^{-1}	s_{max} nm^{-1}	p/h	Scale factor
$CH_3Re(CO)_5$	250	4	68	104	220	260	0.3975	0.864 ± 0.021
	500	2	26	55	138	158	0.4822	0.978 ± 0.021
	1000	1	11	21	62	72	0.1314	0.749 ± 0.012
$SiH_3Re(CO)_5$	250	4	100	140	240	284	0.1369	0.813 ± 0.046
	500	2	26	50	130	154	0.4722	0.762 ± 0.021
	1000	1	12	20	61	71	0.4555	0.713 ± 0.024
$GeH_3Re(CO)_5$	250	4	68	128	230	276	0.3737	0.962 ± 0.039
	500	2	22	40	124	144	0.4283	0.865 ± 0.027
	1000	1	13	23	61	72	0.3954	0.664 ± 0.029

Table 3.3 Molecular parameters for $CH_3Re(CO)_5$

Independent distances	Distance (pm)	Amplitude of vibration (pm)
r_1 C-O	113.0 (4)	4.5 (9)
r_2 Re-$C_{(carbonyl)}$	200.0 (4)	5.6 (4)
r_3 Re-$C_{(methyl)}$	230.8 (17)	5.6 (tied to u 2)
r_4 H-C	110.0 (fixed)	5.0 (fixed)
Dependent distances		
d_1 Re...O_{ax}	312.2 (9)	7.2 (4)
d_2 Re...O_{eq}	312.2 (9)	7.2 (tied to u 6)
d_3 C_{eq}...O_{eq}	506.6 (17)	9.5 (fixed)
d_4 C_{eq}...C_{eq}	395.6 (13)	9.5 (fixed
d_5 O_{eq}...O_{eq}	617.1 (24)	9.5 (fixed)
d_6 C_{eq}...C_{eq}	298.2 (7)	14.7 (18)
d_7 C_{eq}...C_{ax}	280.7 (9)	14.7 (tied to u 10)
d_8 O_{eq}...O_{eq}	464.6 (10)	30.7 (40)
d_9 O_{eq}...O_{ax}	437.8 (16)	30.7 (tied to U 12)
d_{10} C_{eq}...O_{eq}	388.6 (8)	19.1 (13)
d_{11} C_{ax}...O_{eq}	388.6 (7)	19.1 (tied to U 14)

Table 3.3 cont.

d_{12} $C_{eq}\cdots O_{ax}$	368.2 (14)	19.1 (tied to u 14)
d_{13} $C_{met}\cdots C_{ax}$	428.7 (18)	9.5 (fixed)
d_{14} $C_{met}\cdots O_{ax}$	540.3 (20)	10.0 (fixed)
d_{15} $C_{met}\cdots C_{eq}$	287.7 (16)	14.7 (tied to u 10)
d_{16} $C_{met}\cdots O_{eq}$	366.2 (18)	19.1 (tied to u 14)
d_{17} H...Re	286.7 (16)	10.0 (fixed)
d_{18} H...C_{ax}	476.3 (18)	18.0 (fixed)
d_{19} H...O_{ax}	583.1 (18)	18.0 (fixed)
d_{20} H...H	178.9 (fixed)	9.0 (fixed)

H...C_{eq} from 265.4 to 386.7

H...O_{eq} from 314.0 to 471.3

Independent angles

$\angle 1$	(H-C-H)	110° (fixed)
$\angle 2$	(C_{ax}-Re-C_{eq})	96° (2)
$\angle 3$	(Re-C_{eq}-O_{eq})	180° (fixed)

Table 3.4 Least squares correlation matrix for $CH_3Re(CO)_5$, multiplied by 100

r1	r2	r3	<2	u1	u2	u5	u10	u12	u15	k1	k2	k3	
100	7	-2	-4	7	1	9	2	-3	-3	12	9	23	r1
	100	-30	3	19	19	-2	-24	1	4	24	-12	-21	r2
		100	11	-5	-28	-1	2	-11	-13	-27	24	49	r3
			100	-1	1	0	-71	-66	-31	7	-10	-17	<2
				100	16	5	1	3	2	25	-4	7	u1
					100	0	-4	3	4	36	-16	-3	u2
						100	7	5	-2	11	6	19	u5
							100	43	23	-14	19	27	u10
								100	54	11	-7	-19	u12
									100	9	2	-13	u15
										100	-51	-20	k1
											100	16	k2
												100	k3

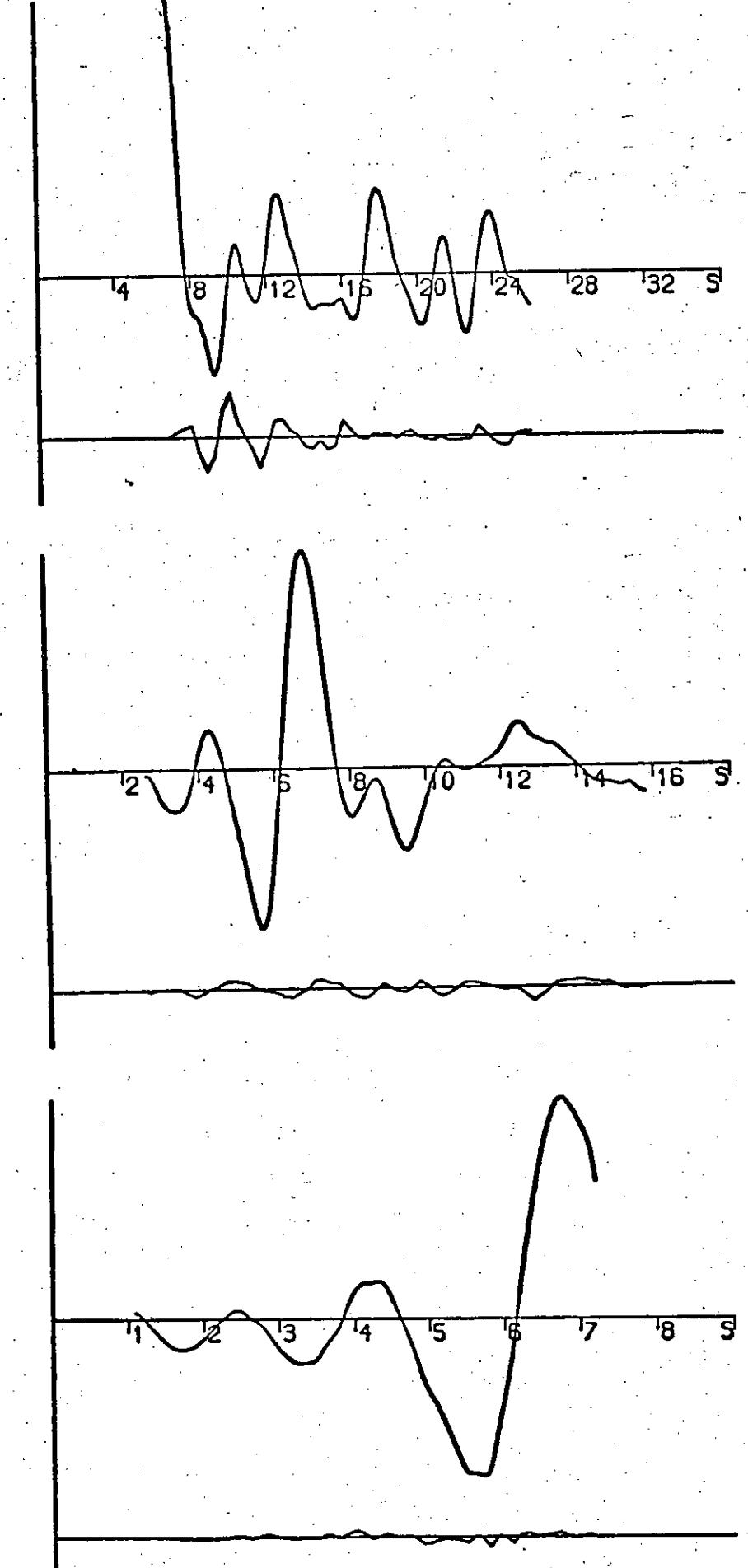

Figure 3.3. Observed and final weighted difference molecular scattering intensities for $CH_3Re(CO)_5$ obtained with nozzle-to-plate distances of 250, 500 and 1000 mm.

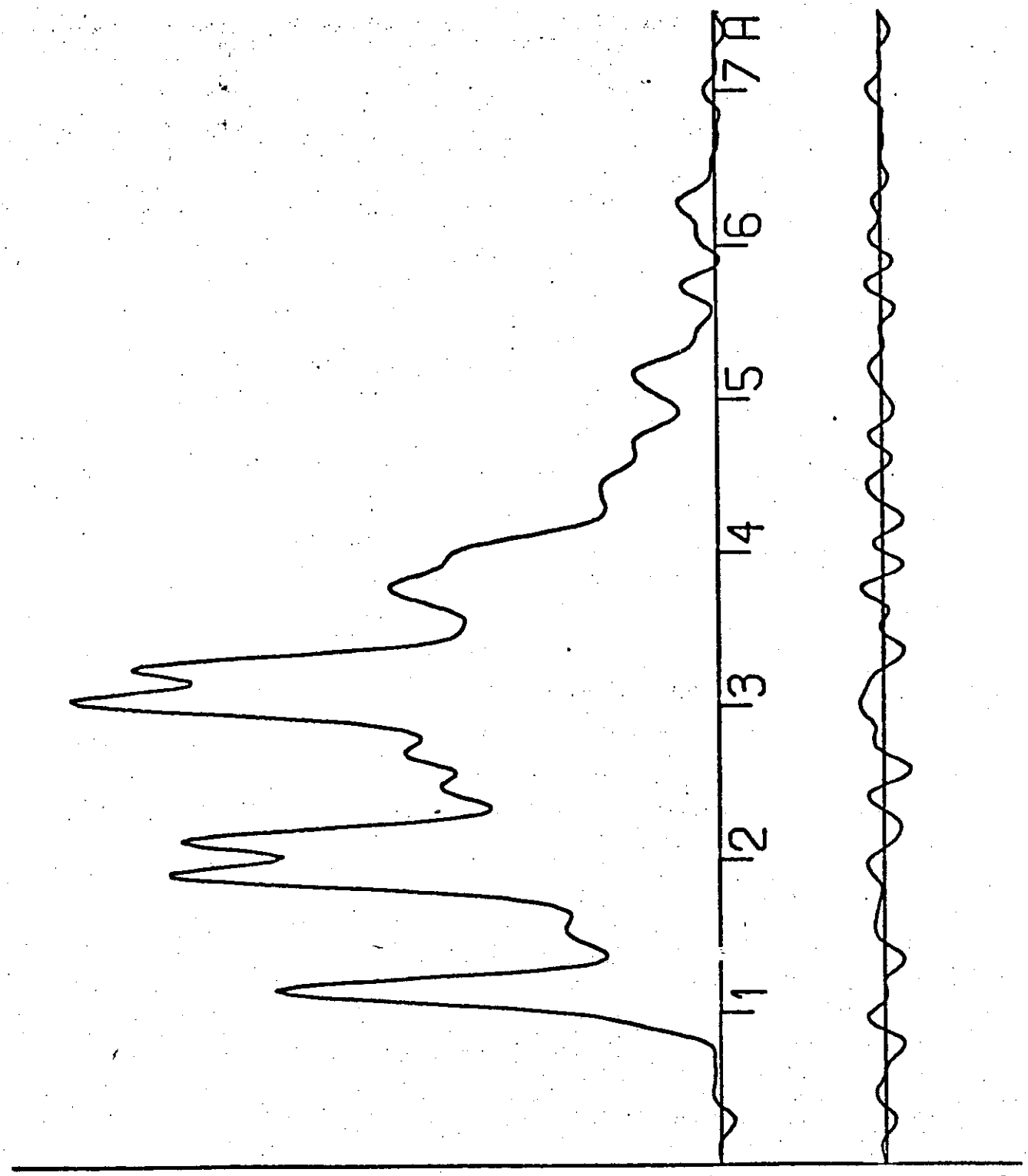

Figure 3.4 Radial distribution curve, P(r)/r, and final differences between experimental and theoretical curves for $SiH_3Re(CO)_5$. Before Fourier inversion the data were multiplied by $s.\exp(-0.000015s^2/(z_{Re}-f_{Re})(z_O-f_O))$

Table 3.5 Molecular parameters for $SiH_3Re(CO)_5$

Independant distances		distance (pm)	amplitude of vibration (pm)
r_1	C-O	113.6 (4)	5.0 (7)
r_2	Re-C	201.0 (4)	6.2 (4)
r_3	Re-Si	256.2 (12)	6.7 (16)
r_4	Si-H	151.4 (37)	8.0 (fixed)
Dependent distances			
d_1	$Re\cdots O_{ax}$	313.8 (9)	5.7 (4)
d_2	$Re\cdots O_{eq}$	313.7 (9)	5.7 (tied to u 5)
d_3	$C_{eq}\cdots O_{eq}$	511.0 (16)	9.5 (fixed)
d_4	$C_{eq}\cdots C_{eq}$	399.2 (12)	9.5 (fixed)
d_5	$O_{eq}\cdots O_{eq}$	622.2 (23)	9.5 (fixed)
d_6	$C_{eq}\cdots C_{eq}$	292.9 (7)	13.0 (fixed)
d_7	$C_{eq}\cdots C_{ax}$	283.3 (9)	13.0 (fixed)
d_8	$O_{eq}\cdots O_{eq}$	459.4 (10)	30.0 (fixed)
d_9	$O_{eq}\cdots O_{ax}$	441.4 (16)	30.0 (fixed)
d_{10}	$C_{eq}\cdots O_{eq}$	382.5 (8)	18.2 (12)
d_{11}	$C_{eq}\cdots O_{ax}$	371.3 (13)	18.2 (tied to u 14)
d_{12}	$C_{ax}\cdots O_{eq}$	384.8 (8)	18.2 (tied to u 14)

Table 3.5 cont.

d_{13}	Si...C_{ax}	455.1 (15)	11.0 (fixed)
d_{14}	Si...O_{ax}	567.3 (17)	11.0 (fixed)
d_{15}	Si...C_{eq}	315.3 (14)	20.0 (fixed)
d_{16}	Si...O_{eq}	388.8 (17)	24.2 (tied to u 14)
d_{17}	H...Re	335.4 (34)	10.0 (fixed)
d_{18}	H...C_{ax}	521.7 (38)	18.0 (fixed)
d_{19}	H...O_{ax}	627.3 (42)	18.0 (fixed)
d_{20}	H...H	248.8 (45)	10.0 (fixed)
	H...C_{eq}	from 299.1 to 447.7	
	H...O_{eq}	from 330.2 to 531.3	

Independent angles

$\angle 1$	H-Si-H	108° (fixed)
$\angle 2$	C_{ax}-Re-C_{eq}	94° (2)
$\angle 3$	O_{eq}-C_{eq}-Re	182° (2)

Table 3.6 Least squares correlation matrix for $SiH_3Re(CO)_5$, multiplied by 100

r1	r2	r3	r4	<2	u1	u2	u3	u5	u12	k1	k2	k3	
100	1	0	-12	-1	12	9	5	12	-1	17	7	9	r1
	100	-4	3	-4	12	12	6	7	-1	11	5	2	r2
		100	-10	0	-3	-3	2	5	9	-3	1	-3	r3
			100	0	-5	-7	-1	-9	1	-11	-1	-4	r4
				100	0	3	-11	4	-20	1	-12	-5	<2
					100	41	19	43	3	67	14	2	u1
						100	-3	46	2	65	14	8	u2
							100	5	4	28	2	-15	u3
								100	3	64	17	7	u5
									100	4	15	-15	u12
										100	14	1	k1
											100	-2	k2
												100	k3

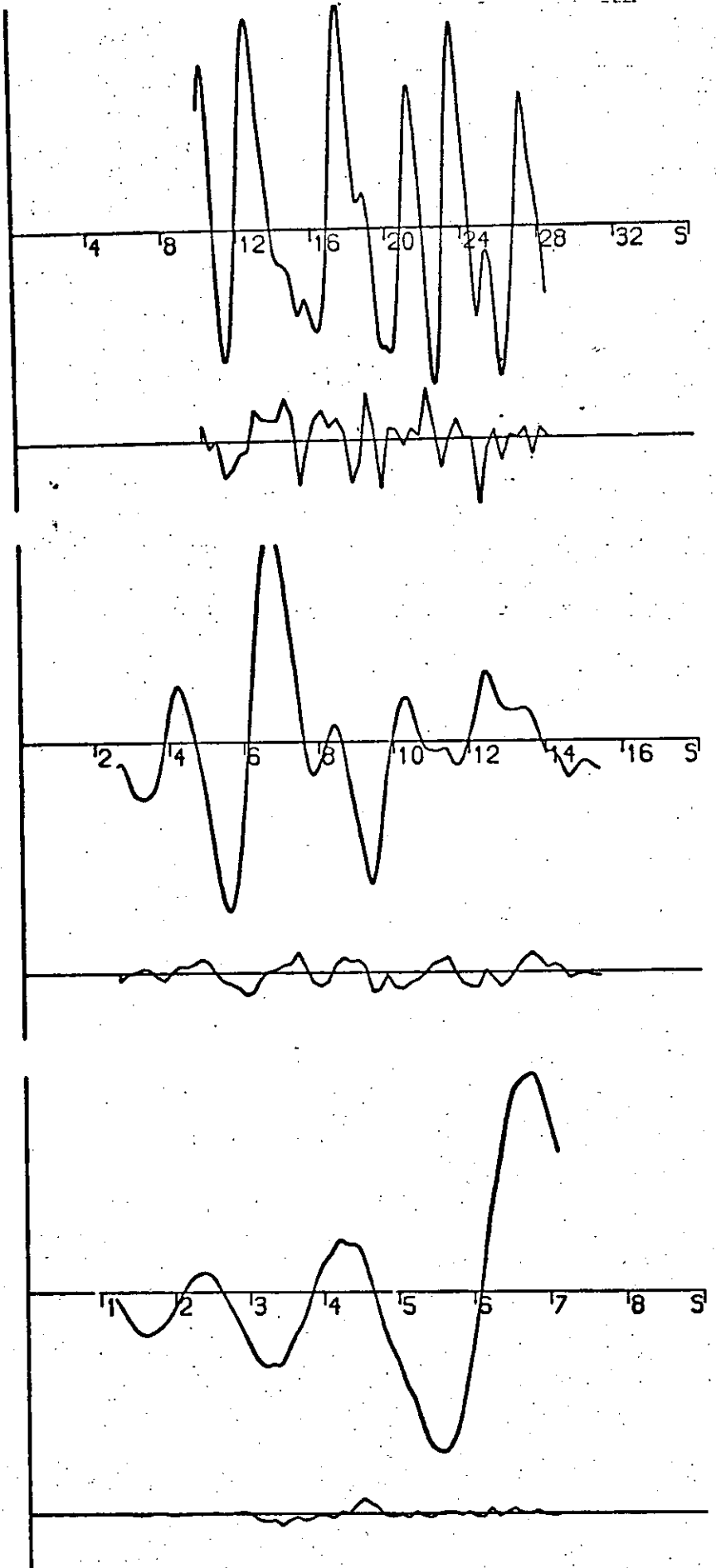

Figure 3.5 Observed and final weights difference molecular scattering curves for $SiH_3Re(CO)_5$ obtained with nozzle-to-plate distances of 250, 500 and 1000mm

b. Silylrheniumpentacarbonyl

Here all the bonded distances refined but only the amplitudes of vibration of the Re-C, Re-Si and C-O bonded distances did so satisfactorily. Both the C_{eq}-Re-C_{ax} and Re-C_{eq}-O_{eq} angles refined satisfactorily. Yet again, due to the overlapping of peaks in the radial distribution curve (figure 3.4), groups of amplitudes of vibration had to be refined as single parameters (table 3.5) though in this case only two such groups refined satisfactorily, the Re...O amplitudes of vibration and the right-angled C...O amplitudes of vibration tied to the right angled Si...O amplitude of vibration. All non-refining parameters were set at reasonable values.

The final R-factor, R_G, is 0.21, final molecular parameters are shown in table 3.5 and the final least squares correlation matrix is shown in table 3.6. In figure 3.5 are the observed and final weighted difference molecular scattering curves.

c. Germylrheniumpentacarbonyl

In this case the refinements were similar to those for $CH_3Re(CO)_5$. All bonded distances other than Ge-H refined satisfactorily and the amplitudes of vibration of the Re-C, Re-Ge and C-O bonded distances also satisfactorily refined as did both the C_{eq}-Re-C_{ax} and Re-C_{eq}-O_{eq} angles. Here also, because of overlapping of peaks in the radial distribution curve (figure 3.6), certain groups of amplitudes had to be refined as single parameters (table 3.7). All groups, other than those involving hydrogen atoms, the group consisting of linear C...C, C...O, O...O, Ge...C and Ge...O amplitudes of vibration and the group consisting of right angled O...O amplitudes of vibration, refined satisfactorily. Reasonable values were given to the non-refining parameters.

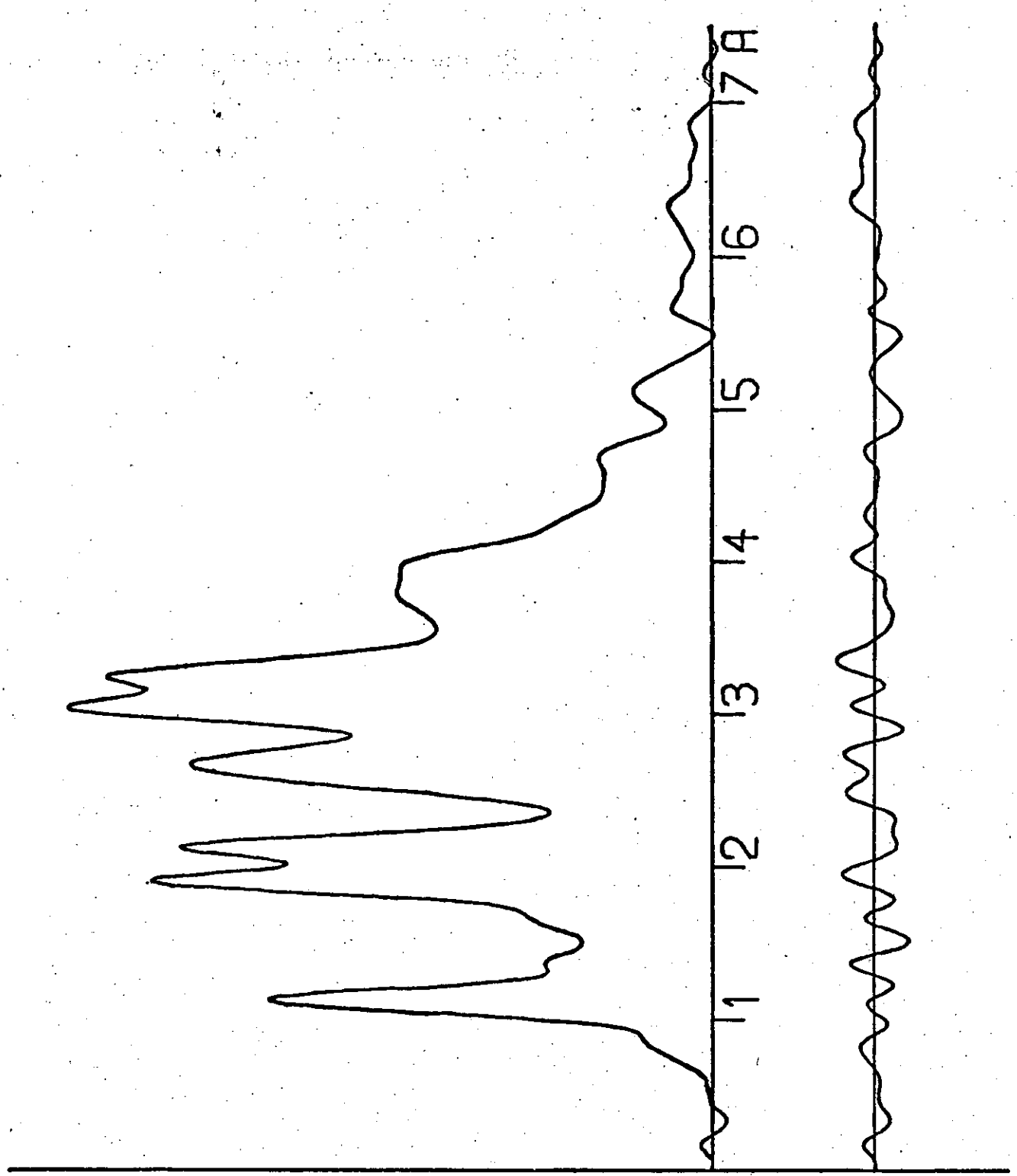

Figure 3.6 Radial distribution curve, P(r)/r, and difference curves for $GeH_3Re(CO)_5$. Before Fourier inversion the data were multiplied by $s.\exp(-0.00001s^2/(z_{Re}-f_{Re})(z_O-f_O))$

Table 3.7 Molecular parameters for $GeH_3Re(CO)_5$

Independent distances		distance (pm)	amplitude of vibration (pm)	shrinkage corrections (pm)
r_1	C-O	112.0 (5)	5.8 (7)	
r_2	Re-C	200.2 (5)	6.4 (5)	
r_3	Re-Ge	262.8 (6)	9.1 (7)	
r_4	Ge-H	152.1 (fixed)	10.0 (fixed)	
dependent distances				
d_1	$Re\cdots O_{ax}$	311.3 (9)	7.2 (6)	0.9
d_2	$Re\cdots O_{eq}$	311.2 (9)	7.2 (tied to u 5)	0.9
d_3	$C_{eq}\cdots O_{eq}$	505.1 (14)	9.5 (fixed)	3.3
d_4	$O_{eq}\cdots O_{eq}$	614.6 (10)	9.5 (fixed)	4.6
d_5	$C_{eq}\cdots C_{eq}$	395.0 (21)	9.5 (fixed)	1.9
d_6	$C_{eq}\cdots C_{eq}$	300.9 (8)	16.8 (30)	0.4
d_7	$C_{eq}\cdots C_{ax}$	280.3 (7)	16.8 (tied to u 10)	0.4
d_8	$O_{eq}\cdots O_{eq}$	465.1 (11)	30.0 (fixed)	2.1
d_9	$O_{eq}\cdots O_{ax}$	436.0 (15)	30.0 fixed)	2.1
d_{10}	$C_{eq}\cdots O_{eq}$	390.8 (8)	21.0 (13)	1.2
d_{11}	$C_{ax}\cdots O_{eq}$	366.9 (11)	21.0 (tied to u 14)	1.2

Table 3.7 cont.

d_{12}	$C_{eq}...O_{ax}$	389.3 (8)	21.0 (tied to u 14)	1.2
d_{13}	$Ge...C_{ax}$	460.9 (10)	10.0 (fixed)	2.1
d_{14}	$Ge...O_{ax}$	571.4 (13)	11.0 (fixed)	3.4
d_{15}	$Ge...C_{eq}$	308.6 (11)	22.4 (tied to u 10)	0.4
d_{16}	$Ge...O_{eq}$	381.6 (15)	28.0 (tied to u 14)	1.5
d_{17}	Re...H	346.7 (8)	10.0 (fixed)	0.9
d_{18}	$H...C_{ax}$	533.2 (11)	18.0 (fixed)	3.3
d_{19}	$H...O_{ax}$	637.8 (13)	18.0 (fixed)	4.6
d_{20}	H...H	246.6 (fixed)	10.0 (fixed)	0.10
	$H...C_{eq}$	from 298.8 to 444.8		
	$H...O_{eq}$	from 328.8 to 526.5		

Independent angles

$\angle 1$	H-Ge-H	111^{o}
$\angle 2$	C_{eq}-Re-C_{ax}	97^{o} (2)
$\angle 3$	Re-C_{eq}-O_{eq}	178^{o} (2)

Table 3.8 Least squares correlation matrix for $GeH_3Re(CO)_5$, multiplied by 100

r1	r2	r3	∠2	u1	u2	u3	u5	u10	u12	k1	k2	k3	
100	2	-2	-3	0	-2	1	-1	7	0	-3	8	15	r1
	100	-4	-6	9	9	-2	6	-3	2	5	11	7	r2
		100	3	6	9	26	-18	25	4	17	7	-4	r3
			100	-12	-13	-5	0	-39	-45	-18	-29	-25	∠2
				100	27	28	15	24	11	47	35	22	u1
					100	29	17	23	11	51	35	25	u2
						100	1	48	9	55	43	21	u3
							100	-13	2	33	15	11	u5
								100	27	33	54	50	u10
									100	17	22	7	u12
										100	42	30	k1
											100	34	k2
												100	k3

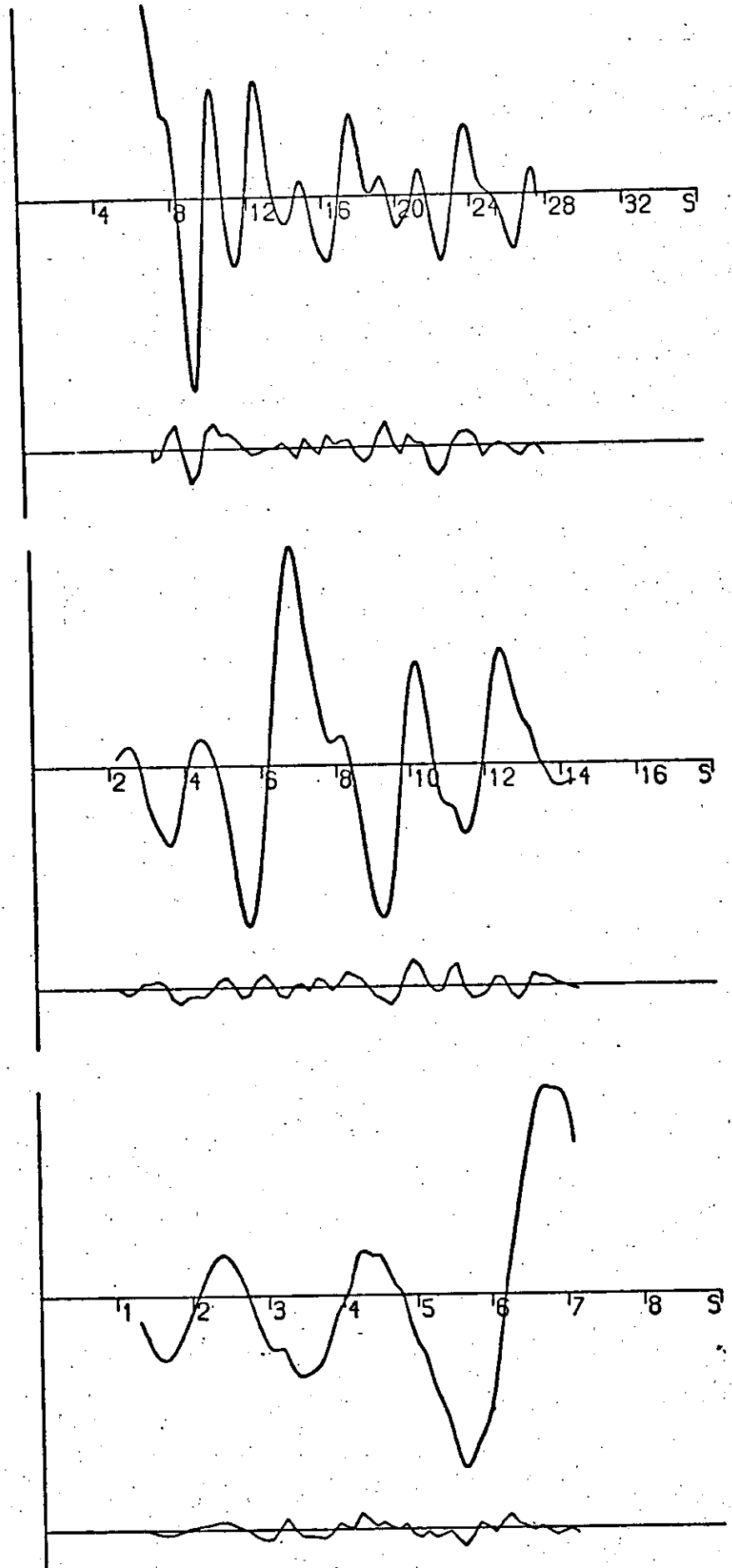

Figure 3.7 Molecular scattering intensity and difference curves for $GeH_3Re(CO)_5$ obtained with nozzle-to-plate distances of 250, 500 and 1000mm.

The final R-factor, R_G, was 0.220; the final molecular parameters are in table 3.7; the least squares correlation matrix is in table 3.8; figure 3.7 gives the observed and final weighted difference molecular scattering curves.

In all of these molecules there are atom pairs of widely differing atomic numbers and, as is usual in such cases, the tabulated phase angles (η) are inadequate. Here cubic functions were derived from the tabulated values of Schäfer, Yates and Bonham[86] and used to calculate the phase angles. The phase shift for the i-j atom pair is given by

$$\eta_i - \eta_j = a_i - a_j + (b_i - b_j)s + (c_i - c_j)s^2 + (d_i - d_j)s^3.$$

This can be written as:

$$\Delta\eta = \pi/2 + \Delta b'(s-s_c) + \Delta c'(s-s_c)^2 + \Delta d'(s-s_c)^3.$$

where s_c is the point where $\cos \Delta\eta = 0$.

The calculated values of s_c for Re-C, Re-O, Re-H, Re-Si and Re-Ge atom pairs were 140, 147, 117, 179 and 333 nm^{-1}. In all three structure determinations the Re-C and Re-O values for s_c were allowed to refine. The optimum s_c values for Re-C and Re-O were 131 nm^{-1} and 138 nm^{-1} and the s_c values for Re-H, Re-Si and Re-Ge were adjusted accordingly to 108, 170 and 324 nm^{-1} respectively.

The same shrinkage corrections were applied to all three rheniumpentacarbonyl derivatives. The values were derived from those used in the structure determination of $PF_3Mo(CO)_5$[79] and are given in table 3.7.

3.3 Discussion

By assuming that the $Re-C_{met}$ bond in $CH_3Re(CO)_5$ is a pure σ bond, a value for the covalent radius of rhenium in rheniumpentacarbonyl compounds can be calculated from $r(Re-C_{met})$ in $CH_3Re(CO)_5$ and r(C-C) in ethane. This value, 154.1 pm, is fairly similar to that derived from

r(Re-Re) in $Re_2(CO)_{10}$[89] and, with the covalent radii of Si and Ge described in chapter 2, is used to predict the Re-Si and Re-Ge bond lengths in $SiH_3Re(CO)_5$ and $GeH_3Re(CO)_5$. Both these predicted bond lengths are substantially longer than those actually observed (table 3.9). However the differences between observed and predicted metal-metal bond lengths in $SiH_3Re(CO)_5$ and $GeH_3Re(CO)_5$ are less than differences between observed and predicted metal-metal bond lengths in $SiH_3Mn(CO)_5$ and $GeH_3Mn(CO)_5$. Such observations are consistent with the published metal-metal bond energies of methyl-, silyl-, and germyl- derivatives of manganese and rheniumpentacarbonyl which indicate that the Re-C_{met} bond in $CH_3Re(CO)_5$ is stronger relative to the Si-Re and Ge-Re bonds in silyl- and germyl-derivatives of rheniumpentacarbonyl than the Mn-C_{met} bond in $CH_3Mn(CO)_5$ is relative to the Mn-Si and Mn-Ge bonds in silyl- and germyl derivatives of manganesepentacarbonyl[28, 29, 90].

In chapters 1 and 2 it was shown that the PE spectra and molecular structures of some methyl-, silyl- and germyl- manganesepentacarbonyl complexes indicated that $(d \rightarrow d)\pi$ bonding was unimportant in silyl- and germyl-manganesepentacarbonyl complexes and that the main change in substituting a methyl- group by a silyl- or germyl-group on manganesepentacarbonyl was to increase the σ-acceptor power of the ligand. If $(d \rightarrow d)\pi$ bonding were important in Si-Re and Ge-Re bonds of rhenium-pentacarbonyl complexes it therefore would be reasonable to expect the Si-Re and Ge-Re bonds of silyl- and germyl-derivatives of rheniumpentacarbonyl to be shorter and stronger relative to the C_{met}-Re bond of $CH_3Re(CO)_5$ than are the Ge-Mn and Si-Mn bonds of silyl- and germyl- derivatives of manganesepentacarbonyl relative to the C_{met}-Mn bond in $CH_3Mn(CO)_5$. The reverse is in fact the case and this seems to be a strong indication of the

Table 3.9 Comparison of observed and calculated Re-Ml distances (pm)

	r(Re-Ml) observed	r(Re-Ml) calculated
$SiH_3Re(CO)_5$	256.2	264.2
$GeH_3Re(CO)_5$	262.8	271.9

unimportance of $(d \rightarrow d)\pi$ in silyl- and germyl-rheniumpentacarbonyl derivatives.

A possible explanation for the relatively strong and short $Re-C_{met}$ bond in $CH_3Re(CO)_5$ could be that the $Re(CO)_5$ group is a less strong σ- donor than the $Mn(CO)_5$ group. Alternatively there may be some steric interaction between the $Mn(CO)_5$ group and CH_3 group in $CH_3Mn(CO)_5$. This would likely be greater than such interaction between the methyl and rheniumpentacarbonyl groups of $CH_3Re(CO)_5$ owing to the longer C-Re bonds.

The $Re(CO)_5$ group changes little with substituent. The $Re-C_{carbonyl}$ bond lengths are virtually the same in all three molecules and even the $C_{ax}-Re-C_{eq}$ angles lie within experimental error.

CHAPTER FOUR

Electron Diffraction Determination of the molecular Structure of hexafluorodisilane in the gas phase

CHAPTER 4

Molecular structure of Hexafluorodisilane.

The He^{I} photoelectron spectra of hexafluorodisilane and disilane indicate that in hexafluorodisilane the electrons involved in the Si-Si σ bond are more tightly bound than those in disilane[91]. Substitution of fluorines for hydrogens in silylmanganesepentacarbonyl has a similar effect in that the photoelectron spectra of $SiF_3Mn(CO)_5$ and $SiH_3Mn(CO)_5$ indicate that the electrons in the Mn-Si σ bond are more tightly bound in $SiF_3Mn(CO)_5$ than in $SiH_3Mn(CO)_5$ (chapter 1). The molecular structures of both $SiF_3Mn(CO)_5$ and $SiH_3Mn(CO)_5$ have been determined (chapter 2) and the Si-Mn bond length is substantially shorter in the case of $SiF_3Mn(CO)_5$. The molecular structure of Si_2F_6 has therefore been determined to find whether the relationship between the binding energy of the Si-Si σ bonding levels in Si_2F_6 and Si_2H_6 and the Si-Si bond lengths in these compounds is like that between the binding energy of the Si-Mn σ bonding levels and the Si-Mn bond lengths in $SiH_3Mn(CO)_5$ and $SiF_3Mn(CO)_5$.

The electron diffraction data for Si_2F_6 was obtained on the Balzer's KD.G2 instrument at the University of Manchester Institute of Science and Technology with the nozzle temperature at 298K and the sample at 209K. Three nozzle-to-plate distances were used, 1000mm, 500mm and 250mm, giving data over a range of scattering variable, s, from 10 to 292 nm^{-1}. The complex scattering factors of Cox & Bonham were used[81]. The molecular parameters are shown in table 4.1 and the least squares correlation matrix in table 4.2. The lowest R-factor (RG) was 0.08 and the combined molecular scattering and difference curves (figure 4.1) and the radial distribution curve (figure 4.2) are from after that refinement. Errors quoted are least squares derived standard deviations with allowances for systematic errors. The twist angle between

Table 4.1 Molecular parameters for Si_2F_6

		distance (pm)	amplitude of vibration (pm)
Independent distances			
r_1	Si-Si	232.4 (6)	6.8 (7)
r_2	Si-F	156.9 (2)	4.7 (2)
Dependent distances			
d_1	F...F	254.5 (7)	8.1 (3)
d_2	Si...F	322.4 (6)	11.0 (3)
d_3	F...F	353.5 (6)	17.3 (21)
d_4	F...F	393.3 (6)	20.5 (24)
d_5	F...F	446.7 (8)	14.4 (10)
Independent angles			
$\angle 1$	F-Si-Si	110.6° (3)	
$\angle 2$	twist	34.6° (see text)	
Dependent angle			
	$\hat{F}$-Si-F	113°	

Table 4.2 Least squares correlation matrix for Si_2F_6 multiplied by 1000

R1	R2	ζ1	U1	U2	U3	U4	U5	U6	U7	K1	K2	K3
1000	22	-253	73	-106	78	-101	-98	-13	-63	-93	-151	-68
	1000	8	27	-26	28	-12	-7	6	6	-17	6	42
		1000	-7	-16	-88	45	258	-23	215	-27	-67	-67
			1000	106	507	50	10	16	11	133	86	57
				1000	267	279	-1	81	11	703	428	109
					1000	153	2	44	-3	353	287	110
						1000	587	126	313	344	278	112
							1000	167	664	-14	1	59
								1000	252	99	85	69
									1000	20	-26	-74
										1000	370	100
											1000	87
												1000

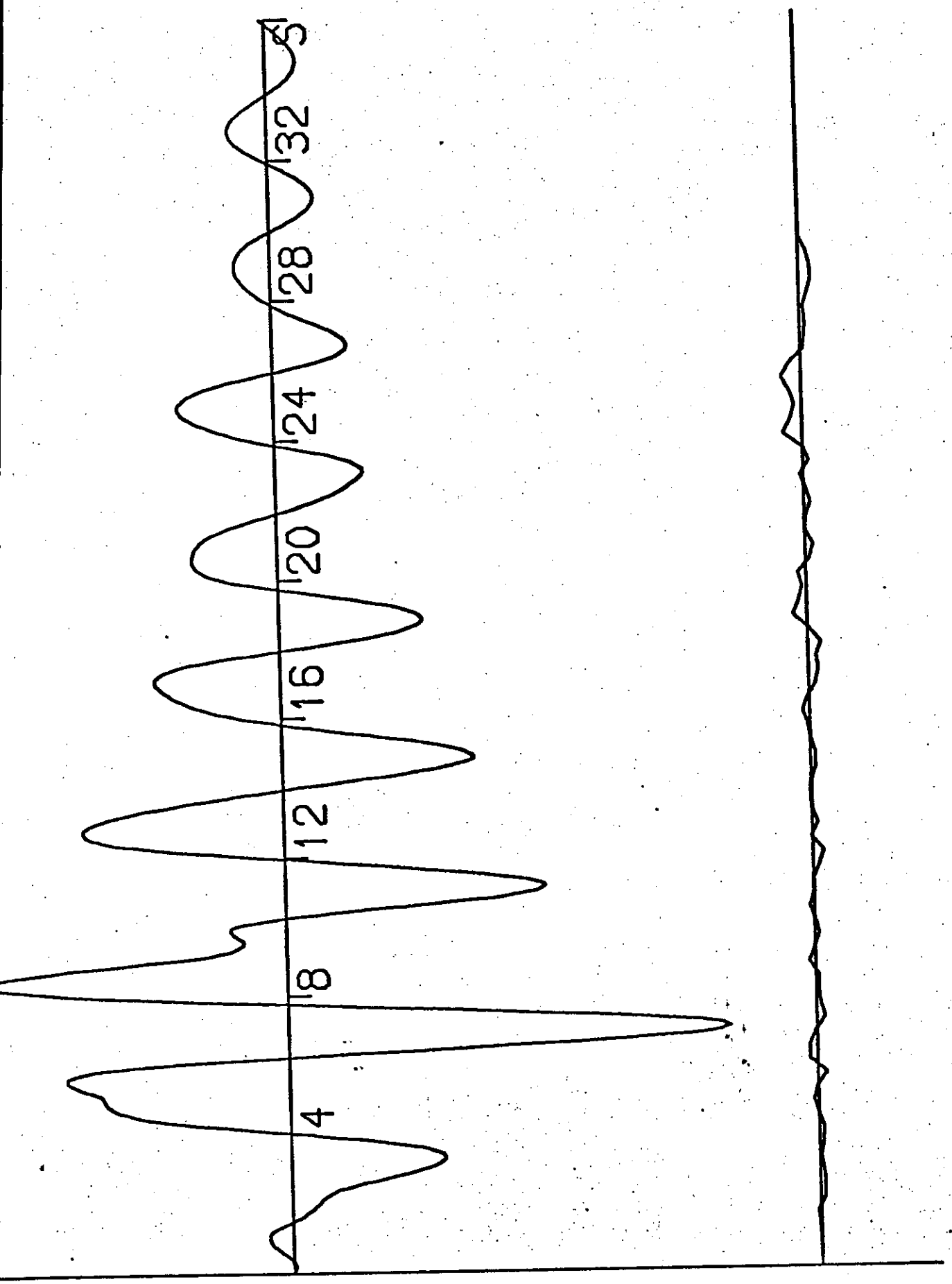

Figure 4.1 Combined molecular scattering and differencecurves for Si_2F_6. In regions where the sum of weights for the 250, 500 and 1000mm data sets was less than 1 theoretical intensity has been included.

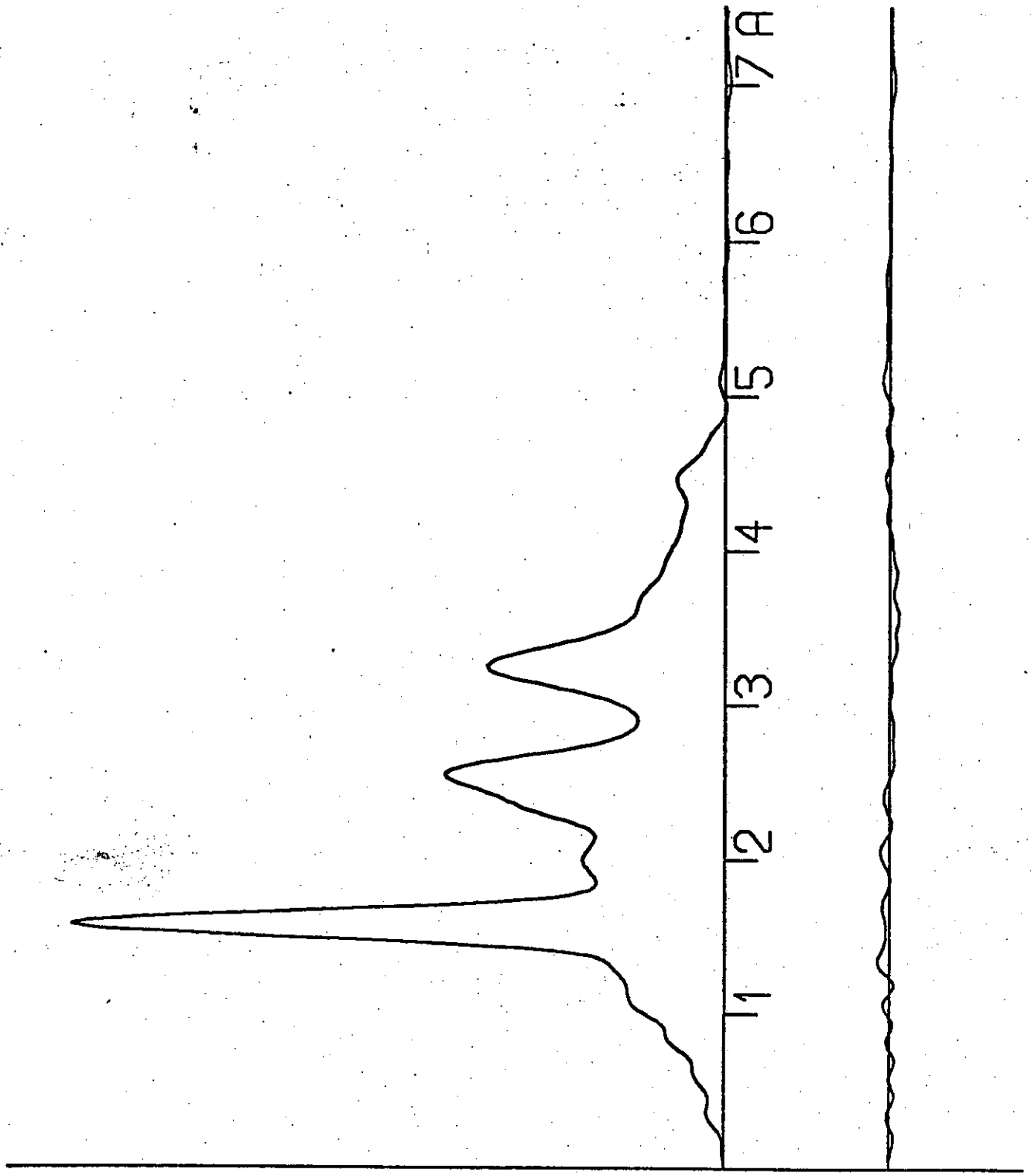

Figure 4.2 Radial distribution curve, P(r)/r and difference curve for Si_2F_6. Before Fourier inversion the data were multiplied by $s.\exp((-0.000025s^2)/(z_{Si}-f_{Si})(z_F-f_F))$

the SiF_3 groups was determined by comparison of R-factors in refinements where that angle was fixed at values between 0° (eclipsed) and 60° (staggered). The twist angle was then fixed at the optimum value.

The Si-Si bond length was found to be 232.4 $\pm$ 0.6 pm, only slightly shorter than in Si_2H_6 (r(Si-Si) = 233.1pm $\pm$ 0.3pm)[92] and Si_2Me_6 (r(Si-Si) = 234.0 $\pm$ 0.9 om)[93]. The high binding energy of the Si-Si σ bonding level in Si_2F_6 therefore does not manifest itself in a short Si-Si bond unlike the case of $SiH_3Mn(CO)_5$ and $SiF_3Mn(CO)_5$ where the higher binding energy of the Si-Mn σ bonding level in $SiF_3Mn(CO)_5$ is reflected in a shorter Si-Mn bond length. In Si_2F_6 it may be that any contraction effect of the fluorines on the Si-Si bond length is almost completely counter balanced by electrostatic repulsion between the two SiF_3 groups.

The molecular structures and PE spectra of Si_2H_6 and Si_2F_6 show the dangers of relating bond lengths to the I.P. of electrons in the appropriate σ bonding levels even where no π bonding is likely.

The Si-F bond length in Si_2F_6 is very similar to that in SiF_3H (156.9 pm in Si_2F_6 and 156.5 in SiF_3H) and the other parameters were very much as expected.

CHAPTER FIVE

Conclusions and Suggestions for further Work

CHAPTER 5

5.1 Conclusions

As was demonstrated in chapter 4, even when no π bonding is likely, there is no relationship between the ionisation potential of electrons from the σ bonding level and the bond length of that bond. One of the main consequences of this is that the molecular structure is no help in the assignment of peaks in the PE spectrum.

However, these PE spectra and molecular structures are consistent with (d → d) π bonding being unimportant in the metal-metal bonds of silyl- and germyl- manganesepentacarbonyl and rheniumpentacarbonyl derivatives. They are more consistent with the main effect of substituting a methyl-group by a silyl- or germyl- group or of halogenating a methyl-, silyl- or germyl group on manganesepentacarbonyl or rheniumpentacarbonyl being to increase the σ acceptor power of the ligand. The unusual order of σ acceptor powers found for methyl-, silyl- and germyl- groups bound to manganese- or rhenium- pentacarbonyl ($CH_3 \ll GeH_3 \leqslant SiH_3$) may be due to the strong σ donor properties and large σ bonding orbital of these transition metal pentacarbonyl groups and may be a reflection of the polarisabilities of the methyl-, silyl-, and germyl- groups.

One possible reason for the apparent unimportance of (d → d) π bonding in these silyl- and germyl- derivatives of manganese and rhenium pentacarbonyl is that since the carbonyl group trans to the silyl- or germyl- group is a strong π acceptor the Mn 3d e or Re 5d e electrons are not available for π backbonding with the silicon or germanium atoms. Ibers suggested the reverse of this, ie., in silyl-transition metal complexes (d→d) π bonding is most important when the group trans to the silyl group is not a strong π acceptor,

as a reason for the short Si-Rh bond in $SiCl_3RhHCl(P(C_6H_5)_3)_2$[42]. That $(d \rightarrow d)\pi$ bonding appears unimportant in silyl- and germyl- manganese and rhenium pentacarbonyl derivatives is consistent with conclusions drawn from the Sn-Fe bond lengths of $SnPh_3Fe(CO)_2(C_5H_5)$, $SnCl_3Fe(CO)_2(C_5H_5)$ and $SnBr_3Fe(CO)_2(C_5H_5)$ [38]. These bond lengths were taken as indicating that the Sn-Fe bonds were all purely σ bonds. The finding that halogenation of a methyl, silyl or germyl group on a manganese- or rhenium- pentacarbonyl group greatly affects the metal-metal σ bonds is also consistent with ^{119}Sn Mossbauer spectra of a wide range of Sn(IV) transition metal carbonyl complexes[64]; these spectra indicate that halogenation of a trialkyl or triaryl stannyl group increases the σ acceptor power of that group. However, conclusions on the nature of metal-metal bonds in Group IVB transition metal carbonyl compounds, based on force field [24, 25] and force constant[14,15, 18,19] calculations are generally in disagreement with the above findings in that differences in force constants in different silyl- and germyl- transition metal carbonyls are normally assigned to differences in $(d \rightarrow d)\pi$ bonding in the metal-metal bonds. There is, however, some doubt as to the validity of the conclusions on metal-metal π bonding based on these calculations.

Little can be concluded from the PE spectra and molecular structures of the Group IVB cobalttetracarbonyl derivatives described in chapters 1 and 2. The metal-metal bond lengths of silyl- and germyl- cobalttetracarbonyl are reduced more by halogenation of the silyl- or germyl- group than the metal-metal bonds of silyl- and germyl- manganesepentacarbonyl. This could result from an increase in $(d \rightarrow d)\pi$ bonding in Si-Co and Ge-Co bonds on halogenation but fluorination of $CH_3Mn(CO)_5$ results in a shortening of $Mn-C_{met}$ [30,31] bond length similar to that observed in r(Si-Co) on fluorination of $SiH_3Co(CO)_4$[23,41]. It also seems difficult to justify

$(d \rightarrow d)\,\pi$ bonding in silyl- and germyl- derivatives of cobalttetracarbonyl from the evidence presented in this work when such bonding is apparently unimportant in silyl- and germyl- derivatives of manganesepentacarbonyl.

5.2 Suggestions for further work.

The molecular structures of $CF_3Re(CO)_5$ and $SiF_3Re(CO)_5$ and the PE spectrum of the former would be useful for comparison with those of analogous manganesepentacarbonyl compounds as they may indicate whether the rheniumpentacarbonyl and manganesepentacarbonyl systems are as similar as they appear from the limited amount of data so far available. They may also give some more information on the nature of the metal-metal bonds in rheniumpentacarbonyl complexes.

An accurate structure determination is still required for silylcobalttetracarbonyl. The molecular structures of methyl- and trifluoromethyl- cobalttetracarbonyl could also be very useful. If the difference between the cobalt-methylcarbon bond lengths in these two compounds is greater than, or as great as, the difference in r(Si-Co) for silyl- and trifluorosilyl- cobalttetracarbonyl it would seem reasonable to assume that the shortening of r(Si-Co) on fluorination is not due to $(d \rightarrow d)\,\pi$ bonding. If, however, the shortening in r(Si-Co) on fluorination of silylcobalttetracarbonyl is greater than that in r(Co-C) on fluorination of methylcobalttetracarbonyl it would be probable that $(d \rightarrow d)\,\pi$ bonding is important in the Co-Si bonds. The PE spectra of $CF_3Co(CO)_4$, $SiCl_3Co(CO)_4$ and $GeCl_3\ Co(CO)_4$ may also be useful in determining the nature of Si-Co and Ge-Co bonds. The molecular structures of trans tetracarbonyl-(triphenylphosphine) silylmanganese (I) and the corresponding germyl- compound would be interesting. Triphenylphosphine groups are generally accepted as poorer π acceptors than

carbonyl groups so, if Ibers' hypothesis on (d→d) π bonding in silicon-transition metal bonds[42] is correct, the Si-Mn and Ge-Mn bonds will be more strongly π bonded and shorter in these compounds than in the corresponding manganesepentacarbonyl compounds. These structures, therefore, may also give some more insight into the nature of bonding in the Si-Mn and Ge-Mn bonds of $SiH_3Mn(CO)_5$ and $GeH_3Mn(CO)_5$.

CHAPTER SIX

Experimental Techniques

CHAPTER 6

6.1 General Experimental Methods

All volatile compounds were handled in a Pyrex glass vacuum system. This was largely conventional though one section of traps and take-off points was fitted with Sovirel greaseless taps. The greaseless taps proved especially useful in the transferring of compounds with low vapour pressures (less than about 1cm. Hg) at room temperature as these dissolve in grease. Involatile, air sensitive solids were handled under oxygen-free nitrogen in a dry-bag. Reactions and preparations were carried out in greaseless tap ampoules. Volatile compounds were normally purified by trap to trap condensation and less volatile compounds by sublimation under vacuo. Purities were checked by i.r., Raman and mass spectra and n.m.r.

Instrumentation

Low resolution infra-red spectra were recorded using a Perkin-Elmer 457 infra-red spectrometer. Spectra were recorded in the normal manner. Raman spectra were recorded with a Cary 83 spectrometer using argon ion excitation at 488 nm. Samples were studied in solution or as solids. A Varian Associates HA100 (operating at 100MHz for ^1H) was used to record nuclear magnetic resonance spectra. Mass spectra were obtained on an A.E.I. MS909 spectrometer. Photoelectron spectra were recorded on a Perkin Elmer PS16 spectrometer some details of which are given in 6.2.

Some details of instrumentation and data treatment used in electron diffraction studies are given in 6.3.

6.2 Photoelectron Spectrometer

The photon source of the spectrometer is an air cooled helium discharge lamp. Since 98% of the emission from this source is of energy 21.22 ev (584 Å wavelength) a monochromator is not necessary. A fine capillary tube connects the target chamber, where photoionisation occurs, to the lamp and this capillary allows radiation to pass out while minimising the diffusion of helium, which is continuously pumped from the lamp, into the target chamber. Electrons resulting from photoionisation are passed through a 1mm slit into the analyser which consists of two concentric plates. Varying the potential between these plates allows electrons of different kinetic energies to be deflected through a variable slit. This slit is adjusted to an optimum width so a balance between high resolution and high sensitivity is obtained. After passing through this slit the electrons pass into an electron multiplier and counting system. The main chamber, (target chamber, analyser and electron multiplier) is kept at 10^{-5} torr by continuous pumping with an oil diffusion pump and an oil rotary pump.

Volatile samples were introduced into this system through a Hoke needle valve from a conventional pyrex glass vacuum system with rotaflo greaseless taps. Most of the compounds studied in this work were sufficiently volatile to be introduced into the spectrometer in this manner. Care had to be taken to ensure no water was adsorbed on the needle valve as, on desorption, it either destroyed the sample or interfered with the spectra obtained. Less volatile compounds were introduced directly into the target chamber by sublimation from a heated probe inside that chamber.

Spectra were recorded using a variable count rate (up to 5000 counts per second) and a slow chart speed to give maximum resolution. Because of charge buildup the spectra were always calibrated in the presence of the sample. This

was done using the doublet peaks of argon at 15.75 ev and 15.93 ev., a reservoir of argon being present in the spectrometer for this purpose.

6.3 Electron diffraction programmes and data treatment.

Electron diffraction scattering data were obtained on photographic plates using Balzer's KDG2 apparatus at either the University of Manchester Institute of Science and Technology[74] or Oslo University[76, 77].

The data from Manchester were digitised on a Joyce-Loebl Microdensitometer and subsequently reduced to molecular scattering curves using a data reduction programme based on one written by Dr. G. M. Sheldrick and Dr. A. G. Robiette[94]. This programme centres the microdensitometer traces, applies corrections for blackness, sector profile and plate planarity, combines the individual traces, subtracts coherent atomic scattering, carries out further levelling by subtracting a fitted cubic and finally applies a seven point smoothing function to the molecular scattering curves thus obtained. The data from Oslo were received as uphill curves having been digitised and reduced to that state in Oslo. Further data reduction to molecular scattering curves was carried out using the above programme.

At this stage a background was subtracted to allow for incoherent atomic scattering and extraneous scattering. Minor background corrections were made later.

The least squares refinement programme used was a development of a programme, Minieldi[94] written by Dr. D. W. H. Rankin and Dr. A. G. Robiette, Minieldi was, itself, developed from Eldi[94], which in turn was based on a Hedberg[95] programme which used a standard full matrix iterative least squares procedure.

The refinements are based on molecular scattering

intensities calculated using the formula

$$I_{calc.} = \sum_{ij}(Z_i - f_i)(Z_j - f_j) \cos(\eta_i - \eta_j)\sin(s(r_{ij} - K_{ij}s^2)) \exp(-u_{ij}s^2/2)/r_{ij}s$$

$$= \sum_{ij} A_{ij} \sin(s(r_{ij} - k_{ij}s^2)) \exp(-u_{ij}s^2/2)\, r_{ij}s$$

where Z_i is the atomic number of the atom, i, f_i its scattering factor at scattering angle, s, $(\eta_i - \eta_j)$ is the phase shift of scattering from the ij atom pair at scattering angle, s, r_{ij} is the interatomic distance of the ij atom pair, K_{ij} is an asymmetry constant for the ij atom pair and u_{ij} is the mean amplitude of vibration of the ij atom pair.

In most cases the phase shift was calculated using the expression:

$$\eta_i - \eta_j = a_i - a_j + (b_i - b_j)s + (c_i - c_j)s^2 + (d_i - d_j)s^3$$

the coefficients a, b, c and d being calculated from tabulated values of phase angles. If these values proved inadequate the phase shift was calculated from refined values of s_c where s_c is the scattering angle where $\cos(\eta_i - \eta_j)=0$ The formula used was:

$$\eta_i - \eta_j = \pi/2 + \Delta b'(s-s_c) + \Delta c'(s-s_c)2 + \Delta d'(s-s_c)^3.$$

Values of K_{ij} were not refined but were set equal to $al^4/6$ where a is a cubic anharmonic constant which was normally set at 2 for bonded distances and zero for non-bonded distances. To allow for correlation between adjacent data points an off diagonal weight matrix was used. If data ran from s_{min} to s_{max} for a particular nozzle to plate distance, t, then two weighting points, s_1 and s_2, could be chosen by inspection. The elements of the weight matrix, W, were therefore written

$$w_{ii} = (s_i - s_{min})/(s_1 - s_{min}) \quad s_{min} \leq s_i \leq s_1$$

$$w_{ii} = 1 \quad s_1 \leq s_i \leq s_2$$

$$w_{ii} = (s_{max} - s_i)/(s_i - s_2) \quad s_2 \leq s_i \leq s_{max}$$

$$w_{ij} = 0 \quad i \neq j \pm 1$$

$$w_{ij} = 0.5(w_{ij} + w_{jj})/(P/h)_t \quad i = j \pm 1$$

$(P/h)_t$ is the correlation parameter for nozzle to plate distance, t, and was calculated by the method of Murato and Morino[96].

For refinements, in all the electron diffraction work

in this thesis, the data were interpolated in s intervals 1, 2 and 4 nm^{-1} for nozzle to plate distances of 1000, 500 and 250 mm respectively as these intervals gave reasonable values for calculated errors. Quoted errors also include increments which allow for systematic errors such as in the measurements of the wavelength. The wavelength was measured from the diffraction pattern of powdered thallous chloride and direct measurement of the accelerating voltage or by determination of the molecular structure of benzene.

Two R-factors were calculated in this programme

$$R_G = (\tilde{U}WU/\tilde{I}WI)^{\frac{1}{2}}$$

and

$$R_D = (\sum w_{jj}U_j^2 / \sum w_{jj}I_j^2)^{\frac{1}{2}}$$

where I is the vector of intensities and U that of residuals W is the weight matrix with elements w_{jk}.

Use of this programme allowed refinements of all independent distances and angles, all amplitudes of vibration and all scale factors. Provision was made for refinement of groups of amplitude of vibration as single parameters. The individual amplitudes within such a group were either held equal to, or at a fixed ratio to, one another. This constraint was especially useful in the larger molecules studied here.

The plotting programme plotted the molecular scattering intensities and the weighted differences between observed and calculated molecular scattering curves. This programme also calculated and plotted the radial distribution curves P(r) and P(r)/r by Fourier inversion. The distances quoted are r_a^{97} and correspond to the centres of gravity of the peaks in P(r)/r

6.4 Preparation of starting materials

compound	method	reference
SiH_3Br	$PhSiCl_3$ + $LiAlH_4$ then HBr	98
SiH_3Cl	SiH_3Br + $HgCl_2$ (streaming)	99
SiH_3I	$(SiH_3)_3N$ + HI	100

SiF_3H	$SiCl_3H + SbF_3$	101
Si_2F_6	$Si_2Cl_6 + SbF_3$ with $SbCl_5$ catalyst	101
GeH_4	$GeO_2 + NaBH_4$ (acid conditions)	103
GeH_3Cl	$GeH_4 + SnCl_4$	104
GeH_3Br	$GeH_3Cl + HBr$	105
GeH_3F	$GeH_3Br + PbF_2$ (streaming)	
HI	$HI_{aq} + P_2O_5$	106
$NaMn(CO)_5$	$Mn_2(CO)_{10} + Na/Hg$	107
$HMn(CO)_5$	$NaMn(CO)_5 + HBr$	107
$SiH_3Mn(CO)_5$	$NaMn(CO)_5 + SiH_3I$	11
$SiCl_3Mn(CO)_5$	$Mn_2(CO)_{10} + SiCl_3H$	108
$SiF_3Mn(CO)_5$	$Mn_2(CO)_{10} + SiF_3H$	109
$GeH_3Mn(CO)_5$	$NaMn(CO)_5 + GeH_3Br$	12
$GeMe_3Mn(CO)_5$	$NaMn(CO)_5 + GeMe_3Cl$	110
$NaCo(CO)_4$	$Co_2(CO)_8 + Na/Hg$	111
$HCo(CO)_4$	$NaCo(CO)_4 + HCl$	112
$SiH_3Co(CO)_4$	$NaCo(CO)_4 + SiH_3I$	5
$SiF_3Co(CO)_4$	$Co_2(CO)_8 + SiF_3H$	113
$SiMe_3Co(CO)_4$	$Co_2(CO)_8 + SiMe_3H$	4
$GeH_3Co(CO)_4$	$NaCo(CO)_4 + GeH_3Br$	8
$GeF_3Co(CO)_4$	$SiMe_3Co(CO)_4 + GeF_4$	114
$NaRe(CO)_5$	$Re_2(CO)_{10} + Na/Hg$	115
$HRe(CO)_5$	$HBr + NaRe(CO)_5$	116
$CH_3Re(CO)_5$	$NaRe(CO)_5 + CH_3I$	117
$SiH_3Re(CO)_5$	$NaRe(CO)_5 + SiH_3Br$	a
$SiF_3Re(CO)_5$	$Re_2(CO)_{10} + SiF_3H$	109
$GeH_3Re(CO)_5$	$NaRe(CO)_5 + GeH_3Br$	115

a see section 6.5

$Mn_2(CO)_{10}$, $Co_2(CO)_8$ and $Re_2(CO)_{10}$ were obtained commercially as were the compounds used other than those listed above.

The following solvents were used and purified as shown below.

diethylether	dried over sodium wire and distilled
tetrahydrofuran	dried over $LiAlH_4$ and distilled.
benzene	Analar grade, dried over sodium wire and distilled.

dichloromethane	distilled off type 4A molecular sieve.
tetramethylsilane	distilled.

6.5 Preparation and Properties of pentacarbonylsilylrhenium(I)

A solution of $Re_2(CO)_{10}$ (1.0g., 1.5mmoles) in 20 ml. tetrahydrofuran was shaken with 4ml sodium amalgam (0.1g, 4.4 mmole sodium) for 4 hours in vacuo. Excess sodium amalgam was poured off under vacuum. SiH_3Br (0.44g, 4.0 mmole) was distilled into the reaction mixture at -196°C. The mixture was allowed to warm to room temperature and left for 3 hours ; the deep red colour of the $NaRe(CO)_5$ solution faded and a white precipitate was observed. All volatiles were then pumped for several hours through a series of traps the first at -46°C , the second at -78°C and the third at -196°C. A white solid stopped in the first trap with SiH_4, SiH_3Br and t.h.f stopping in the second and third traps. The white solid, $SiH_3Re(CO)_5$, was obtained in a yield of 0.63g (1.8 mmole) or about 60% relative to $Re_2(CO)_{10}$.

The compound has a vapour pressure of around 1mm Hg at 20°C and can be moved slowly in a vacuum system. On melting it decomposes slightly, giving off hydrogen and forming a white involatile solid.

The compound was characterised using I.R., Raman and mass spectroscopy and n.m.r.. The photoelectron spectrum was also run (chapter 1) and gas phase molecular structure was determined by electron diffraction (chapter 3).

Vibrational frequencies and their assignments are given in table 6.1. Force constant calculations on ν(Si-Mn) in $SiH_3Mn(CO)_5$ and any possible values for ν(Si-Re) in $SiH_3Re(CO)_5$ assuming a diatomic model, indicated that the Re-Si stretching frequency is at 300 cm^{-1}. The assignments are generally based on those made for $SiH_3Mn(CO)_5$[12] and $GeH_3Re(CO)_5$[115].

Parameters from the proton n.m.r. are given below

Table 6.1 Vibrational spectra of $SiH_3Re(CO)_5$

IR gas	Raman solid	Raman in $(C_2H_5)_2O$ solution	Assignment
2145sh(cm^{-1})	2140s(cm^{-1})	2140s P(cm^{-1})	ν(SiH) A_1
2111s		2100w P	ν(CO) A_1
2090w sh			ν(SiH) E
	2050s	2056s	ν(CO) B
2020 vvs	2000w	2010m	ν(CO) A_1 and E
1997m	1990w		$\nu(^{13}CO)$
1993m sh			
	950vw		$\delta(SiH_3)$
901s	900vw	926m	
690w	690w		δ(Re H) imp
605s			δ(ReCO) E
	532w	510	δ(ReCO)
	458vs	456vs P	ν(Re C) A_1
398m			ν(Re C) A_1
	351w	376m	ν(Re C) E
300w	304m	296s P	ν(ReSi) A_1
	221m		

τ $Si^{1}H$	$J^{29}Si^{1}H$	^{29}SiH
6.28	184 H_Z	-105.8

The mass spectrum showed peaks at 358 and 356 mass numbers corresponding to $(SiH_3{}^{187}Re(CO)_5)^+$ and $(SiH_3{}^{185}Re(CO)_5)^+$ respectively. Peaks corresponding to the progressive loss of carbonyls and peaks corresponding to the species $(SiH_yRe(CO)_xC)^+$ (y = o-3, x = o-4) were observed. Peaks corresponding to $(Re(CO)_x)^+$ (x = 0-5) could not be clearly observed as they were obscured by peaks corresponding to $(SiH_yRe(CO)_x)^+$ (y = o-3, x = o-4). Peaks were observed which could correspond to $(SiH_y)^+$ (y = o-3), the peak at mass no. 28 was probably due to the species $(CO)^+$. Double ionisation was also observed in the mass spectrum. Exact masses were determined for the peaks at 356 and 358 atomic mass units. At 358 mass units the exact value obtained was 357.9295 as opposed to a theoretical exact mass for $SiH_3{}^{187}Re(CO)_5$ of 357.9314. At 356 mass units two maxima were observed, one was at 355.9282 and the other, 355.9166 atomic mass units. The calculated exact mass for $SiH_3{}^{185}Re(CO)_5$ is 355.9284 and that for $SiH^{187}Re(CO)_5$ is 355.9155.

REFERENCES

1 F. Hein and H. Pobloth, Z. Anorg.Allgem. Chem., 248 (1941) 84.

2 F. Hein and E. Heuser, Z. Anorg. Allgem. Chem., 254 (1947) 138.

3 T.S. Piper, D. Lemal and G. Wilkinson, Naturwiss., 43 (1956) 129.

4 A.J. Chalk and J.F. Harrod, J. Am. Chem. Soc., 87 (1965) 1133.

5 B.J. Aylett and J.M. Campbell, Chem. Comms., (1965) 217.

6 S. Cradock and E.A.V. Ebsworth, J. Chem. Soc., (D), (1971) 57.

7 A. Almennirgen, O. Bastiensen, V. Ewing, K. Hedberg and M. Traetteberg, Acta Chem. Scand., 17 (1963) 2457.

8 R.D. George, K.M. Mackay and S.R. Stobart, J. Chem. Soc., Dalton, (1972) 1974.

9 R.F. Heck and D.S. Breslow, J. Am. Chem. Soc, 83 (1961) 1097.

10 T.H. Coffield, R.D. Closson and J. Kozikowski, J. Org. Chem., 22 (1957) 598.

11 B.J. Aylett and J.M. Campbell, J. Chem. Soc. (A), (1969) 1916.

12 K.M. Mackay and R.D. George, Inorg. Nucl. Chem. Letters, 5 (1969) 797.

13 F. Calderazzo and F.A. Cotton, Inorg. Chem., 1 (1962) 30.

14 A.P. Hagen and A.G. MacDiarmid, Inorg. Chem, 6 (1967) 686.

15 D.J. Patmore and W.A.G. Graham, Inorg. Chem., 6 (1967) 981.

16 J. Dalton, I. Paul, J.G. Smith and F.G.A. Stone, J. Chem. Soc. (A), (1968) 1199.

17 J. Dalton, I. Paul, J.G. Smith and F.G.A. Stone, J. Chem. Soc. (A), (1968) 1195.

18 J.F. Young, "Advances in Inorganic and Radiochemistry", Vol. 11 (Academic Press, London, 1968).

19 D.J. Patmore and W.A.G. Graham, Inorg. Chem., 7 (1968) 315.

20 W. Jetz and W.A.G. Graham, J. Am. Chem. Soc., 89 (1967) 2773.

21 W.A.G. Graham and R.S. Gay , Inorg. Chem., 8 (1969) 1561.

22 K.L. Watters, J.W. Brittain and W.M. Risen, Inorg. Chem., 8 (1969)1347.

23 A.G. Robiette, G.M. Sheldrick, R.N.F. Simpson, B.J. Aylett and J.A. Campbell, J. Organometal Chem., 14 (1968) 279.

24 K.L. Watters, J.A. Brittain and W.M. Risen, Inorg. Chem., 10 (1971) 1970.

25 G.C. Van Den Berg and A. Oskam, J. Organometal. Chem., 78 (1974) 357.

26 F.E. Saalfield, M.V. McDowell and A.G. MacDiarmid, J. Am. Chem. Soc., 90 (1970) 2324.

27 F.E. Saalfield, M.V. McDowell, J.J. DeCorpo, A.D. Berry and A.G. MacDiarmid, Inorg. Chem., 12 (1973) 48.

28 R.A. Burnham and S.R. Stobart, J. Chem. Soc. Dalton, (1973) 1269.

29 R.A. Burnham and S.R. Stobart, J. Organometal. Chem., 86 (1975) C45.

30 H.M. Seip and R. Seip, Acta Chem. Scand., 24 (1970) 3431.

31 B. Beagley, Personal Communication (1975).

32 R.S. Hamilton and E.R. Corey, Abs. Inorg. Div. of 156th National Meeting of Am. Chem. Soc.

33 N.I. Gapotchenko, N.V. Alekseev, A.B. Antonova, K.N. Anisimov, N.E. Kolobova, I.A. Ronova and Y.T. Struchkov, J. Organometallic Chem., 23 (1970) 525.

34 B.J. Kilbourn, T.L. Blundell and H.M. Powell, Chem. Comm., (1965) 444.

35 R.F. Bryan, J. Chem. Soc. (A), (1968) 696.

36 H.P. Weber and R.F. Bryan, Acta Cryst., 22 (1967) 822.

37 L. Manojlovic-Muir, K.W. Muir, J.A. Ibers, Inorg. Chem., 9 (1970) 447.

38 R.F. Bryan, P.T. Green, G.A. Melson and P.F. Stokely J. Chem. Soc. (D),(1969) 722.

39 W.T. Robinson and J.A. Ibers, Inorg. Chem.,6 (1967) 1208.

40 K. Emerson, P.R. Ireland and W.J. Robinson, Inorg. Chem.,9 (1970) 436.

41 G.C.v.d. Berg, A. Oskam and K. Olie, J. Organometallic Chem.,80 (1974) 363.

42 K.W. Muir, J. A. Ibers, Inorg. Chem.,9 (1970) 441.

43 H.C. Allen and E.K. Plyler, J. Chem. Phys., 31 (1959) 1062.

44 R.W. Kilb and L. Pierce, J. Chem Phys.,27 (1957) 108.

45 V. Lawrie, J. Chem. Phys., 30, (1959) 1210.

46 S. Evans, J.C. Green, M.L.H. Green, A.F. Orchard, D.W. Turner, Discuss. Faraday Soc.,47 (1969) 112.

47 R.F. Fenske and R.L. DeKock, Inorg. Chem., 9 (1970) 1053.

48 D.L. Lichtenberger, A.C. Sarapu and R. Fenske, Inorg. Chem.,12 (1973) 702.

49 G.D. Caesar, P. Millazzo, J.L. Cihonski and R.A. Levenson, Inorg. Chem.,13 (1974) 3035.

50 M.B. Hall, M.F. Guest and I.H. Hillier, Chem. Phys. Lett., 15 (1972) 592.

51 M.B. Hall and R.F. Fenske, Inorg. Chem.,11 (1972) 768.

52 D.L. Lichtenberger and R.F. Fenske, Inorg. Chem.,13 (1974) 486.

53 A.D. Berry, E.R. Corey, A.P. Hagen, A.G.MacDiarmid, F.E. Saalfield and B.B. Wayland, J. Am. Chem. Soc., 92 (1970) 1940.

54 R.A.N. McLean, J. Chem. Soc. Dalton,(1974) 1568.

55 T.L. Brown, P.A. Edwards, C.B. Harris and J.L.Kirsch, Inorg. Chem.,8 (1969) 763.

56 D.D. Spencer, J.L. Kirsch and T.L. Brown, Inorg. Chem., 9 (1970) 235.

57 J.D. Cotton, Organometallic Chem.,1,Ed. E.W. Abel and F.G.A. Stone (Chemical Society,London,1972).

58 G.M. Bancroft, H.C. Clark, R.G. Kidd, A.F. Rake and H.G. Spinney, Inorg. Chem.,12 (1973) 728.

59 S.R.A. Bird, J.D. Donaldson, S.A. Keppie and M.F. Lambert, J. Chem. Soc. (A),(1971) 1311.

60 S.R.A. Bird, J.D. Donaldson, A.F.C. LeC. Holding, B.J. Senior and M.J. Tricker, J. Chem. Soc. (A),(1971) 1616.

61 B.A. Goodman, R. Greatrex and N.N. Greenwood, J. Chem. Soc. (A),(1971) 1868.

62 B.V. Liengne, M.J. Newlands and J.R. Sams, Inorg. Nuclear Chem. Letters,7 (1971) 1223.

63 W.R. Cullen, J.R. Sams and J.A.J. Thomson, Inorg. Chem., 10 (1971) 843.

64 S. Cradock, Personal Communication (1971).

65 D.W. Turner and M. Al-Joboury, J. Chem. Phys.,(1962) 3007.

66 D.W. Turner, C. Baker, A.D. Baker and C.R. Brundle, "Molecular Photo-electron Spectroscopy":(Wiley Interscience, London, New York, Sydney, and Toronto, 1970).

67 A.D. Baker and D. Betteridge, 'Photo-Electron Spectroscopy-Chemical and Analytical Aspects', (Pergammon Press, Oxford, 1972).

68 A.D. Baker, Acc. Chem. Research, 3 (1970) 17.

69 S.D. Worley, Chem. Rev., 3 (1971) 295.

70 R.L. DeKock and D. R. Lloyd "Advances in Inorganic Chemistry and Radiochemistry," vol. 16 (Academic Press, London,1974).

71 W.G. Richards, J. Mass Spec. Ion. Phys.,2 (1968) 419.

72 B.R. Higginson, D.R. Lloyd, J.A. Connor and I.A. Hillier J. Chem. Soc. Faraday Trans.,II (1974) 1418.

73 C.R. Brundle, M.B. Robin, N.A. Kuebler and H. Basch, J. Amer. Chem. Soc.,94 (1972) 1451.

74 B. Beagley, A.H. Clarke and T.G. Hewitt, J. Chem. Soc. (A),(1968),658.

76 O. Bastiensen, R. Graber and L. Wegmann, Balzer's High Vacuum Report, 25 (1969) 1.

77 W. Zeil, S. Haase and L. Wegmann, Z. Intrumentenk, 74 (1966) 84.

78 B. Anderson, H.M. Seip, T.G. Strand and R. Stolevic, Acta Chem. Scand., 23 (1969) 3224.

79 D.M. Bridges, G.C. Holywell, D.W.H. Rankin and J.M. Freeman, J. Organometal. Chem., 32 (1971) 87.

80 J. Brunvoll, Acta Chem. Scand., 21 (1967) 1390.

81 H.L. Cox and R.A. Bonham, J. Chem. Phys., 47 (1967) 2599.

82 F.A. Cotton and D.C. Richardson, Inorg. Chem., 5 (1966) 1851.

83 A. Almenningen, G.G. Jacobsen and H.M. Seip, Acta Chem. Scand., 23 (1969) 685.

84 J.A. Ibers, J. Organometal. Chem., 14 (1968) 423.

85 M.J. Bennet and R. Mason, J Chem. Soc. (A), (1968) 75.

86 L.S. Schäfer, A.C. Yates and R.A. Bonham, J. Chem. Phys., 53 (1970) 251.

87 E.J. Jacob and L.S. Bartell, J. Chem. Phys., 53 (1970) 2231.

88 E.J. Jacob and L.S. Bartell, J. Chem. Phys., 53 (1970) 2235.

89 V.G. Adrianov, B.P. Biryukov and Yu. T. Struchkov, Zh. Strukht. Khim., 10 (1969) 1129.

90 D.L.S. Brown, J.A. Connor and H.A. Skinner, J. Organomet. Chem., 81 (1974) 403.

91 R.A. Whiteford, Ph.D. Thesis, Edinburgh, 1974.

92 B. Beagley, A.R. Conrad, J.M. Freeman, J.J. Monaghan and B.G. Norton, J. Mol. Struct., 11 (1972) 371.

93 H. Murata and K. Shimizu, J. Chem. Phys., 23 (1956) 1968.

94 D.W.H. Rankin, Ph.D. Thesis, Cambridge, 1969.

95 K. Hedberg and M.J. Wasaki, Acta Cryst., 17 (1964) 529.

96 Y. Murato and Y. Morino, Acta Cryst., 20 (1966) 605.

97 L.S. Bartell, J. Chem. Phys., 29 (1961) 1219.

98 D. Kumer and G. Fitz, Z. Anorg. Chem., 308 (1961) 105.

99 E.A.V. Ebsworth, J.R. Hall, M.J. Mackillop, D.C. McKean, N. Sheppard and L.A. Woodward, Spectrochim. Acta, 13 (1958) 202.

100 J.C. Thompson, Ph.D. Thesis, Cambridge (1965).

101 H.J. Emeleus and A.G. Maddock, J. Chem. Soc. Trans., (1944) 293.

103 A.G. MacDiarmid, 'Preparative Inorganic Reactions', ed. W.L. Jolly, (Wiley Interscience, New York, 1964).

104 J.E. Bentham, S. Cradock and E.A.V. Ebsworth, Inorg. Nucl. Chem. Letters, 7 (1971) 1077.

105 S. Cradock, E.A.V. Ebsworth, J. Chem. Soc. (A), (1967) 1220.

106 M. Schmeisser 'Handbook of Preparative Ionorganic Chemistry,' Ed. G. Brauer (Academic Press, New York, 1963).

107 R.B. King and F.G.A. Stone, "Inorganic Syntheses", VII, Ed. J. Kleinberg (McGraw-Hill Book Co., 1963).

108 W. Jetz and W.A.G. Graham, J. Am. Chem. Soc., 89 (1967) 2773.

109 M. E. Redwood, B.E. Reichert, R.R. Schreike and B.O. West, Australian J. Chem., 26 (1973) 247.

110 H.C. Clark, J.D. Cotton and J.H. Tsai, Inorg. Chem., 5 (1966) 1582.

111 J.J. Eisch and R. Bruce King, 'Organometallic Syntheses' (Academic Press, London, 1965).

112 P. Gilmont, A.A. Blanchard, 'Inorganic Syntheses', II, Ed, W.C. Fernelius (McGraw-Hill Book Co., New York, 1946).

113 A.P. Hagen and A.G. MacDiarmid, Inorg. Chem., 6 (1967) 686.

114 Y.L. Baayand and A.G. MacDiarmid, Inorg. Nucl. Chem. Lett., 3 (1967) 159.

115 K.M. Mackay and S.R. Stobart, J. Chem. Soc. (A), (1973) 214.

116 W. Beck, W. Hieber and G. Braun, Z. Anorg. Chem., 308 (1961) 23.

117 W. Hieber, G. Braun and W. Beck, Chem. Ber., 93 (1960) 901.

APPENDICES

APPENDIX I

An electron diffraction determination of the molecular structure of trifluoromethylisocyanate in the gas phase .

Interest in the molecular structure of trifluoromethylisocyanate stems from the molecular structures of methyl, silyl, germyl and difluorophosphine pseudohalides. In SiH_3NCO[1] and SiH_3NCS[2] the angle at nitrogen has been found linear by microwave and electron diffraction structure determinations of these molecules are consistent with these findings if large shrinkage corrections are applied[3]. However in SiH_3N_3[4] and all methyl[5], germyl[6,7] and difluorophosphine[8] pseudohalides the heavy atom skeletons have been found bent by both microwave and electron diffraction.

The linearity of the heavy atom skeletons in SiH_3NCO[1], SiF_3NCO[9] and SiH_3NCS[2] have been widely explained as, at least partly, due to (p→d) π bonding. The angles at nitrogen in CH_3NCO and CH_3NCS where there is no possibility of (p→d) π bonding, have recently been found to be greater than 120^{o}[5]. This was simply explained by the valence bond structures

$$CH_3-N=C=X \quad \text{and} \quad CH_3-\overset{+}{N} \equiv C-X^{-},$$

the latter involving linear co-ordination at nitrogen. With CF_3NCO the strong electron withdrawing CF_3 group would be expected to destabilise the linear valence bond structure, hence, if the explanation of the wide angles of nitrogen in CH_3NCO and CH_3NCS is correct, the angle at nitrogen in CF_3NCO will be less than that in CH_3NCO.

Experimental and Results

The sample of trifluoromethylisocyanate was prepared by the reaction scheme below

$$SiMe_3N_3 + CF_3COCl \rightarrow CF_3CON_3 + SiMe_3Cl$$

$$CF_3CON_3 \xrightarrow{\text{heat}} CF_3NCO$$

The sample was purified by fractional condensation and its purity checked by infrared spectroscopy.

Table I.1 Weighting functions, etc., for CF_3NCO

Nozzle Height (mm)	dels (nm^{-1})	s_{min}	s_1	s_2	s_{max}	$P/_h$	Scale Factor
190	4	56	96	320	350	0.4939	0.703 ± 0.017
580	2	22	42	105	125	0.4991	0.792 ± 0.014

The electron diffraction data was obtained from the Balzer's KD.G2 gas diffraction apparatus at Oslo University[10,11]. This data were treated in the same manner as that obtained for $SiF_3Mn(CO)_5$ (see chapters 2 and 6). The scale factors, weighting points and correlation parameter are given in table1.1.

The molecular model used assumed C_3v symmetry for the CF_3 group and a linear NCO group. This enabled the molecule to be described by the four bonded distances, the F-C-N, C-N-C, twist and tilt angles; the twist angle defines the twist of the CF_3 group relative to the NCO group and the tilt angle is the angle between C_3 axis of the CF_3 group and the C-N bond.

Only the C-F bond length, the F-C-N angle and F...F amplitudes of vibration refined satisfactorily. The reason for this can be readily seen in the radial distribution curve (figure 1.1). All bond lengths lay under the peak centred at 135pm and all the two-bond distances lay under the peak centred at about 210pm. A general configuration for this molecule was determined by fixing the C-N-C and twist angles at various values and comparing the R factors. The lowest R factor occurred when the twist angle was 30° and the C-N-C angle, 133°. Since neither the bond lengths nor the 2-bond distances could be clearly defined there is the possibility of considerable errors (perhaps as much as 10 degrees) in these figures.

The molecular structures thus obtained is given in table 1.2. This structure can only be described as consistent with the data obtained; it is not necessarily the only structure that fits the experimental data. The final R factor (R_G) was 0.142. The high values in the least square correlation matrix (table 1.3) also are a reflection of the difficulties involved in this structure determination.

Obviously very little can be taken from this structure. The C-N-C angle of 133° being less than that in

Table I.2 Molecular parameters for CF_3NCO

independant distances		distance (pm)	amplitude of vibration (pm)
r_1	C-F	132.4(3)	4.2 (fixed)
r_2	C-N	142.0(fixed)	4.5 (fixed)
r_3	N-C	117.0(fixed)	3.7 (fixed)
r_4	C-O	119.0(fixed)	3.9 (fixed)
dependant distances			
d_1	F...F	215.3	7.0 (6)
d_2	C...O	348.5	10 (fixed)
d_3	C...C	237.6	7 (fixed)
d_4	F...C	335.5	12(fixed)
d_5	F...C	275.2	20 (fixed)
d_6	F...C	306.8	20 (fixed)
d_7	F...O	451.3	15 (fixed)
d_8	F...O	359.7	25 (fixed)
d_9	F...O	408.1	25 (fixed)
d_{10}	O...N	235.0	4.2 (fixed)
d_{11}	F...N	225.0	7 (fixed)
d_{12}	F...N	225.0	7 (fixed)
d_{13}	F...N	225.0	7 (fixed)

independent angles

$\angle 1$	F-C-N	$110^{\circ} \pm 2^{\circ}$
$\angle 2$	C-N-C	133° (fixed)
$\angle 3$	twist	30° fixed
$\angle 4$	tilt	0 fixed

dependent angles

$\widehat{F\text{-}C\text{-}F}$	109°

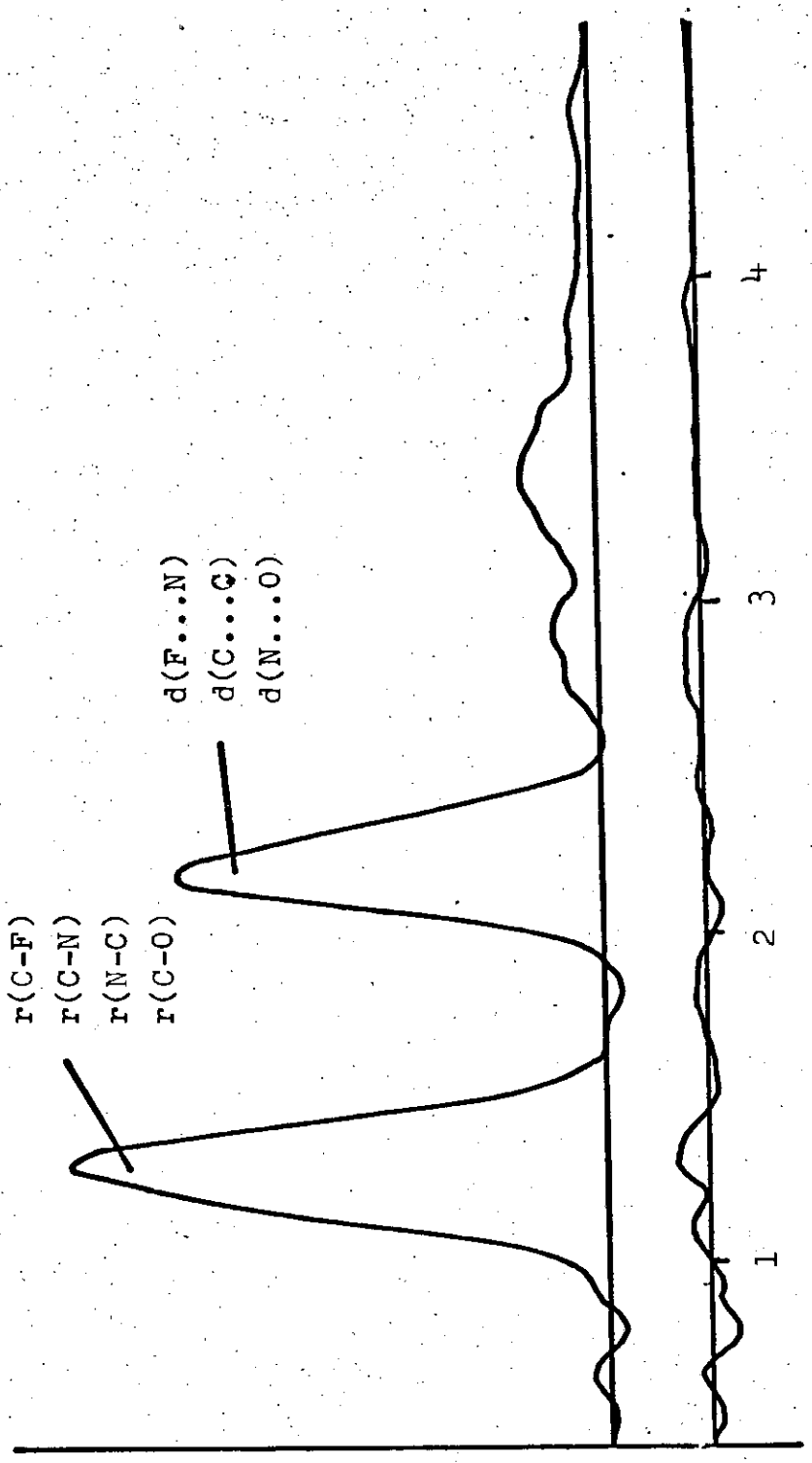

Figure I.1 Radial distribution curve and final difference curve for CF_3NCO. Before Fourier inversion the data were multiplied by $s.\exp((-0.00002s^2)/(z_F-f_F)(z_C-f_C))$.

CH_3NCO is consistent with the explanation given for the wide CNC angle in CH_3NCO.

Table 1.3 Least squares correlation matrix of CF_3NCO multiplied by 1000

R1	∠1	U5	K1	K2	
1000	-803	703	37	98	R1
	1000	-862	-137	-196	∠1
		1000	386	324	U5
			1000	205	K1
				1000	K2

REFERENCES

1 M.C.L. Gerry, J.C. Thompson and T.M. Sugden, Nature (London),211 (1966) 846.

2 D.R. Jenkins, R. Kewley and T.M. Sugden, Trans. Faraday Soc.,58 (1962) 1284.

3 S.J. Cyvin, J. Brunvoll and A.G. Robiette, Chem. Phys. Lett.,11(1971) 263.

4 E.A.V. Ebsworth, D.R. Jenkins, M.J. Mays and T.M. Sugden, Proc. Chem. Soc.,(1963) 21.

5 D.W.W. Anderson, D.W.H. Rankin and A. Robertson, J. Mol. Structure, 14 (1972) 385.

6 J.D. Murdoch, D.W.H. Rankin, Chem Commun.,(1972) 748.

7 K. Ramaprasad, R. Varma and R. Nelson, J. Amer. Chem. Soc., 90 (1968) 6247.

8 D.W.H. Rankin and S.J. Cyvin, J. Chem. Soc. Dalton, (1972) 1277.

9 W. Airey, C. Glidewell, A.G. Robiette and G.M. Sheldrick, J. Mol. Structure,8 (1971) 435.

10 O. Bastiensen, R. Graber and L. Wegmann, Balzer's High Vacuum Report,25 (1969) 1.

11 W. Zeil, J. Haase and L. Wegmann, Z. Instrumentenk., 74 (1966) 84.

APPENDIX II

Molecular structure of hydridotetrakis(trifluorophosphine) rhodium(I) in the gas phase.

Introduction

The molecular structure of hydridotetrakis(trifluorophosphine) rhodium(I) is of interest both in the position of the hydrogen atom and the Rh-P bond length as there is some controversy about the nature of both transition metal-hydrogen and transition metal-phosphorus bonds.

Hydrogen atoms bound to the transition metal are difficult to locate in transition metal phosphine complexes by either X-ray or electron diffraction but their positions normally can be deduced from the configuration of the heavy atom skeleton of the complex. The molecular structures of both $HCo(PF_3)_4$[1] and $HRh(PF_3)(PPh_3)_3$[2] have both been determined and it appears that both molecules are trigonal bipyramids with the hydrogen in axial positions, forming apparently normal covalent bonds with the transition metal atoms.

Multiple bonding is generally regarded as occurring in transition metal-phosphorus bonds in trifluorophosphine complexes to a greater extent than in trialkyl-or triaryl- phosphine complexes and comparison of the Rh-P bond lengths in $HRh(PPh_3)_3(PF_3)$ with the Rh-P bond length in $HRh(PF_3)_4$ may help to confirm that theory.

Experimental

The sample of $HRh(PF_3)_4$ used for structure determination was supplied by J.F. Nixon and J. Sinclair.

Scattering intensities were recorded photographically on Agfa Gevaert replica 23 plates using a Balzer's KD.G2 gas diffraction apparatus at the University of Manchester Institute of Science and Technology[3]. Three nozzle to plate distances, 1000, 500 and 250mm, were used giving a range of scattering variable, s, of 10 to 300nm^{-1}. The samples were held at 273 K and the nozzle at 298K for the 250mm nozzle to plate exposures and 328 K for the remaining data.

Data reduction and refinements were carried out as described in chapter 6.

The scattering factors of Cox and Bonham[4] were used. Table II.1 shows weighting points (used to set up the off-diagonal weight matrix for least squares refinements), correlation parameters and scale factors. Two wavelengths were used. one was determined by direct measurement of the accelerating voltage and the diffraction pattern of powdered thallous chloride and the other by the molecular structure of benzene.

Molecular Model

All Rh-P and P-F bondlengths were assumed equal, the molecule was assumed to have C_3 symmetry and the PF_3 groups were assumed to have C_{3v} symmetry. With these assumptions the molecule can be described by the P-F, Rh-P, and Rh-H bond lengths, the F-P-F angle, the H-Rh-P_{eq} angle and two twist angles, one describing the axial PF_3 group's twist, the other describing the equatorial PF_3 groups' twist. When these angles are zero the axial PF_3 group's configuration is eclipsed with the equatorial phosphine groups and, on each of the equatorial PF_3 groups, one fluorine points towards the axial PF_3 group.

Refinements

The rhodium-phosphorus and phosphorus-fluorine bonded distances and their amplitudes of vibration refined satisfactorily as did the Rh...F amplitude of vibration. H-Rh-P angles did not refine satisfactorily together but did so separately. In the final refinement it was the H-Rh-P angle which refined. The two twist angles were set by carrying out series of refinements with these parameters set at various values and comparing R-factors. The Rh-H bond length was set using a similar procedure.

As can be seen in figureII.1 there is much overlapping of peaks in the radial distribution curve and this rendered impossible the refinement of other amplitudes of vibration, even in groups. All non-refining parameters were set at

Tbale II.1 Weighting Functions, Correlation Parameters and Scale Factors for Tetrakis(trifluorophosphine)rhodiumhydride

Height (mm)	del s nm^{-1}	s_{min} nm^{-1}	s_1 nm^{-1}	s_2 nm^{-1}	s_{max} nm^{-1}	$p/_h$	Scale Factor	Wave Length
250.0380	0.400	6.000	10.000	26.000	30.000	0.4026	0.750 $\pm$ 0.026	0.05660
500.0579	0.200	2.800	5.800	13.600	15.600	0.4909	0.846 $\pm$ 0.023	0.05663
1000.0618	0.100	1.000	2.000	6.700	7.700	0.4971	1.349 $\pm$ 0.038	0.05663

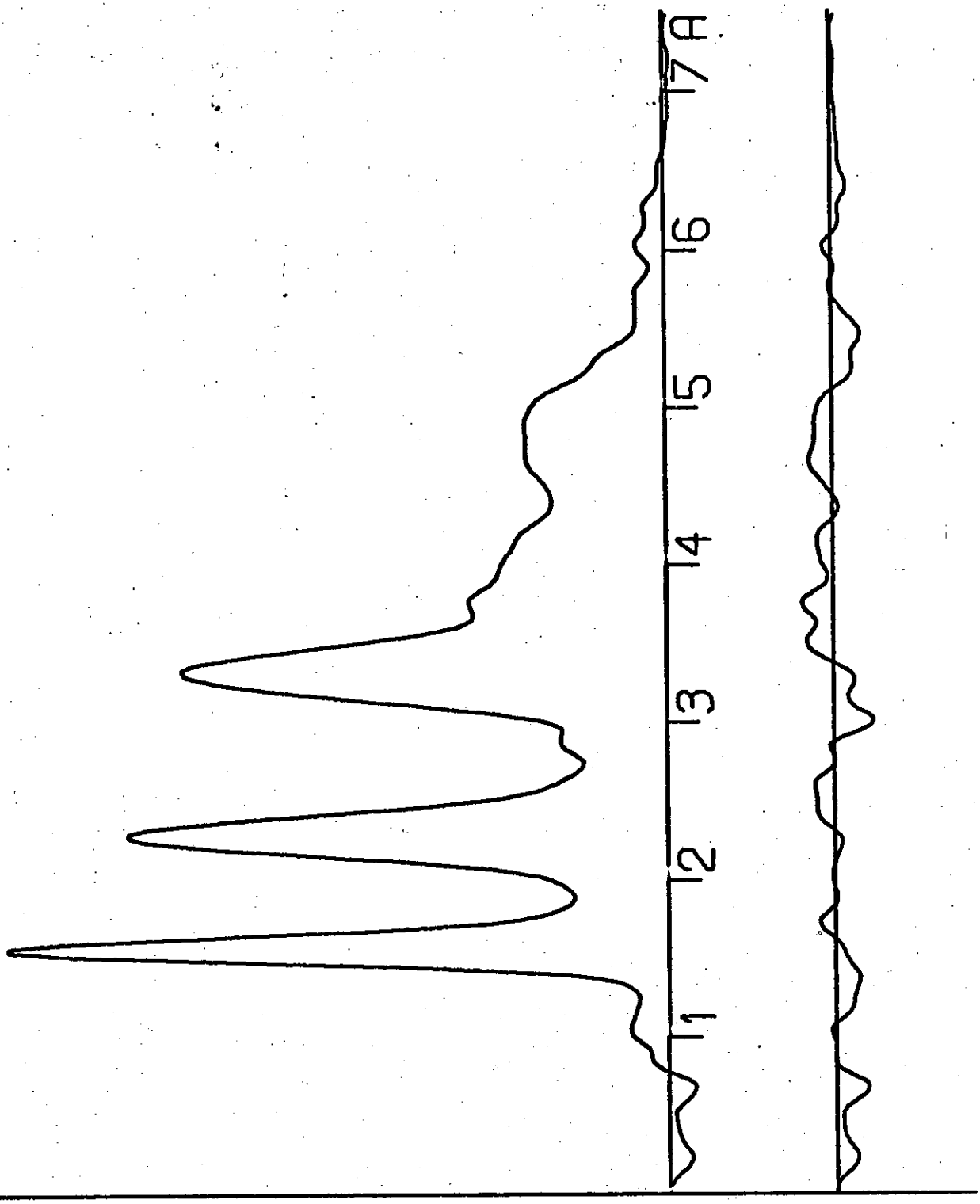

Figure II.1 Radial distribution curve, P(r)/r, and final difference curve for $HRh(PF_3)_4$. Before Fourier inversion the data were multiplied by $s.\exp(-0.00002 5s^2/(z_{Rh}-f_{Rh})(z_F-f_F))$

seemingly reasonable values.

The molecular parameters are given in table II.2 The final R-factor was 0.19. The estimated standard deviations quoted include allowances for systematic errors and constraints applied during refinements. The least square correlation matrix is given in table II.3 and the molecular intensity data is given in figure II.2.

Discussion

As in $HCo(PF_3)_4$[1] and $HRh(P'F_3)(P''Ph_3)_3$[2] the hydrogen atom appears to occupy the axial position of a trigonal bipyramid. What little data is available on the Rh-H bond length indicates that it is a normal co-valent bond.

The Rh-P bond length of 222.2pm found in $HRh(PF_3)_4$ is considerably longer that the Rh-P' bond length (215.9) of $HRh(P'F_3)(P''Ph_3)_3$ and considerably shorter than the Rh-P" bond length. This is consistent with the PPh_3 groups being less π bonded to the Rh atom than the PF_3 groups. Also, the Rh-P bonds of $HRh(PF_3)_4$ are shorter than the Rh-P" bond in $HRh(P'F_3)(P''Ph_3)_3$. This is consistent with the equatorial PPh_3 groups on $HRh(PF_3)(PPh_3)_3$ being less strongly π bonded to the rhodium atom than are the equatorial PF_3 groups on $HRh(PF_3)_4$ thus allowing the axial PF_3 group in the former complex to be more strongly π bonded than in the latter complex. Were the main effect of fluorination of the phosphines an electron withdrawal then the Rh-P bonds in $HRh(PF_3)_4$ would probably be shorter than the Rh-P' bond in $HRh(P'F_3)(PPh_3)_3$.

Table II.2 Molecular Parameters for $HRh(PF_3)_4$

independent distances and amplitudes		distance (pm)	amplitude (pm)
r_1	(P-F)	154.5 (3)	4.1 (6)
r_2	(Rh-P)	222.2 (7)	6.8 (9)
r_3	(Rh-H)	168 (fixed)	6.0 (fixed)
dependent distances and amplitudes			
d_1	(Rh...F)	327.8 (9)	9.5 (7)
d_2	(P...H)	283.8 (11)	8.0 (fixed)
d_3	(P...H)	389.2 (10)	7.0 (fixed)
d_4	(F...H)	400.2 (9)	18 (fixed)
d_5	(F...H)	294.7 (8)	18 (fixed)
d_6	(F...H)	381.4 (8)	18 (fixed)
d_7	(F...H)	484.6 (10)	15 (fixed)
d_8	(P...P)	385.0 (12)	13.5
d_9	(P...P)	307.5 (9)	16
d_{10}	(P...F)	511.7 (17)	20
d_{11}	(P...F)	484.5 (15)	20
d_{12}	(P...F)	417.4 (13)	20
d_{13}	(P...F)	428.8 (11)	20
d_{14}	(P...F)	463.8 (15)	20
d_{15}	(P...F)	521.6 (15)	20
d_{16}	(P...F)	341.1 (10)	20
d_{17}	(P...F)	458.9 (17)	20

d_{18}	(P...F)	355.3 (11)	20 (fixed)
d_{19}	(P...F)	351.6 (15)	20
d_{20}	(P...F)	470.7 (17)	20
d_{21}	(P...F)	378.5 (15)	20
d_{22}	(F...F)	233.0 (7)	8
d_{23}	(F...F)	552.8 (19)	20
d_{24}	(F...F)	538.1 (15)	20
d_{25}	(F...F)	410.9 (13)	20
d_{26}	(F...F)	605.0 (15)	20
d_{27}	(F...F)	509.0 (13)	20
d_{28}	(F...F)	480.5 (13)	20
d_{29}	(F...F)	638.6 (17)	20
d_{30}	(F...F)	621.6 (16)	20
d_{31}	(F...F)	565.3 (17)	20
d_{32}	(F...F)	317.3 (16)	20
d_{33}	(F...F)	500.5 (16)	20
d_{34}	(F...F)	421.3 (16)	20
d_{35}	(F...F)	498.7 (16)	20
d_{36}	(F...F)	616.0 (17)	20
d_{37}	(F...F)	529.4 (17)	20

c independent angles

$\angle_1$	F-P-F	97.7 (fixed)
$\angle_2$	P-Rh-H	87.5 (10)
$\angle_3$	axial PF_3 twist	54.5 (fixed)
$\angle_4$	equatorial PF_3 twist	49 (fixed)

Table II.3 Least squares Correlation Matrix Multiplied by 1000 for Tetrakis (Trifluorophosphine) Rhodium Hydride

r1	r2	2	u1	u2	u4	k1	k2	k3	
1000	18	-26	-27	34	-7	-22	11	76	r1
18	1000	-230	-188	-33	-130	-244	-198	-76	r2
-26	-230	1000	34	-352	-26	51	14	-87	2
-27	-188	34	1000	311	300	641	306	147	u1
34	-33	-352	311	1000	249	427	302	207	u2
-7	-130	-26	300	249	1000	422	429	311	u4
-22	-244	51	641	427	422	1000	334	185	k1
11	-198	14	306	302	429	334	1000	158	k2
76	-76	-87	147	207	311	185	158	1000	k3

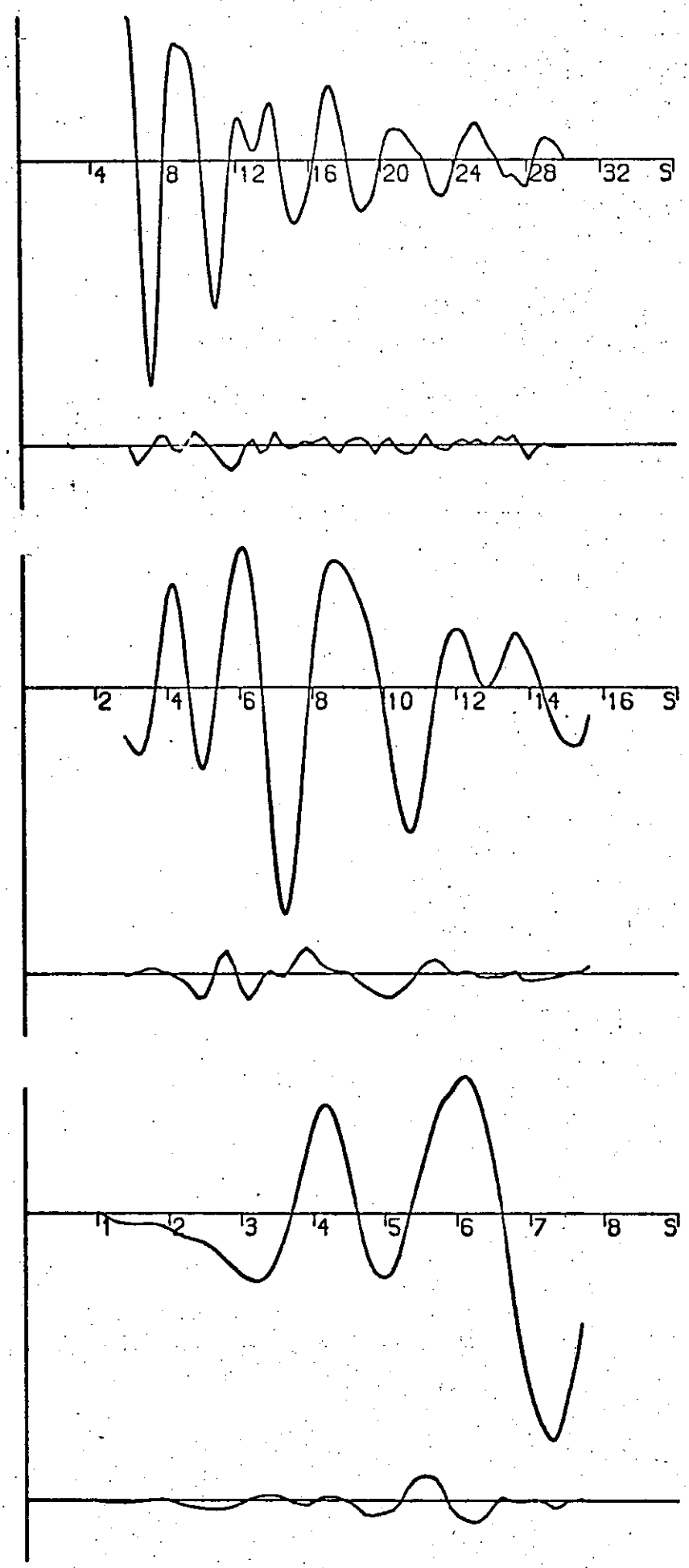

Figure II.2 Molecular scattering intensity and final weighted difference curves for $HRh(PF_3)_4$ obtained from nozzle-to-plate distances of 250mm, 500mm and 1000mm.

REFERENCES

1 B. A. Frenz and J. A. Ibers, Inorg. Chem.,9(1970) 2403.

2 J. Sinclair, PhD thesis, Sussex,1975.

3 B. Beagley, A. H. Clark and T. G. Hewitt, J. Chem. Soc. (A),(1968) 658.

4 H. L. Cox and R. A. Bonham, J. Chem. Phys.,47 (1967) 2599.

Photoelectron Spectra of Some Silyl and Germyl Transition-metal Carbonyls and Related Species

By **S. Cradock, E. A. V. Ebsworth,*** and **A. Robertson,** Department of Chemistry, University of Edinburgh, West Mains Road, Edinburgh EH9 3JJ

Reprinted from

JOURNAL
OF
THE CHEMICAL SOCIETY

DALTON TRANSACTIONS

1973

Photoelectron Spectra of Some Silyl and Germyl Transition-metal Carbonyls and Related Species

By **S. Cradock, E. A. V. Ebsworth,* and A. Robertson,** Department of Chemistry, University of Edinburgh, West Mains Road, Edinburgh EH9 3JJ

The He I (21·22 eV) photoelectron spectra of six silyl and germyl (M^1H_3) derivatives of Mn, Re, and Co (M^2) carbonyls show bands attributable to (*a*) transition-metal unshared *d*-electrons (M^2 *n'd*) in the range 8—10 eV binding energy; (*b*) to the M^1H σ-bonding levels derived from M^1 *np* orbitals (11—12 eV), and (*c*) the carbonyl groups (13—19 eV). Correlation with related hydride and methyl derivatives, where known, suggests that the M^1M^2 σ-bonding level gives rise to a band in the 9—10 eV region, where it is obscured by the M^2 *n'd* bands. No evidence for any π-interaction between the M^2 *n'd* orbitals and the M^1H_3 group is observed; it is concluded that the observed shifts in M^2 *n'd* reflect the varying σ-acceptor powers of the M^1H_3 groups, methyl being a poorer σ-acceptor than silyl or germyl.

SEVERAL SiH_3 and GeH_3 derivatives of transition-metal carbonyls are known;[1] we report here studies on $M^1H_3Mn(CO)_5$, $M^1H_3Re(CO)_5$, and $M^1H_3Co(CO)_4$ for M^1 = Si and Ge. All these compounds obey the 18-electron rule, but it is puzzling that they are comparatively stable at room temperature; of the methyl analogues only $CH_3Mn(CO)_5$ is of comparable stability. It has been suggested[2] that ($d \rightarrow d$) π-bonding might stabilise the Si and Ge compounds relative to the carbon ana-

[1] B. J. Aylett and J. M. Campbell, *J. Chem. Soc.* (*A*), 1969, 1910, 1916; K. M. Mackay and R. D. George, *Inorg. Nuclear Chem. Letters*, 1969, **5**, 797; 1970, **6**, 289; K. M. Mackay and S. R. Stobart, *ibid.*, p. 687.

[2] A. G. Robiette, G. M. Sheldrick, R. N. F. Simpson, B. J. Aylett, and J. M. Campbell, *J. Organometallic Chem.*, 1968, **14**, 279.

logues, and it has been argued that the exceptionally short Si–M bonds in $SiF_3Co(CO)_4$ and various $SiCl_3$–transition metal derivatives [3] are due to similar π-donation from transition-metal *d*-levels to Si 3*d*.

We have attempted to study the electronic structures of these compounds using He I photoelectron spectroscopy, which we have used earlier [4] to demonstrate the occurrence of $(p \rightarrow d)$ π-bonding between Cl and SiH_3 or GeH_3 groups. We have also recorded the spectra of $HRe(CO)_5$ and $HCo(CO)_4$ for comparison; spectra of $HMn(CO)_5$ and $CH_3Mn(CO)_5$ have already been published.[5] The spectrum of $Me_3SiMn(CO)_5$ was also recorded.

EXPERIMENTAL

The compounds were prepared by standard routes [1] as shown in the Scheme, purified by vacuum fractionation, and characterised by i.r. spectroscopy. $SiH_3Re(CO)_5$ does not seem to have been reported; full details of the preparation and characterisation will be reported elsewhere.

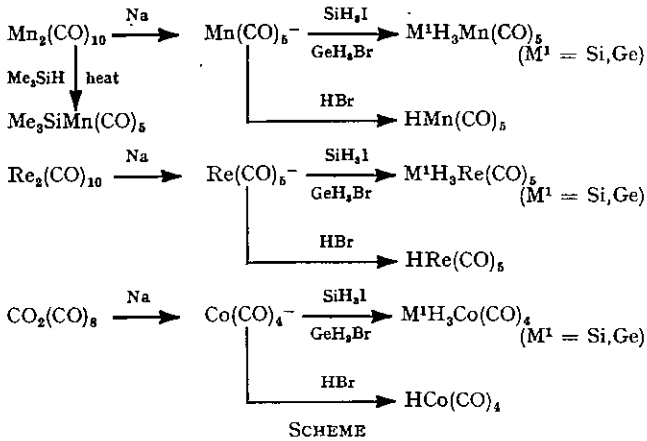

SCHEME

He I (21·22 eV) photoelectron spectra were recorded by use of a small spectrometer described earlier [5] or a Perkin-Elmer PS16 instrument. The effective resolution achievable with the two instruments was of the order of 50 and 30 meV respectively; no fine-structure attributable to vibration was observed on any band, and all bands were broad. The compounds were introduced into the spectrometers as vapours at room temperature; the low vapour pressures of some of the compounds under these conditions made it necessary to use slow scanning and long integration times to achieve reasonable count rate : noise ratios. Calibration was achieved with rare gases, N_2 or H_2O entering the target chamber concurrently with the compound.

RESULTS

The spectra are illustrated in Figures 1—3 and the vertical ionisation potentials (I.P.s) of the bands collected in Tables 1—3, together with data for some related compounds and for the free transition-metal atoms (Table 4). In each spectrum a set of overlapping bands cover the 13—17 eV region; for these the onset-to-tail ranges are given rather than the vertical I.P. The onset in each case is fairly sharp and well-located; the position of the tail is less well-defined.

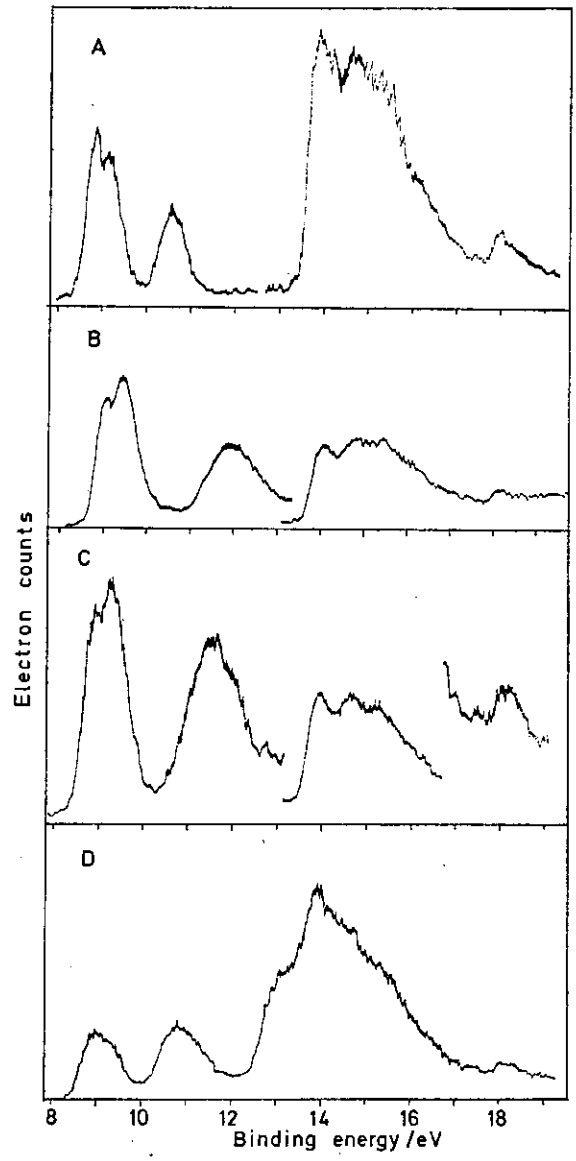

FIGURE 1 Photoelectron spectra of A, $HMn(CO)_5$; B, $SiH_3Mn(CO)_5$; C, $GeH_3Mn(CO)_5$; and D, $Me_3SiMn(CO)_5$. The apparent sharp peaks near 15 eV in A are due to the use of too short an integrating time

TABLE 1

Vertical ionisation potentials/eV for $LMn(CO)_5$

Region [a]	*A*				*B*		*C*
Levels	Mn 3*d*				Mn–Cσ	C–Oπ	
	e	b_2	Mn–H	M^1–H	onset	tail	C–Oσ
L							
H [a]	8·85	9·14	10·55	—	13·4	17	18·0
CH_3 [a]	8·46	9·10	—	12·6	13·5	17	18·0
SiH_3	8·99	9·38	—	11·9	13·7	17	18·0
GeH_3	8·90	9·26	—	11·5	13·4	17	18·1
Me_3Si	9·0	9·3	—	10·8 Si–C 13·1 C–H	13·5	17	18·1

[a] See ref. 5. Vertical I.P.s $\pm$0·02 or $\pm$0·1 eV depending on number of figures given.

[3] L. Manojlovic-Muir, K. W. Muir, and J. A. Ibers, *Inorg. Chem.*, 1970, **9**, 447.

[4] S. Cradock and R. A. Whiteford, *Trans. Faraday Soc.*, 1971, **67**, 3425.

[5] S. Evans, J. C. Green, M. L. H. Green, A. F. Orchard, and D. W. Turner, *Discuss. Faraday Soc.*, 1969, **47**, 112.

TABLE 2

Vertical ionisation potentials/eV for $LRe(CO)_5$

Region	A				B		C
Levels	Re 5d				Re–Cσ	C–Oπ	
	e	b_2	Re–H	M^1–H	onset	tail	C–Oσ
L							
H	8·86, 9·15	9·53	10·5	—	13·5	17	n.o.
SiH_3	8·9?, 9·1	9·5, 9·6	—	11·6	13·6	17	18·2
GeH_3	8·9?, 9·13	9·4, 9·6	—	11·4	13·6	17	18·1

n.o. = Not observed.

TABLE 3

Vertical ionisation potentials/eV for $LCo(CO)_4$

Region	A				B		C
Levels	Co 3d				Co–Cσ	C–Oπ	
	e	e	Co–H	M^1–H	onset	tail	C–Oσ
L							
H	8·90	9·90	11·5	—	13·8	17	18·2
SiH_3	8·85	9·90	—	11·9	13·8	17	18·2
GeH_3	8·80	9·80	—	11·9	13·5	17	18·1

TABLE 4

First ionisation potentials/eV for metal atoms

Metal	Mn	Re	Co
I.P.	7·43	7·87	7·86

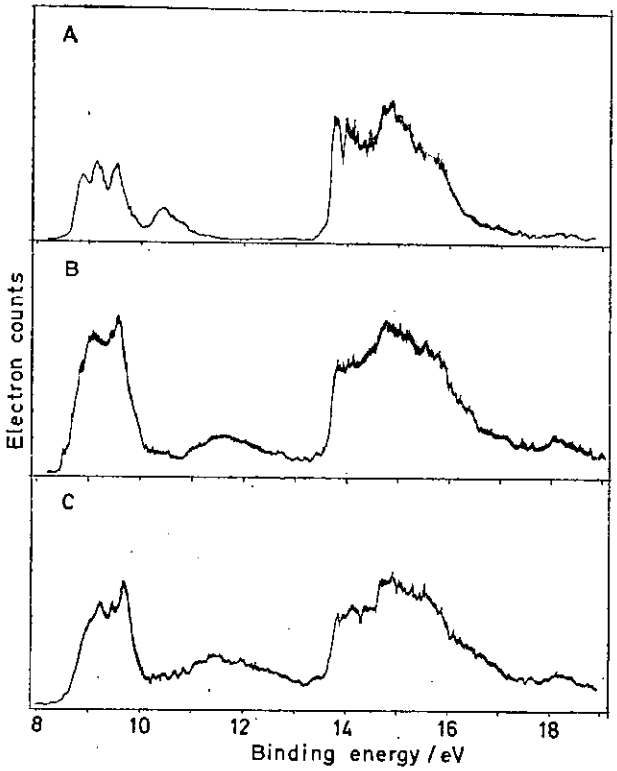

FIGURE 2 Photoelectron spectra of A, $HRe(CO)_5$; B, $SiH_3Re(CO)_5$; and C, $GeH_3Re(CO)_5$

DISCUSSION

In order to analyse our spectra we must establish an approximate scheme to describe the molecular orbitals of the molecules we are studying. Molecules of the form $M^1H_3M^2(CO)_5$ will be assumed to belong to the effective point group C_{4v}, the 3-fold symmetry of the M^1H_3 group being over-ridden by the four-fold symmetry of the $M^2(CO)_5$ group. The occupied molecular orbitals of the valence shell can be subdivided into four groups: those associated with the CO groups and the M^2–C

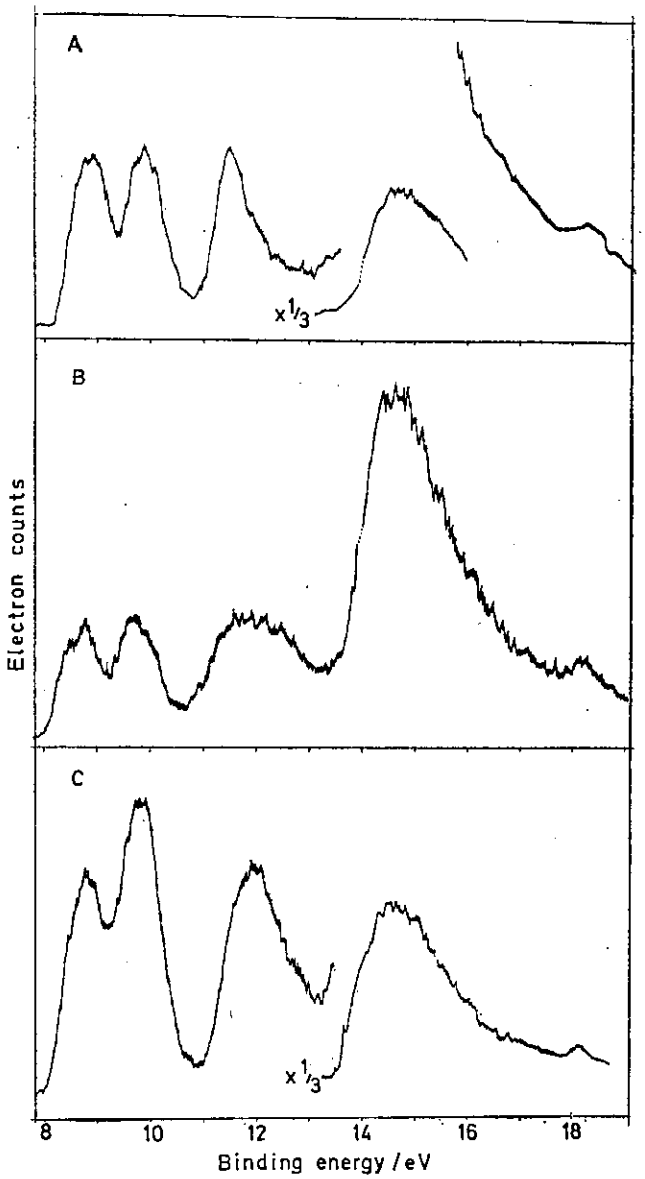

FIGURE 3 Photoelectron spectra of A, $HCo(CO)_4$; B, $SiH_3Co(CO)_4$; and C, $GeH_3Co(CO)_4$

σ-bonds; those associated with the M^1–H σ-bonds (symmetry species a_1 and e); that associated with the M^1–M^2 σ-bond (symmetry species a_1); and those associated with the formally non-bonding metal M^2 d-orbitals (symmetry species b_2 and e). The orbitals of molecules $M^1H_3Co(CO)_4$, point-group C_{3v}, can be classified in very similar terms; the most important difference is that the formally non-bonding d-levels now comprise two doubly-degenerate sets.

A recent experimental and theoretical study [5] of the

photoelectron spectra of compounds containing the $-Mn(CO)_5$ group gives us a valuable basis for our assignment. These spectra were discussed in terms of three regions: *A*, 13—18 eV; *BA*, 8—13 eV; *B* 13—17 eV; and *C* 17—19 eV. In region *C* a broad and relatively weak band is derived from 4σ of CO; region *B* contains a set of overlapping strong bands due to Mn–C σ-bonding and C–O π-bonding levels, while the bands in region *A* were assigned to excitation from the formally non-bonding Mn 3*d*-orbitals, from the sixth σ-bond to Mn and from levels associated mainly with the sixth ligand. Information about the interaction between the transition metal and the M^1H_3 group should therefore be obtainable from the bands in region *A*. It seems very probable that the spectra of the cobalt complexes can be analysed in similar terms. In the discussion that follows we shall deal mainly with region *A*.

The spectra of the hydrides $HMn(CO)_5$, $HRe(CO)_5$, and $HCo(CO)_4$ help us to identify the bands due to the metal *d*-levels. In each spectrum there is a set of strong bands between 8 and 10 eV, with a single weaker band near 11 eV; we assign the bands near 9 eV to the non-bonding metal *d*-levels and the band near 11 eV to the M^2–H σ-bonding level. This assignment differs from that suggested earlier [5] for $HMn(CO)_5$. For M^2 = Mn and Re the bands at lower binding energy overlap, but in both cases more than one maximum can be distinguished. For M^2 = Co there are clearly two bands of equal intensity separated by 1 eV, assigned to the two expected levels of symmetry species *e*. The spectra of the corresponding M^1H_3 derivatives show a superficially similar pattern, a group of strong bands near 9 eV and a broad, weaker band near 12 eV, but while we believe that in these spectra too the bands near 9 eV are due to excitation from the metal *d*-levels, we do not assign the band 12 eV to the M^1–M^2 σ-bonding level.

Each M^1H_3 group has two levels associated with M^1H σ-bonding, derived respectively from *ns* (a_1) and *np* (*e*) levels of M^1. The former are found in the spectra [4] of simple molecules MH_3X to appear in region *C* or at even higher binding energies. The *e*-levels give bands near 15 eV for methyl halides and near 13 eV for silyl and germyl halides; [4] the bands shift to lower binding energies as the group bound to M^1H_3 becomes less electronegative.[6] Thus it is not unreasonable to assign bands near 12 eV in the spectra of $M^1H_3Mn(CO)_5$ to the M^1H_3 *e*-symmetry levels shifted greatly to lower binding energies by the very electropositive $-Mn(CO)_5$ group. Similar bands in the spectra of the other silyl and germyl derivatives are assigned in the same way.

We are now left with no resolved bands which we could assign to the M^1–M^2 σ-bonding levels. From assignments in the spectra of hydrogen, methyl, silyl, and germyl compounds we believe that the binding energies of the M^1–M^2 σ-bonding level is likely to be 2—3 eV less than that of the corresponding H–M^2 level. As in the hydrides we assign the H–M^2 bonding level to the band near 11 eV we may expect M^1–M^2 bonding levels to give bands near 9 eV, where they will be obscured by the M^2 non-bonding *d*-levels.

Having made tentative assignments for the bands in region *A* we may attempt to draw some conclusions from the differences in the spectra. Thus for M^1H_3-$Mn(CO)_5$ (M^1 = C, Si, and Ge) the Mn 3*d* bands (probably including the Mn–M^1 bonding level) near 9 eV shift so that the order of *d*-electron binding energies is Si > Ge > C, rather than C > Si ≈ Ge (as expected on the basis of most electronegativity scales). In the past we [4,6,7] and others [8] have attributed such 'anomalous' shifts in π-levels of groups attached to Si or Ge as being due to π-donation to vacant 3*d* or 4*d* orbitals of Si or Ge respectively. This type of interaction cannot provide the whole explanation here, as one of the Mn 3*d*-levels is of b_2 symmetry, which could only δ-bond to Si or Ge [unless the overall interaction between the C_{3v} M^1H_3 and C_{4v} $Mn(CO)_5$ groups is rigid enough to reduce the effective symmetry to C_s, which seems unlikely].

We believe that the differences in binding energies can be rationalised in terms of differences in σ-accepting power of the M^1H_3 groups, which will determine the effective nuclear charge of the Mn atom. The observed order of binding energies implies that the net positive charge on Mn varies in the order Si > Ge > C, so that the order of decreasing σ-accepting power for the M^1H_3 groups is $SiH_3 > GeH_3 > CH_3$. This would account for shifts in both the *e* and the b_2 Mn 3*d*-levels, whereas ($d \rightarrow d$) π-bonding would produce a shift only in the *e*-level. We conclude that the photoelectron spectra afford no evidence for ($d \rightarrow d$) π-bonding in $SiH_3Mn(CO)_5$ or $GeH_3Mn(CO)_5$. The great similarities of the spectra of the Re derivatives to those of the Mn compounds suggests a similar conclusion in this case also. We are not able to explain why the SiH_3 group should act as a better σ-acceptor than the CH_3 group; it may be that the larger size of the Si atom or of the SiH_3 group allows for more diffusion of charge, or the polarities and polarisabilities of the M^1–H bonds may be a determining factor.

The case of $Me_3SiMn(CO)_5$ is interesting. We [4] and others [9] have found that in compounds such as Me_3SiCl the Me_3Si groups interact strongly with neighbouring π-levels (σ–π mixing). In the present compound we find no marked difference in the positions of the Mn 3*d*-levels from those in the silyl compound. The level mainly responsible for the interaction, the *e*-symmetry Si–C bonding level, occurs at 10·8 eV, very close to its position in Me_3SiH, where no such interaction can occur.

In $HRe(CO)_5$ the first strong band (assigned in the hydride to the $b_2 + e$ Re 5*d*-levels only) shows three peaks, at 8·86, 9·15, and 9·53 eV, whereas $HMn(CO)_5$

[6] S. Cradock and R. A. Whiteford, *J.C.S. Faraday II*, 1972, **68**, 281.
[7] S. Cradock, E. A. V. Ebsworth, W. J. Savage, and R. A. Whiteford, *J.C.S. Faraday II*, 1972, **68**, 934.
[8] D. C. Frost, F. G. Herring, A. Katrib, R. A. N. McLean, J. E. Drake, and N. P. C. Westwood, *Canad. J. Chem.*, 1971, **49**, 4033.
[9] C. G. Pitt and H. Bock, *Chem. Comm.*, 1972, 28.

gives only two peaks, at 8·85 and 9·14 eV. As the spin–orbit coupling parameter ζ_{5d} for Re is of the order of 0·30 eV, while that for Mn, ζ_{3d}, is only 0·03 eV, we assign the extra peak for the Re compound as due to spin–orbit coupling in the ^2E state of the ion $HRe(CO)_5^+$. The first atomic I.P. for Re is 0·44 eV greater than that for Mn, so it seems likely that the peaks at 9·14 eV (Mn) and 9·53 eV (Re) can be assigned to the b_2 level in each case, while the peak at 8·85 eV (Mn) and the doublet at 8·86 and 9·15 eV (Re) are assigned to the e-level. The spectra of $SiH_3Re(CO)_5$ and $GeH_3Re(CO)_5$ are less clearly resolved in this region, probably because of the additional Re–M^1 bonding level, but seem to show a first peak near 9·1 eV with a shoulder at 8·9 eV that may well be the two components derived from the e-level. In each case there are two further peaks near 9·5 eV that we may assign to the b_2 non-bonding and a_1 Re–M^1 bonding levels.

In summary, we are unable to adduce any evidence for π-interactions between transition-metal d-orbitals and SiH_3, GeH_3, or Me_3Si groups. The changes in binding energy of the transition-metal d-electrons seem more probably to be caused by changes in the σ-accepting abilities of the M^1H_3 groups.

We thank Drs. A. F. Orchard and S. Evans of the Inorganic Chemical Laboratories, Oxford, for spectra and discussions; the S.R.C. for a grant, and Edinburgh University for a Dewar Scholarship (to A. R.).

[2/1187 *Received*, 24*th May*, 1972]

PHOTOELECTRON SPECTRUM AND BONDING IN $SiF_3Mn(CO)_5$

Stephen CRADOCK, E.A.V. EBSWORTH and Alastair ROBERTSON
Department of Chemistry, University of Edinburgh, Edinburgh EH9 3JJ, UK

Received 14 October 1974

The He I photoelectron spectrum of pentacarbonyltrifluorosilylmanganese contains a band attributable to the Si–Mn bonding level, at a binding energy of 10.4 eV. The corresponding band for the SiH_3- derivative is probably obscured by the stronger bands near 9 eV due to the Mn 3d levels.

1. Introduction

We have published [1] the photoelectron spectra of some silyl transition metal carbonyl derivatives, $SiH_3Mn(CO)_5$, $SiH_3Re(CO)_5$ and $SiH_3Co(CO)_4$, and the related germyl compounds. It was not possible to resolve any bands in these spectra that could be assigned to the M^1-M^2 σ-bonding level, but we suggested that such bands were among or beneath the stronger bands due to formally non-bonding M^2 d levels. This assignment is in accord with theoretical studies [2] on $CH_3Mn(CO)_5$, but experimental evidence to support it has been lacking.

We here report that the photoelectron spectrum of $SiF_3Mn(CO)_5$ [3] contains a band clearly separated from the Mn 3d level bands. This we assign to the Si–Mn σ-bonding level; the separation arises from the effect of the fluorine atoms attached to Si.

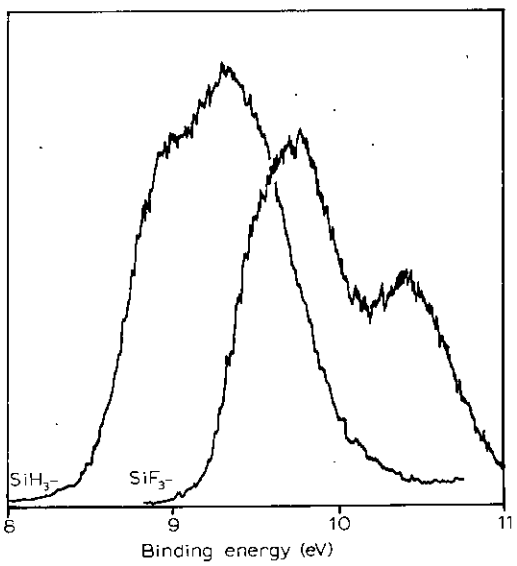

Fig. 1. Photoelectron spectra of $SiH_3Mn(CO)_5$ and $SiF_3Mn(CO)_5$ between 8 eV and 11 eV binding energy.

2. Experimental

Pentacarbonyltrifluorosilylmanganese was prepared [3] from dimanganesedecacarbonyl and trifluorosilane heated together in an evacuated tube:

$$2HSiF_3 + Mn_2(CO)_{10} = 2SiF_3Mn(CO)_5 + H_2.$$

The product was purified by fractional condensation in a vacuum system. The sample was introduced into the photoelectron spectrometer (Perkin–Elmer PS16) from a vacuum manifold, and the photoelectron spectrum obtained using He I (21.22 eV) excitation.

3. Discussion

Fig. 1 shows a comparison of the 8–11 eV binding energy regions of the spectra of the SiH_3- and SiF_3- derivatives. The 0.5 eV shift to higher binding energy

of the main Mn 3d band reflects the higher effective electronegativity of the SiF_3- group [4]. Much more striking is the appearance (at 10.4 eV binding energy) of an additional band in the spectrum of $SiF_3Mn(CO)_5$.

There seem to be two main possibilities:

(a) that this band is due to some component of the Mn 3d levels shifted by a strong π-interaction with the SiF_3- group, or

(b) that it represents the missing Si–Mn σ-bonding level, shifted some 1.5 eV to higher binding energy by the influence of the three F atoms.

There are several clear-cut precedents for the latter assignment, including our study [4] of a variety of SiF_3- compounds, and the so-called "perfluoro effect" in planar compounds [5]. This being so it is unnecessary to postulate enhanced (d → d) π-bonding in $SiF_3Mn(CO)_5$.

Our assignment of the band at 10.4 eV binding energy in the spectrum of $SiF_3Mn(CO)_5$ to the Si–Mn σ-bonding level reinforces our earlier suggestion that the corresponding bands in SiH_3-transition metal carbonyls are hidden by the stronger transition metal d-level bands near 9 eV. This accounts at least in part for the difficulty in establishing clearly the positions of the two components (e and b_2 in a C_{4v} molecule) of the Mn 3d levels. Even when this complication is removed, as in the spectrum of the SiF_3 derivative, there is no clear splitting into two peaks, and it would be unjustifiable to assign any particular value to the splitting between the components. From the breadth of the band near 9.8 eV it is clear that the splitting cannot be greater than about 0.3 eV.

The implications of these observations for the bonding in silyl-transition metal carbonyls are that even in this most favourable case no evidence of (d → d) π-bonding can be found. The variations found in various properties are more likely to reflect changes in σ-bonding. The increase in the binding energy of the Si–Mn bonding level need not correspond to a great change in the bond *strength*, but may have important implications for possible reaction pathways and the relative stabilities of the compounds to chemical reactions.

References

[1] S. Cradock, E.A.V. Ebsworth and A. Robertson, J. Chem. Soc. Dalton (1973) 22.

[2] M.B. Hall, M.F. Guest and I.H. Hillier, Chem. Phys. Letters 15 (1972) 592.

[3] M.E. Redwood, B.E. Reichert, R.R. Schrieke and B.O. West, Australian J. Chem. 26 (1973) 247.

[4] S. Cradock, E.A.V. Ebsworth and R.A. Whiteford, J. Chem. Soc. Dalton (1973) 2401.

[5] C.R. Brundle, M.B. Robin, N.A. Kuebler and H. Basch, J. Am. Chem. Soc. 94 (1972) 1451.

Journal of Molecular Structure, 27 (1975) 438—439

Short communication

THE MOLECULAR STRUCTURE OF HEXAFLUORODISILANE, DETERMINED BY GAS PHASE ELECTRON DIFFRACTION

D. W. H. RANKIN and A. ROBERTSON

Department of Chemistry, University of Edinburgh, West Mains Road, Edinburgh EH9 3JJ (Gt. Britain)

(Received 3 October 1974)

The He^I photoelectron spectrum of hexafluorodisilane implies that the pair of electrons involved in the Si—Si bond is much more tightly bound than the corresponding one in disilane [1]. We have therefore undertaken a determination of the molecular structure of hexafluorodisilane, to see whether the lowering of orbital energy results in a shortening of the Si—Si bond.

A sample of Si_2F_6 was prepared by fluorination of Si_2Cl_6 with antimony trifluoride and antimony pentachloride catalyst [2], and was used to obtain electron diffraction data out to $s = 292$ nm^{-1} using a Balzers' KD.G2 instrument, with a nozzle temperature of 298 K and a sample temperature of 209 K. Computation of results by standard procedures [3, 4], using the scattering factors of Cox and Bonham [5], led to the parameters given in Table 1. Errors quoted are least-squares derived standard deviations with an allowance for systematic errors. The twist angle (between the SiF_3 groups) was determined by comparison of R factors for refinements in which it was

TABLE 1

Molecular parameters of Si_2F_6

	Distance (r_a)	Amplitude (pm)
Si—F	156.9(2)	4.7(2)
Si—Si	232.4(6)	6.8(7)
F(Si)F	254.5(7)	8.1(3)
F(Si)Si	322.4(6)	11.0(3)
F(SiSi)F	353.5(6)	17.3(21)
F(SiSi)F	396.3(6)	20.5(24)
F(SiSi)F	446.7(8)	14.4(10)
	Angle (deg)	
Si—Si—F	110.6(3)	
Twist[a]	34.6 (see text)	

[a] From eclipsed conformation

fixed at values between 0° (eclipsed) and 60° (staggered), and was thereafter fixed at the optimum value. The R factor (R_G) in the best refinement was 0.08: the radial distribution curve and difference curve after this refinement are shown in Fig. 1.

The Si—Si bond length found for Si_2F_6 (232.4 ± 0.6 pm) is only slightly less than those in Si_2H_6 (233.1 ± 0.3 pm) [6] and Si_2Me_6 (234.0 ± 0.9 pm) [7]. It seems than any contraction caused by the fluorine atoms lowering the Si—Si bonding orbital energy is almost balanced by repulsion between the electrons on the fluorine atoms. We expect that in SiH_3SiF_3, where there may be attractive H · · · F forces, a shorter Si—Si bond will be found.

The Si—F bond length (156.9 pm: compare [8] r_0 156.5 pm in $HSiF_3$) and other parameters are much as would be expected.

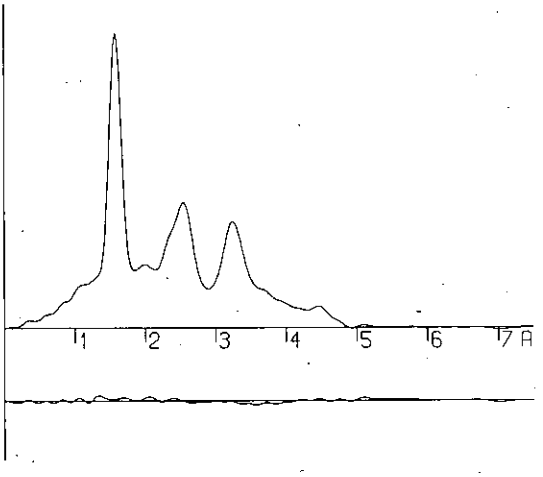

Fig. 1. Radial distribution curve, $P(r)/r$, and difference curve, for Si_2F_6. Before Fourier inversion the data were multiplied by $s.\exp[-0.0025\, s^2(z_{Si}-f_{Si})(z_F-f_F)]$.

REFERENCES

1 S. Cradock, E. A. V. Ebsworth and R. A. Whiteford, J. Chem. Soc. Dalton., (1973) 2401.
2 H. J. Emeléus and A. G. Maddock, J. Chem. Soc., (1944) 293.
3 G. C. Holywell, D. W. H. Rankin, B. Beagley and J. M. Freeman, J. Chem. Soc. A, (1971) 785.
4 D. M. Bridges, G. C. Holywell, D. W. H. Rankin and J. M. Freeman, J. Organometal. Chem., 32 (1971) 87.
5 H. L. Cox and R. A. Bonham, J. Chem. Phys., 47 (1967) 605.
6 B. Beagley, A. R. Conrad, J. M. Freeman, J. J. Monaghan, B. G. Norton and G. C. Holywell, J. Mol. Struct., 11 (1972) 371.
7 B. Beagley, J. J. Monaghan and T. G. Hewitt, J. Mol. Struct., 8 (1971) 401.
8 G. A. Heath, L. F. Thomas and J. Sheridan, Trans. Faraday Soc., 50 (1954) 779.

Journal of Organometallic Chemistry, 85 (1975) 225—235

AN ELECTRON DIFFRACTION DETERMINATION OF THE MOLECULAR STRUCTURES OF SILYL- AND GERMYL-MANGANESE PENTACARBONYL IN THE GAS PHASE

D.W.H. RANKIN and A. ROBERTSON

Department of Chemistry, University of Edinburgh, West Mains Road, Edinburgh, EH9 3JJ. (Great Britain)

(Received September 3rd, 1974)

Summary

The molecular structures of the title compounds have been determined by gas phase electron diffraction methods. The Si—Mn and Ge—Mn bond lengths are 240.7 ± 0.5 and 248.7 ± 0.2 pm respectively and the C—Mn—C angles in the silyl and germyl cases are 94.5 ± 2° and 97 ± 2° respectively. Comparisons are made with the reported structure of $CH_3Mn(CO)_5$ and He^I photoelectron spectra of these compounds in an attempt to determine the extent of $d \rightarrow d$ π-bonding in the Si—Mn or Ge—Mn bonds.

Introduction

In silyl- and germyl-transition metal complexes there exists the possibility of multiple bonding between the silicon, or germanium, atom and the transition metal atom, involving unoccupied silicon or germanium *d* orbitals. It is therefore of interest to determine the molecular structures of some of these complexes to see whether there is any stereochemical evidence for multiple bonding. However up to the present the only compound of this type whose gas phase structure has been determined is silylcobalt tetracarbonyl [1], so we have determined the gas phase structures of silylmanganese pentacarbonyl and germylmanganese pentacarbonyl by electron diffraction.

From a multiple bonding point of view the most important parameters are the silicon—manganese and germanium—manganese bond lengths. These will be compared with the (methyl)carbon—manganese bond length in methylmanganese pentacarbonyl [2] where there is no possibility of such multiple bonding.

It is also interesting to find out whether these structures bear out the conclusions from the He^I photoelectron spectra of these compounds [3] that

TABLE 1

WEIGHTING FUNCTIONS, CORRELATION PARAMETERS AND SCALE FACTORS

Compound	Camera height (mm)	dels (nm^{-1})	s_{min}	s_1	s_2	s_{max}	P/h	Scale factor
$SiH_3Mn(CO)_5$	250	4	68	108	250	280	0.4448	1.056 ± 0.038
	500	2	36	60	135	155	0.4763	1.168 ± 0.029
	1000	1	10	17.5	62.5	70	0.4920	0.900 ± 0.047
$GeH_3Mn(CO)_5$	250	4	68	108	248	288	0.4207	1.067 ± 0.033
	500	2	28	53	130	150	0.2475	0.907 ± 0.020
	1000	1	12	20	65	73	0.4587	0.851 ± 0.039

$d \rightarrow d$ π-bonding is not important in the silicon—manganese and germanium—manganese bonds and that the main effect in changing from methyl to germyl to silyl is an increase in the strength of the σ bond.

Experimental

Samples of silylmanganese and germylmanganese pentacarbonyl were prepared by reacting silyl iodide or germyl bromide with sodiummanganese pentacarbonyl in diethyl ether [4, 5]. The products were collected at 77 K and purified by fractional condensation. Purities were checked spectroscopically.

Scattering intensities were recorded photographically using a Balzers KDG2 gas diffraction apparatus and were digitised on a Joyce Loebl microdensitometer. During exposures the samples were kept at 323 K [$SiH_3Mn(CO)_5$] and 328 K [$GeH_3Mn(CO)_5$] and the nozzle at 333 K. Three nozzle to plate distances were used (1000, 500 and 250 mm) giving data over a range of the scattering variable, s, of about 10-300 nm^{-1}.

Calculations were carried out on an IBM 370/155 computer at the Edinburgh Regional Computing Centre with data reduction and least squares refinement programs previously described [6, 7].

Table 1 shows weighting points (used to set up the off diagonal weight matrix), correlation parameters and scale factors. The complex scattering factors of Cox and Bonham [8] were used and all distances are r_a. The electron wavelength used was determined by direct measurement of the accelerating voltage and from the diffraction pattern of powdered thallous chloride.

Molecular model

For the purposes of least squares refinements it was assumed for each molecule that the manganese pentacarbonyl group had local C_{4v} symmetry, the MH_3 group had local C_{3v} symmetry and all the manganese—carbon and carbon—oxygen bonded distances were equal; since there is a twelve fold barrier to rotation about the M—Mn bond, free rotation about this bond was assumed. These assumptions allowed the molecule to be described uning the 4 bonded distances and the following angles: H—M—H, Mn—C_{eq}—O_{eq} and C_{ax}—Mn—C_{eq}.

The assumption that the manganese—carbon distances are equal for axial and equatorial carbons might have proved to be unjustified, but it is unlikely that the difference will be greater than the 4 pm found in methylmanganese pentacarbonyl and may be around 2 pm as in manganese pentacarbonyl hydride, or even less. Such small differences within the molecule would be very difficult to determine reliably by electron diffraction. There is no evidence for any asymmetry of the Mn—C peak in the radial distribution curves nor are the experimental Mn—C or Mn ... O amplitudes of vibration significantly greater than values found in other manganese pentacarbonyl derivatives.

Refinements

Silylmanganese pentacarbonyl

The silicon—manganese, manganese—carbon, and carbon—oxygen bonded

TABLE 2. MOLECULAR PARAMETERS FOR $MH_3Mn(CO)_5$

	$SiH_3Mn(CO)_5$		$GeH_3Mn(CO)_5$		
	Distance	Amplitude	Distance	Amplitude	Shrinkage correction
a. Independent distances					
r_1(C—O)	113.2 (0.3)	4.2 (0.8)	113.9 (0.2)	4.3 (0.8)	
r_2(Mn—C)	184.7 (0.2)	7.5 (0.6)	184.9 (0.2)	6.8 (0.6)	
r_3(Mn—M)	240.7 (0.5)	7.4 (0.9)	248.7 (0.2)	5.7 (0.6)	
r_4(M—H)	149.0 (fixed)	8.5 (fixed)	153.5 (fixed)	12.0 (fixed)	
b. Dependent distances					
d_5(Mn···O_{ax})	297.4 (1.0)	8.2 (0.6)	298.2 (1.0)	6.8 (0.6)	0.59
d_6(Mn···O_{eq})	297.4 (1.0)		298.2 (1.0)		0.59
d_7(C_{eq}···O_{eq})	474.2 (1.7)	11.5 (1.4)	478.2 (1.5)	8.5 (1.3)	2.27
d_8(O_{eq}···O_{eq})	590.6 (2.0)		590.0 (2.0)		3.42
d_9(C_{eq}···C_{eq})	367.0 (1.1)		365.9 (1.1)		1.33
d_{10}(C_{eq}···C_{eq})	271.2 (0.6)	10.7 (1.4)	276.3 (0.6)	15.9 (fixed)	0.25
d_{11}(C_{eq}···C_{ax})	260.1 (0.7)		259.4 (0.7)		0.25
d_{12}(O_{eq}···O_{eq})	436.0 (0.7)	28.7 (3.6)	445.5 (1.4)	27.7 (fixed)	1.40
d_{13}(O_{eq}···O_{ax})	418.6 (1.4)		418.1 (1.4)		1.40
d_{14}(C_{eq}···O_{eq})	362.0 (0.7)	18.4 (0.9)	368.8 (0.7)	19.3 (fixed)	0.82
d_{15}(C_{ax}···O_{eq})	362.0 (0.7)		368.8 (0.7)		0.82
d_{16}(C_{eq}···O_{ax})	348.8 (1.0)		348.4 (1.0)		0.82
d_{17}(M···C_{ax})	424.0 (1.1)	19.4	432.2 (1.0)	7.1	1.43
d_{18}(M···O_{ax})	536.3 (1.5)	21.7 (7)	545.1 (1.4)	7.9 (1.5)	2.38
d_{19}(M···C_{eq})	291.3 (1.4)	25.0	291.9 (0.8)	15.5	0.28
d_{20}(M···O_{eq})	367.0 (1.8)	36.0 (fixed)	364.5 (1.4)	19.4 (1.0)	0.90
d_{21}(H···Mn)	322.9 (0.9)	12.0 (fixed)	333.3 (1.0)	12.0 (fixed)	0.59
d_{22}(H···C_{ax})	494.3 (1.1)	15.0 (fixed)	504.8 (1.3)	15.0 (fixed)	2.27
d_{23}(H···O_{ax})	602.6 (1.8)	18.0 (fixed)	613.6 (1.7)	18.0 (fixed)	3.42
d_{24}(H···H)	242.4 (0.2)	10.0 (fixed)	249.7 (0.7)	10.0 (fixed)	0.07
(H···C_{eq})	Between 282.0 and 423.4		Between 286.0 and 427.7		
(H···O_{eq})	Between 313.7 and 508.5		Between 309.7 and 510.5		
c. Independent angles					
< 1 (H—M—H)		110° (fixed)		110° (fixed)	
< 2 (C_{ax}—Mn—C_{eq})		94.5° (2°)		97° (2°)	
< 3 (Mn—C_{eq}—O_{eq})		180° (fixed)		180° (fixed)	

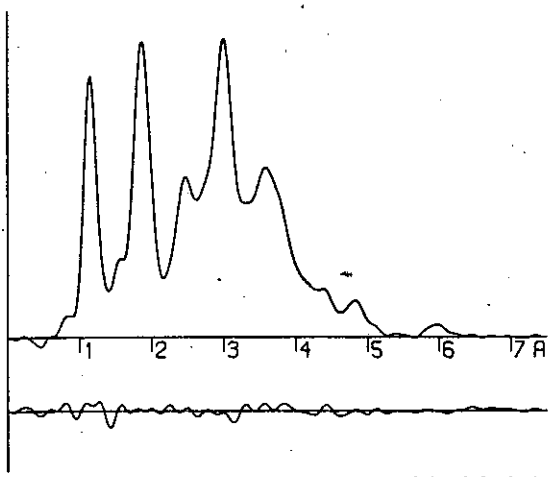

Fig. 1. Radial distribution curve, $P(r)/r$, and final deviations between experimental and theoretical curves for $SiH_3Mn(CO)_5$. Before Fourier inversion the data were multiplied by $s.\exp(-0.0025\,s^2)/(Z_{Mn}-F_{Mn})(Z_O-F_O)$.

distances and their amplitudes of vibration all refined satisfactorily, as did the Mn—C—O and C—Mn—C angles. The overlapping of large numbers of peaks in the radial distribution curve (Fig. 1) necessitated the refinement of certain groups of vibrational amplitudes as single parameters (see Table 2). Most groups, other than those involving hydrogen atoms, refined satisfactorily; the amplitudes of vibration of the silicon to axial carbon and silicon to axial oxygen being the only exceptions. These amplitudes along with all parameters involving hydrogen were set at fixed values.

The final R factor was 0.16. Table 3 shows the least squares correlation matrix, and final molecular scattering intensity and difference curves are shown in Fig. 2. The intensity data or uphill curves may be obtained from the authors on request.

Germyl manganese pentacarbonyl

The refinements were very similar to those of silylmanganese pentacarbonyl. The germanium—manganese, carbon—manganese and carbon—oxygen bonded distances and their amplitudes of vibration and the Mn—C—O and C—Mn—C angles all refined satisfactorily.

Here also there is considerable overlapping in the radial distribution curve (Fig. 3) which necessitated the constraint of certain groups of amplitudes (Table 2). Amplitudes of vibration involving right angled carbon···carbon, carbon···oxygen and oxygen···oxygen distances did not refine, nor did any parameters involving hydrogen. These parameters were set at fixed values. The final R factor was 0.13.

Table 4 shows the least squares correlation matrix, and final molecular scattering intensity and difference curves are shown in Fig. 4. The intensity data or uphill curves can be obtained from the authors on request.

Shrinkage corrections applied were the same as those applied in the structure determination of pentacarbonyl(trifluorophosphine)molybdenum [7].

(continued on p. 233)

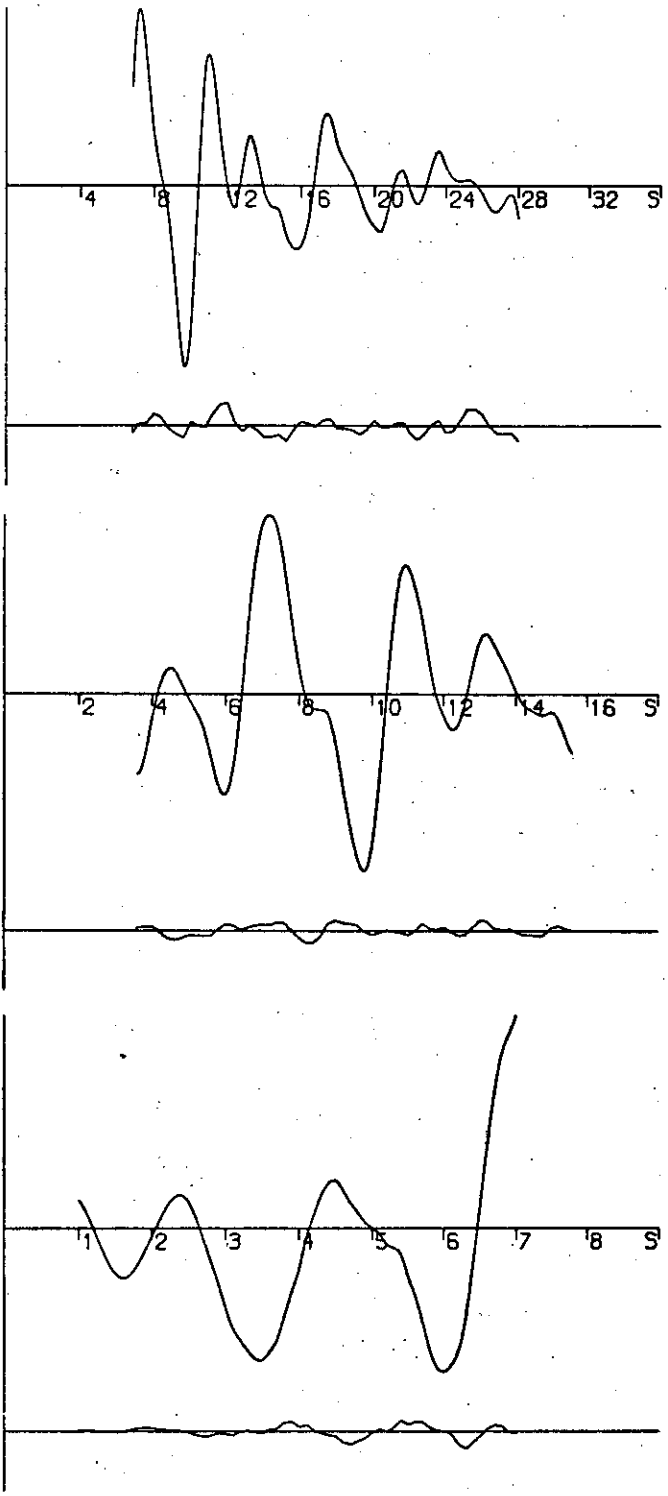

Fig. 2. Observed and final weighted difference molecular intensities for $SiH_3Mn(CO)_5$ for data sets obtained with nozzle-to-plate distances of 250, 500 and 1000 mm.

TABLE 3

LEAST SQUARES CORRELATION MATRIX MULTIPLIED BY 1000 FOR $SiH_3Mn(CO)_5$

R_1	R_2	R_3	< 2	U_1	U_2	U_3	U_5	U_7	U_{10}	U_{12}	U_{14}	U_{17}	K_1	K_2	K_3
1000	−23	−114	−635	11	70	6	71	19	60	77	108	30	27	142	84
	1000	−15	−481	9	33	−11	38	2	19	20	−79	52	46	−7	−30
		1000	47	−33	−94	195	53	−57	272	23	−18	1	−49	−97	−40
			1000	−78	−141	16	−87	−6	50	−150	−268	−19	−145	−169	−30
				1000	459	109	374	124	−69	16	188	1	586	438	52
					1000	39	467	152	−113	17	230	0	682	589	104
						1000	228	39	542	28	1	0	195	123	−52
							1000	146	258	19	59	7	602	502	104
								1000	−23	472	3	−422	188	199	86
									1000	22	−170	11	−106	−116	−16
										1000	167	−756	33	12	−25
											1000	−137	292	260	−56
												1000	14	−27	−74
													1000	572	72
														1000	52
															1000

TABLE 4

LEAST SQUARES CORRELATION MATRIX MULTIPLIED BY 1000 FOR $GeH_3Mn(CO)_5$

R_1	R_2	R_3	< 2	U_1	U_2	U_3	U_5	U_7	U_{17}	U_{19}	K_1	K_2	K_3
1000	51	25	−606	8	85	54	42	83	16	−95	18	101	96
	1000	−59	−615	38	112	134	107	48	59	50	113	122	85
		1000	−120	−65	−181	−28	−36	−44	−29	−224	−92	−146	−178
			1000	−83	−177	−156	−46	−89	−30	−132	−150	−225	−140
				1000	445	335	259	117	100	318	530	511	157
					1000	410	338	151	124	384	624	656	247
						1000	176	118	104	344	579	496	135
							1000	161	113	−131	480	369	86
								1000	−65	−3	199	172	92
									1000	49	180	136	5
										1000	438	542	293
											1000	636	227
												1000	258
													1000

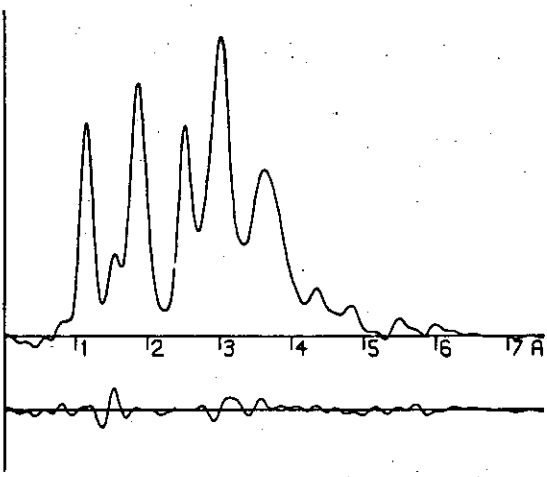

Fig. 3. Radial distribution curve, P(r)/r, and final differences between experimental and calculated curves for $GeH_3Mn(CO)_5$. Before Fourier inversion the data were multiplied by $s \cdot \exp(0.0025\, s^2)/(Z_{Mn}-F_{Mn})\cdot(Z_O-F_O)$.

Discussion

In methylmanganese pentacarbonyl the covalent radius of manganese has been found to be 141.8 pm [2]. Using this, and taking the covalent radii of silicon and germanium to be 110.0 and 117.8 pm respectively (calculated from bond lengths between tetrahedrally coordinated atoms in ethane [9], methylsilane [10] and methylgermane [11]), we would expect the silicon—manganese bond length to be 251.9 pm and the germanium—manganese bond length to be 259.6 pm. In fact these two bond lengths turn out as 240.7 and 248.7 pm respectively.

These two bond lengths could be taken to indicate that multiple bonding does exist between the manganese and silicon or germanium atoms in these compounds. This multiple bonding would involve the π 3*d* orbitals of manganese and the 3*d* (or 4*d*) π-orbitals of silicon (or germanium). However, He^I photoelectron spectra of these compounds [3] indicate that the main change in going from a methyl to a silyl to a germyl substituent on manganese pentacarbonyl is a σ effect, and that silyl is a slightly better σ acceptor than germyl which is a much better σ acceptor than methyl; that is, silyl is slightly more electropositive than germyl which is very much more electropositive than methyl. This theory would also lead to similar results to those we have found here. We intend to make further studies to find out more about these effects.

Acknowledgements

We thank Professor D.W.J. Cruickshank, Dr. B. Beagley, Mrs. V. Ulbrecht and Dr. M.J. Smyth for the experimental facilities. We also thank the Dewar Foundation for a grant to A.R.

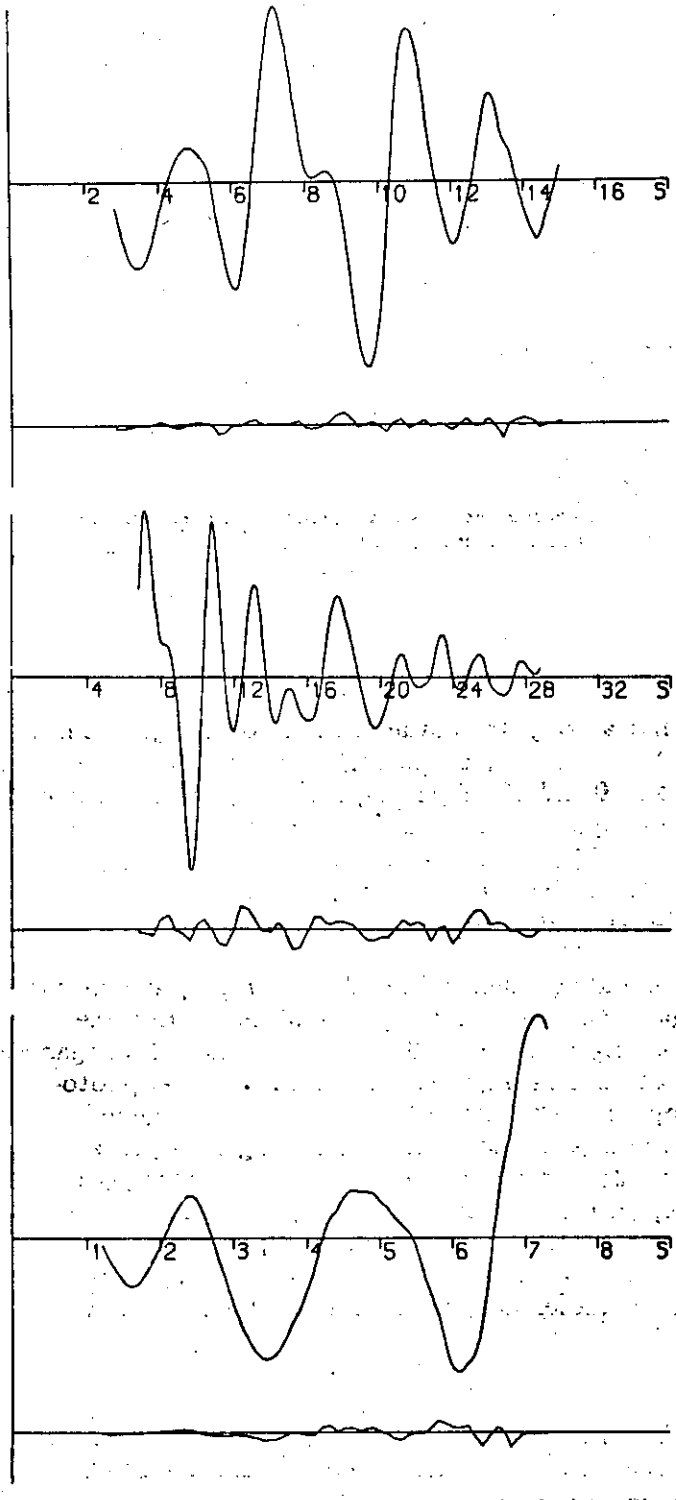

Fig. 4. Observed and final weighted difference molecular intensities for $GeH_3Mn(CO)_5$ for data sets obtained with nozzle-to-plate distances of 250, 500 and 1000 mm.

References

1 A.G. Robiette, G.M. Sheldrick, R.N.F. Simpson, B.J. Aylett and J.A. Campbell, J. Organometal. Chem., 14 (1968) 279.
2 H.M. Seip and R. Seip, Acta Chem. Scand., 24 (1970) 3431.
3 S. Cradock, E.A.V. Ebsworth and A. Robertson, J. Chem. Soc. Dalton Trans., (1973) 22.
4 B.J. Aylett and J.M. Campbell, J. Chem. Soc. A, (1969) 1916.
5 R.D. George, K.M. Mackay and S.R. Stobart, J. Chem. Soc. Dalton Trans., (1972) 1505.
6 G.C. Holywell, D.W.H. Rankin, B. Beagley and J.M. Freeman, J. Chem. Soc. A, (1971) 785.
7 D.M. Bridges, G.C. Holywell, D.W.H. Rankin and J.M. Freeman, J. Organometal. Chem., 32 (1971) 87.
8 H.L. Cox and R.A. Bonham, J. Chem. Phys., 47 (1967) 605.
9 H.C. Allen and E.K. Plyler, J. Chem. Phys., 31 (1959) 1062.
10 R.W. Kilb and L. Pierce, J. Chem. Phys., 27 (1957) 108.
11 V. Laurie, J. Chem. Phys., 30 (1959) 1210.

Journal of Organometallic Chemistry, 88 (1975) 191—197

AN ELECTRON DIFFRACTION DETERMINATION OF THE MOLECULAR STRUCTURE OF TRIFLUOROSILYLMANGANESE PENTACARBONYL IN THE GAS PHASE

D.W.H. RANKIN and A. ROBERTSON

Department of Chemistry, University of Edinburgh, West Mains Road, Edinburgh EH9 3JJ (Great Britain)

R. SEIP

Department of Chemistry, University of Oslo, P.O. Box 1033, Blindern, Oslo 3 (Norway)

(Received October 29th, 1974)

Summary

The molecular structure of trifluorosilylmanganese pentacarbonyl, SiF_3-$Mn(CO)_5$, in the gas phase has been determined by electron diffraction. The principle parameters are: r_a (C—O) 113.1(3); r(Mn—C)$_{av}$ 186.0(6); r(Mn—Si) 236.0(7); r(Si—F) 158.3(4) pm: ∠ (F—Si—F) 112.5(4); ∠ (C_{ax}—Mn—C_{eq}) 92.9(4)°.

Introduction

In compounds containing elements such as silicon or germanium bonded to a transition metal, there is the possibility of $(d \rightarrow d)\pi$ interactions involving vacant 3*d* or 4*d* orbitals of the Main Group atoms, and filled *d* levels of the transition metal atoms. If this type of interaction does occur, then the reduction, in both size and energy, of the silicon 3*d* orbitals on replacement of a silyl group by a trifluorosilyl group, should lead to an increase in the extent of the π-bonding.

We have therefore determined the gas phase molecular structure of trifluorosilylmanganese pentacarbonyl by electron diffraction and have compared it with the gas phase structures of silylmanganese pentacarbonyl [1] and silylcobalt tetracarbonyl [2], and with the solid phase structure of trifluorosilylcobalt tetracarbonyl [3]. In silyl- and trifluorosilyl-cobalt tetracarbonyl there is a large difference (15 pm) between the two silicon—cobalt bond lengths, and this has been explained in terms of more extensive $(d \rightarrow d)\pi$ bonding in the trifluorosilyl compound. It is interesting to determine whether a similar difference exists for the silicon—manganese bonds in silyl- and trifluorosilyl-manganese pentacarbonyl.

The He(I) photoelectron spectra of silylmanganese pentacarbonyl [4] and trifluorosilylmanganese pentacarbonyl [5] indicate that the main effect of changing the silyl substituents from protons to fluorine atoms is to strengthen the manganese—silicon σ bond: π interaction seems to be unimportant. This would again lead to a shortening of the manganese—silicon bond.

Experimental

A sample of trifluorosilylmanganese pentacarbonyl was prepared by treating trifluorosilane with dimanganese decacarbonyl at 450 K and three atmospheres pressure [6]. The products were collected at 77 K and purified by fractional condensation. The purity was checked spectroscopically.

Scattering intensities were collected photographically on Agfa—Gevaert Replica 23 plates using a Balzer's KD.G2 Eldigraph in Oslo [7, 8]. Two nozzle-to-plate distances were used, 580 mm (5 plates) and 190 mm (4 plates), giving data over a range of the scattering variable, s, of about 10 to 360 nm^{-1}. The compound sample was maintained at 334 K and the nozzle at 343 K for the 580 mm exposures: temperatures of 338 and 348 K were used for the 190 mm exposures.

Apart from data reduction as far as uphill curves, all data reduction and refinements were carried out on an ICL 4-75 computer at the Edinburgh Regional Computing Centre using established programmes [9,10]. The complex scattering factors of Cox and Bonham [11] were used.

Table 1 shows weighting points (used in setting up the off-diagonal weight matrix for least-squares refinements), correlation parameters and scale factors. The electron wavelength, determined from the diffraction pattern of powdered zinc oxide, was 5.846(3) pm.*

Molecular model

Local C_{4v} symmetry was assumed for the manganese pentacarbonyl group, and local C_{3v} symmetry for the trifluorosilyl group. Free rotation about the silicon—manganese bond was also assumed, as the 12-fold barrier is almost certainly very low. All carbon—oxygen bonds were assumed to be of equal length.

The molecular structure was therefore described in terms of silicon—fluorine, silicon—manganese, carbon—oxygen and average manganese—carbon

TABLE 1

WEIGHTING FUNCTIONS, SCALE FACTORS AND CORRELATION PARAMETERS

Camera height (mm)	s (nm^{-1})	s_{min} (nm^{-1})	sw_1 (nm^{-1})	sw_2 (nm^{-1})	s_{max} (nm^{-1})	p/h	Scale factor
190	4	48	76	300	340	0.4549	0.979 ± 0.021
580	2	24	36	120	130	0.4902	0.836 ± 0.021

* Studies of benzene and CO_2 show that the wavelength determined in this way gives distances about 0.1% too small. Allowance for this has been made in calculating distances quoted in this paper.

bond lengths, the difference between axial and equatorial manganese—carbon bond lengths, and the three angles F—Si—F, Mn—C_{eq}—O_{eq} and C_{ax}—Mn—C_{eq}.

Refinements

All bonded distances and their amplitudes of vibration, except u(C—O), refined satisfactorily, as did the C_{eq}—Mn—C_{ax} and F—Si—F angles. Owing to the overlap of many peaks in the radial distribution curve (Fig. 1) certain amplitudes of vibration had to be refined in groups. Even then, not all groups of amplitudes could be refined simultaneously, and so several amplitudes were fixed at typical values, as shown in Table 2.

The difference between axial and equatorial manganese—carbon bond lengths and the Mn—C_{eq}—O_{eq} angle were both determined by doing series of

(continued on p. 196)

TABLE 2

MOLECULAR PARAMETERS FOR $SiF_3Mn(CO)_5$[a]

(a). Independent distances and amplitudes[b]				
$r1$	(C—O)	113.1(3)	3.5 (fixed)	
$r2$	$(Mn—C)_{av}$	186.0(6)	5.4(5)	
$r3$	(Mn—Si)	236.0(7)	7.6(7)	
$r4$	(Si—F)	158.3(4)	4.7(5)	
(b). Dependent distances, amplitudes and shrinkage corrections applied[c]				
$d5$	($Mn—C_{eq}$)	185.6(8)	5.4	0.00
$d6$	($Mn—C_{ax}$)	187.6(8)	5.4	0.00
$d7$	($Mn \cdots O_{eq}$)	298.1(13)	6.8(5)	0.59
$d8$	($Mn \cdots O_{ax}$)	300.1(13)		0.59
$d9$	($C_{eq} \cdots C_{eq}$)	369.4(20)	11.4(14)	1.33
$d10$	($C_{eq} \cdots O_{eq}$)	481.5(24)		2.27
$d11$	($O_{eq} \cdots O_{eq}$)	593.4(28)		3.42
$d12$	($C_{eq} \cdots C_{eq}$)	270.5(12)	14.6(fixed)[d]	0.25
$d13$	($C_{eq} \cdots C_{ax}$)	261.9(15)		0.25
$d14$	($O_{eq} \cdots O_{eq}$)	430.5(16)	25.0(fixed)[d]	1.40
$d15$	($O_{eq} \cdots O_{ax}$)	420.5(19)		1.40
$d16$	($C_{eq} \cdots O_{eq}$)	360.4(15)	15.9(9)	0.82
$d17$	($C_{ax} \cdots O_{eq}$)	358.0(13)		0.82
$d18$	($C_{eq} \cdots O_{ax}$)	350.5(18)		0.82
$d19$	($Si \cdots C_{ax}$)	422.2(15)	11.9 (28)	1.43
$d20$	($Si \cdots O_{ax}$)	534.3(20)	13.2	2.38
$d21$	($Si \cdots C_{eq}$)	292.5(16)	15.3 (14)	0.28
$d22$	($Si \cdots O_{eq}$)	372.5(20)	18.5	0.90
$d23$	($Mn \cdots F$)	330.1(8)	10.5(7)	0.59
$d24$	($F \cdots C_{ax}$)	503.5(14)	16.7(fixed)	2.27
$d25$	($F \cdots O_{ax}$)	611.5(18)	16.7(fixed)	3.42
$d26$	($F \cdots F$)	253.2(12)	9.9(fixed)	0.07
	($F \cdots C_{eq}$)	Between 295 and 439		
	($F \cdots O_{eq}$)	Between 329 and 528		
(c). Angles				
<1	(F—Si—F)	112.5(4)		
<2	(C_{ax}—Mn—C_{eq})	92.9(4)		
<3	(Mn—C_{eq}—O_{eq})	178.3(fixed)		

[a] All distances and amplitudes are given in pm; angles in degrees. [b] Independent distances are r_a. [c] Shrinkages applied were the same as those used for $SiH_3Mn(CO)_5$ [1]. [d] Derived from calculated amplitudes of vibration for $Mn_2(CO)_{10}$ [13].

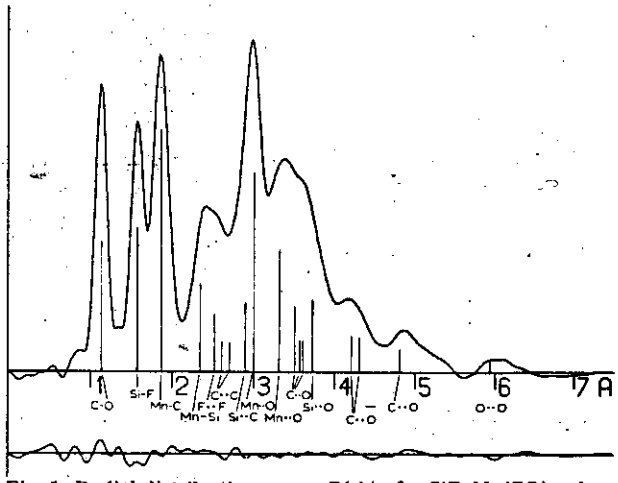

Fig. 1. Radial distribution curve, $P(r)/r$, for $SiF_3Mn(CO)_5$, showing principal interatomic distances. Before Fourier inversion the data were multiplied by $s \exp[-0.0015s^2/(z_{Mn}-f_{Mn})(z_O-f_O)]$.

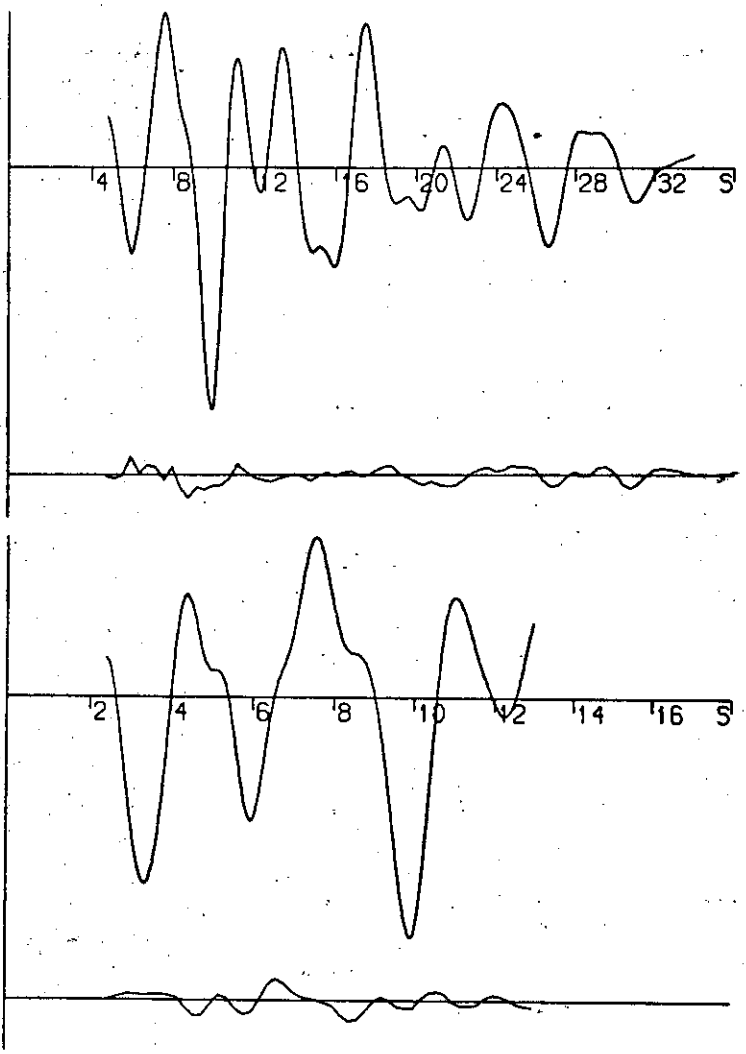

Fig. 2. Observed and final weighted difference molecular scattering intensities for $SiF_3Mn(CO)_5$.

TABLE 3

LEAST SQUARES CORELATION MATRIX MULTIPLIED BY 100

r1	r2	r3	r4	< 1	< 2	u3	u4	u5	u7	u9	u16	u19	u21	u23	k1	k2
100	16	12	13	−25	−17	9	−4	4	6	12	−32	0	−24	−25	3	−8
	100	24	44	−43	−57	6	3	−11	2	5	−40	1	−9	−11	−8	−8
		100	1	−62	28	−10	−11	−5	−10	1	2	−11	12	7	−22	−13
			100	−5	−38	−10	−2	−18	−1	−11	2	3	−16	4	−15	−16
				100	−39	19	5	0	29	−30	37	13	−39	4	8	13
					100	−30	−4	8	−30	19	2	−13	48	−2	2	1
						100	9	7	19	−3	5	6	−20	1	20	12
							100	11	15	2	−1	5	3	−3	34	7
								100	21	8	3	6	11	−1	53	25
									100	−3	11	8	−42	1	41	18
										100	−17	−32	5	−9	11	6
											100	−8	−1	58	3	6
												100	1	−2	12	5
													100	33	12	8
														100	−4	−7
															100	26
																100

refinements with different fixed values of these parameters and comparing R factors. Once determined in this way, these parameters were fixed at their optimum values in subsequent refinements.

Under these conditions refinement converged to give the parameters of Table 2, with an R factor (R_G) of 0.129. The estimated standard deviations quoted include random errors determined in the least squares analysis, and allowances for systematic errors and any constraints applied during refinement [12]. The final least-squares correlation matrix is given in Table 3. Molecular intensity data, shown diagrammatically in Fig. 2, is available from the authors on request.

Discussion

In silylmanganese pentacarbonyl the silicon—manganese bond length is 240.7 ± 0.5 pm [1], whereas in the trifluoro derivative the length is 236.0 ± 0.7 pm. This shortening is consistent both with $(d \rightarrow d)\pi$ bonding, as suggested for the cobalt carbonyl compounds [2], and with the purely σ effects that have been proposed, based on evidence from photoelectron spectra. It is unfortunate that the molecular structures provide no evidence that enables us to say that the observed shortening is due mainly to one of the two effects.

Despite this, there are features of interest in the structure of trifluorosilylmanganese pentacarbonyl. In particular, it should be noted that the difference in silicon—manganese distances in the compounds under consideration is only about 5 pm, whereas the difference for the cobalt tetracarbonyls is more than 15 pm. This difference cannot entirely be due to phase effects (the trifluorosilylcobalt tetracarbonyl structure is for a crystal) or to the rather poor data used for silylcobalt tetracarbonyl. Steric crowding should be considered, since at least one fluorine—carbon distance must be shorter in trifluorosilylmanganese pentacarbonyl (292 pm) with C_{3v} and C_{4v} groups, than in trifluorosilylcobalt tetracarbonyl (ca. 316 pm) where all the fluorines are staggered with respect to the equatorial carbonyl groups. However, the C_{eq}—M—C_{ax} angles in the trifluorosilyl compounds are the same as in other manganese and cobalt carbonyl derivatives, and the F—Si—F angle is smaller in the cobalt compound than in the manganese one. One would expect crowding of the fluorine atoms to show itself in changes of valence angles, before bond lengths were affected significantly.

We therefore suggest that the differences may be due to the larger number of d electrons in cobalt than in manganese, making the silicon—cobalt bond length more susceptible to changes of substituent at silicon. More data is required if this is to be confirmed: we intend to carry out further studies of structures of carbonyl derivatives, so that the nature of silicon—metal bonds may be better understood.

References

1 D.W.H. Rankin and A. Robertson, J. Organometal. Chem., 85 (1975) 225.
2 A.G. Robiette, G.M. Sheldrick, R.N.F. Simpson, B.J. Aylett and J.A. Campbell, J. Organometal. Chem., 14 (1968) 279.
3 K. Emerson, P.R. Ireland and W.T. Robinson, Inorg. Chem., 9 (1970) 436.

4 S. Cradock, E.A.V. Ebsworth and A. Robertson, J. Chem. Soc. Dalton Trans., (1973) 22.
5 S. Cradock and A. Robertson, unpublished results.
6 M.E. Redwood, B.E. Reichert, R.R. Schrieke and B.O. West, Aust. J. Chem., 26 (1973) 247.
7 O. Bastiansen, R. Graber and L. Wegmann, Balzer's High Vacuum Report, 25 (1969) 1.
8 W. Zeil, J. Haase and L. Wegmann, Z. Instrumentenk., 74 (1966) 84.
9 G.C. Holywell, D.W.H. Rankin, B. Beagley and J.M. Freeman, J. Chem. Soc. A, (1971) 785.
10 D.M. Bridges, G.C. Holywell, D.W.H. Rankin and J.M. Freeman, J. Organometal. Chem., 32 (1971) 87.
11 H.L. Cox and R.A. Bonham, J. Chem. Phys., 47 (1967) 605.
12 M.A. MacGregor and R.K. Bohn, Chem. Phys. Lett., 11 (1971) 29.
13 J. Brunvoll and S.J. Cyvin, Acta Chem. Scand., 22 (1968) 2709.

Journal of Organometallic Chemistry, 104 (1976) 179—186

AN ELECTRON DIFFRACTION DETERMINATION OF THE GAS PHASE STRUCTURE OF GERMYLCOBALT TETRACARBONYL *

D.W.H. RANKIN* and A. ROBERTSON

Department of Chemistry, University of Edinburgh, West Mains Road, Edinburgh EH9 3JJ (Great Britain)

(Received July 18th, 1975)

Summary

The molecular structure of germylcobalt tetracarbonyl in the gas phase has been determined by electron diffraction. Principal parameters (r_a) are: r(C—O), 112.8(4); r(Co—C)(average), 180.0(6); r(Co—Ge), 241.6(4) pm. The difference between axial and equatorial Co—C distances is very small. The equatorial carbonyl groups are bent towards the germyl group, with C_{eq}—Co—Ge angles of 83.8(3)°.

Introduction

Although multiple bonding in silyl and germyl transition metal complexes, involving overlap of filled metal *d* orbitals with vacant silicon 3*d* or germanium 4*d* orbitals, is possible on symmetry grounds, there is little experimental evidence for or against it. Study of Si—M and Ge—M bond lengths may provide some such evidence, particularly by showing the effects of changing the metal, or the Group IV atom or its substituents. We have recently studied by electron diffraction the structures of silyl-, trifluorosilyl- and germyl-manganese pentacarbonyl [1,2]. The gas phase structure of silylcobalt carbonyl was studied some years ago [3], but otherwise only solid phase structures have been reported. As part of a series of structural studies of this type of compound, we present here the results of a determination of the gas phase structure of germylcobalt tetracarbonyl, and compare them with those for related compounds.

Experimental

Germylcobalt tetracarbonyl was prepared by addition of germyl bromide to a solution of sodium cobalt tetracarbonyl in diethyl ether at room tempera-

* No reprints available.

TABLE 1

WEIGHTING FUNCTIONS, CORRELATION PARAMETERS AND SCALE FACTORS

Camera height (mm)	Δs (nm^{-1})	s_{min} (nm^{-1})	s_1 (nm^{-1})	s_2 (nm^{-1})	s_{max} (nm^{-1})	p/h	Scale factor
250	4	76	105	260	300	0.4201	1.069 ± 0.032
500	2	28	40	120	140	0.4795	1.020 ± 0.026
1000	1	10	17	64	72	0.4994	1.033 ± 0.052

ture, and purified by fractional condensation in vacuo [4]. Purity was checked spectroscopically.

Electron diffraction scattering intensities were collected photographically using Ilford N60 plates and a Balzers' KD G2 gas diffraction apparatus, and were obtained in digital form using a Joyce—Loebl microdensitometer. During the exposures the sample was maintained at 313 K and the nozzle at 328 K. Nozzle-to-plate distances of 250, 500 and 1000 mm were used, giving data over a range of the scattering variable, s, from 10 to 300 nm^{-1}. Calculations were carried out on an ICL 4-75 computer at the Edinburgh Regional Computing Centre using data reduction and least squares refinement programmes previously described [5,6], and the complex scattering factors of Cox and Bonham [7]. Table 1 shows weighting points (used to set up the off-diagonal weight matrix), correlation parameters and scale factors. The electron wavelength of 5.663 pm was determined by direct measurement of the accelerating voltage and from the diffraction pattern of powdered thallous chloride.

Refinements

The molecule was assumed to have C_3 symmetry, with all C—O bonds of equal length. The structure was then defined by the distances Co—C_{ax}, Co—C_{eq},

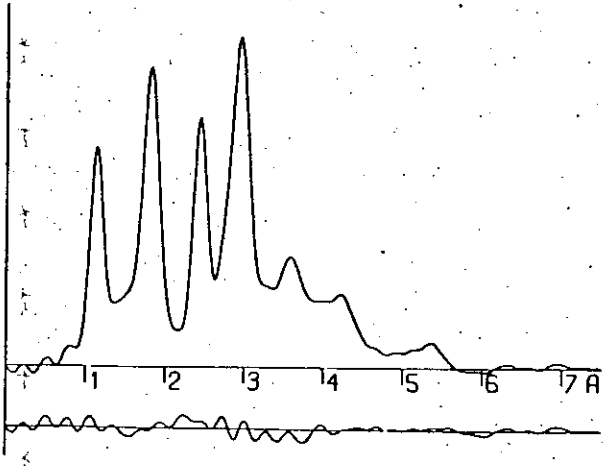

Fig. 1. Radial distribution curve, $I'(r)/r$. Before Fourier inversion the data were multiplied by $s \exp(-0.000025\ s^2)/(z_C - f_C)(z_O - f_O)$.

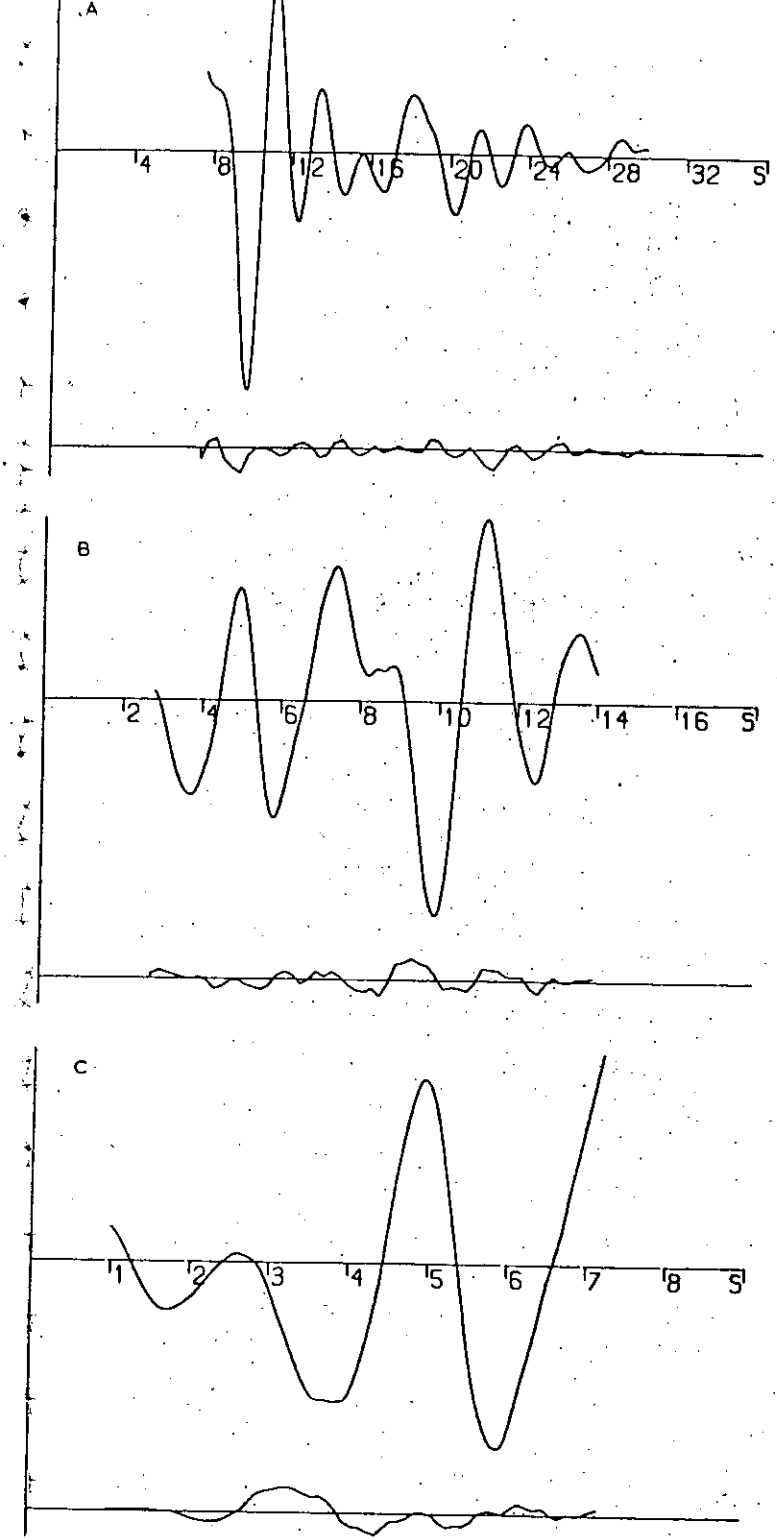

Fig. 2. Observed and final weighted difference molecular scattering intensities for $GeH_3Co(CO)_4$ for data sets obtained with nozzle-to-plate distances of 250, 500 and 1000 mm.

C—O, Co—Ge and Ge—H, the angles C_{eq}—Co—Ge, Co—C_{eq}—O_{eq} and Co—Ge—H, and the twist angle of the germyl group away from the position in which it was eclipsed with respect to the $Co(CO)_4$ group. Of these, the C—O, Co—C(average) and Co—Ge distances and associated amplitudes of vibration all refined satisfactorily, as did the Co—C—O and C—Co—Ge angles. The dihedral angle was set at the value that was found to give the lowest R factor, but was not included in subsequent refinements. The difference between axial and equatorial Co—C bond lengths was allowed to refine, but the estimated error in the value obtained is greater than the value itself. In any case, electron diffraction is not a good method for determining small deviations from idealised models, and any error in this parameter will be reflected in the amplitude of vibration associated with the Co—C distances.

TABLE 2

MOLECULAR PARAMETERS[a]

(a). Independent distances and amplitudes (pm)			
r1	(Co—C)(mean)	180.0(6)	
δ	(Co—C)(eq-ax)	−1.0(16)	
r2	(C—O)	112.8(4)	5.2(7)
r3	(Co—Ge)	241.6(4)	6.9(5)
r4	(Ge—H)	152.5(fixed)	10.0(fixed)
(b). Dependent distances and amplitudes (pm)			
d5	(Co—C_{eq})	179.8(8)	6.1(6)
d6	(Co—C_{ax})	180.8(15)	6.1(tied to u 5)
d7	(Co···O_{eq})	291.7(13)	6.8(5)
d8	(Co···O_{ax})	292.8(18)	6.8(tied to u 7)
d9	(C_{eq}···C_{eq})	308.7(14)	13.0(18)
d10	(C_{eq}···O_{eq})	408.6(18)	15.7(tied to u 9)
d11	(O_{eq}···O_{eq})	500.2(25)	18.6(tied to u 9)
d12	(C_{ax}···C_{eq})	268.3(18)	14.5(fixed)
d13	(C_{ax}···O_{eq})	361.3(24)	17.5(fixed)
d14	(C_{eq}···O_{ax})	360.0(23)	17.5(fixed)
d15	(O_{ax}···O_{eq})	437.4(30)	21.0(fixed)
d16	(Ge···C_{ax})	420.3(19)	10.0(16)
d17	(Ge···O_{ax})	532.1(23)	11.0(tied to u 16)
d18	(Ge···C_{eq})	284.2(6)	16.5(14)
d19	(Ge···O_{eq})	355.0(8)	19.9(tied to u 18)
d20	(Co···H)	325.1(12)	15.0(fixed)
d21	(H···C_{eq})	274.8(8)	15.0(fixed)
d22	(H···C_{eq})	379.1(9)	15.0(fixed)
d23	(H···C_{eq})	395.1(11)	15.0(fixed)
d24	(H···O_{eq})	295.0(8)	15.0(fixed)
d25	(H···O_{eq})	445.5(13)	15.0(fixed)
d26	(H···O_{eq})	472.7(14)	15.0(fixed)
d27	(H···C_{ax})	491.7(22)	20.0(fixed)
d28	(H···O_{ax})	599.6(29)	20.0(fixed)
d29	(H···H)	248.9(fixed)	11.0(fixed)
(c). Angles			
<1	(Co—Ge—H)	109.1(fixed)	
<2	(C_{eq}—Co—Ge)	83.8(3)	
<3	(twist)	10.0(see text)	
<4	(Co—C_{eq}—O_{eq})	178.3(fixed)	

[a] Distances (r_a) are given in pm, and angles in degrees. The angle Co—C—O, fixed in the final refinement, had been included in earlier refinements, in which the quoted value was obtained.

TABLE 3

LEAST SQUARES CORRELATION MATRIX MULTIPLIED BY 100

r1	δ	r2	r3	<2	u3	u4	u5	u7	u9	u16	u18	h1	h2	h3	
100	−4	36	−4	−86	3	11	8	−6	−15	−3	10	17	15	−1	r1
	100	4	11	−2	4	7	17	24	54	32	−6	6	15	19	δ
		100	−4	−67	0	1	7	−4	−1	−3	−5	4	3	−1	r2
			100	−2	0	8	−3	7	−4	3	−17	4	−2	−9	r3
				100	−6	−12	−15	5	12	4	−19	−30	−19	1	<2
					100	30	28	25	10	8	19	−44	30	6	u3
						100	40	30	14	13	25	65	44	5	u4
							100	37	22	16	28	62	52	15	u5
								100	29	21	−9	54	42	16	u7
									100	16	15	18	27	26	u9
										100	−14	39	41	11	u16
											100	17	16	10	u18
												100	57	12	h1
													100	14	h2
														100	h3

Owing to the overlapping of peaks in the outer part of the radial distribution curve (Fig. 1) certain groups of amplitudes of vibration were refined together (see Table 2). Apart from those involving the hydrogen atoms, most of these groups refined satisfactorily, the exception being that involving axial···equatorial C···C, C···O and O···O amplitudes of vibration. These non-refining parameters were fixed at typical values. Under these conditions refinement converged to give an R factor (R_G) of 0.14. The molecular scattering intensities, and differences calculated using the final refined parameters, are shown in Figure 2.

Final parameters are given in Table 2. The estimated standard deviations quoted in the table include the random errors determined in the least squares analysis, and allowances for both systematic errors and any constraints applied during the refinements. The least squares correlation matrix is shown in Table 3.

Discussion

The bond lengths in some silyl and germyl compounds, listed in Table 4, show that, in general, the difference between distances Ge—X and Si—X depends on the electronegativity of X. This trend is found also for the halides, results for which are not included in the table. The Co—Ge bond length that we have determined [241.4(4) pm] is only 3.3 pm longer than the Co—Si distance in silylcobalt tetracarbonyl [3], and this small difference, compared with 8.0 pm for the manganese pentacarbonyl derivatives [1] may be due to the presence of two more *d* electrons on cobalt than on manganese, making the $Co(CO)_4$ group effectively more electropositive than $Mn(CO)_5$. However, the Co—Si distance also seems long relative to Mn—Si in silylmanganese pentacarbonyl after allowing for the change in radius of the metal, and relative to Co—Si in trifluorosilylcobalt tetracarbonyl (222.5 pm in the solid phase) [8]. Of course, these differences may also reflect the differing electronegativities of the groups involved.

The Co—Ge distance found is considerably longer than that in $GeCl_3Co(CO)_4$

TABLE 4

COMPARISON OF SOME BOND LENGTHS[a] INVOLVING SILICON AND GERMANIUM

Silicon			Germanium			Ge—Si difference
Compound	Bond length	Ref.	Compound	Bond length	Ref.	
$(SiH_3)_2O$	163.4(2)	13	$(GeH_3)_2O$	176.6(4)	14	13.2
$(SiH_3)_3N$	173.4(2)	15	$(GeH_3)_3N$	183.6(5)	16	10.2
$SiH_3Mn(CO)_5$	240.7(5)	1	$GeH_3Mn(CO)_5$	248.7(2)	1	8.0
SiH_3CH_3	186.7(1)[b]	17	GeH_3CH_3	194.5(1)[b]	18	7.8
$(SiH_3)_2S$	213.6(2)	19	$(GeH_3)_2S$	220.9(4)	14	7.3
$(SiH_3)_2Se$	227.3(4)	20	$(GeH_3)_2Se$	234.4(3)	21	7.1
$(SiH_3)_3P$	224.8(3)	22	$(GeH_3)_3P$	230.8(3)	23	6.0
Si_2H_6	233.1(3)	24	Ge_2H_6	240.3(3)	25	7.2/2 = 3.6
$SiH_3Co(CO)_4$	238.1(7)	3	$GeH_3Co(CO)_4$	241.4(4)		3.3

[a] Bond lengths are given in pm, and are r_a values unless stated otherwise. [b] r_s.

(231.0 pm) [9], but is still some 15 pm shorter than the sum of Co and Ge covalent radii [10,11].

The other structural parameters are much as one would expect. It should be noted that the evidence suggests that the axial Co—C bond is longer than th equatorial ones in germylcobalt tetracarbonyl, whereas the reverse is true in iro pentacarbonyl [12].

Acknowledgements

We thank Professor D.W.J. Cruickshank, Dr. B. Beagley, Mrs. V. Ulbrecht and Dr. M.J. Smyth for the use of experimental facilities. We also thank the Dewar foundation for a grant to A.R.

References

1 D.W.H. Rankin and A. Robertson, J. Organometal. Chem., 85 (1975) 225.
2 D.W.H. Rankin and A. Robertson, J. Organometal. Chem., 88 (1975) 191.
3 A.G. Robiette, G.M. Sheldrick, R.N.F. Simpson, B.J. Aylett and J.A. Campbell, J. Organometal. Chem 14 (1968) 279.
4 R.D. George, K.M. Mackay and S.R. Stobart, J. Chem. Soc., Dalton Trans., (1972) 974.
5 G.C. Holywell, D.W.H. Rankin, B. Beagley and J.M. Freeman, J. Chem. Soc. A, (1971) 785.
6 D.M. Bridges, G.C. Holywell, D.W.H. Rankin and J.M. Freeman, J. Organometal. Chem., 32 (1971) 87
7 H.L. Cox and R.A. Bonham, J. Chem. Phys., 47 (1967) 605.
8 K. Emerson, P.R. Ireland and W.T. Robinson, Inorg. Chem., 9 (1970) 436.
9 G.C. v.d. Berg, A. Oskam and K. Olie, J. Organometal. Chem., 80 (1974) 363.
10 J.A. Ibers, J. Organometal. Chem., 14 (1968) 423.
11 L. Pauling, The Nature of the Chemical Bond, 3rd ed., Cornell University Press, Ithaca, 1960.
12 B. Beagley and D.G. Schmidling, J. Mol. Struct., 22 (1974) 466.
13 A. Almenningen, O. Bastiansen, V. Ewing, K. Hedberg and M. Trætteberg, Acta Chem. Scand., 17 (1963) 2455.
14 C. Glidewell, D.W.H. Rankin, A.G. Robiette, G.M. Sheldrick, B. Beagley and S. Cradock, J. Chem. Soc A, (1970) 315.
15 B. Beagley and A.R. Conrad, Trans. Faraday Soc., 66 (1970) 2740.
16 C. Glidewell, D.W.H. Rankin and A.G. Robiette, J. Chem. Soc. A, (1970) 2935.
17 R.W. Kilb and L. Pierce, J. Chem. Phys., 27 (1957) 108.
18 V.W. Laurie, J. Chem. Phys., 30 (1959) 1210.

19 A. Almenningen, K. Hedberg and R. Seip, Acta Chem. Scand., 17 (1963) 2264.
20 A. Almenningen, L. Fernholt and H.M. Seip, Acta Chem. Scand., 22 (1968) 51.
21 J.D. Murdoch, D.W.H. Rankin and C. Glidewell, J. Mol. Struct., 9 (1971) 17.
22 B. Beagley, A.G. Robiette and G.M. Sheldrick, J. Chem. Soc. A, (1968) 3002.
23 D.W.H. Rankin, A.G. Robiette, G.M. Sheldrick, B. Beagley and T.G. Hewitt, J. Inorg. Nucl. Chem., 31 (1969) 2351.
24 B. Beagley, A.R. Conrad, J.M. Freeman, J.J. Monaghan and B.G. Norton, J. Mol. Struct., 11 (1972) 371.
25 B. Beagley and J.J. Monaghan, Trans. Faraday Soc., 66 (1970) 2745.

Journal of Organometallic Chemistry, 105 (1976) 331—340

THE GAS PHASE MOLECULAR STRUCTURES OF METHYL-, SILYL- AND GERMYL-RHENIUM PENTACARBONYL, DETERMINED BY ELECTRON DIFFRACTION *

D.W.H. RANKIN * and A. ROBERTSON

Department of Chemistry, University of Edinburgh, West Mains Road, Edinburgh, EH9 3JJ (Great Britain)

(Received August 27th, 1975)

Summary

The molecular structures of the title compounds in the gas phase have been determined by electron diffraction. The C(methyl)—Re, Si—Re and Ge—Re bond lengths (r_a) are 230.8 ± 1.7, 256.2 ± 1.2 and 262.8 ± 0.6 pm respectively. The $Re(CO)_5$ groups in the molecules have almost identical structures, with r(Re—C) 200-201 pm, r(C—O) 113 pm, and the equatorial carbonyl groups bent towards the MH_3 group away from the regular octahedral positions by 4-7°.

Introduction

Studies of the structures of methyl-, silyl- and germyl-manganese pentacarbonyl [1,2] have shown that the Mn—Si and Mn—Ge bonds are about 11 pm shorter than would be expected on the basis of covalent radii. This may be attributed to π-bonding between silicon or germanium and the metal, or to differences of σ-acceptor properties of the methyl, silyl and germyl substituents, but the differences seem to be rather large to be purely electronegativity effects.

There are some surprising differences between manganese and rhenium carbonyl derivatives. For example, the metal carbonyls not only have different conformations, one having D_{4d} symmetry, and the other D_{4h}, but also the Re—Re bond length in $Re_2(CO)_{10}$ is about twice the covalent radius of rhenium [3], whereas the Mn—Mn bond in $Mn_2(CO)_{10}$ [4] is 10-20 pm longer than twice the mangenese covalent radius (depending on how the radius is defined). These observations are consistent with estimates of the metal—metal bond dissociation energies, which are reported as 104 and 187 kJ mol^{-1} for Mn—Mn and Re—Re respectively [5]. Morevoer, the dissociation energies for the metal—carbon (methyl) bonds in methyl-manganese and -rhenium carbonyls have been reported as being 117-129 and 222 kJ mol^{-1} respectively [6], and the Si—metal and Ge—metal stretching force constants for silyl- and germyl-rhenium pentacar-

* No reprints available.

bonyls are considerably greater than those for the manganese derivatives [7]. As all this evidence implies that bonds from rhenium to carbon, silicon and germanium are all stronger than those from mangenese, we have determined the structures of three rhenium pentacarbonyl derivatives, to see whether the bond lengths are consistent with the other evidence.

Experimental

Samples of methyl-, silyl- and germyl-rhenium pentacarbonyl were prepared by reaction of methyl iodide, silyl bromide or germyl bromide with sodium rhenium pentacarbonyl [7,8], and purified by fractional condensation in vacuo.

Scattering intensities were recorded photographically on Agfa Gevaert Replica 23 plates using a Balzers' KD.G2 gas diffraction apparatus, and were converted to digital form with a Joyce-Loebl microdensitometer. During exposures the samples were maintained at 333 K, and the inlet nozzle at 340 K. For each compound, three nozzle-to-plate distances (250, 500 and 1000 mm) were used, (usually two plates at each distance), giving scattering intensities over a range of s from about 10 to 280 nm^{-1}. The electron wavelength used, 5.660(5) pm, was determined from diffraction patterns for gaseous benzene.

Calculations were carried out on an ICL 4-75 computer at the Edinburgh Regional Computing Centre with data reduction and least squares refinement programs described elsewhere [9,10]. The refinement program uses an off-diagonal weight matrix: weighting points used in setting it up are given in Table 1, together with scale factors and correlation parameters.

In early refinements, the scattering factors of Schäfer, Yates and Bonham [11] were used. However, both the real and imaginary parts of the scattering factor for rhenium were found to be inadequate, and were modified in the light of the experimental data. The real part was observed to have an oscillation of frequency about 80 nm^{-1} at high s values. This oscillation, which has been noticed before [12] was removed by smoothing the appropriate part of the scattering factor, resulting in a considerable improvement of the fit of experimental and calculated scattering, both atomic and molecular. The original and modified forms are shown in Fig. 1.

For the imaginary part of the scattering factor, we normally use cubic func-

TABLE 1

WEIGHTING FUNCTIONS, CORRELATION PARAMETERS AND SCALE FACTORS

Compound	Camera height (mm)	del s (nm^{-1})	s_{min} (nm^{-1})	s_1 (nm^{-1})	s_2 (nm^{-1})	s_{max} (nm^{-1})	p/h	scale factor
$CH_3Re(CO)_5$	250	4	68	104	220	260	0.3975	0.864 ± 0.021
	500	2	26	55	138	158	0.4822	0.978 ± 0.021
	1000	1	11	21	62	72	0.1314	0.749 ± 0.01
$SiH_3Re(CO)_5$	250	4	100	140	240	284	0.1369	0.813 ± 0.04
	500	2	26	50	130	154	0.4722	0.762 ± 0.02
	1000	1	12	20	61	71	0.4555	0.713 ± 0.02
$GeH_3Re(CO)_5$	250	4	68	128	230	276	0.3737	0.962 ± 0.03
	500	2	22	40	124	144	0.4283	0.865 ± 0.02
	1000	1	13	23	61	72	0.3954	0.664 ± 0.02

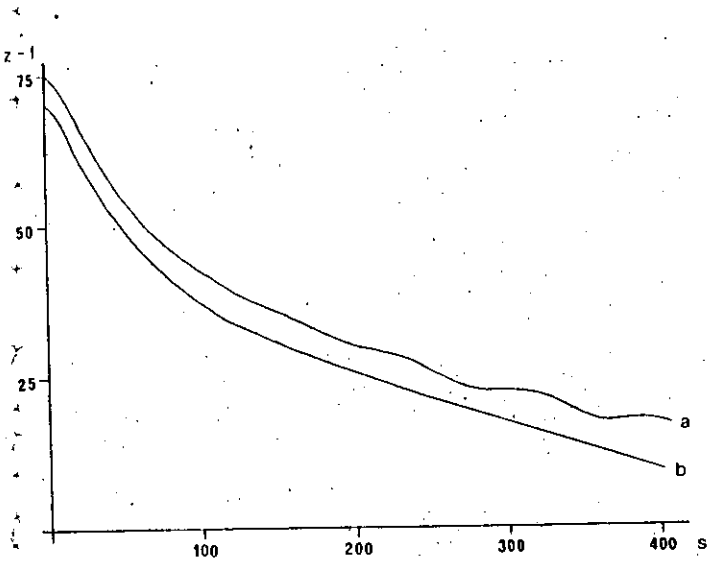

Fig. 1. Scattering factor, $z - f$, for rhenium, (a) derived from data by Schäfer et al. [11] and (b) as modified and used in this work. The second curve is displaced 5 units downwards, for clarity.

tions fitted to the tabulated phase angles [11]. Thus for the atom pair i—j the phase shift is given by:

$$\eta_i - \eta_j = a_i - a_j + (b_i - b_j)s + (c_i - c_j)s^2 + (d_i - d_j)s^3.$$

This may be rewritten as:

$$\Delta\eta = \pi/2 + \Delta b'(s - s_c) + \Delta c'(s - s_c)^2 + \Delta d'(s - s_c)^3,$$

where s_c is the "beat-out" point, where $\cos(\Delta\eta) = 0$. Using tabulated values for $\eta_i(s)$, the beat-out points for Re—C, Re—O, Re—H, Re—Si and Re—Ge atom pairs were calculated to be 140, 147, 117, 179 and 333 nm^{-1} respectively. In all three structure determinations, the values for Re—C and Re—O were allowed to refine. Optimum values in each case were close to 131 and 138 nm^{-1} for Re—C and Re—O: in subsequent refinements they were fixed at these values, with those for Re—H, Re—Si and Re—Ge adjusted to 108, 170 and 324 nm^{-1} respectively.

Approximate shrinkage corrections, as listed in Table 2, were applied to non-bonded distances.

Refinements

Molecular model

For each compound, the model used was the same as that used for manganese carbonyl derivatives [2]. This assumed C_{4v} symmetry for the $Re(CO)_5$ group, C_{3v} for the $ReMH_3$ group, and free rotation about the Re—M bond. In view of the problems caused by inadequate scattering factors, and the correla-

(continued on p. 336)

TABLE 2

MOLECULAR PARAMETERS FOR $MH_3Re(CO)_5$

	$CH_3Re(CO)_5$		$SiH_3Re(CO)_5$		$GeH_3Re(CO)_5$		Shrinkage correction
	Distance (pm)	Amplitude	Distance (pm)	Amplitude	Distance (pm)	Amplitude	
(a) Independent distances							
r_1(C—O)	113.0(4)	4.5(9)	113.6(4)	5.0(7)	112.0(5)	5.8(7)	—
r_2(Re—C)	200.0(4)	5.6(4)	201.0(4)	6.2(4)	200.2(5)	6.4(5)	—
r_3(Re—M)	230.8(17)		256.2(12)	6.7(16)	262.8(6)	9.1(7)	—
r_4(M—H)	110.0(fixed)	5.0(fixed)	151.4(37)	8.0(fixed)	152.1(fixed)	10.0(fixed)	—
(b) Dependent distances							
d_5(Re···O_{ax})	312.2(9)	7.2(4)	313.8(9)	5.7(4)	311.3(9)	7.2(6)	0.6
d_6(Re···O_{eq})	312.2(9)		313.7(9)		311.2(9)		0.6
d_7(C_{eq}···C_{eq})	395.6(13)	9.5(fixed)	399.2(12)	9.5(fixed)	395.0(10)	9.5(fixed)	1.3
d_8(C_{eq}···O_{eq})	506.6(17)		511.0(16)		505.1(14)		2.3
d_9(O_{eq}···O_{eq})	617.1(24)		622.2(23)		614.6(21)		3.4
d_{10}(C_{eq}···C_{ax})	280.7(9)	14.7(18)	283.3(9)	13.0(fixed)	280.3(7)	16.8(30)	0.3
d_{11}(C_{eq}···C_{eq})	298.2(7)		292.9(7)		300.9(8)		0.3
d_{12}(C_{eq}···O_{eq})	388.6(8)	19.1(13)	382.5(8)	18.2(12)	390.8(8)	21.0(13)	0.8
d_{13}(C_{eq}···O_{ax})	368.2(14)		371.3(13)		366.9(11)		0.8
d_{14}(C_{ax}···O_{eq})	388.6(7)		384.8(8)		389.3(8)		0.8
d_{15}(O_{eq}···O_{eq})	464.6(10)	30.7(40)	459.4(10)	30.0(fixed)	465.1(11)	30.0(fixed)	1.4
d_{16}(O_{eq}···O_{ax})	437.8(16)		441.4(16)		436.0(15)		1.4
d_{17}(M···C_{ax})	428.7(18)	9.5(fixed)	455.1(15)	11.1(fixed)	460.9(10)	10.0(fixed)	1.4
d_{18}(M···O_{ax})	540.3(20)	10.0(fixed)	567.3(17)	11.0(fixed)	571.4(13)	11.0(fixed)	2.4
d_{19}(M···C_{eq})	287.7(16)	14.7[a]	315.3(14)	20.0(fixed)	308.6(11)	22.4[a]	0.3
d_{20}(M···O_{eq})	366.2(18)	19.1[b]	388.8(17)	24.2[b]	381.6(15)	28.0[b]	0.9
d_{21}(Re···H)	286.7(16)	10.0(fixed)	335.4(34)	10.0(fixed)	346.7(8)	12.0(fixed)	0.6
d_{22}(C_{ax}···H)	476.3(18)	18.0(fixed)	521.7(38)	18.0(fixed)	533.2(11)	18.0(fixed)	2.3
d_{23}(O_{ax}···H)	583.1(21)	18.0(fixed)	627.3(42)	18.0(fixed)	637.8(13)	18.0(fixed)	3.4
d_{24}(H···H)	178.9(fixed)	9.0(fixed)	248.8(45)	10.0(fixed)	246.6(fixed)	10.0(fixed)	0.1
(C_{eq}···H)	265-387		299-448		299-445		
(O_{eq}···H)	314-471		330-531		329-527		
(c) Angles (°)							
∠1(Re—M—H)	110(fixed)		108(fixed)		111(fixed)		
∠2(C_{ax}—Re—C_{eq})	96(2)		94(2)		97(2)		
∠3(Re—C_{eq}—O_{eq})	180(fixed)		182(2)[c]		178(2)[d]		

[a] Tied to u10. [b] Tied to u12. [c] Bent towards Si. Not included in final refinement. [d] Bent away from Ge.

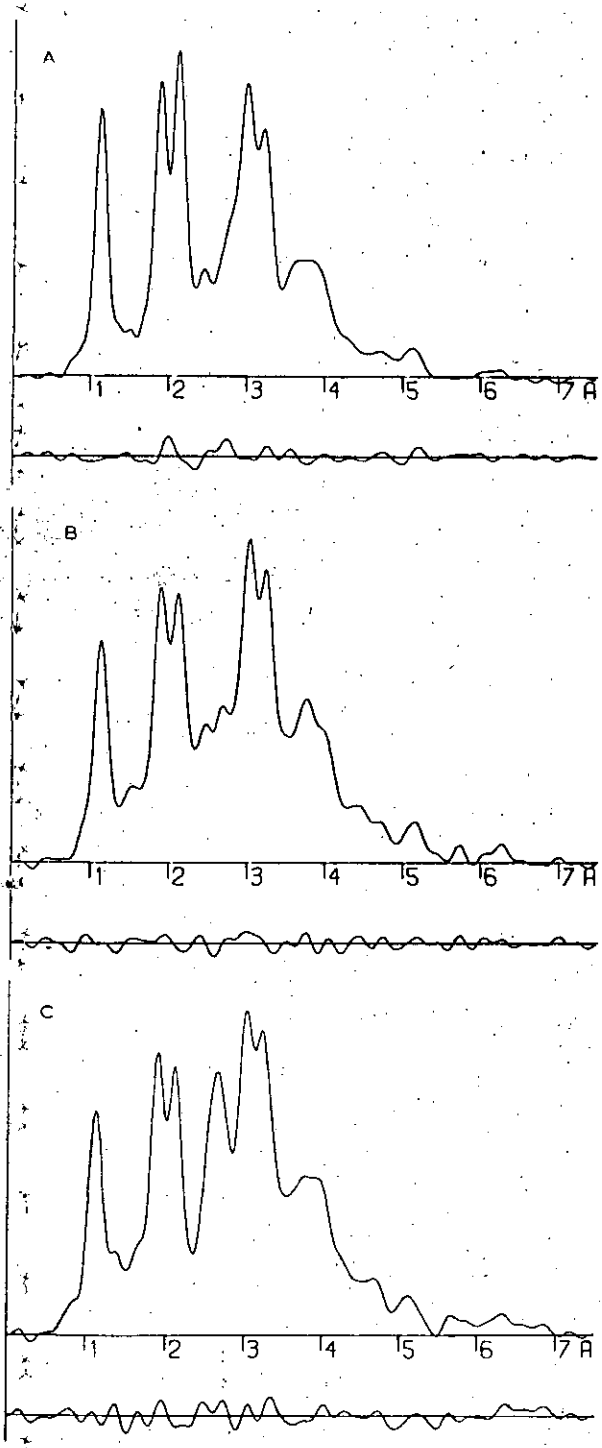

Fig. 2. Radial distribution curves, $P(r)/r$, and difference curves, for (a) $CH_3Re(CO)_5$, (b) $SiH_3Re(CO)_5$ and (c) $GeH_3Re(CO)_5$. In each case, before Fourier inversion, the data were multiplied by: $s \times \exp(-d \times s^2)/(z_{Re} - f_{Re})(z_0 - f_0)$, where the damping factor, d, was 0.000015 nm^{-2} for $SiH_3Re(CO)_5$, and otherwise 0.00001 nm^{-2}.

TABLE 3

LEAST SQUARES CORRELATION MATRIX FOR $CH_3Re(CO)_5$, MULTIPLIED BY 100

r1	r2	r3	∠2	u1	u2	u5	u10	u12	u15	k1	k2	k3	
100	7	−2	−4	7	1	9	2	−3	−3	12	9	23	r1
	100	−30	3	19	19	−2	−24	1	4	24	−12	−21	r2
		100	11	−5	−28	−1	2	−11	−13	−27	24	49	r3
			100	−1	1	0	−71	−66	−31	7	−10	−17	∠2
				100	16	5	1	3	2	25	−4	7	u1
					100	0	−4	3	4	36	−16	−3	u2
						100	7	5	−2	11	6	19	u5
							100	43	23	−14	19	27	u10
								100	54	11	−7	−19	u12
									100	9	2	−13	u15
										100	−51	−20	k1
											100	16	k2
												100	k3

tion of refined "beat-out" parameters for Re—C and Re—O with the amplitudes of vibration for these distances, no attempt was made to differentiate between axial and equatorial Re—C distances. Such a difference would in any case be small.

Methyl-rhenium pentacarbonyl

The bond lengths Re—C(methyl), Re—C(carbonyl) and C—O, and their amplitudes of vibration, and the angle C_{ax}—Re—C_{eq}, all refined satisfactorily. In the radial distribution curve (Fig. 2a) there is much overlapping of peaks due to non-bonded pairs of atoms, and groups of amplitudes of vibration were refined together, as shown in Table 2. All parameters involving hydrogen, and one group of vibration amplitudes, were fixed at reasonable values, as they were not well enough defined to be included in refinements. The parameters from the final refinement, for which R_G was 0.12, are given in Table 2. The least squares

TABLE 4

LEAST SQUARES CORRELATION MATRIX FOR $SiH_3Re(CO)_5$, MULTIPLIED BY 100

r1	r2	r3	r4	∠2	u1	u2	u3	u5	u12	k1	k2	k3	
100	1	0	−12	−1	12	9	5	12	−1	17	7	9	r1
	100	−4	3	−4	12	12	6	7	−1	11	5	2	r2
		100	−10	0	−3	−3	2	5	9	−3	1	−3	r3
			100	0	−5	−7	−1	−9	1	−11	−1	−4	r4
				100	0	3	−11	4	−20	1	−12	−5	∠2
					100	41	19	43	3	67	14	2	u1
						100	−3	46	2	65	14	8	u2
							100	5	4	28	2	−15	u3
								100	3	64	17	7	u5
									100	4	15	−15	u12
										100	14	1	k1
											100	−2	k2
												100	k3

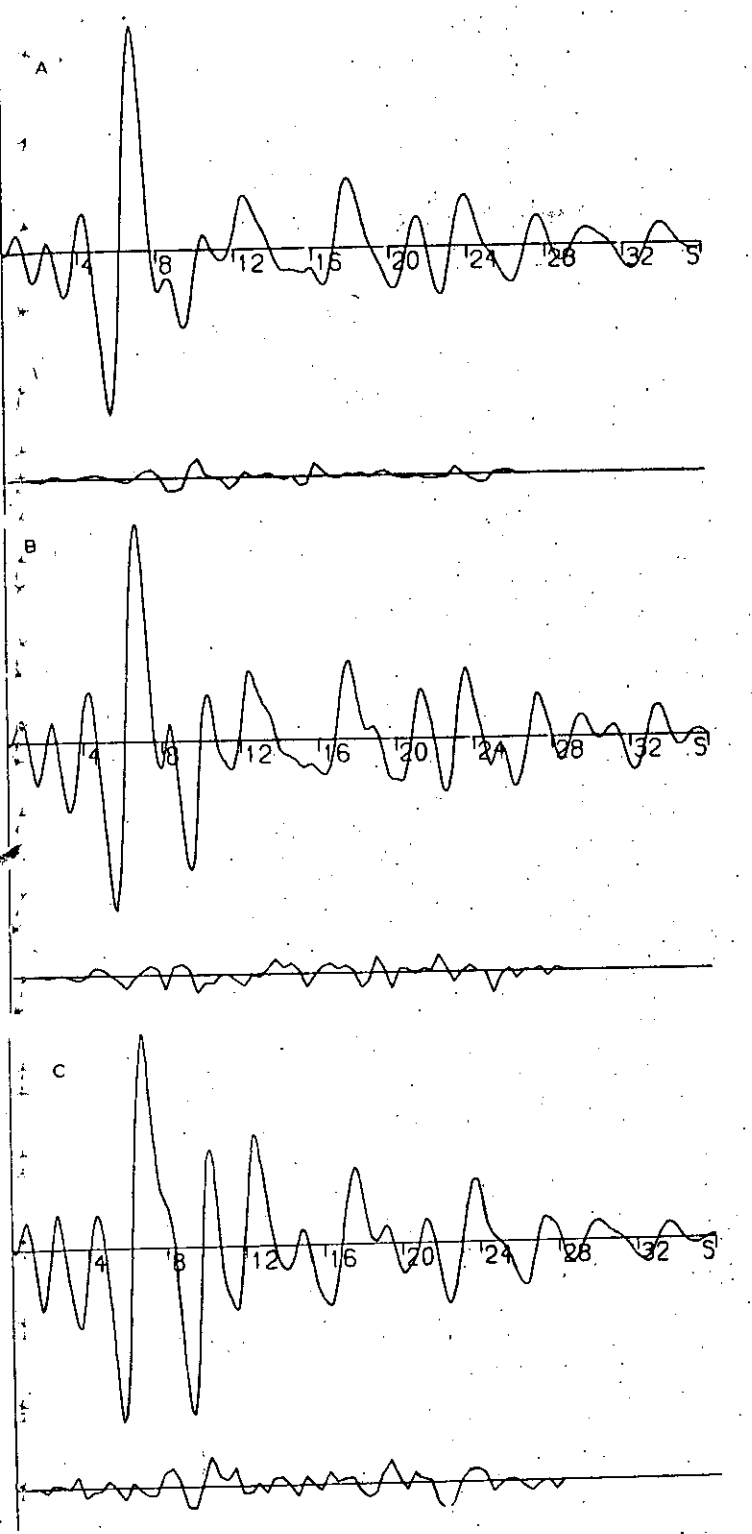

Fig. 3. Combined molecular scattering intensity and difference curves for (a) $CH_3Re(CO)_5$, (b) $SiH_3Re(CO)_5$ and (c) $GeH_3Re(CO)_5$. In regions where the sum of the weights for the 250, 500 and 100 mm data sets was less than 1, theoretical intensity has been included.

correlation matrix is presented in Table 3. It should be noted that the errors quoted included those derived from the least squares analysis, and an allowance for systematic errors. The use of an off-diagonal weight matrix takes care of the problem of correlation between observations.

The combined molecular intensity curves for the three molecules are shown in Fig. 3. Intensity data may be obtained from the authors on request.

Silylrhenium pentacarbonyl

The four bond lengths Re—Si, Re—C, C—O and Si—H, their amplitudes of vibration (except that for Si—H) and the angles C_{ax}—Re—C_{eq} and Re—C_{eq}—O_{eq}, were refined, with some amplitudes of vibration for non-bonded atom pairs. The results of a refinement for which R_G was 0.21, are shown in Table 2, together with details of constraints on vibrational parameters. The least squares correlation matrix is given in Table 4. The values of R_G for this compound and for the germyl analogue are larger than usual, mainly because the scattering intensities due to atom pairs involving rhenium are reduced by the phase shift term discussed earlier. The poor rhenium scattering factor adds to the problem.

Germylrhenium pentacarbonyl

The results of a refinement with R_G equal to 0.22 are given in Table 2, and the least squares correlation matrix is in Table 5. In this case it was found to be possible to refine the Re—C, Re—Ge and C—O distances and vibrational amplitudes, the angles C_{ax}—Re—C_{eq}, Re—C_{eq}—O_{eq} and three groups of amplitudes of vibration for non-bonded distances. As with the other compounds, the Re—C and Re—O "beat-out" points were included in early refinements, but subsequently fixed.

Discussion

It is not easy to define a covalent radius for a metal such as manganese or rhenium, but the best estimates available for these atoms are 139 [13] and 153

TABLE 5

LEAST SQUARES CORRELATION MATRIX FOR $GeH_3Re(CO)_5$, MULTIPLIED BY 100

r1	r2	r3	∠2	u1	u2	u3	u5	u10	u12	k1	k2	k3	
100	2	−2	−3	0	−2	1	−1	7	0	−3	8	15	r1
	100	−4	−6	9	9	−2	6	−3	2	5	11	7	r2
		100	3	6	9	26	−18	25	4	17	7	−4	r3
			100	−12	−13	−5	0	−39	−45	−18	−29	−25	∠2
				100	27	28	15	24	11	47	35	22	u1
					100	29	17	23	11	51	35	25	u2
						100	1	48	9	55	43	21	u3
							100	−13	2	33	15	11	u5
								100	27	33	54	50	u10
									100	17	22	7	u12
										100	42	30	k1
											100	34	k2
												100	k3

TABLE 6

BOND LENGTHS INVOLVING Mn OR Re

	Mn	Ref.	Re	Ref.	Difference
$MH_3M(CO)_4—CO^a$	184.9(3)	1,2	200.4(4)	this work	15.5
$(CO)_5M—CH_3$	218.5(11)	1	230.8(17)	this work	12.3
$(CO)_5M—SiH_3$	240.7(5)	2	256.2(12)	this work	15.5
$(CO)_5M—GeH_3$	248.7(2)	2	262.8(6)	this work	14.1
$(CO)_5M—M(CO)_5$	297.7(11)	4	304.0(5)	3	6.3/2 = 3.2
Covalent radius	139	12	153	13	14

[a] Mean of values in CH_3, SiH_3 and GeH_3 derivatives.

pm [14] respectively. The difference between these values, 14 pm, is close to the difference between average metal—carbonyl distances, as shown in Table 6, and so this difference may be taken as being reliable, even if the absolute values are not. Using these covalent radii, and 76.7 pm for carbon, we predict Mn—C and Re—C distances of 215.7 and 229.7 pm. Thus the Mn—C bond in methylmanganese pentacarbonyl does seem to be anomalously long, consistent with estimates of its bond dissociation energy [6]. The Mn—Mn bond in dimanganese decacarbonyl is even more remarkably long. In contrast, Table 6 shows that the bonds in silyl- and germyl-rhenium pentacarbonyls are 14-15 pm longer than the bonds in the manganese derivatives. These bonds are still short compared to those to a methyl group carbon, which may reflect some multiple bond character in the silicon and germanium bonds, but there is no evidence that the extent of this is different for the two metals, rhenium and manganese. This is not consistent with results based on metal—metal stretching force constants [7], but those estimates depended on some assumptions and simplifications that could lead to large errors.

On the other hand, there are estimates of the manganese covalent radius up to 146 pm (based on a value for cobalt [15]), and using this we find our results to agree with all the earlier work, except that concerning bond dissociation energies in methyl derivatives.

The structures of the $—Re(CO)_5$ groups are exactly as would be expected. The parameters seem to depend very little on the substituent, although small variations in the $Re—C_{ax}$ distance would not be easily detected by electron diffraction.

Acknowledgements

We thank Professor D.W.J. Cruickshank, Dr. B. Beagley, Mrs. V. Ulbrecht and Dr. M.J. Smyth for their assistance in the experimental work, and the Dewar Foundation for a grant to A.R.

References

1 H.M. Seip and R.M. Seip, Acta Chem. Scand., 24 (1970) 3431.
2 D.W.H. Rankin and A. Robertson, J. Organometal. Chem., 85 (1975) 225.
3 N.I. Gapotchenko, Yu.T. Struchkov, N.V. Alekseev and I.A. Ronova, Zh. Strukt. Khim., 14 (1973) 419.
4 A. Almenningen, G.G. Jacobsen and H.M. Seip, Acta Chem. Scand., 23 (1969) 685.

5 G.A. Junk and H.J. Svec, J. Chem. Soc. A, (1970) 2102.
6 D.L.S. Brown, J.A. Connor and H.A. Skinner, J. Organometal. Chem., 81 (1974) 403.
7 K.M. Mackay and S.R. Stobart, J. Chem. Soc. Dalton Trans., (1973) 214.
8 W. Hieber, G. Braun and W. Beck, Chem. Ber., 93 (1960) 901.
9 G.C. Holywell, D.W.H. Rankin, B. Beagley and J.M. Freeman, J. Chem. Soc. A, (1971) 785.
10 D.M. Bridges, G.C. Holywell, D.W.H. Rankin and J.M. Freeman, J. Organometal. Chem., 32 (1971) 87.
11 L.S. Schäfer, A.C. Yates and R.A. Bonham, J. Chem. Phys., 55 (1971) 3055.
12 E.J. Jacob and L.S. Bartell, J. Chem. Phys., 53 (1970) 2231.
13 F.A. Cotton and D.C. Richardson, Inorg. Chem., 5 (1966) 1851.
14 V.G. Adrianov, B.P. Biryukov and Yu.T. Struchkov, Zh. Strukt. Khim., 10 (1969) 1129.
15 J.A. Ibers, J. Organometal. Chem., 14 (1968) 423.

ABSTRACT OF THESIS

Name of Candidate Alastair Robertson

Address 6 Tyler's Acre Road, Edinburgh

Degree PhD *Date* September 1976.

Title of Thesis Structures of some Silyl- and Germyl-Transition Metal Carbonyl Complexes.

The He(I) photo-electron spectra of $HMn(CO)_5$, $SiH_3Mn(CO)_5$, $SiCl_3Mn(CO)_5$, $SiF_3Mn(CO)_5$, $GeH_3Mn(CO)_5$, $GeMe_3Mn(CO)_5$, $HRe(CO)_5$, $CH_3Re(CO)_5$, $SiH_3Re(CO)_5$, $SiF_3Re(CO)_5$, $GeH_3Re(CO)_5$, $Re_2(CO)_{10}$, $HCo(CO)_4$, $SiH_3Co(CO)_4$, $SiMe_3Co(CO)_4$ and $GeH_3Co(CO)_4$ were recorded. These spectra and published photo-electron spectra of $CH_3Mn(CO)_5$, $CF_3Mn(CO)_5$ and $SiMe_3Mn(CO)_5$ and discussed in terms of $(d\rightarrow d)\pi$ bonding in the silicon-transition metal and germanium-transition metal bonds. Due to the overlapping of peaks in the above-mentioned spectra the assignment of all but a few electronic energy levels to peaks in the photo-electron spectra was impossible. However these spectra did indicate that, in at least the manganese-pentacarbonyl derivatives, $(d\rightarrow d)\pi$ bonding was unimportant in the metal-metal bonds. The main change in substituting a silyl- or germyl- group for a methyl- group on manganesepentacarbonyl appeared to be an increase in σ acceptor power of the ligand. Rheniumpentacarbonyl and cobalt-tetracarbonyl derivatives gave photo-electron spectra which are consistent with this observation.

The gas phase molecular structures of $SiH_3Mn(CO)_5$, $SiF_3Mn(CO)_5$, $GeH_3Mn(CO)_5$ $GeH_3Co(CO)_4$, $CH_3Re(CO)_5$, $SiH_3Re(CO)_5$ and $GeH_3Re(CO)_5$ were determined by electron diffraction. Difficulties were encountered in the structure determinations of the rhenium derivatives owing to an oscillation in the published scattering factor for rhenium. This oscillation had to be removed to enable these structure determinations to be carried out. The discussion of the above structures and those available for $CH_3Mn(CO)_5$, $CF_3Mn(CO)_5$, $SiMe_3Mn(CO)_5$, $SiH_3Co(CO)_4$, $SiCl_3Co(CO)_4$, $SiF_3Co(CO)_4$ and $GeCl_3Co(CO)_4$ was also largely in terms of $(d\rightarrow d)\pi$ bonding in the bonds between silicon or germanium and transition metals. These metal-metal bonds were always found to be shorter than would be predicted from the covalent radii of the atoms involved and this could be taken as an indication of $(d\rightarrow d)\pi$ bonding. However, these relatively short silicon-

Use other side if necessary.

and germanium- transition metal bond lengths are also consistent with σ acceptor power increasing as silyl- and germyl- groups are substituted for methyl- groups. Halogenation of a silyl- or germyl- group bound to a transition metal atom shortens the metal-metal bond. This again could be due to an increase in (d→d) π bonding. The very large reduction in the methyl carbon-manganese bond length on fluorination of $CH_3Mn(CO)_5$ and the fact that the silicon-manganese bond length in $SiF_3Mn(CO)_5$ is only slightly shorter than would be predicted from the methyl carbon-manganese bond length in $CF_3Mn(CO)_5$ indicate that halogenation of silyl- and germyl- groups in transition metal carbonyl complexes does not cause an increase in (d→d) π bonding in the metal-metal bonds. It also seems likely that the methyl carbon-manganese bond in $CH_3Mn(CO)_5$ is anomalously weak and long rather than the manganese-silicon and manganese-germanium bonds in $SiH_3Mn(CO)_5$ and $GeH_3Mn(CO)_5$ being anomalously short and strong.

At the start of this work it was hoped that the molecular structures would also enable more information to be obtained from the photoelectron spectra. However, the photoelectron spectra and molecular structures of Si_2H_6, Si_2F_6, $SiH_3Mn(CO)_5$ and $SiF_3Mn(CO)_5$ demonstrated the difficulties involved in trying to correlate bond lengths with binding energies of the σ bonding level. Fluorination of Si_2H_6 results in an increase in binding energy of the electrons in the Si-Si σ bond but no significant decrease in bond length whereas fluorination of $SiH_3Mn(CO)_5$ resulted both in an increase in binding energy of the electrons in the Si-Mn σ bond and a decrease in Si-Mn bond length.

Appendix one describes an attempt to determine the gas phase molecular structure of trifluoromethylisocyanate by electron diffraction. This failed since all the bond lengths are too close together, as are the two-bonded distances.

Appendix two describes the gas phase molecular structure of hydridotetrakis (trifluorophosphine) rhodium (I) determined by electron diffraction. This structure indicates that, with trifluorophosphine ligands, (d→d) π bonding is important in rhodium-phosphorus bonds.

UNIVERSITY OF EDINBURGH THESIS

Author (surname, initials): Degree: Year:

This thesis is an unpublished typescript and the copyright is held by the author. *All persons consulting this thesis, or having copies made, must sign the Copyright Declaration below.*

Copying regulations:

(1) This thesis may be copied in whole or in part for the use of individuals and for libraries wishing to add this thesis to their stock. *Copying must be done by Edinburgh University Library.*

(2) This thesis must not be copied, either in whole or in part, without the applicant obtaining the author's written permission. *If permission is granted, then copying must be done by Edinburgh University Library.* (The bibliography/list of works consulted may be copied without the author's permission, provided the copying is done by Edinburgh University Library.)

(3) This thesis may be copied only in so far as the copying does not contravene the 1956 Copyright Act. *Copying must be done by Edinburgh University Library.*

Copyright Declaration: I undertake fully to observe the author's copyright in this thesis, not to publish the whole or any part of it without the author's written permission, and not to allow any other person to use any copy made for me.

Date	Name and Address (BLOCK CAPITALS)	Signature	Pages copied (if any)